AN ABSTRACT OF THE THESIS OF

Brian P. Malone for the degree of Master of Science in Wood Science and Civil Engineering presented on June 7, 2013

Title: Light-Frame versus Timber Frame: A Study in Quantifying the Differences

Abstract approved:

Rakesh Gupta Thomas H. Miller

The objective of this study was to compare light wood framing and traditional timber framing quantitatively through environmental impact assessment and load path analysis. This research was inspired by a traditional timber frame structure constructed in Vermont in 2011, and the design of structures considered within reflect the general characteristics of this building with some modifications. A light-frame structure was designed for comparison purposes to be equivalent to the timber frame structure in overall dimension and function.

Cradle-to-gate environmental impact assessments were performed with the Athena Impact Estimator for Buildings software, following the standard methodology of life cycle assessment. The environmental impacts for each structural system as well as for multiple material substitutions to each were investigated. Environmental impacts considered included total energy use, fossil fuel consumption, global warming potential, and wood fiber use. Results show that though the timber frame structure has more potential for decreased environmental impact, these measures are driven largely by material choice.

Models for each framing system (light-frame and timber frame) were created using SAP2000 structural analysis software, and load paths generated by applied design loads were investigated and compared. Both structures were modeled with and without openings (doors and windows), and comparisons were made based on resistance to uplift, story drift and twisting, the addition of large openings, a break in load path, and the relative ranges of axial loads in posts and studs. Results show that the timber frame structure outperforms the light-frame structure in many aspects, providing increased resistance to uplift, story drift, and twisting, less sensitivity to the addition of large openings or the loss of a floor-supporting post, and less variability in axial forces in vertical members.

LIGHT-FRAME VERSUS TIMBER FRAME: A STUDY IN QUANTIFYING THE DIFFERENCES

by
Brian P. Malone

A THESIS

submitted to

Oregon State University

in partial fulfillment of
the requirements for the
degree of

Master of Science

Presented: June 7, 2013
Commencement: June 2014

Master of Science thesis of Brian P. Malone presented on June 7, 2013.

APPROVED:

Co-Major Professor representing Wood Science and Engineering

Co-Major Professor representing Civil Engineering

Head of the Department of Wood Science and Engineering

Head of the School of Civil and Construction Engineering

Dean of the Graduate School

I understand that my thesis will become part of the permanent collection of Oregon State University libraries. My signature below authorizes release of my thesis to any reader upon request.

Brian P. Malone, Author

ACKNOWLEDGMENTS

I would like to express my appreciation to the following:

- My advisors, Dr. Rakesh Gupta and Dr. Thomas H. Miller, for their expertise and guidance.
- Maureen Puettmann, PhD., whose expertise in life cycle assessment within the wood products industry added considerably to my research.
- Kenny Martin, whose previous research, development of modeling methods, and guidance in wood structural engineering.
- Katherine Pfretzschner for her previous research and development of modeling methods.
- Arijit Sinha, whose guidance pertaining to life cycle assessment in the early stages of this study was of great assistance.
- The Department of Wood Science & Engineering and the School of Civil & Construction Engineering at Oregon State University for providing the necessary resources and furthering my education, as well as funding this project.
- My friends who helped me raise the barn that inspired this project.

Finally, I would like to thank my family. My parents, Jack and Susan Malone, as well as my sister Kelly have always supported and encouraged me throughout my education and career.

CONTRIBUTION OF AUTHORS

Dr. Rakesh Gupta and Dr. Thomas H. Miller provided technical guidance and support during the research stages. They also provided insight and editing for the final manuscripts and thesis. Additionally, Dr. Maureen Puettmann provided these services for the Environmental Impact Assessment portion of this study.

TABLE OF CONTENTS

TABLE OF CONTENTS (Continued)

TABLE OF CONTENTS (Continued)

Page

LIST OF FIGURES

Figure Page

LIST OF FIGURES (Continued)

Figure Page

LIST OF TABLES

Table Page

LIST OF APPENDICES

LIST OF APPENDIX FIGURES

Figure Page

LIST OF APPENDIX FIGURES (Continued)

Figure Page

LIST OF APPENDIX TABLES

Table Page

LIST OF APPENDIX TABLES (Continued)

Table Page

LIST OF APPENDIX TABLES (Continued)

Table Page

LIGHT-FRAME VERSUS TIMBER FRAME: A STUDY IN QUANTIFYING THE DIFFERENCES

INTRODUCTION

Prior to the advent of light-frame (LF) construction, wood-framed structures were composed of large-dimension timbers fastened with mortise-and-tenon style joinery, a construction method known as timber framing (Allen and Thallon 2011). Modern LF construction practices were developed in the first half of the 19th century when advances in manufacturing for building materials (sawn framing material and machine-made nails) made economically possible a structural system that was more efficient in both time and skill (Allen and Thallon 2011). Furthermore, the structural success of this framing system disproved the belief that large-dimension timbers were necessary for structural stability. In the decades following, the craft of timber framing was abandoned in the US in favor of LF construction due primarily to its economic benefits (Allen and Thallon 2011).

Growing concerns over the performance of LF wood residential structures in the wake of extreme weather events have highlighted the need for improvement in wood framing practices (van de Lindt et al. 2007, Prevatt et al. 2012). Additionally, concerns over the negative environmental effects of the construction industry in general have designers and builders taking a second look at how the decisions they make affect the health of our planet. As two of the largest concerns facing the wood framing industry, safety and environmental responsibility continue to demand closer attention. This study combines the consideration for these concerns simultaneously by performing structural load path analysis alongside an environmental impact analysis. Additionally, traditional timber frame (TF) construction is considered and compared to LF construction to weigh its contribution to structural and environmental effectiveness against that of an equivalent LF. The revival of the craft of timber framing in the 1970's in the U.S. has taken a traditional framing style and turned it into a modern product that deserves attention. Though LF structures have existed for no more than two centuries, many several-hundred-year-old TFs have already been proven by the test of time, and modern advances in engineering and product manufacturing aim only to improve upon this construction style. A quantitative comparison with current LF practice is the best way to determine the differences in these structural systems, as well as what timber framing could offer an industry currently dominated by light framing.

OBJECTIVES

The main objective of this study was to determine differences between an LF structure and a TF structure based on quantitative results from a load path analysis and an environmental impact analysis of each. Additionally, an objective of the structural load path analysis was to compare the behavior of each structural system with several modifications to the designs, and to perform additional investigations based on the results of these comparisons. Within the environmental impact analysis was the objective to analyze the environmental effects of common material substitutions to each structural system.

RESEARCH APPROACH

Theoretical design alterations to an existing TF structure were made to aid research by simplifying and generalizing its assembly. An LF structure was then designed according to the specifications of the International Residential Code (ICC 2009) to reflect the simplified TF structure, equivalent to it in both envelope and general function. For the creation of structural models, the LF was considered sheathed in plywood, and the TF was considered sheathed in structural insulated panels (SIPs). For the environmental impact analysis, the standard LF considered the LF sheathed in OSB, and the traditional TF was sheathed as it was built, in various solid-sawn wood products (described within). Additional alterations to these structures, and the purpose for these alterations, are described within.

Environmental Impact Assessment

This environmental impact assessment (EIA) uses life cycle assessment (LCA) methodology to determine the associated burdens of each structural system on the environment. LCA is comprised of four parts, which include a goal and scope definition phase, a life cycle inventory (LCI), a life cycle impact analysis (LCIA), and an interpretation of results (ISO 2006). All environmental assessment impact models were created using commercially available software, the Athena Materials Institute's Impact Estimator for Buildings (Athena 2012). The Athena Impact Estimator (AIE) was used to perform LCI and LCIA for this study. Observations and conclusions were made based on these LCIA and with the aid of LCI and LCA studies performed by contributing CORRIM researchers pertaining to the wood products industry.

Models developed with the Impact Estimator reflect the standard LF and traditional TF designs created for this study, as well as multiple structural material substitutions to each system.

These material substitutions reflect design options commonly used in industry, and include alternate sheathing materials, changes in framing member dimension, and the use of unseasoned (green) versus kiln-dried solid sawn materials. Environmental burdens examined in this environmental impact assessment include total energy consumption, fossil fuel use, global warming potential (GWP), and wood fiber use and waste. Each environmental impact assessment was considered "cradle-to-gate," including impacts from manufacturing through construction only. The results for the LF structures as a whole were compared to the results for the TF structures as a whole, and material substitutions were compared within each structural system individually.

Structural Load Path Analysis

The modeling methods used in this study were based on the work of Pfretzschner et al. (2013) and Martin et al. (2011). In each case, the methods developed by these studies for light wood frame structures were validated against the results of partial or full-scale assemblies and sub-assemblies (Wolfe et al. 1986; Wolfe and McCarthy 1989; Dolan and Johnson 1996; Paevere et al. 2003; Datin 2009). Good results deemed these modeling methods suitable for direct application to both the LF and TF models developed for this study. All models were created using commercially available structural analysis software, SAP2000 Version 15 (Computers and Structures 2012).

Framing members were modeled using SAP2000's frame element, and connections between frame elements were modeled primarily as pinned connections. Connections to the base of the structure, representing anchor bolts, hold-downs, and post bottom connections were modeled as linear springs. Sheathing was modeled using SAP2000's layered shell element. Material properties assigned within the model were chosen based on industry standards and specifications.

Models developed reflect the LF structure sheathed in plywood and the TF structure sheathed in SIPs. Each structural system was modeled fully enclosed by sheathing, as well as with openings (doors and windows). Design loads were applied to each structure according to allowable stress design (ASD) loading combinations (ASCE 2010), and results obtained were the magnitude of reactions to these loads at foundation connection locations. Load combinations considered included either gravity loads only or gravity loads combined with lateral loads.

MANUSCRIPT: ENVIRONMENTAL IMPACT ASSESSMENT OF LIGHT-FRAME AND TIMBER FRAME BUILDINGS

Brian P. Malone, Maureen E. Puettmann, Rakesh Gupta, and Thomas H. Miller

Journal of Green Building

College Publishing
12309 Lynwood Drive
Glen Allen, VA 23059

Submitted 2013

ABSTRACT

The objective of this study was to analyze the environmental performance of different wood structural assemblies for residential buildings. Two structural systems (a traditional timber frame and a light-frame) were compared together with alternate material options for each system. Environmental impacts were determined using the Athena Impact Estimator for Buildings software. Design alterations for generalization were made to an existing timber frame (TF) structure used as the basis of this analysis, and an equivalent light-frame (LF) structure was designed based on the International Residential Code (IRC). Environmental impacts observed include total energy consumption, fossil fuel consumption, global warming potential (GWP), and wood fiber use. All analyses were considered cradle-to-gate, including the manufacturing and construction life-cycle stages. Results show how GWP is linked to both fossil fuel consumption and wood fiber use, and how ultimate environmental impact is driven by energy source. Environmental impacts of structures are driven by material choice, and levels of carbon stored in structural wood serve to decrease GWP. Of the structural assemblies analyzed, the most traditional TF structure outperformed all other options in almost every measure.

INTRODUCTION

As considerations for the environmental impacts of products become increasingly important to designers and consumers, the ability to determine these effects becomes necessary. Though qualitative reasoning to evaluate sustainability is valid for some decisions, an accurate quantitative analysis of these negative attributes is the only way to arrive at conclusive results and make truly informed decisions. Life-cycle Assessment (LCA) is a procedure by which the environmental burdens of products, assemblies of products, or activities can be measured and evaluated (ISO 2006). This study follows LCA methodology as outlined in the ISO 14040 (2006) Standard, "Environment Management – Life-cycle Assessment – Principles and Framework." According to this standard, LCA can assist in identifying product improvement opportunities, product decision making, identifying indicators of environmental performance, and the marketing of a product (ISO 2006). LCA is comprised of four phases. These include a goal and scope definition phase, a life-cycle inventory (LCI), a life-cycle impact assessment (LCIA), and an interpretation of results (ISO 2006). Figure 2.1 illustrates the interaction of these phases, as well as general LCA input and output points.

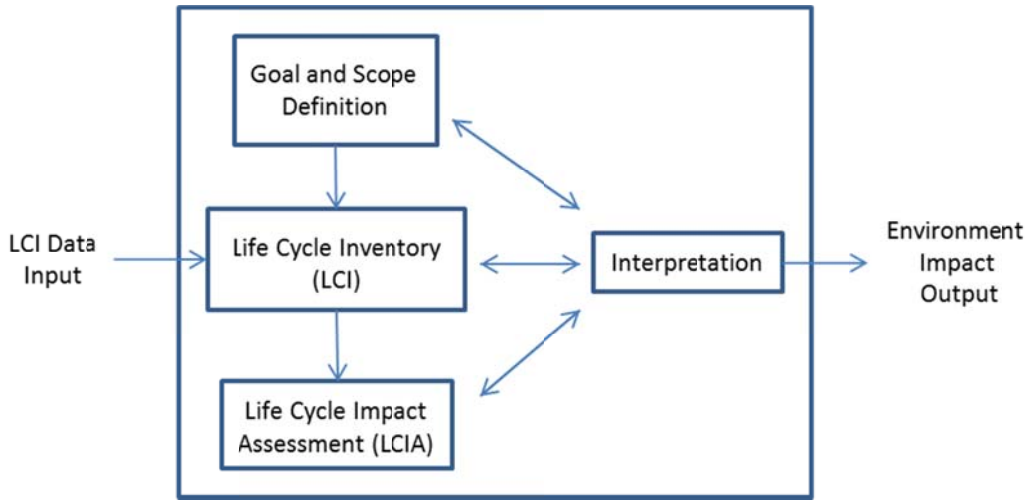

Figure 2.1: Steps to perform a life-cycle assessment

The Athena Impact Estimator software (AIE) (ASMI 2012b), published by the Athena Sustainable Materials Institute (ASMI) simplifies a complex process by providing a database of common building materials and assemblies. This tool combines available information on building materials, and provides cumulative cradle-to-grave environmental impact results (LCIA) for assemblies and whole buildings designed by the user (ASMI 2012a). The LCI that comprise AIE are the result of a vast network of contributing researchers and industry professionals that have determined the material and energy input and environmental releases pertaining to individual building materials (NREL 2012). It is important to note that additional proprietary LCI data gathered by ASMI, itself, is also built into this software. The LCI database provided and maintained by the National Renewable Materials Laboratory (NREL) is called the US Life-cycle Inventory Database (USLCI). The purpose of the USLCI is to provide high-quality and transparent LCI data and that covers commonly used materials, products, and processes in the United States (NREL 2012). The primary contributor of inventory data for wood and other bio-based materials to this database is the Consortium for Research on Renewable Industrial Materials (CORRIM) (CORRIM 2013). CORRIM has performed the most up-to-date research in this field, and has released their findings in two phases (2005 and 2010) of collections of published reports on a wide range of wood products focused on different geographical areas of the United States (Lippke and Wilson 2010). Furthermore, LCI are incorporated into AIE and are used to perform LCIA. Using impact categories based on the Tool for the Reduction and Assessment of Chemical and Other Environmental Impacts (TRACI) (Bare 2011), AIE determines the relative impact of a product or system based on various environmental impact

stressors such as fossil fuel consumption, global warming potential (GWP), or resource use. TRACI was developed by the U.S. Environmental Protection Agency as a tool that offers a framework to achieve consistent long-term environmental effects (Bare 2011).

Objectives

This environmental impact assessment (EIA) is part of a research effort that compares residential wood framing systems. The overall objective of this research was to compare a traditional timber frame (TF) structure with an equivalent light-frame (LF) structure and determine the differences in performance of each based on both EIA results and structural performance. For more information on the structural analysis portion of this research, please see Malone (2013). The objective of this EIA was to determine which structural system performs most favorably in a cradle-to-gate analysis in the categories of total energy consumption, fossil fuel use, GWP, and wood fiber use and waste. Furthermore, this study investigates how the environmental impacts observed within each structural system change with common material substitutions and changes in framing methods. (Note that the term EIA is used to describe this study, because where a true LCA has complete knowledge of all LCI data sources, the use of AIE inhibits some knowledge of this. This is explained further in the following section.)

LCA Limitations and Assumptions

Life-cycle assessment is a complex science that is still developing. As advances are made in the methods and tools for quantifying environmental impact, an increase in the level of accuracy of LCA will continue to emerge. All LCA (or EIA) studies are subject to inherent limitations and assumptions that must be considered for appropriate analysis of results.

AIE is a decision support tool, and is not considered a means of assigning any definitive rating or score (ASMI 2012a). Though AIE is a useful tool for comparing the environmental effects of given options for products or services within given boundaries, it is understood that there are more factors involved in the decision-making process than can be included in an EIA study such as this. These factors include, but are not limited to the structural or isolative capability of materials, or their cost.

A significant assumption made by AIE is that a project lies in one of a list of set geographical locations in North America. Since material sourcing, power generation, and transportation vary highly by geographic region, and do not obey political boundaries, the user

must define a project by the most appropriate city available. From here, AIE ties its analysis to local power sources, electricity grids, transportation modes, average distances to manufacturing, and manufacturing technologies available (ASMI 2012a). Additionally, materials for input are also based on what is most common, and not all specific material data are available. Construction assemblies and material inputs available are, however, applicable to more than 95% of the building stock in North America (ASMI 2012a). Furthermore, analysis is based on data collected from a multitude of sources, and the accuracy of LCI and LCIA results is tied closely to how current and accurate these original data are. Due to "assumptions and uncertainties in the basic LCI data," and the assumptions necessary to develop a tool that is useful to the general public, ASMI "considers any comparative impact measure differences of 15% or less as being equal or insignificant" (ASMI 2012a). For this reason, only generalized statements can be made based on seemingly precise numeric output values.

Wood Structural Systems

Light wood framing is the most commonly existing structural system for residential buildings in the United States (US) today (Allen and Thallon 2011). Light framing methods emerged in the early-to-mid-19th century and evolved as an efficient and economical wood framing system. Light framing involves 38-mm (nominal 2-in) -thick dimensional lumber generally spaced at either 406-mm or 610-mm (16-in or 24-in) on center to construct walls, flooring, and roofing. Sheathing is most commonly performed with oriented strand board (OSB), and structural elements are connected with metal fasteners (nails, screws, and bolts). The design of residential LF structures is dictated (by law only where adopted) by the International Residential Code (IRC), published by the International Code Council (ICC 2009). Where design necessities exceed the limitations of the IRC, structural components must be engineered individually using the International Building Code (ICC 2011). For this purpose, the design of wood components and systems is performed specifically according to the National Design Specification for Wood Construction (NDS) (AF&PA 2005a).

Prior to the development of light-framing methods, wood framing was performed by a technique known as timber framing. Timber framing flourished in the settlement of America from the early 1600's to the mid-19th century, until light framing emerged as a more economic building system. Light-framing took over, and timber framing nearly disappeared in the US until it resurfaced in the 1970's. An appreciation for timber framing and the necessary to repair and

maintain existing structures gave birth to a new sector of the modern wood framing industry (BRT 2010). Today's timber framing industry represents a niche craft in the custom residential and commercial industry. Though the materials and joinery methods reflect historic practices, advances in wood product manufacturing have advanced the traditional TF to today's modern product. Timber framing can be defined as a structural system composed of large-dimension framing members, generally 127-mm x 127-mm (nominal 5-in x 5-in) and larger that are connected with mortise-and-tenon-style wooden joinery and fastened with wooden pins (though metal fasteners are commonly used for some connections today). The engineering of TF structures is typically performed on a case-by-case basis, and design commonly relies on methods dictated by the NDS (AF&PA 2005a). Though no official code specific to TF design currently exists, the "Standard for Design of Timber Frame Structures" has been written and adopted by the TF Engineering Council, a subset of the Timber Framers Guild of North America (TFEC 2010).

Global Warming Potential and Carbon Stored in Wood Products

The phenomenon of global warming has been primarily attributed to the abundant presence of gases in the atmosphere which absorb outgoing infrared radiation rather than allow it to escape. Carbon dioxide (CO_2) is considered to be the primary anthropogenic cause of global temperature increase. Over time, increased concentration of these gasses in the atmosphere increases the Earth's temperature. Among other effects, this causes sea levels to rise, weather patterns to alter, and extreme weather events to occur more frequently and with more intensity (Florides and Christodoulides 2008). GWP is measured in equivalent weight (kg) of CO_2 released. It is important to note that since global warming emissions commonly include gases other than CO_2, all values are normalized to be reported in CO_2-equivalent units.

Values reported by AIE for GWP reflect only the emissions released directly to the atmosphere during manufacturing and construction. It should be noted that emissions related to the burning of biofuels, however, are considered carbon neutral by AIE, and therefore do not contribute to GWP. Though combustion causes the release of carbon stored in tree material to the atmosphere in the form of CO_2, AIE considers this release equal to the amount of carbon that the tree stored during its lifetime (Finlayson 2013). Carbon stored in materials manufactured, however, is not credited by the software (ASMI 2012a). As a tree grows, CO_2 is sequestered from the atmosphere and carbon is stored in the wood as a large percentage of its composition. For as long as the wood does not decay or burn, approximately half of its weight is comprised of

carbon that has been kept from entering the atmosphere, and therefore kept from contributing to global warming. When wood products are employed for the construction of a building, the carbon in these products is stored in the building's structure for at least as long as the building exists, and possibly longer if these wood products are reused or recycled.

RESEARCH METHODS

This EIA was performed using the Athena Impact Estimator for Buildings (AIE). System boundaries were defined by the user, and these boundaries were part of the definition of each structure within AIE by providing necessary inputs. It is important to note that AIE automatically generates results for a cradle-to-grave analysis. Though these results include all of the five life-cycle stages observed by AIE (manufacturing, construction, operations, maintenance, and end-of-life), a boundary ("gate") was easily set to include life-cycle stages through construction only by ignoring results from operations, maintenance, and end-of-life. (Note that to include these life-cycle stages, additional information not included here would be required for meaningful results.) Results were analyzed objectively with the assistance of previously published LCI reports on wood products (Kline 2005, Bergman and Bowe 2010, Lippke et al. 2010, Lippke and Wilson 2010, Puettmann et al. 2010). The parameters concerning the development, analysis, and interpretation of EIA are explained in the following sections.

System Boundaries

Comparisons for this EIA included the wood structural system for each building, as well as necessary metal fasteners (screws, nails, etc.). Insulation was included for two structures. Since foundations would be considered equal for both structures, these components were not included in the study. TF pins are made of wood, and were considered as already included in the volume of large-dimension lumber.

The analysis performed for each structure was cradle-to-gate, cataloguing all material and energy input, and environmental releases from material extraction and product manufacturing through construction. Material extraction of forest products includes seedling production, forest operations, thinning, and logging. Manufacturing includes all of material extraction, as well as log transportation to the sawmill, and all sawmill operations and material processing necessary for the manufacture of each product (Finlayson 2013). OSB manufacturing, for example, requires wood flaking, drying and screening of flakes, blending with adhesives and pressing of the panel product, finishing, as well as heat generation and emission control for these processes (Kline

2005). Product manufacturing phases and LCI results vary for each individual product. Energy and environmental emissions for the manufacture of adhesives and metal connectors (nails, screws, etc.) are also considered, as well as for insulation options for two structures. The construction phase includes transportation of construction materials from the manufacturing site to the construction site, and the on-site energy required to assemble the products and construct the structure (ASMI 2012a). Building operations, maintenance, and end-of-life were not considered in this study. Figure 2.2 provides a visual rendering of the system boundary for this study.

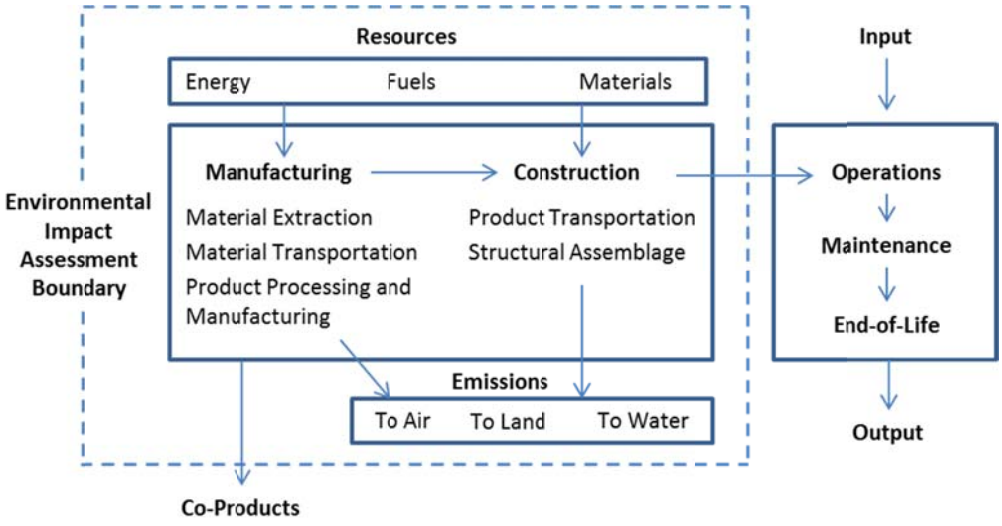

Figure 2.2: Environmental impact assessment boundary for this study

Research Structures

The structures described herein were inspired by a traditional TF building. This building was completed in 2011, and is located in Jay, Vermont. Figure 2.3 and Figure 2.4 are images of the exposed framing system and the completed building, respectively.

Figure 2.3: Exposed timber frame structure in Jay, Vermont, looking north-west

Figure 2.4: Completed timber frame structure in Jay, Vermont, looking north-east

The Vermont structure served as inspiration for this study. For simplicity and generalization, it was necessary to make changes to this design (for research purposes only). Theoretical alterations to the Vermont structure for this study include omission of the cupola and 2nd floor entry dormer, as well as minor adjustments in framing member locations. Additionally, some window locations were assumed and added to the design. This altered version of the Vermont structure is referred to as the "traditional TF" for this study. All other physical and material attributes detailed in the traditional TF design are reflective of the Vermont structure.

The Vermont structure was constructed of solid-sawn, unseasoned (green) eastern hemlock timbers by traditional timber framing methods. All joinery is mortise-and-tenon-style fastened primarily with wooden pins, siding is kiln-dried 19-mm (nominal 1-in) –thick pine shiplap, flooring is green solid-sawn 38-mm x 184-mm (nominal 2-in x 8-in) lumber, and roofing

is kiln-dried 38-mm x 140-mm (nominal 2-in x 6-in) lumber. The traditional TF structure was designed using the NDS (AF&PA 2005) and follows the guidelines outlined by the Standard for Design of TF Structures (TFEC 2010). See Malone (2013) for a thorough description of the design of this structure. Figure 2.5 is a Google Sketch-Up rendering of the traditional TF structure (Google 2012).

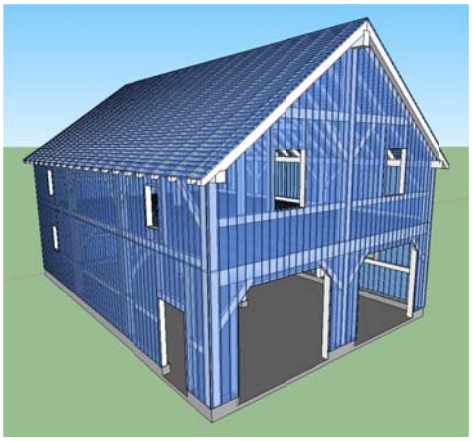

Figure 2.5: Traditional timber frame

All structural systems outlined for this study reflect a rectangular 2-story residential building that has a 7.9-m x 12.2-m (26-ft x40-ft) footprint, is approximately 8-m (26.5-ft)-high at the gable, and has a 9:12-slope gable roof. The bottom story has two garage doors on one gable end, as well as a person door on one side. There are three windows on the first story, and eight on the second. This building is located in the town of Jay, Vermont.

An equivalent LF structure (called the "standard LF" in this study) was designed based on the traditional TF structure. Equivalence for this design was defined as maintaining building envelope and shape, and meeting the same operational needs as the traditional TF structure. The design of the standard LF was performed in accordance with the guidelines outlined in the IRC (ICC 2009). Where design requirements could not be met by these guidelines, necessary components of the structural system were engineered according to the NDS (AF&PA 2005). These components include the beams that support the 2nd floor and the columns that centrally support these beams. Additionally, where available shear wall area on the gable end with garage door openings was deemed insufficient by the IRC, a moment-resisting portal frame was engineered (Martin et al. 2008). Figure 2.6 is a Google Sketch-Up rendering of the standard LF structure (Google 2012).

Figure 2.6: Standard light frame

Material substitutions were made to both the traditional TF and the standard LF structures to determine the environmental impacts of these design options. Changes to structural systems included the following:

Timber Frame

- Replaced large-dimension green framing materials with large-dimension kiln-dried framing materials. ("Kiln-dried TF")
- Installed (kiln-dried) small-dimension light-framing "infill" between timber framing members to serve as connection points for OSB for roof, wall, and floor sheathing. ("TF with light-framing infill")
- Utilized structural insulated panels (SIPs) for roof and wall sheathing. ("TF with SIPs.")

SIPs were explored both with and without considering the environmental contribution of expanded polystyrene insulation (foam). Note that SIPs inherently include foam insulation, and though a TF structure with SIPs neglecting this insulation was considered for this study, it is for comparison only.

Light- Frame

- Decreased stud size, and therefore wall thickness to that of a 38-mm x 89-mm (nominal 2-in x 4-in) stud. ("LF with 38-mm x 89-mm (nominal 2-in x 4-in) walls.")

- Sheathed the roof, walls, and floor with plywood instead of OSB. ("LF with OSB.")

Fiberglass batt insulation was also considered for environmental comparison with the expanded polystyrene in SIPs. (LF with insulation) Design alterations considered but omitted from this study include using green framing material for the LF structure, as well as spacing studs at 610-mm (24-in) o.c. rather than 406-mm (16-in) o.c. Since light-framing with unseasoned material is not a common practice in Vermont, this option was not considered. Though spacing studs at 610-mm (24-in) o.c. is a viable option often considered to increase insulation space, this slight reduction in overall volume of framing material was minimal and was therefore not considered. Table 2.1 outlines the materials used in each structural system.

Table 2.1: Structural system materials description

Structural System		Materials					
Frame	**Option**	**Wall Framing**	**Roofing**	**Flooring**	**Siding**	**Insulation**	
						Wall	**Roof**
Light-Frame	**Standard**	Kiln-Dried 38-mm x 140-mm, 406-mm o.c.	OSB, 12-mm	OSB, 12-mm	OSB, 12-mm	None	None
	2x4 Walls	Kiln-Dried 38-mm x 89-mm, 406-mm o.c.	OSB, 12-mm	OSB, 12-mm	OSB, 12-mm	None	None
	Plywood	Kiln-Dried 38-mm x 140-mm, 406-mm o.c.	Plywood 12-mm	Plywood 12-mm	Plywood 12-mm	None	None
	Standard Insulated	Kiln-Dried 38-mm x 140-mm, 406-mm o.c.	OSB, 12-mm	OSB, 12-mm	OSB, 12-mm	140-mm Fiberglass	235-mm Fiberglass
Timber Frame	**Traditional**	Large-Dimension Solid-Sawn ,Green	Kiln-dried, Solid-Sawn 38-mm x 140-mm Lumber	Green, Solid-Sawn 38-mm x 203-mm Lumber	Kiln-Dried, Solid-Sawn Shiplap Lumber, 19-mm	None	None
	Kiln-dried	Large-Dimension Solid-Sawn, Kiln-Dried	Kiln-dried, Solid-Sawn 38-mm x 140-mm Lumber	Kiln-Dried, Solid-Sawn 38-mm x 203-mm Lumber	Kiln-Dried, Solid-Sawn Shiplap Lumber, 19-mm	None	None
	LF Infill	Large-Dimension Solid-Sawn ,Green	OSB, 12-mm	OSB, 12-mm	OSB, 12-mm	None	None
	SIPs	Large-Dimension Solid-Sawn, Green	SIPs (2 Layers OSB, 9.5-mm)	OSB, 12-mm	SIPs (2 Layers OSB, 9.5-mm)	140-mm Expanded Polystyrene	235-mm Expanded Polystyrene
	SIPs No Foam	Large-Dimension Solid-Sawn ,Green	SIPs (2 Layers OSB, 9.5-mm)	OSB, 12-mm	SIPs (2 Layers OSB, 9.5-mm)	None	None

Life-cycle Inventory and Data Entry

AIE is a software package that was developed to simplify the LCA process and make it more accessible and user-friendly. For this reason, its results are limited to the range of inputs it allows. LCI and LCIA results are based solely on the data entry that it requires, as well as the user-defined material or assembly information for each building to be analyzed. Basic project information for each structure includes a "project location," "building type," "building height," "and "gross floor area." Note that for this cradle-to-gate EIA, "building life expectancy" is negligible because the boundaries of this study include only the manufacturing and construction life-cycle stages. AIE offers only a limited number of building locations, and due to its closest proximity to the actual building site, the "project location" chosen for this study was Montreal, Quebec, Canada. "Building type" was selected as "single-family residential." "Gross floor area" for each structure was 193 m^2 (2,080 ft^2), and building height was either 7.9-m (26.2-ft) for TF structures or 8.2-m (26.8-ft) for LF structures. Note that in order to maintain interior wall and ceiling heights, building height between TF and LF structures varied slightly due to the nature of the construction techniques.

The primary step in performing an analysis with AIE is to create a "bill of materials." The bill of materials is the backbone of all results generated by AIE, and therefore these results are based on each material's volume, surface area, or weight depending on its required functional unit. Functional units are the units by which all building materials are input to AIE by the user or reported by AIE. Functional units vary based on building material and are defined by AIE. Though AIE has the ability to self-calculate a bill of materials based on user-defined construction assemblies (walls, roofs, etc.), this feature was not used for this study. Since AIE does not recognize TF construction practices, material quantity data were input directly using the "extra basic materials" option. This feature allows for the input of user-calculated material quantities to form the bill of materials, which overrides any necessary material calculation by AIE (ASMI 2012a). A bill of materials defined directly by the user also allows for greater accuracy, because the bill of materials calculated by AIE is considered accurate only within +/- 10% (ASMI 2012a). For consistency, this feature was used for each frame analyzed, including LF models. All material quantity inputs for this study are reflective of purchased quantities rather than exact quantities in the final building product, and therefore include the environmental impact of any materials wasted during all life-cycle stages considered. All materials that do not end up as part of a structural system are therefore considered waste. Note that AIE assigns an increase in the

material quantity entered into “extra basic materials” based on a percent of waste automatically assumed. This calculation, however, was mathematically overridden so that the final quantity for each material reflected the user-calculated value (which already included waste).

For the calculation of each bill of materials, a thorough inventory of all materials within each wooden structural system was performed. A three-dimensional model of each structure was created using Google Sketch-up software (Google 2012), providing an interactive visual of all components except small fasteners (nails, screws). Using these models and a working knowledge of standard construction practices, the total quantities of each material were calculated. Material quantities were determined either by volume, surface area, or weight, as dictated by AIE, and were reported in the functional units required by AIE. Material estimates were calculated by hand, and multiple checks were performed to verify accuracy. Due to limitations concerning input categories in AIE, material quantities were entered in their respective most appropriate category. For example, “small dimension lumber” is considered to be 38-mm x 140-mm (nominal size 2-in x 6-in) and smaller, and “large dimension lumber” is considered to be 38-mm x 203-mm (nominal size 2-in x 8-in) and larger (ASMI 2012a). Note also that all OSB and plywood values are entered in the equivalent of 9.5-mm (3/8-in) thickness, and therefore a multiplication factor of 1.25 was applied to calculate the equivalent quantity of 12-mm (15/32-in) -thick sheathing materials. Other materials including insulation were also entered on a per-thickness basis, as required. Fasteners were calculated based on a working knowledge of standard construction practices, and reported by weight. Table 2.2 outlines the “Bill of Materials” for each structure. Each value in this table is presented in the functional unit required by AIE.

Table 2.2: Bill of materials

Material	Units	Light-Frame				Timber Frame				
		Std.	2x4 Walls	Plywood	Std. Insulated	Traditional	Kiln-Dried	LF Infill	SIPs No Foam	SIPs
Large-Dim Softwood Lumber, kiln-dried	m^3	7.861	7.861	7.861	7.861	0	15.55	0	0	0
Small-Dim Softwood Lumber, kiln-dried	m^3	6.396	4.835	6.396	6.396	6.276	6.276	3.511	0.675	0.675
Large-Dim Softwood Lumber, green	m^3	0	0	0	0	15.55	0	12.16	12.16	12.16
Oriented Strand Board	m^2	631.2	631.2	0	631.2	0	0	628.0	918.0	918.0
Softwood Plywood	m^2	0	0	631.2	0	0	0	0	0	0
Pine Wood Shiplap Siding	m^2	0	0	0	0	919	919	0	0	0
Nails	tonnes	0.0701	0.0654	0.0701	0.0701	0.0607	0.0607	0.0622	0.0164	0.0164
Screws Nuts & Bolts	tonnes	0.008	0.008	0.008	0.008	0.0168	0.0168	0.0168	0.0740	0.0740
Hot Rolled Sheet (Steel)	tonnes	0	0	0	0	0.0113	0.0113	0.0113	0.0113	0.0113
Batt Fiberglass	m^2	0	0	0	1,954	0	0	0	0	0
Expanded Polystyrene	m^2	0	0	0	0	0	0	0	0	2,777

Carbon Storage in Wood Products

The amount of carbon stored in each structural system was calculated based on the weight of wood products in each structure. Material weights were based on specific gravities of species and panel products as reported by the NDS and the Panel Design Specification, respectively (AF&PA 2005, APA 2012). Carbon calculations assumed a carbon composition of 50% by weight, which is approximately typical of most softwood species (Lamlom 2003). This value was then scaled to CO_2-equivalence based on molecular weight for direct comparison with AIE GWP values. Since material quantities used for this calculation reflect purchased amounts, a 10% reduction in material weight was assumed to account for construction waste. For a more detailed account of these calculations, see Appendix G of Malone (2013).

RESULTS AND DISCUSSION

Life-cycle impact analysis

Cradle-to-gate environmental impacts analyzed included total energy consumption, fossil fuel consumption, GWP, and wood fiber use and waste.

Though many additional environmental impacts are reported by AIE, these were determined for analysis based on relevance and ease of comparability. For additional EIA data, see Appendix H of Malone (2013). Results of these analyses are presented in Figures 7 through 12. The values contributing to these graphs were determined by AIE.

Energy Consumption

Total energy consumption is defined as the cumulative energy, from all sources, necessary to complete all tasks within the EIA boundary. Total manufacturing energy consumption is a portion of total energy consumption, and is defined as all energy necessary to produce the materials that comprise the structure. Energy consumption is measured in total mega joules (MJ) of energy consumed for the manufacturing of materials (including material extraction) and construction of each structural system (ASMI 2012a). Reports present several types of fuel sources for energy generation. Figure 2.7 shows the LCIA results for total energy consumption for all LF and TF structures considered in this EIA.

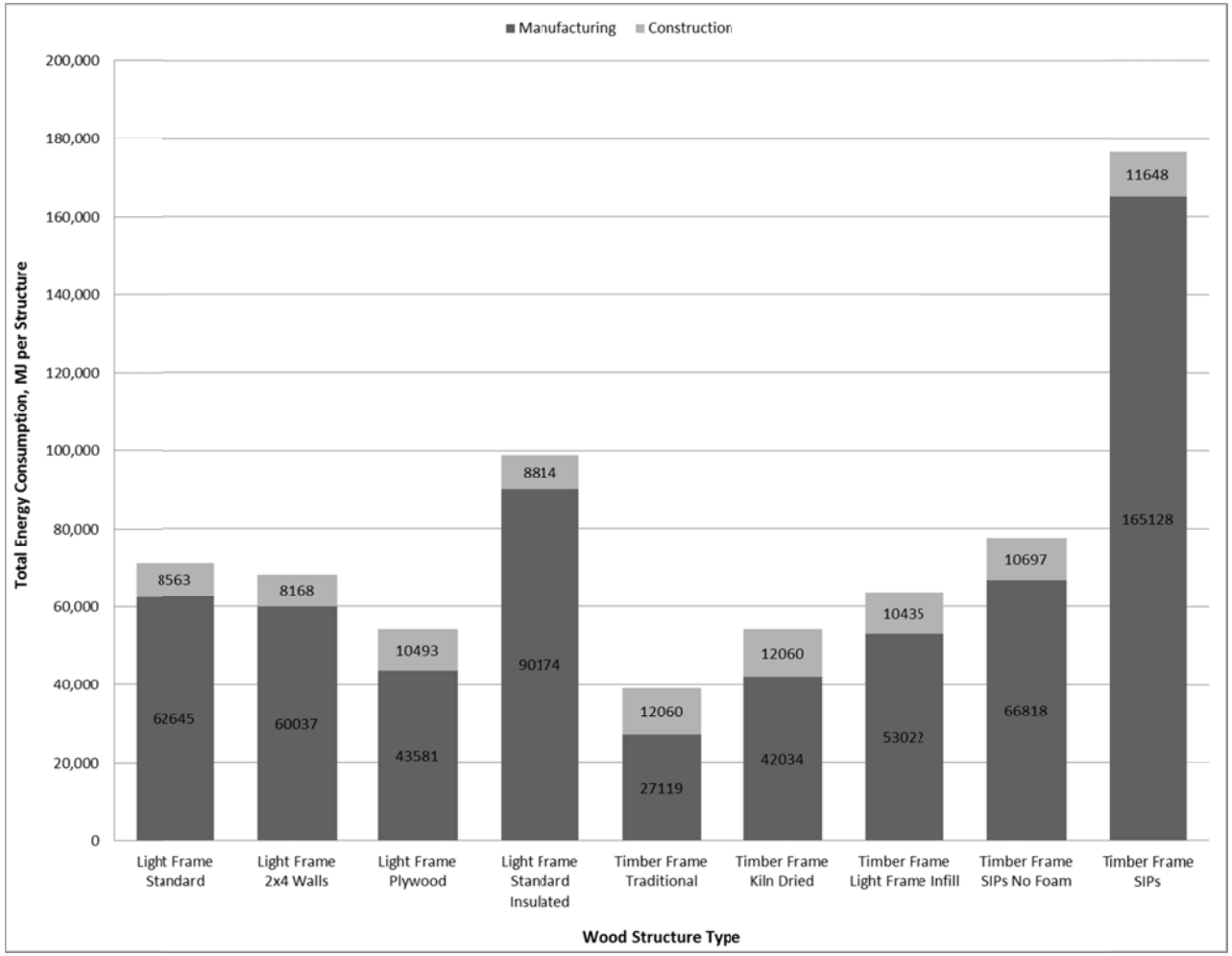

Figure 2.7: Total energy consumption from cradle to construction gate for timber frame and light-frame structures and their alternatives

Cradle-to-gate energy consumption for both designs and their alternatives was dominated by the manufacturing life-cycle stage. Manufacturing energy consumption ranged from 69% of total energy consumption for the traditional TF to 93% for the TF with SIPs. The remaining percentage of total energy consumption was consumed during the construction life-cycle stage. Among the structures that do not include insulation, the total energy consumption ranged from 39,200 MJ (3.71×10^7 btu) to 77,500 MJ (7.35×10^7 btu). Once engineered wood products that require additional processing (OSB, kiln-dried solid-sawn framing, etc.) were added to the traditional TF structure, however, total energy consumption values were comparable to those of light-framing options. Energy consumption therefore increased with the use of materials that require kiln drying or additional mechanical processing (chipping, pressing, etc.). For example, the TF structure with kiln-dried timbers and flooring rather than green materials for these purposes required an increase in manufacturing energy requirement of 55%. Since AMSI considers any comparative difference of 15% or less to be equal or insignificant, some structures required comparatively equal amounts of energy (ASMI 2012a). The option to construct the LF walls with 38-mm x 89-mm (2-in x 4-in) framing material instead of 38-mm x 140-mm (2-in x 6-in) framing material, for example, results in a manufacturing energy consumption decrease of only 4%. This value therefore provides no significant conclusion for comparison. The LF sheathed with plywood, however, consumed 27% less manufacturing energy than the standard LF sheathed with OSB. This reduction can be attributed to the higher level of processing required to manufacture OSB (Kline 2006). When plywood is compared directly to OSB, the energy to manufacture plywood is less than half of the energy required to manufacture OSB (Lippke et al. 2010). Also considered equal or insignificantly different were the kiln-dried TF and the TF with LF infill (of which timbers are green, light-framing infill is kiln-dried, and sheathing is OSB). Both of these structural options required less energy than the TF with SIPs, but more energy than the traditional TF constructed with green timbers and without panel products. With insulation considered, the energy necessary for the manufacture of expanded polystyrene (foam) required more than twice the manufacturing energy of the LF structure with fiberglass batts. Note that these were the only two assemblies that included insulation. Biofuels provided 47% of the energy for manufacturing, followed by diesel fuel (16%), feedstock (15%), natural gas (14%), and hydroelectric power (10%). These values are part of the energy consumption results generated by AIE.

Construction energy varied only slightly among building assemblies, and for many comparisons the difference is less than 15% and therefore considered insignificant. The energy required to construct the standard LF remains comparatively equivalent when stud size is decreased to 38-mm x 89-mm (2-in x 4-in). When plywood is substituted for OSB for siding and roofing, however, construction energy requirements increase by 29%. Here it must be noted that the total energy comparison for these assemblies (standard LF, and LF with plywood) still favors sheathing the LF with plywood. Construction energy requirements for the TF design options were all within 15% difference. Since the TF structures weigh more than the LF structures, they required more energy consumption for construction. The traditional TF structure consumed 40% more energy than the standard LF structure. It should be noted that moisture content (green versus kiln-dried) does not affect the assumed weight of wood products within AIE, which assumes kiln-dried weight, and therefore it is likely that a green TF would require significantly more energy for construction than reported. The calculation for construction energy by AIE is based on the energy necessary to lift the mass of construction materials to one half the height of the building with a crane (ASMI 2012a). For this reason, the source of construction energy is primarily diesel fuel. Transportation from the manufacturing site to the construction site is included, and also consumes diesel fuel.

Cradle-to-gate total energy for the traditional TF structure consumed the least amount of energy. The addition of further-processed materials such as OSB or kiln-dried lumber, however, increased the energy requirement, as did the increased weight of the structural assembly. The kiln-dried TF and TF utilizing light-framing infill required 38% and 62% more energy (total) than the traditional TF, respectively. Though the TF options generally required less energy to create than the light-framing options, this was only true for the TF structures that were not constructed with SIPs. Sheathing the TF in SIPs increased the energy consumption requirement of the traditional TF (sheathed in less processed kiln-dried sawn lumber products) to more than double, even without the consideration of expanded polystyrene. The standard LF consumed 40% more energy (total) than the traditional TF, however other TF options, such as the TF with light-framing infill, were similar to light-framing options in total energy consumed. Considering the addition of insulation, the standard LF outperformed the TF with SIPs, consuming only approximately half of its total requirement of energy.

Fossil Fuel Consumption

Fossil fuel consumption represents fuel utilized for energy in resources extraction, manufacturing, and construction, whether used directly (e.g. as diesel fuel) or for the production of electricity. Fossil fuels are also used as feedstock ingredients necessary for some product manufacturing, namely insulation and adhesives in this study. Figure 2.8 shows the LCIA results for fossil fuel consumption for all LF and TF structures considered in this EIA.

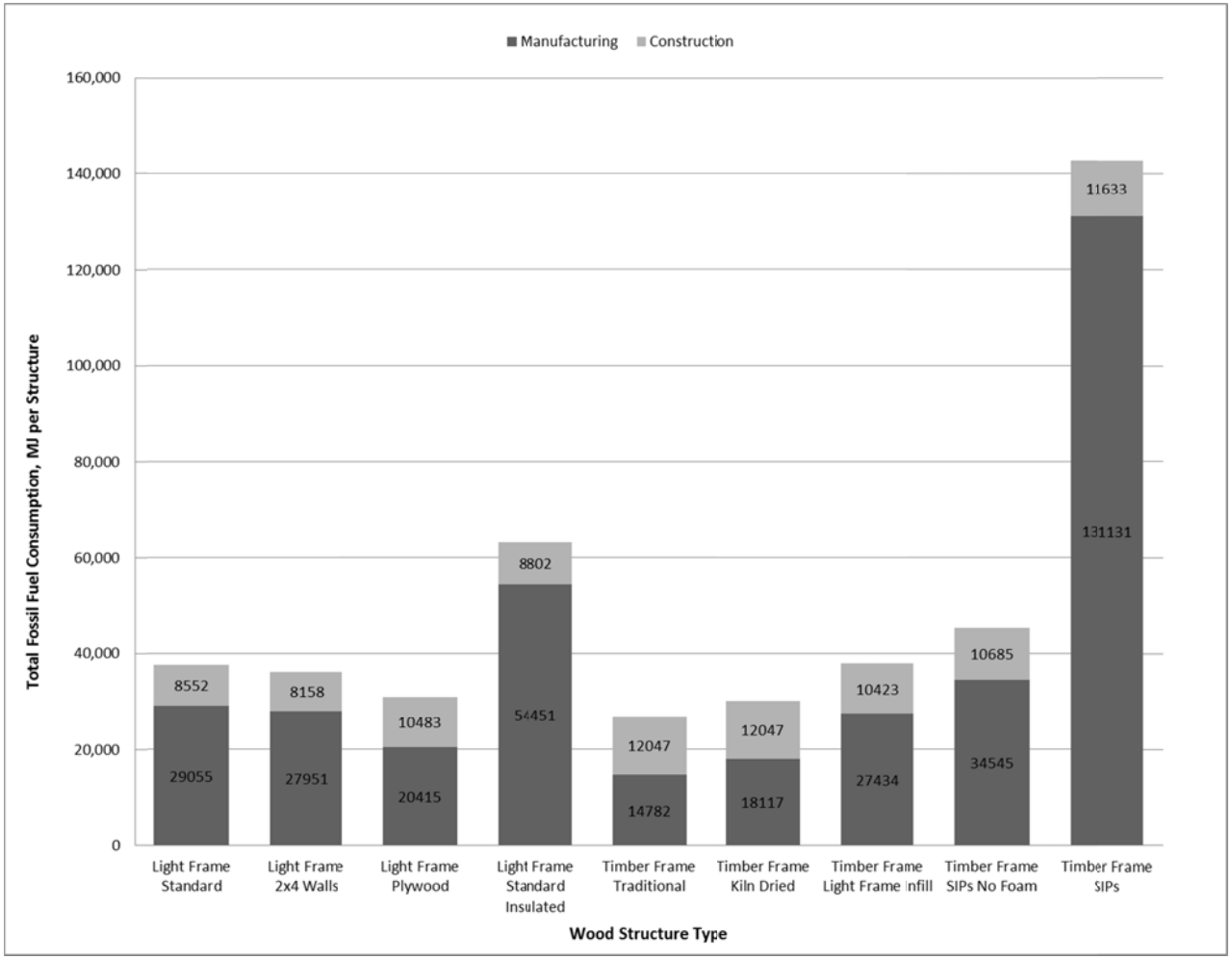

Figure 2.8: Total fossil fuel consumption from cradle to construction gate for timber frame and light-frame structures and their alternatives

Total fossil fuel consumption was also dominated by the manufacturing life-cycle stage. Due to the use of biofuels, namely hog fuel (wood waste) used on-site by wood product manufacturers for heat generation, fossil fuel consumption levels were considerably lower than total energy consumption values. Over half (58-60%) of the total energy required to manufacture kiln-dried softwoods (and hardwoods) in the Northeast and North Central USA is generated by burning wood biomass (Puettmann et al. 2010). This difference, however, is evident only in the manufacturing life-cycle stage because construction energy is provided primarily by diesel. Manufacturing fossil fuel consumption increases with increased kiln drying, and this is apparent by an increase of 23% of fossil fuels necessary for the manufacture of the kiln-dried TF. It is important to note that though this comparison is valid for current typical Northeastern mills, biofuels contribute a large amount of energy to the drying process and their increased or decreased utilization can cause this percentage to vary considerably. Fossil fuel consumption increase is more prevalent, however, for structures constructed with more processed wood products that require resins and further mechanical processing such as chipping or pressing. The LF structure sheathed with OSB (standard LF) requires 37% more fossil fuels for manufacturing than the LF sheathed with plywood. Manufacturing requires electricity, and fossil fuels are the primary source of off-site electricity in the Northeast (Puettmann et al. 2010). Coal represents 59% of off-site electricity, 11% by burning natural gas, and a small percentage is provided by petroleum. Non-fossil fuel sources of electricity include nuclear (25%) and hydroelectric (3%), and renewable energy accounts for less than 2% (Bergman and Bowe et al. 2010). Off-site electricity for the production of kiln-dried softwood in the Northeast, for example, comprises 85% of total electrical energy required for production (Bergman and Bowe 2010). The difference in fossil fuel consumption between the manufacture of the standard LF structure with 38-mm x 140-mm (nominal 2-in x 4-in) wall framing and the LF structure with 38-mm x 89-mm (nominal 2-in x 4-in) wall framing is insignificant, results showing a decrease of only 5%, respectively. Since expanded polystyrene is a petroleum product and requires a significant energy contribution, its introduction to the TF sheathed with SIPs increases fossil fuel consumption drastically. Comparatively, fiberglass batts introduced to the LF double the fossil fuel consumption of the standard LF, though still consuming less fossil fuel than the expanded polystyrene.

Fossil fuel use accounts for nearly 100% of the energy consumption required for the construction of each structure. The construction life-cycle stage is dominated by the use of diesel fuel on-site to assemble the structure with a crane, as well the diesel fuel required for material

transportation from the manufacturing site to the construction site. Travel distance is assumed by AIE, and is based on average distances from manufacturing sites to construction sites in the region. Since these differences are based on building weight (transportation distances assumed equal by AIE), heavier structures require the consumption of more fossil fuels during construction. Notable observations for the fossil fuel consumption for construction include an increase of 29% when plywood is used rather than OSB for the LF (LF with plywood vs. standard LF, respectively). Additionally, the traditional TF requires significantly more fossil fuel for its construction than any LF option since it is a heavier structure. Specifically, the traditional TF structure requires 23% more fossil fuels to construct than the standard LF structure. As noted previously, AIE does not account for the increased weight of a green wood product over a kiln-dried wood product, and therefore a difference in fossil fuel consumption between the traditional TF structure and the kiln-dried TF is not notable here. For this same reason, it is likely that the gap between the amount of fossil fuel consumed constructing the traditional TF and the standard LF is even greater. Adding to this likelihood is the fact that though a crane is commonly employed for the erection of a TF structure, this is rarely necessary when constructing an LF (Allen and Thallon 2011).

Fossil fuel sources account for slightly over half of the total energy required for the manufacturing and construction life-cycle stages for most structures analyzed. Considering fossil fuel consumption as an important factor when evaluating the environmental impact of a wood structure, the traditional TF structure constructed of green timbers and less-processed sheathing materials performs most favorably. Comparing this structure to the kiln-dried TF option shows that kiln drying (alone) increases fossil fuel consumption by an insignificant amount. This is due to the large percentage of biofuels used to generate energy during manufacturing (Puettmann et al. 2010). Constructing the TF with light-framing infill, however, increases fossil fuel consumption by 41% over the traditional TF, yet this assembly still out-performs the standard LF structure. Constructing the standard LF requires an increase in fossil fuel consumption of 40 % over the traditional TF. Replacing the OSB of the standard LF with plywood, however, provides a decrease of 18% in fossil fuel consumption, and brings the LF to a fossil fuel consumption level equivalent to both the traditional and the kiln-dried TF options. The wooden structural system that requires the highest consumption of fossil fuels is the TF sheathed with SIPs, and when the expanded polystyrene foam is considered this requirement increases drastically. The TF sheathed with SIPs (no insulation considered) requires double the fossil fuel consumption than the

traditional TF. Considering insulation, the TF with SIPs requires more than twice the fossil fuel consumption of the LF insulated with fiberglass batts.

Global Warming Potential and Carbon Stored in Wood

GWP is widely recognized as an important indicator of overall environmental impact. This value represents the total emissions of gasses that are known to contribute to global temperature increase. Since increased atmospheric concentration of CO_2 is considered to be the primary anthropogenic cause of global temperature increase, GWP is reported in kilograms (kg) of equivalent CO_2 emissions. Though CO_2 is considered the primary contributor to global warming (largely from the combustion of fossil fuels), other gaseous emissions including water vapor and methane also contribute to this phenomenon. These compounds are collectively referred to as greenhouse gasses, and since each contributor has a different effect on the atmosphere, GWP is normalized to values equivalent to CO_2 for reporting purposes (Florides and Christodoulides 2008).

Figure 2.9 depicts the total emission of greenhouse gasses from manufacturing and construction for each structure, represented as equivalent emissions of CO_2. These emissions are caused primarily by the burning of fossil fuels for logging, transportation, sawmill and construction site operations, and manufacturing processes. Emissions from biofuels are considered carbon neutral and therefore are not represented in either graph. Values for the carbon stored in wood products that comprise each structure are also not represented by this graph.

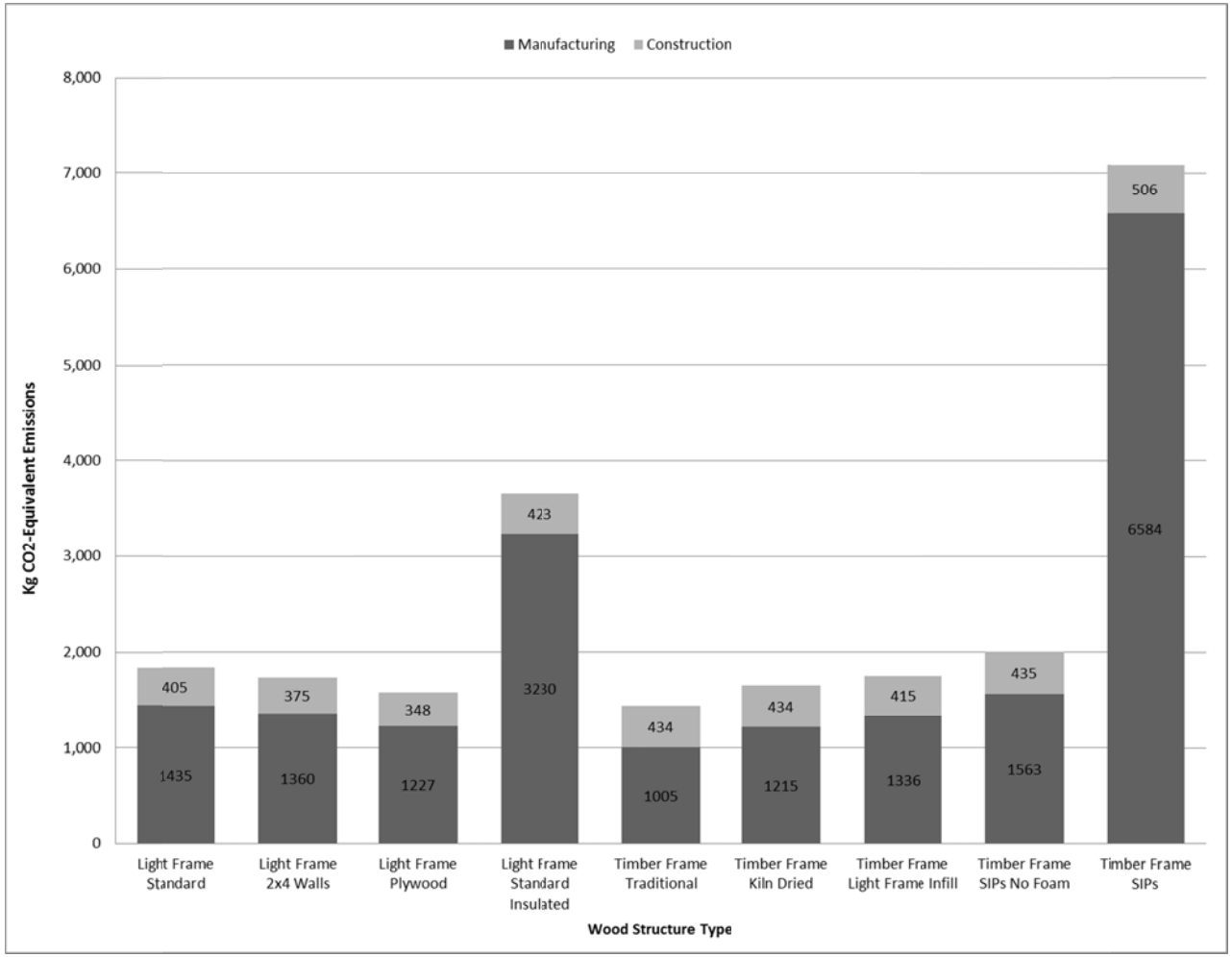

Figure 2.9: Global warming potential (GWP) from cradle to construction gate for timber frame and light-frame structures and their alternatives

GWP emissions for each structure analyzed are affected most by the manufacturing life-cycle stage. Not considering insulation options, manufacturing emissions range from 1,000 kg (2,210 lb) CO_2-equivalent released for the manufacture of the products that comprise the traditional TF structure, to 1,560 kg (3,440 lb) CO_2-equivalent for the manufacture of the products in the TF with SIPs. Among TF options, this value increased with added material processing. Utilizing kiln-dried material for framing and flooring materials increased GWP by 21% over the traditional TF structure. Likewise, manufacturing GWP for the TF with light-framing infill and OSB siding was 33% greater than the traditional TF. Steadily increasing with increased use of OSB, the TF with SIPs generated 56% more GWP than the traditional TF. Comparing LF options to TF options, it is not evident which framing system outperforms as a whole. Though the standard LF structure caused 43% more GWP than the traditional TF structure, other LF options performed more favorable than some TF options. Of notable interest is the LF sheathed in plywood, which has nearly the exact same GWP affect as the kiln-dried TF. Among light-framing options, the frame sheathed in plywood produced the lowest GWP. (Though the GWP of the LF sheathed with plywood is only 15% less than the GWP of the standard LF, and therefore considered to be of equal or insignificant difference by Athena, it is still considered to have the lowest effect among LF options). This value was still, however, 22% greater than the lowest GWP value from the traditional TF. Considering insulation, the addition of expanded polystyrene to the TF with SIPs quadrupled its GWP. This structural option also produced two times the GWP of the standard LF sheathed with fiberglass batt insulation.

GWP generated during the construction phase represented approximately 1/3 of the total GWP for most structural assemblies, and is attributed to the burning of fossil fuels (diesel) for transportation and construction site operations. These calculations are based on transportation distances (which are assumed equal for all structures) and weight of materials. For this reason, the LF sheathed in plywood performed most favorably at 350 kg (770 lb) CO_2-equivalent, and the traditional (or kiln-dried) TF options produced the highest GWP at 430 kg (960 lb) CO_2-equivalent. Many construction GWP comparisons are considered to be of equal or insignificant difference (ASMI 2012a).

Table 2.3 shows GWP emissions and carbon stored. Emission values are those generated by AIE and account for the total release of greenhouse gasses to the atmosphere from manufacturing and construction. Values for carbon stored represent a calculated sum of carbon in the wood products that comprise each structure. Wood fiber is comprised of approximately 50%

carbon by weight, and was stored throughout the tree's life by photosynthesis. Since these structures store carbon indefinitely as long as their wood products do not break down (burn, decay), and the life of a structure is on the order of decades or more, it is appropriate to present these stored values alongside the values for carbon emitted to the atmosphere. Note that the values for carbon stored in each structure have been converted to CO_2-equivalent to facilitate comparison.

Table 2.3: Global warming potential compared with carbon stored in wood products

Framing System		Emissions (Kg CO_2-Equivalent)			Carbon Stored in Wood Products (Kg)
		Manufacturing	Construction	Total Emissions	
Light Frame	Standard	1,402	398	1,800	16,340
	2x4 Walls	1,327	377	1,704	16,807
	Plywood	1,204	352	1,556	14,100
	Standard Insulated	3,198	416	3,614	16,340
Timber Frame	Traditional	1,037	462	1,499	24,245
	Kiln Dried	1,261	462	1,723	24,245
	Light Frame Infill	1,343	436	1,779	21,656
	SIPs (No Foam)	1,755	498	2,253	19,773
	SIPs (No Foam)	6,773	570	7,343	19,772

The amount of carbon stored in each structure is inherently tied to the total weight of the wood products utilized. For this reason, a structure that utilizes a higher total weight of wood products stores more carbon. The traditional TF structure stores 36% more carbon than the standard LF structure, which indicates that the sum of the weight of its wood products is 36% greater. Though TF structures have been accused of being wasteful of wood fiber, the increased "permanent" storage of carbon in these materials is favorable in this regard (Allen and Thallon 2011). Among most TF options there is very little difference in the amount of carbon stored, however carbon stores for the TF with SIPs are 10% lower than the traditional TF. LF options also show a similar level of carbon stores to one another. Of notable difference from the standard LF is the LF sheathed in plywood, which stores 11% less carbon. Calculations for the inclusion of insulation are not applicable because neither of the types of insulation considered are derived from wood fiber. Note that since these values were hand-calculated based on the actual volumes of wood products in each structure (not generated by AIE), their comparative results are not subject to the same assumption that a value of 15% difference or less is of equal or insignificant difference.

Values for the quantity of carbon stored were considerably greater than the total GWP emissions produced by the manufacturing and construction life-cycle stages, as reported by AIE. Since the emissions and stores of bioenergy materials are not included (and are considered to be carbon neutral), these values are not reported as a total sum of carbon stores and emissions. Results show that for the construction of any of the structural assemblies considered (even including insulation), the final product is carbon-negative. Values for carbon storage range from 9 times greater than carbon emitted for the LF sheathed in plywood, to 15 times greater for the traditional TF. Overall, TF structures have a lower cumulative impact on GWP when carbon stores are considered. The higher the total weight of wood products drives carbon stores up, and the lower the amount of manufacturing energy (particularly manufacturing energy generated by the combustion of fossil fuels), the lower the carbon emissions. The amount of wood fiber utilized has the greatest impact on this overall result.

Wood fiber Use and Waste

Wood fiber use refers to the total raw wood material necessary to create the wood products used for the construction of each structural system, as well as the material burned for the production of heat and electricity as biofuel utilized in the manufacturing process (ASMI 2012a).

Wood fiber use and waste are reported in kilograms of material on an oven-dry basis. AIE does not attribute any wood fiber use to the construction life-cycle stage, since all wood fiber is initially used in manufacturing, and therefore all results indicate wood fiber use during manufacturing only (ASMI 2012a). Note that the results reflect each structural assembly's bill of materials, and include the manufacture of all materials purchased, some of which become on-site material waste (cut-offs, sawdust, etc.). Wood fiber waste includes the portion of wood fiber use from manufacturing that is not ultimately part of the final wood product (lost as sawdust, woodchips, etc.). Construction site waste or wood fiber burned for biofuel are not included here as wood fiber waste. Figure 2.10 and Figure 2.11 show the LCIA results for wood fiber use and wood fiber waste, respectively, for all LF and TF structures considered in this EIA.

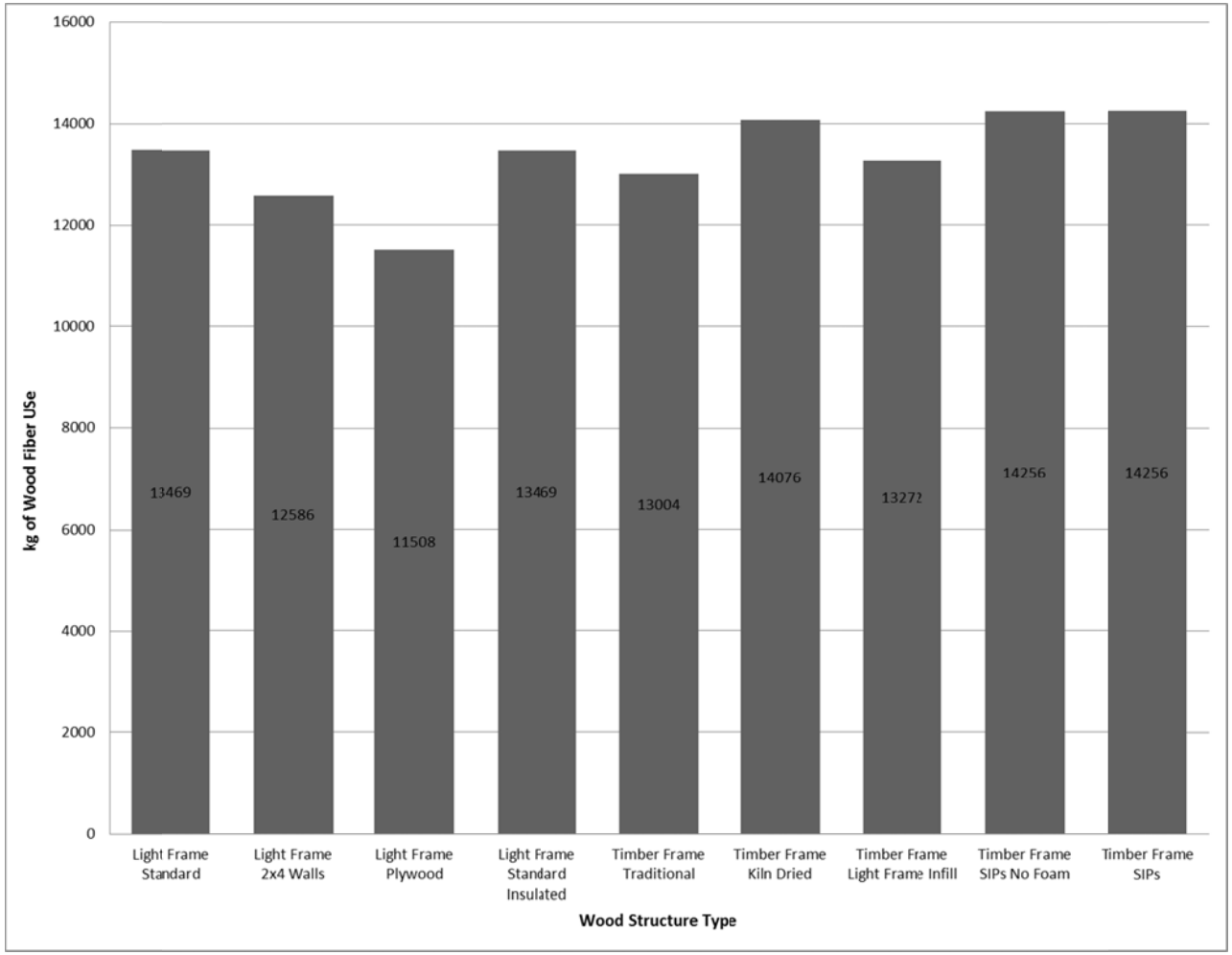

Figure 2.10: Wood fiber use from manufacturing from cradle to construction gate for timber frame and light frame structures and their alternatives

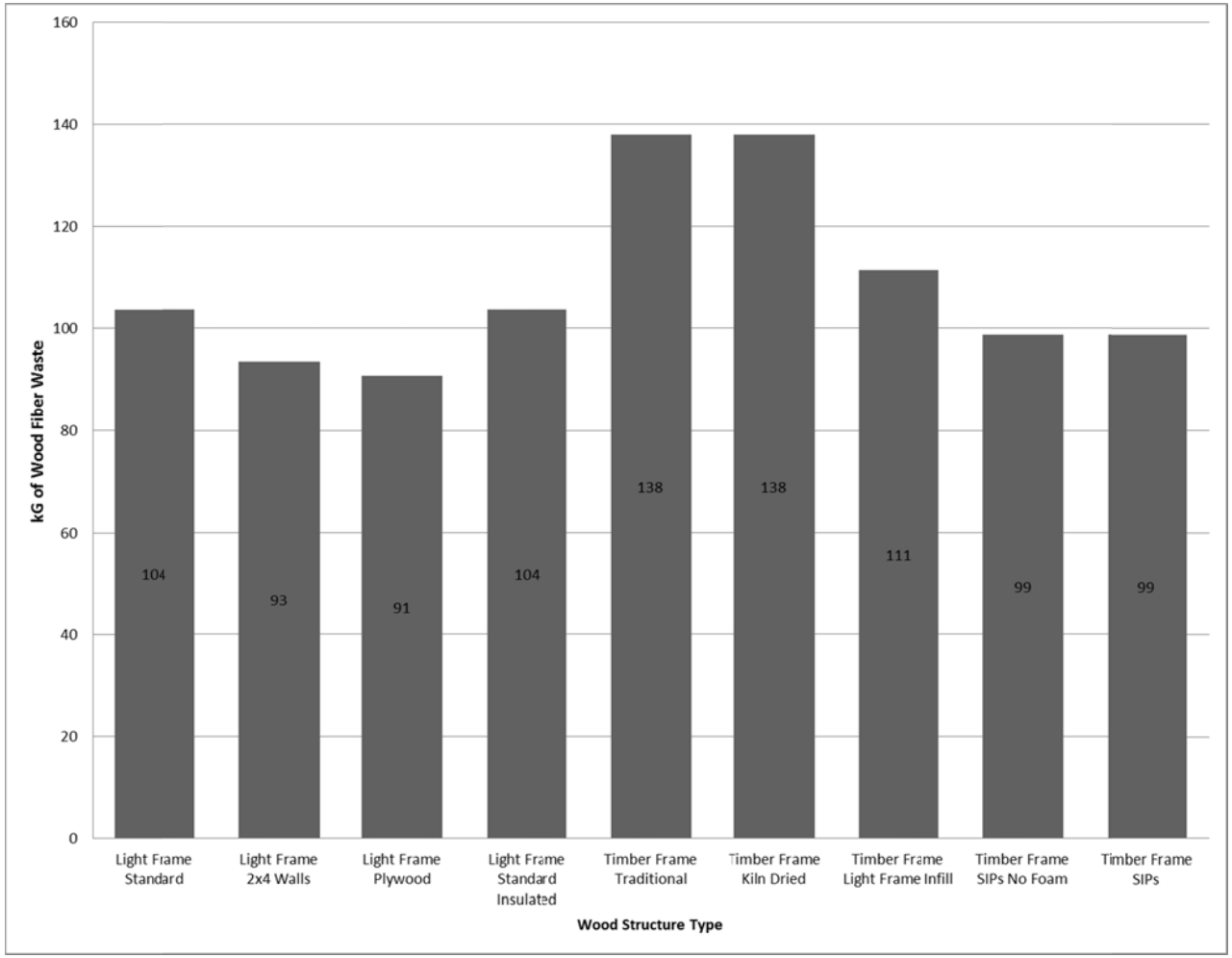

Figure 2.11: Wood fiber waste from manufacturing from cradle to construction gate for timber frame and light-frame structures and their alternatives

Results for wood fiber use are reported in kilograms of wood fiber. Values range from 11,500 kg (25,300 lb) for the LF sheathed with plywood to 14,300 (31,400 lb) for the TF with SIPs. Wood fiber utilization among TF options differ within a range considered equal or insignificant difference. Similarly, LF structures were comparable, and many LF structures were comparable with TF options. Of notable difference among light-framing options is the LF sheathed in plywood, which requires 17% less wood fiber than the standard LF (sheathed with OSB). The difference between the standard LF structure and the traditional TF structure is insignificant. It should be noted, however, that the apparent increase in wood fiber use from the traditional TF to the kiln-dried TF indicates wood fiber burned for heat and energy required for the kiln drying process. This comparison, however, is technically insignificant, showing an increase of only 8% (attributed to biofuel material). Wood fiber use for the traditional TF and the TF constructed with light-framing infill are equivalent. Overall, wood fiber use appears to be higher among structural systems comprised of less-processed materials.

Wood fiber waste, also represented in kilograms of wood fiber, ranges from 0.7 to 1.1% of total wood fiber use. Lower percentages of wood fiber waste are prevalent in results from both the LF structure with walls framed with 38-mm x 89-mm (2-in x 4-in) material, as well as with the TF with SIPs. The highest percentage of wood fiber waste of wood fiber use is from the traditional TF. Specific values for wood fiber waste range from 91 kg (200 lb) for the LF sheathed with plywood to 140 kg (300 lb) for the traditional TF. Though wood fiber waste does not vary significantly among most structural options analyzed, of interest is a comparison between the standard LF structure (sheathed with OSB) and the same structure sheathed in plywood (LF with plywood). The LF structure with plywood wastes 14% less wood fiber than the LF structure with OSB. This implies (non-conclusively since this comparison shows less than a 15% difference) a more efficient use of wood fiber when manufacturing plywood as compared to manufacturing OSB. Additionally, systems requiring larger cross-section solid-sawn materials appear to waste more wood fiber than some light-framing options.

For specific results discussed but not reported here, or for further LCIA results, please see Appendix H of Malone (2013).

CONCLUSIONS

It is widely recognized that the energy demands and environmental emissions associated with the construction industry are of considerable proportion. For this reason it is important for designers to make informed decisions with the environment in mind. LCA is a tool to aid this decision process which analyzes all environmental inputs and outputs associated with the life-cycle of some product, assembly of products, or process. An LCI is created that catalogues these inputs and outputs, and an LCIA is performed to produce results based on specific environmental burdens of concern, and these results are interpreted based on calculated evidence of environmental impact. This study was considered an environmental impact assessment that utilizes LCA methodology, differentiated from a true LCA with respect to the fact that some data are not traceable through use of AIE.

Two wood structural systems were designed, a light frame (LF) and a timber frame (TF), and several material substitutions were considered for each. A cradle-to-gate environmental impact assessment was performed on each structural assembly based on LCA methodology with the aid of AIE for Buildings software. These structures were analyzed based on total energy consumption, fossil fuel consumption, global warming potential (GWP), and wood fiber use and waste. Quantities for structural assembly materials were catalogued (bill of materials), and AIE provided LCI and LCIA results. Results and conclusions were determined based on these results, as well as reports filed by CORRIM.

LCIA results for fossil fuel consumption represent some portion of total energy use. (Note that some percentage of fossil fuel use is attributed to feedstock). Additionally, GWP is closely tied to fossil fuel consumption since the combustion of fossil fuels is the primary contributor of greenhouse gas emissions. GWP can then be compared directly with the quantifiable amount of carbon stored in wood products, and therefore wood fiber use directly affects cumulative GWP. Considering these interactions and LCIA results, the traditional TF structure (constructed of green framing material and less-processed sheathing materials) performed most favorably with respect to environmental impact. It requires the lowest amount of total energy input for manufacturing and construction, as well as the lowest level of fossil fuel consumption. Additionally, the traditional TF had the least net impact on GWP, a result of less-processed materials and high carbon storage.

The environmental impact of other structural systems analyzed varied with respect to choice of materials. These materials varied in this regard based on manufacturing requirements and weight. The use of products requiring a significant amount of mechanical processing (chipping, pressing, etc.), such as OSB, contributed to increased energy consumption, as well as fossil fuel consumption, and therefore GWP. This is true for the use of plywood as well, though increases were not as dramatic. For this reason, analysis of the environmental impact of the TF with SIPs (which requires two layers of OSB) resulted in the highest environmental impact. Considering insulation, impacts increased dramatically, and were still more environmentally damaging than the LF insulated with fiberglass batts. The necessity to provide energy for heat in the drying process was also a contributor to negative environmental impacts. Quantities of wood fiber used do not correspond directly with other environmental impacts. It can therefore be concluded that environmental impact is driven primarily by product manufacturing requirements, and the amount of wood in a structure is no implication of negative environmental impact as compared here. Ultimately, it is the source from which energy is generated that has the greatest impact on environmental impact. Further development and utilization of non-fossil fuel-based energy sources will have the greatest effect on mitigating these environmental burdens.

FUTURE RESEARCH

The necessity to make decisions based on an accurate assessment of wood structural systems and materials is clear. Decisions made possible based on this research, however, are limited. Since only the manufacturing and construction phases lie within the scope of this study, the environmental effects of the life of these structures have not been considered. It is widely recognized that heating and cooling are the most contributing operations to a building's overall negative environmental impact, and so the operational life-cycle stage must also be examined. This will require extending this research beyond that of only the structural system to include a complete building envelope. For this reason, future research is necessary to capture a complete picture of each structure's effect on our planet for informed decision-making purposes.

ACKNOWLEDGMENTS

It is recognized that previous LCA-related research performed by all CORRIM contributors to quantify the environmental effects of wood products is what made this study a reality. Technical assistance by Grant Finlayson of the Athena Institute was also an important contribution. Guidance with LCA methodology in the early stages of this research provided by

Arijit Sinha is greatly appreciated. Finally, funding and support from the Wood Science and Engineering Department and School of Civil and Construction Engineering Oregon State University made this research possible.

References

AF&PA (2005). *National Design Specification for Wood Construction (NDS).* ANSI/AF&PA NDS-2005. Washington, DC.

Allen, E., and Thallon, R. (2011). *Fundamentals of Residential Construction*. 3rd ed. Hoboken: John Wiley & Sons, 2011.

APA – The Engineered Wood Association (2012). *Panel Design Specification*. The Engineered Wood Association. Tacoma, WA.

Athena Sustainable Materials Institute (ASMI) (2012a). Athena Impact Estimator for Buildings V 4.2 Software and Database Overview. Toronto, Ontario.

Athena Sustainable Materials Institute (ASMI) (2012b). Athena Impact Estimator for Buildings. Version 4.2 Build 01 Hotfix. Athena, 2012.

Bare, J. (2012). "TRACI 2.0: The tool for the reduction and assessment of chemical and other environmental impacts 2.0." *Clean Technologies and Environmental Policy*, 13(5), 687-696.

Bergman, R.D., and Bowe, S.A. (2010). "Environmental Impact of Manufacturing Softwood Lumber in Northeastern and North Central United States." *Wood and Fiber Science*, 42, 76-78.

Blue Ridge Timberwrights (BRT). 2010. "A History of Timber Framing." 15, April 2013. *<http://brtw.com/historyoftimberframing.php>*

Consortium for Research on Renewable Industrial Materials (CORRIM). 2013. "Life-cycle Inventory & Life-cycle Assessment."15, April 2013. < http://www.corrim.org/research/lci_lca.asp>

Finlayson, G. "Re: Query from contact us page." Inquiries to Grant Finlayson of Athena. Jan. 24, 2013. E-mail.

Florides, G.A., and Christodoulides, P. (2008). "Global warming and carbon dioxide through sciences." *Environment International*, 35, 390-401.

Google Sketch-Up Pro. Version 8.0.15158. Google, Mountain View, CA, 2012.

ICC – International Code Council (2009). International Residential Code for One- and Two-Family Dwellings – 2009. Country Club Hills, IL.

ICC – International Code Council (2011). International Building Code - 2012. Country Club Hills, IL.

ISO 14040 (2006): Environmental management – Life-cycle assessment – Principles and framework, International Organization for Standardization (ISO), Genève.

Kline, D. Earl. (2005). "Gate-To-Gate Life-Cycle Inventory of Oriented Strandboard Production." *Wood and Fiber Science*, 37, 74-84.

Lamlom, S.H., and Savidge, R.A. (2003). "A Reassessment of Carbon Content in Wood: Variation Within and Between 41 North American Species." *Biomass & Bioenergy*, 25, 381-388.

Lippke, B., and Wilson, J.B. (2010). "Introduction to Special Issue: Extending the Findings on the Environmental Performance of Wood Building Materials." *Wood and Fiber Science*, 42, 1-4.

Lippke, B., Wilson, J., Meil, J., Taylor, A. (2010). "Characterizing the Importance of Carbon Stored in Wood Products." *Wood and Fiber Science*, 42, 5-14.

Malone, B.P. (2013). "LF Versus Traditional TF: A Study in Comparing the Differences." M.S Thesis, Oregon State University, Corvallis, OR.

Martin, Z., Skaggs, T.D., Keith, E.L., Yeh, B. (2008). "Principles of Mechanics Model for Wood Structural Panel Portal Frames." *Proceedings of the 2008 Structures Congress - Structures 2008: Crossing Borders*, 314.

National Renewable Energy Laboratory (NREL). 2012. "U.S. Life-cycle Database." http://www.nrel.gov/lci/ (April 15, 2013).

Puettmann, M., Bergman, R., Hubbard, S., Johnson, L., Lippke, L., Oneil, E., Wagner, F.G. (2010). "Cradle-to-Gate Life-Cycle Inventory of US Wood Products Production: CORRIM Phase I and Phase II Products." *Wood and Fiber Science*, 42, 15-28.

TFEC (2010). *Standard for Design of TF Structures and Commentary*. TF Engineering Council. Becket, MA.

MANUSCRIPT: STRUCTURAL LOAD PATH ANALYSIS OF LIGHT-FRAME AND TIMBER FRAME BUILDINGS

Brian P. Malone, Thomas H. Miller, and Rakesh Gupta

American Society of Civil Engineers
Journal of Performance of Constructed Facilities

ASCE Journal Services
1801 Alexander Bell Drive
Reston, VA 20191

Submitted 2013

ABSTRACT

The objective of this study was to compare structural load path and system behavior of a light-frame (LF) and a timber frame (TF) structure. This load path analysis is part of a research effort that compares LF to TF residential structures, and was performed simultaneously with an environmental impact assessment. SAP2000 structural analysis software was used to create a model of each structure. The TF structure was composed of large-dimension timbers and structural insulated panels (SIPs). An equivalent LF structure was designed for comparison, following the guidelines of the International Residential Code. Results show that the TF outperforms the LF in resisting uplift, as well as in story drift. The TF also provides load paths that are less sensitive to the introduction to large openings and the loss of a central post. Observed axial loads in posts show smaller ranges compared to LF studs.

INTRODUCTION

Investigations on structural load path and system behavior of light-frame (LF) wooden structural systems have been performed in the wake of poor performance of these buildings when subject to extreme weather events (such as hurricanes and tornados) (van de Lindt et al. 2007, Prevatt et al. 2012). Recent studies have involved the development of modeling techniques based on experimental results from partial or full-scale testing (Doudak 2005, Martin et al. 2011, Pfretzschner et al. 2013). Wood LF structures comprise the majority of residential structures in the US (Allen and Thallon 2011), yet have proven to be particularly vulnerable to high wind-induced damage (van de Lindt et al. 2007). Where there is room to improve, computer modeling of these structures can aid designers and builders in predicting performance and therefore in making more informed design decisions for safety and durability.

Prior to the introduction of light-framing practices, wood frames were constructed from large-dimension timber, connected by mortise-and-tenon-style joinery and fastened with wooden pins, a structural system known as a timber frame (TF). Today, timber framing has evolved from its traditional roots to offer a modern product, an alternative to light framing that is worth investigating with respect to structural performance. In an industry where the safety of inhabitants is of utmost concern and improvements are necessary, a comparison of available structural systems can highlight the strengths and weaknesses of different structural systems for the application of this knowledge to future design and structural system selection. Though qualitative reasoning to evaluate the structural characteristics of each is valid for some decisions,

an accurate quantitative analysis of performance is the only way to arrive at conclusive results and make truly informed decisions. Structural analysis of each is necessary, and the creation of models with structural analysis software makes this possible during the design stage. Research efforts to model traditional TF structural performance have primarily focused on the behavior of mortise-and-tenon joints (Erikson and Schmidt 2003, Shanks and Walker 2009, Bulliet et al. 1999). Structural modeling of whole-system TFs, however, has not been performed and presented in the literature as for LFs. Furthermore, no modeling method has been applied to both structural systems for direct comparison.

Objectives

The main objective of this study was to create structural analysis models of a TF and an LF for structural load path comparison. This objective accompanies that of an ancillary environmental impact study to analyze the environmental burdens of wood frame structures. (For more information pertaining to this additional study, see Malone (2013)). Additionally, objectives include comparing the TF structure with the LF structure with respect to uplift, story drift, the introduction of large openings, a break in load path, and range of axial loading in vertical members (posts and studs).

Wood Structural Systems

Of the structural systems available to designers and builders, light wood framing is the most commonly existing structural system for residential buildings in the United States (US) today (Allen and Thallon 2011). Light-framing with dimensional lumber emerged in the early-to-mid-19th century and evolved as an efficient and economical wood framing system. Light framing involves 38-mm (nominal 2-in) -thick dimensional lumber generally spaced at either 406-mm or 610-mm (16-in or 24-in) on center to construct walls, flooring, and roofing. Walls, floors, and roofs are sheathed most commonly with oriented strand board (OSB). Building elements are connected with metal fasteners including nails, screws, and bolts. The design of residential LF structures is dictated (by law only where adopted) by the International Residential Code (IRC), published by the International Code Council (ICC 2009). Where design necessities exceed the limitations of the IRC, structural components must be engineered individually using the International Building Code (ICC 2011). For this purpose, the design of wood components and systems is performed according to the National Design Specification for Wood Construction (NDS) (AF&PA 2005a).

The origins of timber framing predate light framing, and define the early evolution of wood framed structures. Timber framing flourished in the settlement of America from the early 1600's to the mid-19th century, until light framing emerged and proved to be a faster method of construction that required less-refined skills (BRT 2010). Though the practice of timber framing continued overseas (due largely to the demand for maintenance of existing infrastructure), it nearly disappeared in the US until it resurfaced in the 1970's (BRT 2010). An appreciation for timber framing and the necessity to repair and maintain existing structures gave birth to a new sector of the modern wood framing industry (BRT 2010). Alongside historical restoration, today's timber framing industry represents a niche craft in the custom residential and commercial industry. Though the materials and basic methods reflect historic practices, advances in wood product manufacturing, as well as the fields of architecture and engineering in general, have advanced the traditional TF to today's modern product. Timber framing can be defined as a structural system composed of large-dimension framing members, generally 127-mm x 127-mm (nominal 5-in x 5-in) and larger that are connected with mortise-and-tenon-style wooden joinery and fastened with wooden pins (though metal fasteners are commonly used for some connections today). The engineering of TF structures is typically performed on a case-by-case basis, and design commonly relies on methods dictated by the NDS (AF&PA 2005a). Though no official code specific to TF design currently exists, the "Standard for Design of TF Structures" has been written and adopted by the Timber Frame Engineering Council, a subset of the Timber Framers Guild of North America (TFEC 2010).

METHODS AND MATERIALS

Structural System Design

Timber Frame

The TF structure designed for this study was based on an existing TF built by the primary author. This building was completed in 2011, and is located in Jay, Vermont. Figure 3.1 shows the framing system for this building.

Figure 3.1: Exposed timber frame structure in Jay, Vermont, looking south-west

The Vermont structure served as the inspiration for this study. For simplicity and generalization, it was necessary to make changes to this design (for comparison purposes in this study). Alterations to the Vermont structure include omission of the cupola and floor entry dormer (not visible in Figure 3.), as well as minor adjustments in framing member locations. Additionally, some window locations were assumed and added to the model. Structural design of the (amended) TF structure was verified with the NDS (AF&PA 2005), and member size was dictated largely by the size necessary to facilitate mortise-and-tenon-style joinery. Verification calculations show that some members, such as posts, are over-conservative, where others, such as rafters, are adequate.

The Vermont structure was constructed of solid-sawn, unseasoned (green) eastern hemlock (*Tsuga canadensis*) timbers by traditional timber framing methods. All joinery was mortise-and-tenon-style fastened primarily with wooden pins. The TF structure for this study was designed using the NDS (AF&PA 2005a), and follows the guidelines outlined by the Standard for Design of Timber Frame Structures (TFEC 2010). See Malone (2013) for a thorough description of the design of this structure.

Though the Vermont structure is sheathed with solid-sawn materials, the model created for this study is sheathed with SIPs due to their current popularity in industry. Figure 2 shows a rendering of this structure shown without SIPs (for clarity) (Google 2012).

The structural systems designed for this study reflect a rectangular 2-story residential building that has a 7.9-m (26-ft) x 12.2-m (40-ft) footprint, is approximately 8.0-m (26-ft, 6-in)

high at the gable, and has a 9:12-slope gable roof. The bottom story has two garage doors on one gable end, as well as a person door on one side. There are three windows on the first story, and eight on the second. This building is located in the town of Jay, Vermont. All design loads applied for this analysis are based on the requirements for this location.

Light-Frame

An equivalent LF structure was designed based on the modified Vermont TF structure. Equivalence for this design was defined as maintaining building envelope and shape, and meeting the same operational needs as the modified TF structure. Structures designed for this study reflect a typical design for each framing method, and therefore equivalence was not based on structural capacity. This structure is framed with "spruce-pine-fir" (SPF) dimensional lumber with 38-mm x 140-mm (2-in x 6-in) walls and sheathed with plywood. The design of the LF was performed in accordance with the prescriptive guidelines outlined in the 2009 IRC (ICC 2009). Where design requirements could not be met by these guidelines, necessary components of the structural system were engineered according to the NDS (AF&PA 2005a). These components include the beams that support the floor and the columns that centrally support these beams. Additionally, where available shear wall area on the gable end with garage door openings was deemed insufficient by the IRC for lateral force resistance, a moment-resisting portal frame was engineered following the guidelines published by Martin et al. (2008). Figure 3.2 also shows a rendering of the TF structure and LF structure designed for modeling in this study (Google 2012).

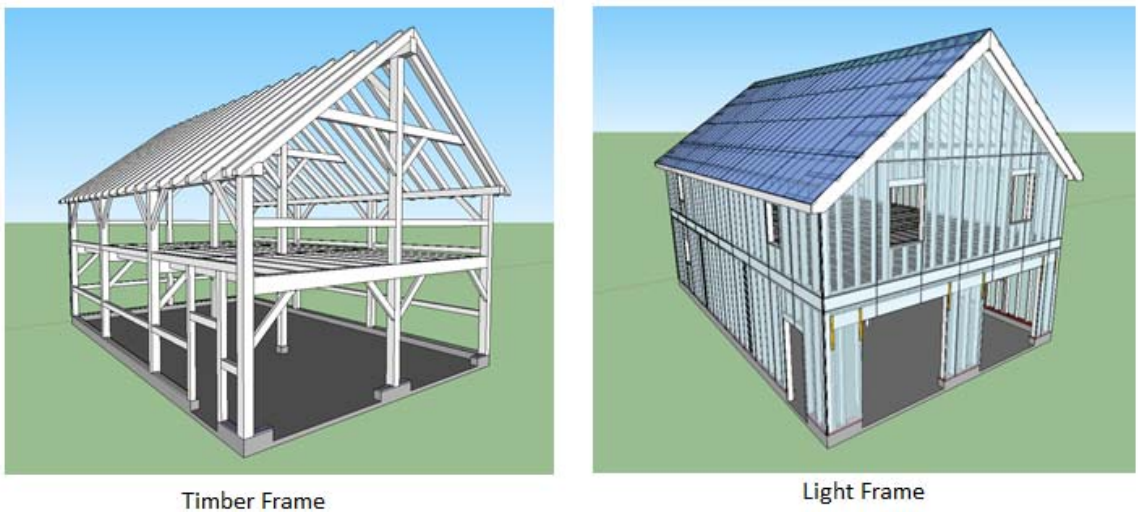

Figure 3.2: Timber frame design (without SIPs) and light-frame design

Design Loading

Design loads applied to each structure included dead, live, snow, and wind loads, and were assigned based on the location of the Jay, Vermont structure. Dead loads were assigned using material properties (weights) for frame and shell elements, and were based on species and product type. Panel product (OSB and plywood) specific gravities were provided by the APA Panel Design Specification (APA 2012) and solid-sawn material densities were based on the specific gravity (SG) on an oven-dry (OD) basis of species selected (to conservatively estimate the weights of members), and were provided by the NDS (AF&PA 2005a). Live, wind, and snow loads were applied directly to appropriate sheathing elements within the model, and lateral (wind) loads were considered from both general directions. Note that each general wind direction refers to a range of wind angle. Live loads applied to the floor of each structure were determined with ASCE 7-10, Minimum Design Loads for Buildings and Other Structures (ASCE 2010). Similarly, ASCE 7-10 was used to calculate wind loading. Wind pressures were determined using the simplified envelope procedure for low-rise buildings as outlined in part 2 of chapter 28 of ASCE 7-10 (ASCE 2010). For a detailed description of these wind loading calculations, see Appendix E of Malone (2013). Design snow loads were dictated by the town of Jay, Vermont.

Table 3.1 is an overview of all loads applied to the structures considered in this study. Figure 3.3 indicates calculated wind load assignments (wind pressures) from the general east-west and north-south directions (ASCE 2010).

Table 3.1: Load assignments for structures studied

Loading	Application	Magnitude	Unit	Based on	Source
Dead	SPF Framing	420 (26.2)	kg/m^3 (lb/ft^3)	SG = 0.42 (OD)	NDS (AF&PA 2005a)
	Eastern Hemlock Framing	420 (26.2)	kg/m^3 (lb/ft^3)	SG = 0.42 (OD)	NDS (AF&PA 2005a)
	Plywood	420 (26.2)	kg/m^3 (lb/ft^3)	SG = 0.42 (OD)	Panel Design Spec. (APA 2012)
	OSB	500 (31.2)	kg/m^3 (lb/ft^3)	SG = 0.50 (OD)	Panel Design Spec. (APA 2012)
Live	Floor Sheathing	195 (40)	kg/m^3 (lb/ft^3)	Residential	ASCE 7-10 (ASCE 2010)
Wind	Wall and Roof Sheathing	Varies	kg/m^3 (lb/ft^3)	Simplified Envelope Method	ASCE 7-10 (ASCE 2010)
Snow	Roof Sheathing	293 (60)	kg/m^3 (lb/ft^3)	Local Requirements	Town of Jay, Vermont

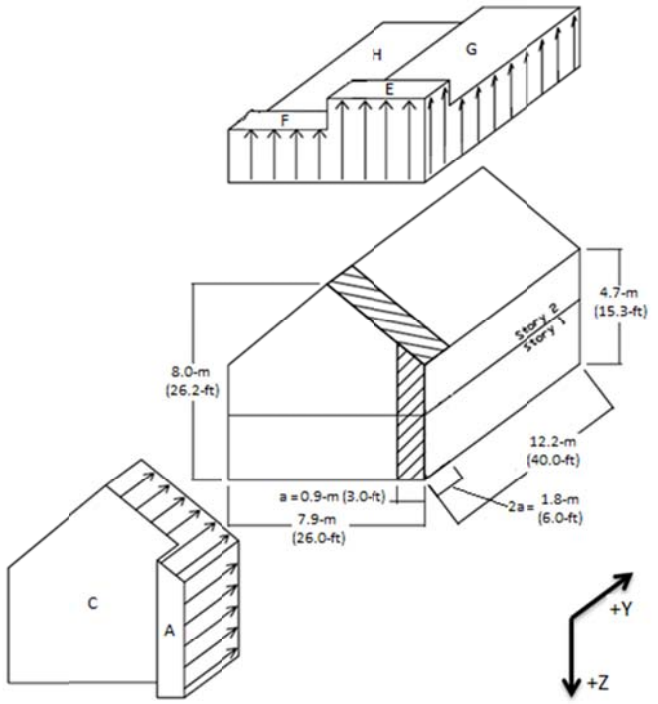

Zone	A	C	E	F	G	H	E_{OH*}	G_{OH*}
Wind Pressure kN/m^2 (lb/ft^2)	1.00 (21.0)	0.67 (13.9)	-1.21 (-25.2)	-0.68 (-14.3)	-0.84 (-17.5)	-0.53 (-11.1)	-1.30 (-27.2)	-1.69 (-35.3)

*Overhang wind pressures not shown in figure

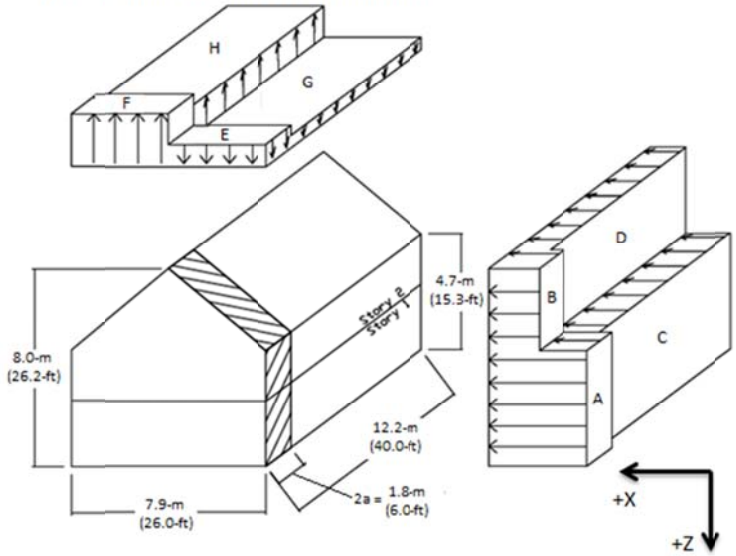

Zone	A	B	C	D	E	F	G	H	E_{OH*}	G_{OH*}
Wind Pressure kN/m^2 (lb/ft^2)	1.13 (23.6)	0.77 (16.1)	0.90 (18.8)	0.62 (12.9)	0.09 (1.8)	-0.68 (-14.3)	0.03 (0.6)	-0.59 (-12.3)	-0.46 (-9.5)	-0.40 (-8.3)

*Overhang wind pressures not shown in figure

Figure 3.3: General north-south direction wind loading (ASCE 2010)

Allowable stress design (ASD) load combinations 4, 5, and 6a (ASCE 2010), indicated below in Equations 1, 2 and 3, were chosen for the application of design loads to each structure.

Load Combination 4: $D + 0.75L + 0.75S$ **(1)**

Load Combination 5: $D + 0.6W$ **(2)**

Load Combination 6a: $D + 0.75L + 0.75(0.6W) + 0.75S$ **(3)**

Where: D = dead load, L = live load, S = snow load, and W = wind load.

These load combinations were used to observe load path and system behavior based on gravity loads only, loading considering the effects of wind and 100% of dead load only, and from the interaction of all applicable loads, respectively. Where openings did not allow direct application of these loads to sheathing, their equivalent effects on door and window framing were calculated and applied as appropriately distributed loads to these framing elements.

Modeling Methods

Modeling methods developed by Martin et al. (2011) and further developed and validated by Pfretzschner et al. (2013) were used for the creation of structural models. These methods were developed using SAP2000 software, and therefore all models in this study were created with this commercially available program (Computers and Structures, Inc. 2012). Both the TF and the LF structures were modeled with and without openings (doors, windows), referred to as "standard" and "enclosed," respectively. Figure 3.4 shows the LF structure model, depicted both completely enclosed and with openings (standard), as well as similar images of the TF structure.

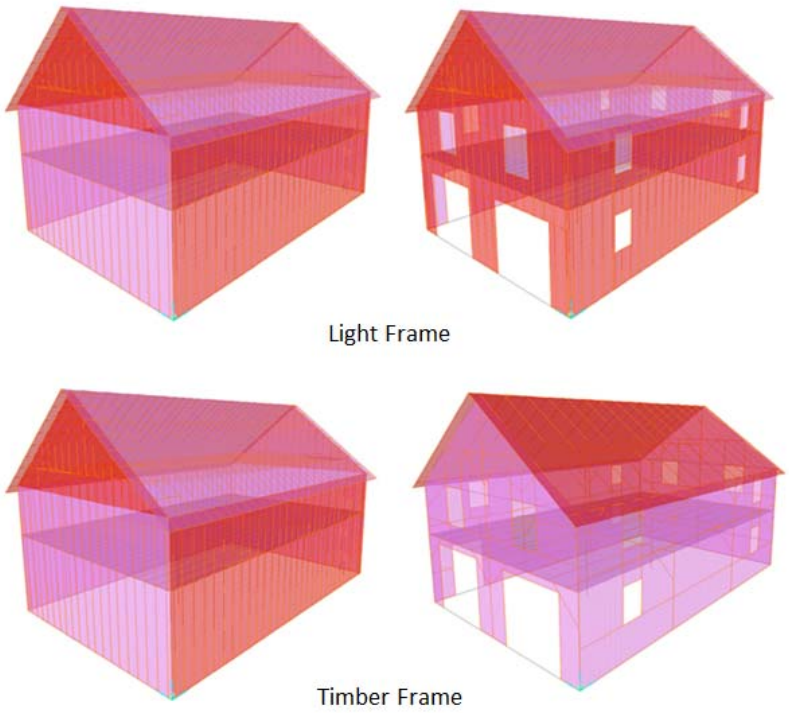

Figure 3.4: Light-frame and timber frame models, fully-enclosed and with openings

Framing Members

Framing members were modeled according to methods developed by Martin et al. (2011) and Pfretzschner et al. (2013). Framing members for both the TF and the LF were modeled using SAP2000's frame element (Computers and Structures, Inc. 2012). Framing elements of all sizes, 38-mm x 140-mm (2-in x 6-in) LF studs and 203-mm x 203-mm (8-in x 8-in) TF posts alike, were modeled similarly and assigned isotropic material properties. Multiple members framed longitudinally adjacent in the LF, such as a double top plate or a built-up post, were modeled using a single framing element with a cross-section equal to the sum of their individual cross-sections. Isotropic material properties for framing members were assigned based on those provided by the NDS (AF&PA 2005a). Properties were assigned based on species and grade selection. LF members were No.1/No.2 SPF and TF members were No.1 eastern hemlock.

Sheathing

Sheathing was also modeled according to methods developed by Martin et al. (2011) and Pfretzschner et al. (2013). Wall sheathing was modeled using SAP2000's layered shell element as one continuous shell element applied to each wall, floor, or roof. Each shell element was then

meshed into approximately 8-in x 8-in sections. Wall shell elements were modeled through the center of wall framing members (LF studs or TF posts), and assigned an offset from this center line to the appropriate location on the outside surface of the wall. Similarly, floor and roof sheathing were modeled through the center of joists and rafters, respectively, and displaced to their correct location in the assembly as well. LF plywood was modeled as a single shell element on each surface, and assigned its appropriate thickness. SIPs were modeled as two layers of OSB sheathing with thickness assigned, and each layer was offset to its respective location. Expanded polystyrene (isolative foam) in SIPs was not modeled.

Similar to Pfretzschner et al. (2013), LF plywood sheathing properties, including moduli of elasticity (MOE) and Poisson's ratios for both in-plane and out-of-plane behavior, were calculated using Nairn's (2007) OSULaminates software. In-plane and out-of-plane sheathing MOE values for OSB for the TF SIPs were determined based on values provided in the Panel Design Specification (APA 2012). Poisson's ratios assigned to OSB were based on the findings of research performed by Thomas (2003). Stiffness values (G_{12}) for sheathing products were determined by G_{12} calibration, as explained below. Material properties for sheathing elements were assigned as in-plane or out-of-plane values, based on lateral loading direction. Note that for gravity loading only, wall sheathing is considered to act in-plane, and diaphragms (roof and floor) are considered to act out-of-plane.

Framing Connectivity

With the exception of the connections at rafter peaks for the LF structure, all framing connections for both structures were modeled as "pinned." Where the design calls for gusset plates at the aforementioned location on the LF only, connections were modeled as "rigid."

Sheathing Stiffness (G_{12}) Adjustment

To model the in-plane shear stiffness (G_{12}) of shear walls and diaphragms (roof and floor), which includes accounting for the effects of edge nail spacing of sheathing, calibrations were performed against known or calculated displacements. The procedure outlined in Pfretzschner et al. (2013), similar to the "correlation procedure" used by Martin et al. (2011) was used to determine the shear modulus (G_{12}) for the LF plywood sheathing. For each wall, roof, or floor of the LF structure, the G_{12} value for the sheathing material of a simple calibration model created in SAP2000 was adjusted until its deflection matched that calculated by equation C4.3.2-2 in the Wind and Seismic supplement to the NDS (AF&PA 2005b). Calibration models matched

the height and length of each TF wall, and one was created for each story of each side wall and gable-end. Each model reflected a wall with no openings, sheathed on one side. Framing and sheathing were modeled with identical methods to those presented above. Material properties for the calibration model matched those for plywood as determined by Nairn's (2007) OSULaminates software. The effects of anchor bolts and hold downs were omitted from these calibrations (and all others) by defining all supports in the calibration model as rigid. These foundation connections were incorporated into the structural models, themselves, and their effects were modeled as spring elements and therefore accounted for. G_{12} values for the LF structure varied based on wall length and height, and varied linearly with length for a given wall height (Pfretzschner et al. 2013). For more information on this general procedure, see Pfretzschner (2012).

Due to the limitations of the IRC (ICC 2009), sufficient shear wall area was not available on the gable end of the LF structure due to the garage doors. A portal frame was therefore designed for the necessary lateral force resistance of this wall (Martin et al. 2008). Due to the structural differences and increased stiffness of this moment-resisting frame per unit of sheathing area, a separate stiffness calibration method was necessary. Note that NDS equation C4.3.2-2 (AF&PA 2005b) applies only to standard light framing practices, which do not include the presence of a portal frame. Full-scale testing to determine the deflection and stiffness of a portal frame was performed by Al Mamun et al. (2011). A calibration model was created in SAP2000 depicting an identical setup to these tests. The G_{12} value of the sheathing elements was then adjusted until deflection results (and therefore stiffness) from testing where matched. Note that even though the entire portal frame system was modeled, assigning "pinned" connections to joints allows stiffness to be controlled entirely by sheathing elements. This stiffness value was, therefore, assigned to the shell element material that represents the sheathing on the portal frame.

TF wall and roof sheathing elements were also calibrated against existing full-scale test results on actual TF elements. TF/SIP wall stiffness was calibrated against stiffness tests performed by Erikson et al. (2003) on a two-story, two-bay TF wall section with SIP panels attached. Panel joints coincided with frame members, and wall framing included a sill member, a system of fabrication similar to the TF modeled for this study. A simple calibration model was created in SAP2000 depicting this identical testing setup, and the G_{12} value for the model sheathing material was adjusted until the deflection from testing was attained by the model. The calibration model was created with two sets of sheathing elements representing the OSB SIP face

panels, each offset the appropriate distance from the center line of wall framing. G_{12} values determined from this calibration procedure were then applied to all TF wall sheathing elements on TF models created for this study. Roof SIP sheathing stiffness was determined in a similar manner by calibrating against stiffness results from tests performed by Carradine et al. (2004) on a TF roof system sheathed in SIPs.

Wall Anchorage

Similar to Pfretzschner et al. (2013), anchor bolt and hold-down foundation connections were modeled in SAP2000 with directional linear spring elements. Hold-down connections in the LF were modeled as springs in the vertical (Z) direction only, and anchor bolt connections in both structures were modeled as springs in all three orthogonal directions (X, Y, and Z). Note that where anchor bolts resist uplift, overturning, and horizontal movement, hold-downs are designed to resist uplift only. Axial stiffness of hold-downs (Z direction) was determined based on published properties provided by the manufacturer, Simpson Strong-Tie, and the specific hold-down model selected, model number HDU8-SDS2.5, was based on portal frame design requirements (Simpson Strong-Tie, 2013). In accordance with both Martin et al. (2011) and Pfretzschner et al. (2013), the axial stiffness of anchor bolts (Z direction) was based on testing performed by Seaders (2004). Shear stiffness values (X and Y directions) were determined in agreement with Martin et al. (2011) using the NDS equation for the load/slip modulus for a dowel-type fastener wood-to-wood connection (AF&PA 2005a). Post bottom connections for the TF were modeled similarly as a linear spring, but with twice the stiffness of a typical anchor bolt (for all three orthogonal directions) since each post bottom connection was performed with two anchor bolts.

Load Path Investigations

Load path investigations were performed by applying design loads in ASD loading combinations and observing and comparing the relative magnitude of reactions at each structure's foundation. Specifically, the reactions resulting at anchor bolts, hold-downs, and post bottom connections were observed. Additionally, system behavior, most notably member and system deflections were observed in SAP2000. Observations from an initial overall comparison were made based on patterns in load path from gravity loading, as well as resistance to uplift. Additionally, investigations pertaining to story drift and twisting, the introduction of large wall

openings, a break in load path, and the variation of axial forces in studs and posts, were performed.

Timber Frame vs. Light Frame Structural Load Path Comparison Investigation

Similar to analysis methods used by Pfretzschner et al. (2013), reactions to design loadings were observed at connection points to the foundation. These connections were the anchor bolts and hold-downs for the LF, and post bottoms and anchor bolts for the TF. Each structure therefore had reactions determined along all four walls, as well as at two central locations within the building representing the reactions at the foundation from posts that support second floor beams in each structural system. Locations for the reactions observed, and their connection type, for the LF and the TF, both enclosed and without openings are shown in Figure 3.5.

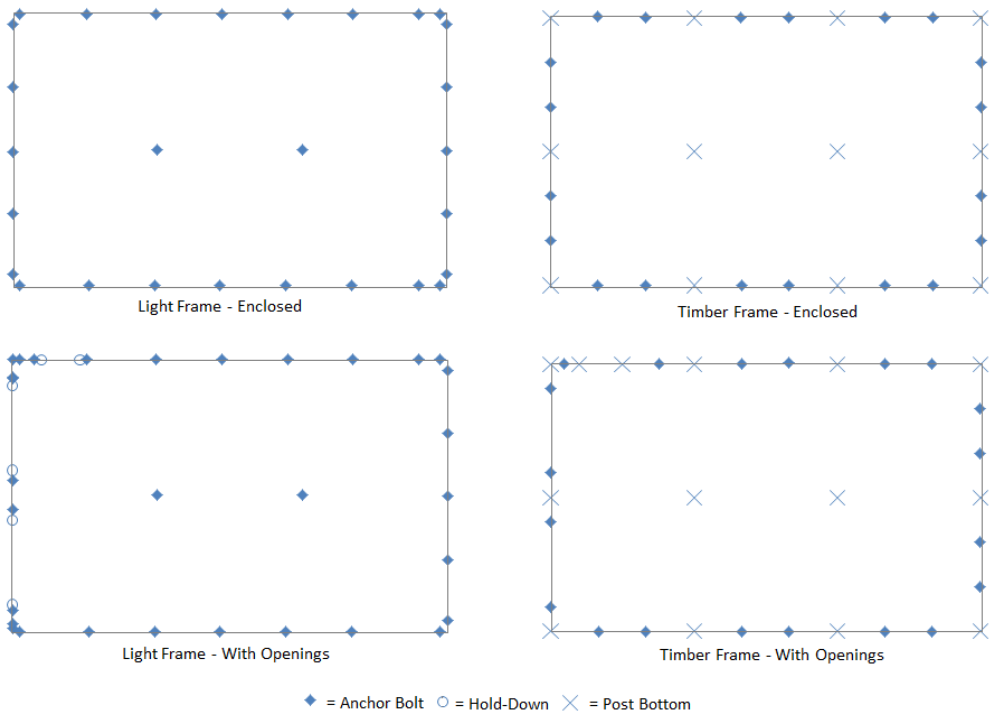

Figure 3.5: Foundation connection locations for LF and TF structures, enclosed and with openings

Reactions were then represented graphically such that both their magnitude and location were apparent. Comparisons focused on the differences between reactions in the TF versus the LF without openings for identical loadings, and then similarly across framing systems with

openings. Additionally, the effects of introducing openings (doors and windows) on each separate structural system individually were observed. Finally, observations based on the deflected shapes of each structure in SAP2000 were also made.

Observations were made in an initial comparison between the LF structure and the TF structure (both with and without openings) subject to all load combinations considered. Notable observations further investigated include a variation in pattern of load path between the two structural systems, as well as each structural system's relative resistance to wind-induced uplift.

Story Drift and Gable-End Stiffness

TF construction typically employs vertical posts on exterior walls that span from the foundation to roof line. Light framing techniques (platform framing), however, call for a separate stud at each story for exterior walls, introducing a joint at every level. To investigate the difference between these wall framing methods with respect to deflection under lateral loads, each standard structure (with openings) was modeled with load combination 5 (dead and wind loads) to observe the maximum effect of north-south wind.

A simultaneous investigation was also performed on the aforementioned structures with the same loading to examine twisting and gable-end stiffness. Where LF design with the IRC required the additional engineering of a portal frame to sufficiently resist lateral loads, no similar design was added to enhance the stiffness of the gable end with garage doors for the TF. To compare the stiffness of each gable-end wall with garage doors, load combination 5 with north-south wind loading was applied to each structure.

Large Opening Investigation

To compare the effects of introducing large openings in walls for each structural system, large doorways were introduced to the LF and TF models. These additional openings were introduced to the (standard) versions of each structure, already having doors and windows. This was done to mimic the effect of making additional alterations to an actual structure. A large opening was created in the gable end of each structure by removing the wall section between the two garage doors. For the LF, this meant removing several studs and their associated sheathing. For the TF, this meant removing one post, as well as its surrounding garage door (small-dimension) framing and associated SIP sheathing. A 140-mm x 286-mm (nominal 6-in x 12-in) header was introduced to the LF, which is the largest typical built-up solid-sawn header available

for use in LF construction. Note that though this alteration to the gable end of the LF introduces a clear-span opening of 6.3-m (20-ft, 8-in), which is greater than that allowed by the IRC (ICC 2009) for this header size, this modification was introduced for comparison purposes in this study only. Similarly, an identical size and position opening was introduced to the TF. Due to typical timber framing construction methods, no additional framing members (such as a header) were necessary. Figure 3.6 shows this alteration to the LF structure and the TF structure, respectively.

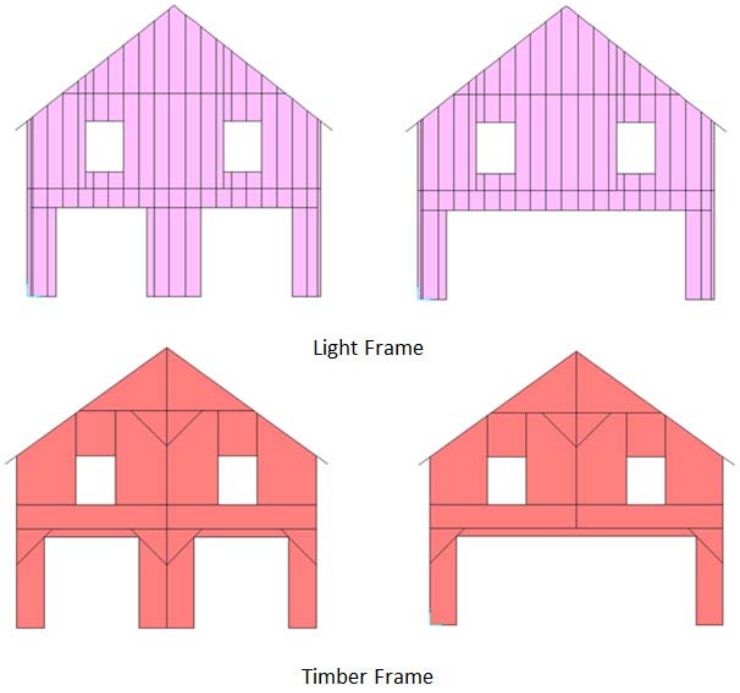

Figure 3.6: Large gable-end opening introduced to light-frame and timber frame

A large opening was also introduced to the side of each structure. The size of this opening was dictated by the space available between the two central posts in this wall of the TF. A 140-mm x 286-mm (nominal 6-in x 12-in) header was added above this opening in the LF, however with a clear span of approximately 4.0-m (13-ft, 1-in), this header is still considered insufficient by the IRC (ICC 2009). As noted previously, this is the largest typical header size available in light framing construction. This large opening has again been introduced for comparison purposes only. Due to typical timber framing construction methods, no additional framing members (such as a header) were added. Figure 3.7 shows this alteration to the LF structure and the TF structure, respectively.

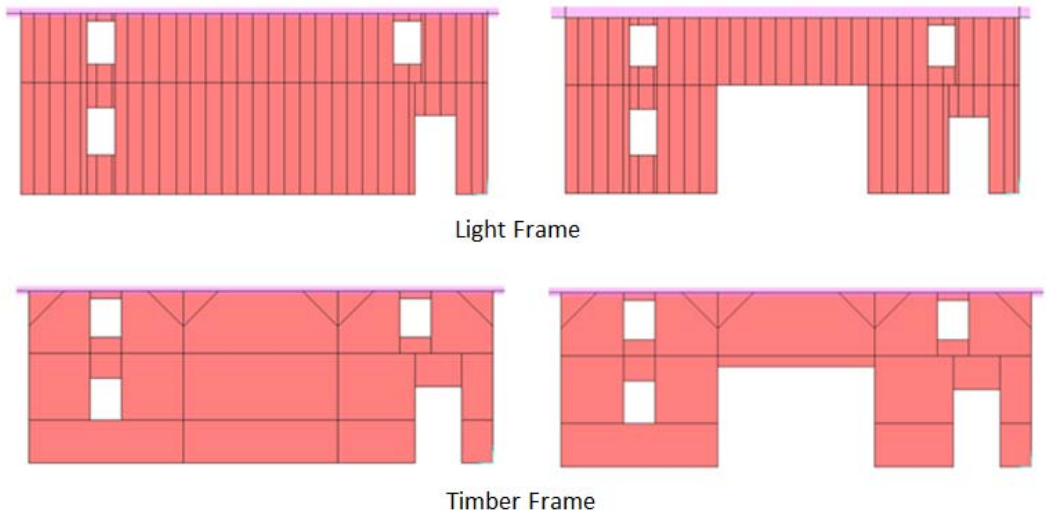

Figure 3.7: Large side opening introduced to the light-frame and timber frame

Break-in-Load-Path Investigation

One of the structural differences between an LF and a TF is the number of total vertical members transmitting loads to the ground. Where an LF is composed of many small studs, a TF relies on a smaller number of larger posts to transmit loads. This comparison is similar for rafters and joists as well. A TF simply employs fewer structural framing members. An LF, therefore, inherently offers a more redundant design than the TF when studs, joists or rafters are considered, providing an increased number of possible load paths directly to the ground. For this reason, it is clear that the omission of one stud in the LF would have considerably less effect on load paths than the omission of one post in the TF. To investigate the effect of a break in the load path for both structural systems, an investigation was carried out to determine the effect of losing one common member considered critical to each structure, a 1st floor central post. The central post furthest from the gable end with garage doors was removed from both the standard TF and the standard LF model.

Post vs. Stud Range of Axial Load Investigation

Axial loads in the 38-mm x 140-mm (nominal 2-in x 6-in) LF studs and 203-mm x 203-mm (8-in x 8-in) TF posts based on gravity loadings were observed for the range in magnitude. Each structural system was examined fully-enclosed, with openings (standard), and with large gable and side openings introduced separately to standard models. Maximum axial forces were observed, and average axial forces were calculated for posts and studs in each model. A value for the ratio of maximum load to the average load was calculated for each, indicating a range in variability of the loads. Load variability between LF studs and TF posts was compared.

RESULTS AND DISCUSSION

Timber Frame vs. Light-Frame Structural Load Path Comparison Investigation

Patterns in Load Path from Gravity Loading

Results for the magnitudes and locations of base reactions for the structural load paths show a distinctly different pattern for the LF and the TF. This observation is seen most clearly by considering gravity loading only (dead, live, and snow loads) with load combination 4. Where load transfer to the foundation in the LF shows an even distribution of magnitudes, the TF displays two separate ranges of reaction magnitudes, one at post bottom connections and the other at anchor bolts (where sheathing transmits vertical loads). Figure 3.8 shows the foundation connection reactions for the LF structure and the TF structure subject to uniform gravity loads only.

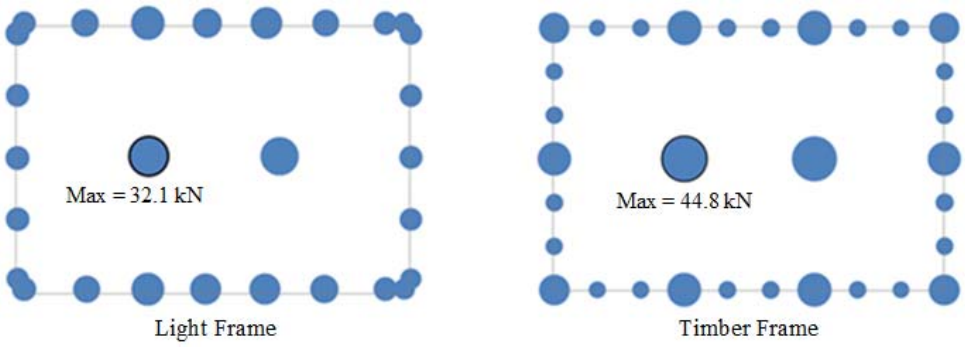

Figure 3.8: Fully-enclosed light-frame and timber frame foundation reactions, ASD load combination 4

LF reactions range from 9.60 kN (2,150 lb) to 32.1 kN (7,220 lb), and show a symmetrical pattern. Load distribution shows a generally higher concentration of reaction at the

center of the side walls, and they are reduced as anchor bolt reactions closer to gable-end walls are considered. Load distribution along gable-end walls, however, shows a more consistent magnitude along the length of the wall. These results are in good agreement with patterns observed in a uniform uplift investigation by Pfretzschner et al. (2013), validating correct application of modeling methods.

Load path is inherently dependent on the structural assembly, and a higher concentration of load on the side walls of the LF is due to the fact that roof loading is transmitted primarily to these walls by rafters. Gable-end walls transmit their own dead load, as well as a small tributary area of roof and a portion of the floor load, each. Central posts support central floor dead and live load only, and show a maximum reaction of 32.1 KN (7,220 lb) each.

TF foundation reactions from the same load combination show a pattern that is different from the LF structure. Reactions are segregated by magnitude between post bottoms and anchor bolts. As expected, a smaller number of higher-magnitude loads are transmitted to the foundation in the TF, as compared to the more uniform distribution observed in the LF assembly. Anchor bolts are located along sill plates that span from one post bottom to the next, and serve as connection points for SIP sheathing. Two anchor bolts exist between each post. This allows the sheathing to transmit loads to the foundation. Where post bottom connection reactions show gravity loads transmitted directly by the frame, anchor bolt reactions indicate gravity loads transmitted by SIP sheathing. Though framing members are typically designed to resist 100% of vertical loads, results show that approximately 30% of gravity loads for this assembly have been transmitted to the foundation through the sheathing. Wall post reactions vary due to structural configuration, however, they are fairly consistent, ranging between 20.0 kN (4,500 lb) and 26.3 kN (5,910 lb). Anchor bolts experience reactions from 6.17 kN (1.390 lb) to 7.13 kN (1,600 lb). Contrary to LF reactions, the higher values here are observed in the gable end of the structure. Note that since the TF structure employs a ridge beam and central posts that span the height of the floor as well, much of the roof load is transmitted directly to the foundation through this central load path. Where the LF structure uses collar ties and rafter ties to safely transmit roof loads to side walls, the TF configuration creates a load path that does not rely as heavily on side walls. For this reason the foundation reactions at the central posts in the TF are approximately 44.8 kN (10,100 lb), a value 40% higher than the reactions for the LF. Also for this reason, the tapering off of reactions observed in the side walls of the LF is not present in the TF.

Wind Uplift Resistance

Results from the application of load combination 5, considering the dead load of the structure and wind loading only, reflect the behavior of each structure when additional gravity loads (live and snow) are not present to assist in the resistance of uplift. Figure 9 shows the results from this loading on both the LF and the TF considering wind in the general east-west direction. Arrows indicate wind loading direction.

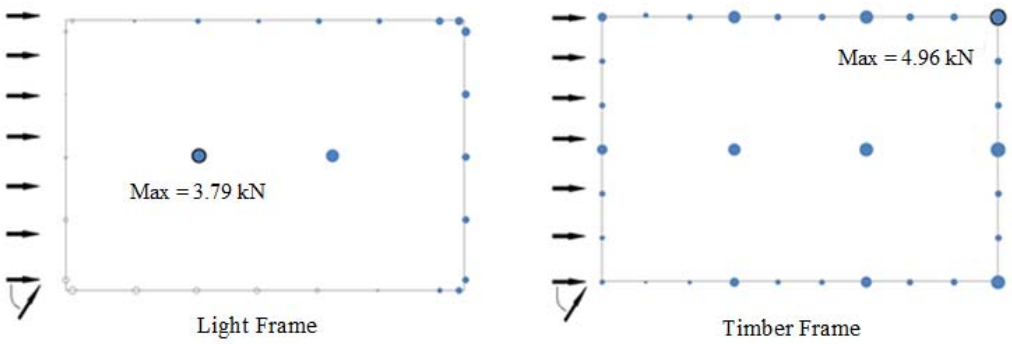

Figure 3.9: Fully-enclosed light-frame and timber frame foundation reactions, ASD load combination 5

Dark bubble points in Figure 3.9 indicate a downward force at the foundation connection (and therefore a positive, upward reaction), and clear bubble points indicate a point of uplift (a negative, downward reaction). At these points the foundation connections are in compression and tension, respectively. These results show that the windward gable-end and the windward side of the LF structure experience uplift along nearly their entire length. Uplift reaction magnitudes are greatest at the windward corner and taper away from this location along both the gable-end and side wall.

Where the LF structure exhibits uplift along both windward sides of the building, the TF maintains compressive forces (positive foundation reactions) along both sides, therefore more effectively resisting uplift forces due to wind load. Additionally, foundation connection reactions at post bottom connections continue to be higher in magnitude than anchor bolt connections. This indicates that the fewer number of higher magnitude gravity load reactions more effectively resist uplift.

Since increased gravity loads including dead load are an effective means of resisting uplift, a heavier structure is inherently more likely to maintain compressive (downward) forces

along the foundation than a lighter structure, when subjected to wind forces. A sum of the reactions at the foundation indicates that the TF modeled in this study is 32% heavier than the LF. For the purpose of examining the structural effects of the TF composition on uplift resistance without the advantage of increased dead load, a self-weight multiplier was introduced to the load pattern. A self-weight multiplier of 0.76 equates the weight of the TF to the weight of the LF. Where Figure 3. indicates the results for foundation reactions for the actual TF subjected to wind and dead load (load combination 5), Figure 3.10 shows these results for the TF structure with an identical total dead load to the LF structure.

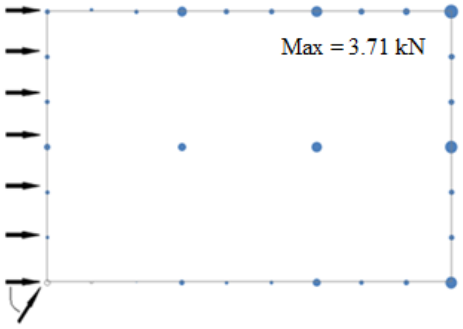

Figure 3.10: Fully-enclosed timber frame foundation reactions, equivalent dead load to light-frame, ASD load combination 5

Though these results indicate uplift forces at the windward corner of the TF, the region experiencing uplift in this structure is considerably smaller than the uplift seen in the LF under identical loading (Figure 3.9). Since the dead load for the TF has been scaled to equal the dead load for the LF, results indicate that the structural configuration of the TF, itself, is more capable of resisting uplift than the structural configuration of the LF.

Story Drift and Gable-End Stiffness

Deflections observed based on dead and wind loading (load combination 5) considering wind loading from the general north-south direction indicated an increased resistance to story drift in the TF as compared to the LF. Figure 3.11 compares the deflection of the TF and LF structures subjected to identical north-south wind loading. Images are viewed at a deflection scale factor of 200 for clarity.

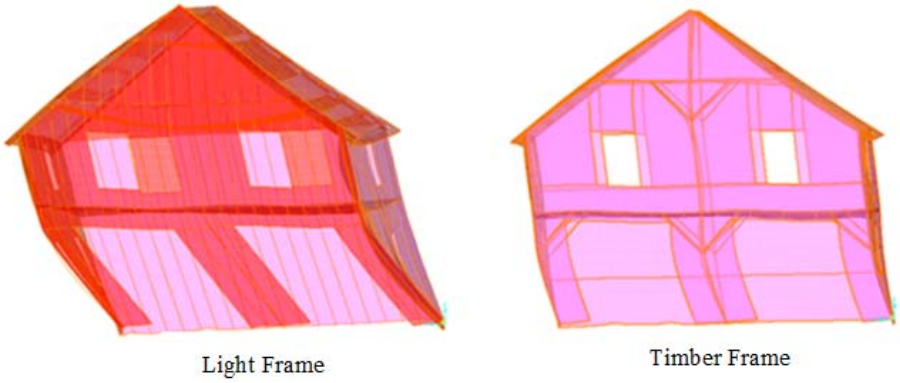

Figure 3.11: Light-frame and timber frame deflection, respectively, standard structures with openings, subjected to north-south wind loading, load combination 5, deflection scale: 200

Where TF construction often employs continuous posts that span from the foundation to the roof line, the LF construction method of platform framing introduces a joint at each story. Structures designed for this study employ platform framing because this is the primary method of light framing employed in the US today (Allen and Thallon, 2011). Construction sequence calls for first-floor studs to terminate at a top plate so that the second floor can be installed to serve as a work platform. Installation of the second floor walls follows. The exterior wall of a typical LF structure, therefore, consists of multiple story-high studs joined vertically at points which essentially act as hinges when subjected to lateral loads (such as wind). (Platform framing replaced balloon framing, a light framing technique that employs continuous studs for framing exterior walls, in the mid 1950's. Among other deficiencies of balloon framing, it gave way to platform framing because it was more difficult to construct (Allen and Thallon, 2011).) The effects of the discontinuous nature of the exterior wall framing in the LF are clear in Figure 3., where story drift is great. Deflection at floor level of the second story was approximately 3.5 times greater in the LF than in the TF.

Observations between each gable end on the LF and each gable end on the TF show the effects of gable-end stiffness. Figure 3.12 shows the deformations from load combination 5 with a north-south wind direction.

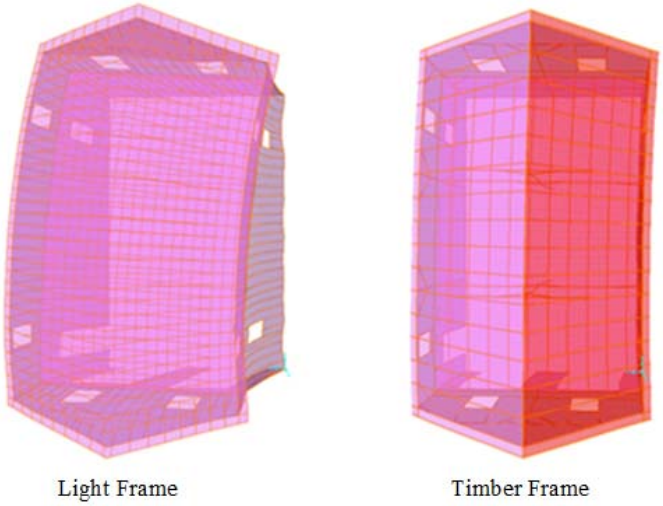

Figure 3.12: Light-frame and timber frame: effects of gable-end stiffness, load combination 5, north-south wind direction, deflection scale: 200

As expected, the deflection is greater (70%) on the gable end with garage doors than the gable end without these openings on the TF. Deflections were measured at floor level of the 2nd story. The LF gable-end wall with garage door openings, however, deflects considerably (over 200%) more than the gable end without openings on the LF. For deflection comparison between the two structural systems, note that the gable-end of the LF without garage doors deflected approximately three times further than the similar gable-end of the TF. Note that the wall with the garage door in the LF was designed with a moment-resisting frame to increase the stiffness. However, the results show that a TF is more resilient to openings introduced in shear walls with respect to lateral stiffness. The deflected shape of the LF also shows more twisting than the TF, both of which employ diaphragms considered to be semi-rigid. Lateral loads are transmitted to shear walls in rigid (or semi-rigid) structures based on the stiffness of each shear wall, and therefore twisting occurs in the LF structure because the stiffness of the portal frame is less than the stiffness of the opposing gable-end shear wall. It is important to note that for all results based on loads applied laterally to the timber frame structure, lateral behavior is dictated by the stiffness of the sheathing, determined by calibration with experimental results.

Large Opening Investigation

The effects of introducing large openings to the gable end and side of each structure were investigated. Load combination 4 (gravity loads only) was applied to the TF and LF structures with each large opening. Results, based on observing the deflected shape of each structure with

the introduction of a large gable opening, show that both structures behave similarly. Deflections due to the introduction of a large opening in the side of each structure, however, are considerably different. Figure 3.13 shows the deformed shape of the gable-end and side of each structure at a deflection scale factor of 100.

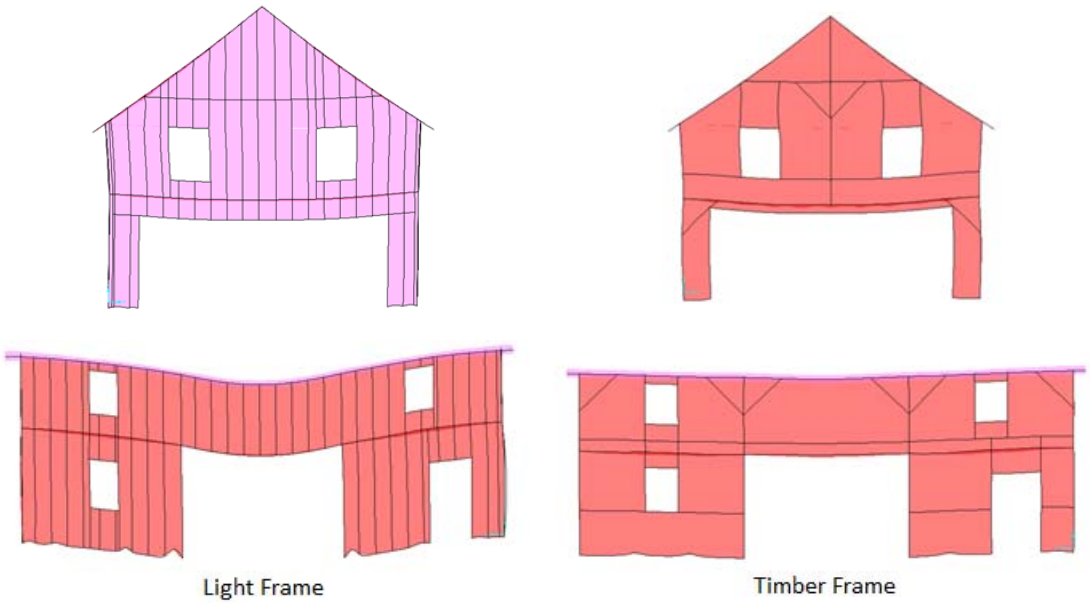

Figure 3.13: Light-frame and timber frame deflection, respectively, large openings, subjected to gravity loading, load combination 4, deflection scale: 100.

TF load paths appear to adapt easily to the presence of a large opening in the side of the structure. This can be attributed to the smaller-magnitude loads that are transmitted by the sheathing that has been removed to create the opening. Since gravity load paths within the timber frame structure rely primarily on posts for transmission to the foundation, and post locations have not been altered to include the opening, little change in load path is observed. The LF, however, experiences considerable deflection in the header above the opening, as well as in the eave line of the roof. Change in load path within the LF structure due to a large opening in the side of the structure relies on the header, installed above the opening, to transmit loads to adjacent studs. Additionally, the location of this opening is where the magnitudes of loads transmitted by the side wall are the greatest (See Figure 3.). This investigation further supports the conclusion that a TF structure is more resilient to the introduction of large openings than an LF, provided posts are unaltered and available for load transmission. Furthermore, it is more responsible to locate a

large opening in a gable-end rather than the side of an LF structure. This conclusion is in agreement with the findings of Martin et al. (2011) and Pfretzschner et al. (2013).

Break-in-Load-Path Investigation

Figure 3.14 shows the resulting deflection in floor systems for the LF and the TF when a 1st-floor central post is removed. Even though the removed central post in the TF supports additional roof load (the 1st-floor central post in the LF do not support roof load), the TF floor system deflects only 25% as much as the LF floor system. The TF is, therefore, less sensitive to this break in load path than the LF.

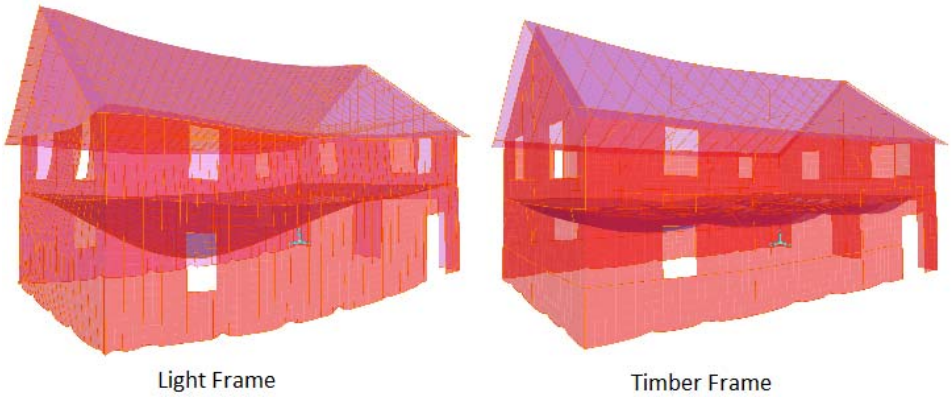

Figure 3.14: Break in load path, deflection from central post removal from light-frame and timber frame, deflection scale: 100

Post vs. Stud Range of Axial Load Investigation

Table 3.2 shows the maximum axial loads in the LF studs and TF posts as well as average loads for each based on gravity loading only (load combination 4). When the maximum is considerably above the average, the actual factor of safety is diminished due to the concentration of loadings. The TF posts consistently show a maximum to average axial load ratio of approximately 2.0 for all of the structural options examined. The LF, however, shows an increase in load variability as the frame complexity increases and openings are introduced. Though the ratio of maximum load divided by average load is only 1.43 for the fully-enclosed LF, the ratio increases to 3.72 for the LF with a large side opening. Though a factor of safety is applied during design to typical elements of the structure, variability reduces the actual effective factor of safety. TF posts must be designed to withstand at least two times the average load expected. LF studs,

however, must be designed to carry significantly more due to even greater variability of loads in some cases.

Table 3.2: Axial load distribution in light-frame studs and timber frame posts

Structural Composition	LF Studs 38-mm x 140-mm (2-in x 6-in)			TF Posts 203-mm x 203-mm (8-in x 8-in)		
	Maximum Axial Load kN (lb)	Average Axial Load kN (lb)	Max/Ave.	Maximum Axial Load kN (lb)	Average Axial Load kN (lb)	Max/Ave.
Fully-Enclosed	4.54 (1,020)	3.15 (709)	**1.44**	71.2 (16,003)	35.6 (7,993)	**2.00**
Standard (with openings)	5.23 (1,175)	3.13 (704)	**1.67**	70.7 (15,905)	36.2 (8,140)	**1.95**
Large Gable-End Opening	6.30 (1,416)	3.14 (705)	**2.00**	76.6 (17,226)	37.8 (8,493)	**2.03**
Large Side Opening	11.93 (2,681)	3.21 (721)	**3.72**	71.0 (15,962)	34.9 (7,836)	**2.04**

CONCLUSIONS

Structural models of a timber frame (TF) and a light-frame (LF) were created in SAP2000 using modeling methods developed by Martin et al. (2011) and Pfretzschner et al. (2013). Comparisons were made between structural systems (with and without openings) based on the behavior of each model subjected to design gravity and wind loads. Results were based on observed reaction forces at the foundation in each structure, as well as observed deflections of members and assemblies. Specifically, observations considering reaction patterns from uniform gravity loading, as well as uplift resistance from wind loading were made. Additional investigations performed included observing story drift and twist, introducing large wall openings, introducing a break in load path, and observing the range of axial loads in TF posts and LF studs.

Results show that the TF structure outperforms the LF structure in many aspects. TFs more effectively resist uplift with fewer, more heavily (gravity) loaded posts. Story drift and twisting were also more effectively resisted by the TF, due to continuous posts resisting out-of-plane wind loading more effectively than platform-framed exterior walls. Additionally, TFs are

more suitable for the addition of large openings in the side of a structure provided these openings are introduced in between posts. Where the LF in this study relies on side walls (perpendicular to the rafter direction) for the primary transmission of roof loads, the TF employs central posts that carry a large percentage of gravity loads through the center of the structure. Based on observations of axial loads in studs and posts in variations of the models, the range of loads is smaller in TF members.

ACKNOWLEDGMENTS

Previous research performed by Kenny Martin and Kate Pfretzschner to develop and validate the modeling methods utilized in this study was crucial in creating the structural models. Additionally further assistance provided by Kenny Martin and Kate Pfretzschner while applying these modeling methods was greatly appreciated. Finally, funding and support from the Wood Science and Engineering Department and the School of Civil and Construction Engineering of Oregon State University made this research possible.

References

AF&PA (2005a). *National Design Specification for Wood Construction (NDS).* ANSI/AF&PA NDS-2005. Washington, DC.

AF&PA (2005b). *Special Design Provisions for Wind and Seismic.* ANSI/AF&PA NDS-2005. Washington, DC.

Al Mamun A., Ghasan, D., Ni, C., Mohammad, M., Chui, Y.H., and Asiz, A. (2011). "Alternative Bracing Systems in Light-Wood Frame Buildings." *CSCE 2011 General Conference*. Ottowa, Ontario.

Allen, E., Thallon, R. (2011). *Fundamentals of Residential Construction*. 3rd ed. Hoboken: John Wiley & Sons, 2011.

APA – The Engineered Wood Association (2012). *Panel Design Specification*. The Engineered Wood Association. Tacoma, Washington.

ASCE – American Society of Civil Engineers. (2010). *ASCE/SEI 7-10 Minimum Design Loads for Buildings and Other Structures.* ASCE, New York, NY.

Bergman, R., Zhiyong, C., Carll, C.G., Clausen, C.A., Dietenberger, M.A., Falk, R.H., Frihart, C.R., Glass, S.V., Hunt, C.G., Ibach, R.E., Kretschmann, D.E., Rammer, D.R., Ross, R.J., Stark, N.M., Wacker, J.P., Wang, X., White, R.H., Wiedenhoeft, A.C., Wiemann, M.C., and Zelinka, S.L. *Wood Handbook, Wood as an Engineering Material.* U.S. Department of Agriculture, Forest Service, Forest Products Laboratory, Madison, WI, 2010.

Blue Ridge Timberwrights (BRT). 2010. "A History of Timber Framing." <*http://brtw.com/historyoftimberframing.php*> (April 15, 2013).

Bulliet, W.M., Sandberg, B.L., Drewek, M.W., O'Bryant, T.L. (1999). "Behavior and Modeling of Wood-Pegged TFs." *Journal of Structural Engineering*, 125, 3-9.

Carradine, D.M., Woeste, F.E., Dolan, J.D., and Loferski, J.R. (2004). "Utilizing diaphragm action for wind load design of TF and structural insulated panel buildings." *Forest Products Journal*, 54(5), 73-80.

Computers and Structures, Inc. (2012). *CSI Analysis Reference Manual: For SAP2000, ETABS and SAFE*. Berkeley, CA.

Doudak, G. (2005). "Field Determination and Modeling of Load Paths in Wood Light-Frame Structures." PhD. Thesis, McGill University, Montreal, Quebec.

Erikson, R.G., and Schmidt, R.J. (2003). "Behavior of Traditional TF Structures Subjected to Lateral Load." Ph.D. Thesis, University of Wyoming, Laramie, WY.

Google Sketch-Up Pro. Version 8.0.15158. Google, Mountain View, CA, 2012.

ICC – International Code Council (2009). International Residential Code for One- and Two-Family Dwellings – 2009. Country Club Hills, IL.

ICC – International Code Council (2011). International Building Code - 2012. Country Club Hills, IL.

Malone, B.P. (2013). "LF Versus Traditional TF: A Study in Comparing the Differences." M.S Thesis, Oregon State University, Corvallis, OR.

Martin et al., Z., Skaggs, T.D., Keith, E.L., and Yeh, B. (2008). "Principles of Mechanics Model for Wood Structural Panel Portal Frames." *Proceedings of the 2008 Structures Congress - Structures 2008: Crossing Borders*, 314.

Martin, K.G., Gupta, R. Prevatt, D.O., Datin, P. and van de Lindt J. 2011 "Modeling System Effects and Structural Load Paths in a Wood-Framed Structure." *Journal of Architectural Engineering (Special issue on residential construction)*, 17(4), 1-12

Nairn, J. (2007). *OSULaminates – Java Application for Laminated Theory Analysis, Version 2.1.* < http://www.cof.orst.edu/cof/wse/faculty/Nairn/OSU Laminates.html> (Feb 1, 2013).

Pfretzschner, K.S. (2012). "Practical Modeling for Load Paths in a Realistic, LF Wood House." M.S Thesis, Oregon State University, Corvallis, OR.

Pfretzschner, K., Gupta, R., and Miller, T.H. (2013). "Practical Modeling for Load Paths in a Realistic, LF Wood House" *Journal of Performance of Constructed Facilities*, accepted for publication, 2013.

Prevatt, D.O., Roueche, D.B., van de Lindt, J.W., Pei, S., Dao, T., Coulbourne, W., Graettinger, A.J., Gupta, R., and Grau, D., (2012). "Building Damage Observations and EF Classifications from the Tuscaloosa, AL and Joplin, MO Tornadoes."

Structures Congress 2012, ASCE 2012, 999-1010.

Seaders, P. (2004). "Performance of Partially and Fully Anchored Wood Frame Shear Walls Under Monotonic, Cyclic and Earthquake Loads." M.S. Thesis, Oregon State University, Corvallis, OR.

Simpson Strong-Tie (2013) "LTT/HTT Tension Ties." *Simpson Strong-Tie,* < http://www.strongtie.com/products/connectors/HDU-DTT2.asp> (May 5, 2013)

Shanks, J., and Walker, P. (2009). "Strength and Stiffness of All-Timber Pegged Connections." *Journal of Materials in Civil Engineering*, 21, 10-18.

TFEC (2010). *Standard for Design of TF Structures and Commentary*. TF Engineering Council. Becket, MA.

Thomas, W.H. (2003). "Poisson's ratios of an oriented strand board." *Wood Science Technology*, 37, 259-268.

van de Lindt, J. W., Graettinger, A., Gupta, R., Skaggs, T., Pryor, S., and Fridley, K. (2007). "Performance of Wood frame Structures during Hurricane Katrina." Journal of Performance of Constructed Facilities, 21(2), 108-116.

CONCLUSIONS

A qualitative understanding of the difference between structural options lends itself useful for some improvements. A quantitative analysis, however, is often necessary to track these differences and make truly informed decisions for improvements upon structural assembly and environmental impact. This study compares light-frame (LF) construction with timber frame (TF) construction by performing an environmental impact analysis (EIA) and a structural load path analysis of each framing system. An LF structure was designed based on a simplified version of an existing TF structure. Analyses were performed by modeling these structures with SAP2000 structural analysis software, as well as with the Athena Impact Estimator (AIE), life cycle assessment software. Structural investigations were performed to compare these framing systems with respect to gravity loading pattern, resistance to uplift, story drift, and twisting, to the introduction of large openings, and the range of axial loading observed in vertical members (posts and studs). Environmental impact investigations were performed to determine the relative impact of these structures with respect to total energy use, fossil fuel use, global warming impact (GWP), and wood fiber use and waste. Additionally, several material alternatives were explored for environmental impact.

Results from the EIA show that though the timber frame structure has the highest potential for mitigating the environmental burdens of these structures, impact was driven primarily by material choice. Structures utilizing OSB instead of solid-sawn products or plywood siding, or employing materials requiring a high level of kiln-drying, were shown to have the highest energy requirements and highest GWP. Insulation options increased these impacts considerably, and expanded polystyrene (TF insulation) proved to be considerably more damaging than fiberglass batts (LF insulation). Additionally, results show that all environmental impact categories observed are interrelated, and comparative trends showing the relative burden of each structure show a similar pattern for total energy consumption, fossil fuel consumption, and GWP. This is due to the fact that a major cause of global warming is due to the burning of fossil fuels. This suggests that though decisions based on differences in framing systems or choice of structural materials do have an effect on the environment, it is the source of energy used that can has the greatest impact. The wood product industry generates a large percentage of necessary manufacturing energy and heat from renewable sources (namely the burning of biofuels), however, it still uses electricity and fuels generated from non-renewable sources such

as natural gas or coal. Ultimately, we must strive for the utilization of renewable energy sources to most effectively mitigate environmental impacts.

Structural models developed in SAP2000 to investigate the differences between TF construction and LF construction revealed a number of measures in which the TF outperformed the LF. A difference in the load pattern observed at foundation reactions shows that where the LF structure provides a more evenly-distributed load path, the timber frame loads are transmitted to fewer points with higher-magnitude reactions. Assuming the foundation design has accounted for increased point loads at post bottoms, results show that this load pattern more effectively resists uplift. The TF structure also resisted twisting and story shear more effectively than the LF. This can be attributed to the difference between exterior wall framing techniques among these two framing systems. Where a TF employs continuous vertical members (posts) that span from the foundation to the roof line, LF exterior walls are framed with a separate stud at each story level, thereby introducing a joint that deflects under lateral loading. This deflection allows story-shear, and also reduces the lateral stiffness of this wall. A difference in the lateral stiffness between this wall and its opposing shear wall was the cause of twisting. The TF and LF structures performed equally under gravity loads when a large opening was introduced to the gable-end of each structure. When a large opening was introduced to the side of each structure, however, the TF proved to be far less sensitive to header and eave deflection than the LF, which showed considerable deflection at this location. Additionally, the TF floor system deflected considerably less than the LF floor system when a primary support column was removed. Lastly, axial forces observed in TF posts showed considerably less variation when subjected to gravity loads than LF studs.

Results from this study were limited to the individual investigations performed on the individual structures considered. Additionally for the EIA, results were limited to the construction and manufacturing life-cycle stages considered. Future research on the environmental impact of these structures should take into account a more complete building system, so that operations, maintenance, and end-of-life life-cycle stages can be included. Future research pertaining to the load path analysis should explore more complex shaped structures, structures incorporating commonly used engineered wood products (such as I-Joists), and common designs for TF/LF hybrids.

BIBIOLOGRAPHY

AF&PA (2005a). *National Design Specification for Wood Construction (NDS).* ANSI/AF&PA NDS-2005. Washington, DC.

AF&PA (2005b). *Special Design Provisions for Wind and Seismic.* ANSI/AF&PA NDS-2005. Washington, DC.

Al Mamun A., Ghasan, D., Ni, C., Mohammad, M., Chui, Y.H., and Asiz, A. (2011). "Alternative Bracing Systems in Light-Wood Frame Buildings." *CSCE 2011 General Conference*. Ottawa, Ontario.

Allen, E., and Thallon, R. (2011). *Fundamentals of Residential Construction*. 3rd ed. Hoboken: John Wiley & Sons, 2011.

APA – The Engineered Wood Association (2012). *Panel Design Specification*. The Engineered Wood Association. Tacoma, WA.

ASCE – American Society of Civil Engineers. (2010). *ASCE/SEI 7-10 Minimum Design Loads for Buildings and Other Structures.* ASCE, New York, NY.

Athena Sustainable Materials Institute (ASMI) (2012a). Athena Impact Estimator for Buildings V 4.2 Software and Database Overview. Toronto, Ontario.

Athena Sustainable Materials Institute (ASMI) (2012b). Athena Impact Estimator for Buildings. Version 4.2 Build 01 Hotfix. Athena, 2012.

Bare, J. (2012). "TRACI 2.0: The tool for the reduction and assessment of chemical and other environmental impacts 2.0." *Clean Technologies and Environmental Policy*, 13(5), 687-696.

Bergman, R.D., Bowe, S.A. 2010. "Environmental impact of manufacturing softwood lumber in northeastern and north central united states." *Wood and Fiber Science (CORRIM Special Issue),* 42, 67-78.

Bergman, R., Zhiyong, C., Carll, C.G., Clausen, C.A., Dietenberger, M.A., Falk, R.H., Frihart, C.R., Glass, S.V., Hunt, C.G., Ibach, R.E., Kretschmann, D.E., Rammer, D.R., Ross, R.J., Stark, N.M., Wacker, J.P., Wang, X., White, R.H., Wiedenhoeft, A.C., Wiemann, M.C., and Zelinka, S.L. *Wood Handbook, Wood as an Engineering Material.* U.S. Department of Agriculture, Forest Service, Forest Products Laboratory, Madison, WI, 2010.

Blue Ridge Timberwrights (BRT). 2010. "A History of Timber Framing." <*http://brtw.com/historyoftimberframing.php*> (April 15, 2013).

Brungraber, R. L. (1985). "Traditional Timber Joinery: A Modern Analysis," Ph.D. Dissertation, Stanford University, Palo Alto, CA.

Bulliet, W.M., Sandberg, B.L., Drewek, M.W., O'Bryant, T.L. (1999). "Behavior and Modeling of Wood-Pegged Timber Frames." *Journal of Structural Engineering*, 125, 3-9.

Carradine, D.M., Woeste, F.E., Dolan, J.D., Loferski, J.R. (2000). "Demonstration of Wind Load Design for Timber Frame Structures Using Diaphragm Action." *Transactionf of the American Society of Agricultural* Engineers, 43(3), 729-734.

Carradine, D.M., Woeste, F.E., Dolan, J.D., and Loferski, J.R. (2004). "Utilizing diaphragm action for wind load design of timber frame and structural insulated panel buildings." *Forest Products Journal*, 54(5), 73-80.

Computers and Structures, Inc. (2012). *CSI Analysis Reference Manual: For SAP2000, ETABS and SAFE*. Berkeley, CA.

Consortium for Research on Renewable Industrial Materials (CORRIM). 2013. "Life-cycle Inventory & Life-cycle Assessment."15, April 2013. http://www.corrim.org/research/lci_lca.asp

Datin, P. L. (2009). "Structural Load Paths in Low-Rise, Wood-Frame Structures." Ph.D. Proposal, University of Florida, Gainesville, Florida.

Delabruere, K. "Re: SIP technical info." Inquiries to Kyle Delabruere of Foam Laminates of Vermont. October 29, 2012. E-mail.

Doudak, G. (2005). "Field Determination and Modeling of Load Paths in Wood Light-Frame Structures." PhD. Thesis, McGill University, Montreal, Quebec.

Erikson, R.G., and Schmidt, R.J. (2003). "Behavior of Traditional Timber Frame Structures Subjected to Lateral Load." Ph.D. Thesis, University of Wyoming, Laramie, WY.

Finlayson, G. "Re: Query from contact us page." Inquiries to Grant Finlayson of Athena. Jan. 24, 2013. E-mail.

Florides, G.A., and Christodoulides, P. (2008). "Global warming and carbon dioxide through sciences." *Environment International*, 35, 390-401.

Frenette, C.D., Bulle, C., Beauregard, R., Salenikovich, A., Derome, D. 2010. "Defining an environmental index to compare light-frame wood wall assemblies using life-cycle assessment." *12th World Conference on Timber Engineering, 2010.*

Gerilla, G.P., Teknomo, K., Hokao, K. 2007. "An environmental assessment of wood and steel reinforced concrete housing construction." *Building and Environment,* 42, 2778-2784.

Glover, J., White, D.O., Langrish, T.A.G. 2002. "Wood versus concrete and steel in house construction: a life cycle assessment." *Journal of Forestry,* Dec. 2002, 34-41.

Google Sketch-Up Pro. Version 8.0.15158. Google, Mountain View, CA, 2012.

He, M., Lu, T. 2011. "Research on Lateral Performance of Hybrid Structure Based on Post-beam construction and Light Wood Frame Construction." *International Conference on M Multimedia Technology, 2011.*

Hindman, D.P. 2011. “Life cycle analysis and life cycle costing tools applied to post-frame building systems.” National Frame Builders Association, 2001. <nfba.org> (May 20, 2013)

ICC – International Code Council (2009). International Residential Code for One- and Two-Family Dwellings – 2009. Country Club Hills, IL.

ICC – International Code Council (2011). International Building Code - 2012. Country Club Hills, IL.

ISO 14040 (2006): Environmental management – Life-cycle assessment – Principles and Framework, International Organization for Standardization (ISO), Genève.

Kellenberger, D., Althaus, H.J. 2008. “Relevance of simplifications in LCA of building components.” *Building and Environment,* 44, 818-825.

Kermani, A., Hairstans, R. 2006. “Racking Performance of Structural Insulated Panels.” *Journal of Structural Engineering*, 132, 1806-1812.

Kline, D.E. (2005). “Gate-To-Gate Life-Cycle Inventory of Oriented Strandboard Production.” *Wood and Fiber Science*, 37, 74-84.

Lamlom, S.H., Savidge, R.A. (2003). “A Reassessment of Carbon Content in Wood: Variation Within and Between 41 North American Species.” *Biomass and Bioenergy,* 25, 381-388.

Lippke, B., and Wilson, J.B. (2010a). “Introduction to Special Issue: Extending the Findings on the Environmental Performance of Wood Building Materials.” *Wood and Fiber Science*, 42, 1-4.

Lippke, B., Wilson, J., Meil, J., Taylor, A. (2010b). “Characterizing the Importance of Carbon Stored in Wood Products.” *Wood and Fiber Science*, 42, 5-14.

Manthey, C., Guenther, E., Heiduschke, A., Haller, P., Heistermann, T., Veljkovic, M., Hajek, P. 2012. “Structural, economic and environmental performance of fiber reinforced wood provies vs. solutions made of steel and concrete.” *Life-Cycle and Sustainability of Civil Infrastructure Systems – Proceedings of the 3rd International Symposium on Life-Cycle Civil Engineering, IALCCE 2012,* 483-490.

Martin, K.G., Gupta, R. Prevatt, D.O., Datin, P. and van de Lindt J. 2011. “Modeling System Effects and Structural Load Paths in a Wood-Framed Structure.” *Journal of Architectural Engineering (Special issue on residential construction)*, 17(4), 1-12

Martin, Z., Skaggs, T.D., Keith, E.L., Yeh, B. (2008). “Principles of Mechanics Model for Wood Structural Panel Portal Frames.” *Proceedings of the 2008 Structures Congress - Structures 2008: Crossing Borders*, 314.

Meil, J., Wilson, J., O’Connor, J., Dangerfield, J. 2007. “An assessment of wood product processing technology advancements between the CORRIM I and II studies.” *Forest Products Journal,* 57(7/8), 83-89.

Milota, M.R., West, C.D., Hartley, I.D. (2005). "Gate-to gate life-cycle inventory of softwood lumber production." *Wood and Fiber Science (CORRIM Special Issue)*, 37, 47-57.

Nairn, J. (2007). *OSULaminates – Java Application for Laminated Theory Analysis, Version 2.1.* < http://www.cof.orst.edu/cof/wse/faculty/Nairn/OSU Laminates.html> (Feb 1, 2013).

National Renewable Energy Laboratory (NREL). 2012. "U.S. Life-cycle Database." http://www.nrel.gov/lci/ (April 15, 2013).

National Research Council. (1976). Renewable resources for industrial materials. National Academy of Sciences, Washington, DC.

Paevere, P., Foliente, A.M., and Kasal, B. (2003). "Load-Sharing and Redistribution in a One-Story Woodframe Building." *Journal of Structural Engineering*, 129 (9), 1275-1284.

Perez-Garcia, J., Lippke, B., Briggs, D., Wilson, J.B., Bowyer, J., Meil, J. 2005a. "The environmental performance of renewable building materials in the context of residential construction." *Wood and Fiber Science (CORRIM Special Issue)*, 42, 3-17.

Perez-Garcia, J., Lippke, B., Comnick, J., Manriquez, C. 2005b. "An assessment of carbon pools, storage, and wood products market substitution using life-cycle analysis results." *Wood and Fiber Science (CORRIM Special Issue),* 37, 140-148.

Pfretzschner, K.S. (2012). "Practical Modeling for Load Paths in a Realistic, Light-Frame Wood House." M.S Thesis, Oregon State University, Corvallis, OR.

Pfretzschner, K., Gupta, R., and Miller, T.H. (2013). "Practical Modeling for Load Paths in a Realistic, Light-Frame Wood House" *Journal of Performance of Constructed Facilities*, accepted for publication, 2013.

Puettmann, M., Bergman, R., Hubbard, S., Johnson, L., Lippke, L., Oneil, E., Wagner, F.G. (2010a). "Cradle-to-Gate Life-Cycle Inventory of US Wood Products Production: CORRIM Phase I and Phase II Products." *Wood and Fiber Science*, 42, 15-28.

Puettmann, M.E., Wagner, F.G., Johnson, L. 2010b. "Life cycle inventory of softwood lumber from the inland northeast US." *Wood and Fiber Science (CORRIM Special Issue)*, 42, 52-66.

Prevatt, D.O., Roueche, D.B., van de Lindt, J.W., Pei, S., Dao, T., Coulbourne, W.,Graettinger, A.J., Gupta, R., and Grau, D., (2012). "Building Damage Observations and EF Classifications from the Tuscaloosa, AL and Joplin, MO Tornadoes." Structures Congress 2012, ASCE 2012, 999-1010.

Salazar, J., Meil, J. 2009. "Prospects for carbon-neutral housing: the influence of greater wood use on the carbon footprint of a single-family residence." *Journal of Cleaner Production,* 17, 1563-1571.

Sandberg, L. B., Bulleit, W. M., O'Bryant, T. L., Postlewaite, J. J., and Schaffer, J. J. (1996). "Experimental Evaluation of Traditional Timber Connections," *Proceedings*, I International Wood Engineering Conference, New Orleans, LA, 4, 225-231.

Schmidt, R. J., and Daniels, C. E. (1999). "Design Considerations for Mortise and Tenon Connections," Research Report, Department of Civil and Architectural Engineering, University of Wyoming, Laramie, WY.

Schmidt, R. J., and Scholl, G. F. (2000). "Load Duration and Seasoning Effects on Mortise and Tenon Joints," Research Report, Department of Civil and Architectural Engineering, University of Wyoming, Laramie, WY.

Seaders, P. (2004). "Performance of Partially and Fully Anchored Wood Frame Shear Walls Under Monotonic, Cyclic and Earthquake Loads." M.S. Thesis, Oregon State University, Corvallis, OR.

Simpson Strong-Tie (2013) "LTT/HTT Tension Ties." *Simpson Strong-Tie,* < http://www.strongtie.com/products/connectors/HDU-DTT2.asp> (May 5, 2013)

Shanks, J., and Walker, P. (2009). "Strength and Stiffness of All-Timber Pegged Connections." *Journal of Materials in Civil Engineering*, 21, 10-18.

Terentiuk, S, Memari, A. 2012. "In-Plane Monotonic and Cyclic Racking Load Testing of S Structural Insulated Panels." *Journal of Architectural Engineering*, 18(4), 261-275.

TFEC (2010). *Standard for Design of Timber Frame Structures and Commentary*. Timber Frame Engineering Council. Becket, MA.

Thomas, W.H. (2003). "Poisson's ratios of an oriented strand board." *Wood Science Technology*, 37, 259-268.

U.S. EPA. "Tool for the Reduction and Assessment of Chemical and Other Environmental Impacts (TRACI)." 15 April, 2013. < *http://www.epa.gov/nrmrl/std/traci/traci.html*>

van de Lindt, J. W., Graettinger, A., Gupta, R., Skaggs, T., Pryor, S., and Fridley, K. (2007). "Performance of Wood frame Structures during Hurricane Katrina." Journal of Performance of Constructed Facilities, 21(2), 108-116.

Western Wood Products Association (WWPA). 2012. < *http://www2.wwpa.org*> (May 14, 2013).

Wilson, J.B. 2005. "Documenting the environmental performance of wood building materials." *Wood and Fiber Science (CORRIM Special Issue)*, 37, 1-2.

Wilson, J.B. and Sakimoto, E.T. (2005). "Gate-to-gate life-cycle inventory of softwood plywood production." Wood and Fiber Science (CORRIM Special Issue), 37, 58-73.

Xiong, H., and Zhao, Y. 2011. "Environment impact comparison of different structure system based on life cycle assessment methodology." Advanced Materials Research, 243-249, 5275-5279.

APPENDIX

APPENDIX A

EXTENDED LITERATURE REVIEW

ENVIRONMENTAL IMPACT ASSESSMENT

A large percentage of the life cycle assessment (LCA) research that has been performed to date concerning wood products has been a comparison with other structural materials, such as steel or concrete, and studies have been numerous. These LCA have been performed to compare individual products, assemblies of products, and whole buildings. A study was performed in 1976 by the Academy of Science/National Research Council that compared wood products to other materials, and results showed wood to perform favorably (NRC 1976). Since this landmark study, LCA has developed to a standardized science (ISO 2006), and additional studies comparing wood to similar-use structural products have been performed. Very often, life cycle impact assessment (LCIA) results show that structural assemblies and whole buildings employing wood-based materials for the majority of their structural assembly have significantly less environmental impact than designs utilizing concrete or steel material options (Glover et al. 2002, Perez-Garcia et al. 2005a, Gerilla et al. 2007, Xiong and Zhao 2011, Manthey et al. 2012). Manufacturing for wood-based materials requires less energy than other equivalent-use materials, less dependence on fossil fuel sources, and stores atmospheric carbon which acts to mitigate global warming potential (GWP) (Glover et al. 2002, Perez-Garcia et al. 2005a, Gerilla et al. 2007, Xiong and Zhao 2011, Manthey et al. 2012). Energy consumption and global warming potential are both widely recognized as key indicators of environmental sustainability.

The most comprehensive research pertaining to the life cycle inventory (LCI) of wood products in the U.S. has been performed by the Consortium for Research on Renewable Industrial Materials (CORRIM). CORRIM is a collective group of research institutions founded in 1996 to expand upon a 1976 National Academy of Science study on the energy requirements of renewable building materials (Wilson 2005). This research, performed prior to the standardization of LCA, defined the original efforts to catalogue the energy consumption for LCI of wood products, and many advancements to LCA have been made since its publication. It is CORRIM's goal to compile an accurate database for the LCI of common wood products for all life-cycle stages of LCA (material extraction through end-of-life), and to make this information publicly available and useful (Wilson 2005). Results from CORRIM's expansion on the 1976 study were published in special editions of Wood and Fiber Science (volumes 37 and 42) in two

phases of reports (Phase I and Phase II). References in the literature refer to the 1976 study as the original CORRIM study, and the Phase I and II studies published in 2005 and 2010, respectively, as the CORRIM II study. Phase I covered the first six steps of the 22-step research initiative, compiling LCI data for the production of softwood lumber, plywood, I-joists, glue-laminated timbers, and laminated veneer lumber. Additionally, this phase of reports included the results from research on forest activities, disposal of residential structures, implications of carbon storage, as well as a comparison LCA of two residential structures (Wilson 2005). Phase I focused specifically on the Pacific Northwest U.S. (PNW) and the southeast U.S. (SE). Phase II of this research focused on the northeastern (NE) and north central (NC) U.S, as well as to some extent on the inland northwest (INW). This phase compiled LCI data for the production of softwood lumber, hardwood flooring, particleboard, medium density fiberboard (MDF), and resins. Additionally, research was performed on carbon storage in wood products and forest resources, among other efforts (Lippke and Wilson 2010a). The results of these research efforts have been added to the US Life Cycle Inventory database (USLCI), maintained by the National Renewable Energy Laboratory (NREL), and are accessed by LCA software including the Athena Impact Estimator (AIE) (ASMI 2012b). All research performed by CORRIM follows ISO 14040 protocols (ISO 2006). Specific results of CORRIM research from both phases of the CORRIM II research initiative pertaining to this study are further explained below.

Milota et al (2005) compiled survey data from sawmills in the PNW and SW U.S. to determine quantitative values for the energy and materials, as well as the environmental releases required to produce softwood lumber. The primary use of softwood sawn lumber in the U.S. is for residential construction. LCI data gathered were for the manufacturing phase only, cataloguing the inputs and releases from log to final kiln-dried, planed product. Results show that aside from logs, water, natural gas, and diesel are the primary resources consumed during production, and emission sources are dominated by fuel burned for the drying process. The most significant results from a study by Meil et al.(2007) comparing the results of the original CORRIM study with the CORRIM Phase 1 study, pertaining to softwood lumber production, show the increase in efficiency of utilization of raw materials in the manufacturing life-cycle phase. Puettmann et al. (2010b) continued to develop LCI for softwood lumber by examining production in the inland Northwest U.S. Results show similar input and releases, but also that energy source varies considerably by region. A look at kiln-drying showed that it requires a significant portion of the total energy consumed. Electricity use, however was dominated by

equipment use for planing of lumber. The most significant emission was carbon dioxide (CO_2), and approximately two thirds of CO_2 emissions were due to the burning of biomass. LCI development for softwood lumber production was continued by Bergman et al. (2010) to include manufacturing in the NE and NC US. For each mill, material, energy type, and energy amount were again determined. Log conversion to product showed a final material use of 42%. Values for total energy required and total CO_2 emissions were calculated. Conclusions show the necessity to lower energy consumption in sawmills, especially in sawing, drying, and planing, the three main processes necessary for the production. Drying was shown again to consume the highest proportion of fuel, however the burning of biomass for heat generation accounts for 87% of thermal energy used, and conclusions point out that replacing kilns with progressive kilns or providing more air drying would greatly reduce energy requirements. Results for the consumption of electricity for this region were attributed to sawing operations. This study suggested many ways in which energy (electricity and fuel) needs could be reduced at the mill site.

Puettmann et al. (2010a) performed LCI and comparisons for softwood lumber, hardwood lumber, and hardwood flooring manufactured in the inland NW, NE, and NC U.S. The bounds of this study included forestry, material extraction, transportation, and product manufacturing. The manufacturing life-cycle stage demonstrated the highest demand of total energy, and the energy requirement for hardwood manufacturing was approximately twice that of the manufacturing of softwood. This can be attributed to the energy required for heat generation for kiln-drying. Environmental releases were due primarily to the use of fuels and electricity, a small percentage of which was due to transportation. These products are shown to be manufactured primarily with energy provided biofuels. Additionally, comparisons between regions show more energy demand in the North-Central and Northeastern parts of the country than the inland Northwest.

LCI data for the production of softwood plywood were gathered by research performed by Wilson and Sakimoto (2005). This gate-to-gate study included only the manufacturing phase, compiling all material and energy input and environmental releases applicable to all material processing and plywood production. Survey results from PNW and SW plywood manufacturers provided the high-quality data, which were processed with SimaPro LCI software. Results show that inputs included logs, fuel and electricity, veneer, and resin, and outputs included emissions to air, land, and water, as well as a variety of co-products. The primary emission of carbon dioxide

(CO2) was attributed to the burning of biofuels. Variation in energy source showed a high contribution from hydro power in the PNW, where the SW relies considerably on fossil fuels. Primary energy use was provided by the burning of biofuels, representing nearly half of the total energy used in both the PNW and SW.

LCI data for oriented strand board for the SW U.S. were gathered by Kline (2005) from surveying OSB manufacturing plants. Results show that 71% of material input (logs) contributes to the final product, and the remaining 29% is burned as biofuels or used for co-products. Over half of the energy necessary for the production of OSB is generated on-site (primarily from burning biofuels), and the remainder of this energy comes from natural gas. Additional inputs include resin/wax and other fuels. Environmental releases generated at the manufacturing plant include CO_2, volatile organic compounds, and particulates, and additional releases for the production of resin, wax, and electricity, are generated off-site. The release of atmospheric CO_2 from burning biofuels is a significant environmental burden in the production of OSB, however, 69% of carbon stored in the raw material input remains in the final product.

An essential component to many composite wood products is formaldehyde-based resins. LCI research was performed by Wilson (2005) because the material and energy inputs and environmental releases associated with resins are an essential component in the LCI of wood composites. This study determined the LCI for all applicable resins produced in the U.S. through survey responses representing a large percentage of manufacturers. Environmental impacts were determined for operations at the manufacturing site, as well as cradle-to-gate, including resource extraction and manufacturing. Cradle-to-gate results showed a significantly higher impact than results from the manufacturing site alone, indicating that the material extraction has a high environmental burden and that resin manufacturing operations are resource-efficient and have relatively little environmental burden.

The LCI research efforts detailed above represent the portion of studies performed on wood structural materials applicable to this study. Additional studies have been performed on specific wood products that have not been included here, but are available in phases I and II of the CORROM II reports. An important focus of additional investigations performed by CORRIM is the relevance of carbon storage with respect to the wood products industry.

Perez-Garcia et al. (2005b) performed analytical research that identifies three separate carbon pools related to carbon storage and wood products, and observed the effects of forestry

practices on total carbon balance. These carbon pools include the forest, wood products, and the displacement of carbon emissions provided by utilization of wood products. Carbon is stored in wood fiber as a tree grows, and wood products continue to store this carbon. Furthermore, the use of wood products displaces the additional energy required (and therefore the additional emissions) from the manufacture of products of equivalent function that require increased levels of processing. Results show that a significant reduction in atmospheric carbon is shown only when all three carbon pools are considered, and wood products are not only manufactured, but are also considered as product substitutes for more carbon-intensive materials such as concrete or steel. Lippke et al. (2010b) examined carbon emissions and storage, and compared the important contribution of wood products to alternative materials including steel and concrete. The LCA of a residential building composed of these varying products was performed and its impact on global warming potential (GWP) was observed. Results show that carbon stored in wood products makes a wooden structure's contribution to reducing GWP significant. The use of wood-based structural materials reduces carbon emissions due to "fossil fuel combustion, carbon stored in products, permanent avoidance of emissions from fossil fuel-intensive products, and use of a sustainable and renewable resource." Lippke et al. (2010b) also recognize that carbon stored in wood products offers the possibility of offsetting the emissions from residential building products that do not store carbon. Results point back to the forest, and offer a sound argument for sustainable forest management, harvesting, and use of wood products.

An opportunity taken by Meil et al. (2007) to compare the original CORRIM study (NRC 1976) with phase I of the CORRIM II study outlined the advances made in the production and utilization of wood products over the preceding 30 years. LCA inherently relies on the most recent LCI data available, and since the forest products industry is always changing and improving, these changes provide perspective on the necessity of continual research. Additionally, an understanding of the general direction of the forest products industry lends perspective on its future, and points out where improvements are still needed. This comparison focuses on the production of softwood lumber, plywood, and OSB, three wood products that were analyzed in both reports. Fuel source is trending more towards the burning of biofuels, and volume of waste products are reduced due to this trend. Increased use of biofuels has led to a decreased dependence on fossil fuel sources, and this has resulted in a decreased GWP. Overall, observations of total energy use show a significant decrease in consumption for all three products. Though mechanical processing requires more electricity than in the 1970's, advances made in

kiln-drying operations provide for a decrease in energy requirement. As stated above, results show the most significant improvement in the efficient utilization of raw materials for the manufacture of softwood lumber. Plywood and OSB production efficiency have remained constant, however with decreased available log size and quality, this still shows improvement. The forest products industry is utilizing more species and lower qualities of raw materials, yet producing higher if not equal quality products.

Research aimed at the development of the U.S. Life Cycle Inventory (USLCI), such as the research performed on wood products by CORRIM serves the purpose of providing data for LCA studies. LCA studies have been performed on the comparison of wood structures with those comprised of other materials, as well as comparing wood products directly to one another in building systems. Perez-Garcia et al. (2005a) performed cradle-to-gate and cradle-to-grave comparative LCA of two residential structures, each with alternative building materials reflective of common construction practices in their respective region, either Atlanta, GA, or Minneapolis, MN. Material selection for the Atlanta house included a structural system that employed primarily wood or concrete, and material selection for structural system for the Minneapolis house was either wood or steel. Note that Atlanta is considered warm climate, and the Minneapolis location is considered a cold climate. LCA were performed on complete building assemblies and individual structural sections of each house (walls, floors, etc.). Though each residential design employed many similar non-wood materials for non-structural purposes, differences in environmental impact were considerable. Results from these comparisons show that wood employed for the structural system outperformed the steel or concrete systems in almost every impact category considered for this cradle-to-grave assessment. Additionally, investigations were made on wood-based material substitutions within the wood structures, themselves. The substitution of plywood instead of OSB sheathing showed a decrease in environmental burden. Questions, however, were raised concerning net gain with this substitution due to the efficient use of wood fiber in the manufacture of OSB. With respect to GWP, it was noted that the emissions generated from drying operations to produce wood products were only a fraction of those generated by the manufacture of steel or concrete. Additionally, it was shown that use of steel or concrete requires significantly more non-bio-based fuels than the use of wood does.

Salazar and Meil (2009) investigated the energy and carbon balances of two residential buildings designed with typical light-frame structural support. Beyond the wood structural

system, one building was designed to employ common building materials that are typically not wood-based, including asphalt shingles, fiberglass insulation, brick cladding, and vinyl siding, but are more typical of residential construction today. The second residential building, however, was designed to be "wood-intensive," utilizing wood products such as cedar shingles, cellulose insulation, and wood windows and siding. Investigations performed focused on three separate carbon systems: forest sequestration, product manufacturing, and end-of-life. Where results showed net carbon emissions for a cradle-to-gate LCA, the "wood-intensive" building was approximately carbon neutral, storing approximately three times the carbon in its structure than the typical structure. Additionally, the wood-intensive structure consumed less than half of the fossil fuels consumed throughout the typical structure. The maintenance life-cycle stage shows that wood materials such as shingles and siding require more maintenance, and therefore drive up the environmental impact of this life-cycle stage. When compared to manufacturing and construction life-cycle stages, however, the increase in burden from manufacturing non-wood cladding and roofing more than justifies the impact of maintenance of wood cladding and roofing.

Frenette et al. (2010) performed research to aid the performance measuring of light-frame wood wall systems with LCA. This research was performed to determine the positive and negative attributes of different accepted methods of conducting LCIA. A case study was performed comparing 5 light-frame wooden wall systems in a residential building located in Quebec City. Life-cycle stages considered include construction and maintenance. LCI was generated by the Athena Environmental Impact Estimator, and LCIA is performed according to three separate tools: Impact 2002+ and Eco-Indicator 99 (both using SimaPro software), and TRACI (using Athena software). Initial results from use of different software and varying LCIA methods show that while SimaPro software allows for a more generic LCA approach, the Athena software is easier to use and provides sufficient LCI.

With respect to LCA accuracy, Kellenberger and Althaus (2008) performed a detailed analysis of LCA results from various building assemblies with varying degrees of simplicity. The objective was to observe how simplifications and generalizations that are often made in LCA studies affect the outcome of impact results. Simplifications to LCA included five separate levels of detailing, from complete to significantly reduced. Results show that neglecting ancillary materials in a wooden structure (nails, screws) had significant effect on LCA outcomes. Results also show that close attention to cutting waste has little impact on overall LCA results.

Hindman (2011) performed research on the LCA of "post-frame" buildings for the purpose of developing tools for LCA and life cycle costing (LCC) that include this type of construction. Hindman recognizes that currently there are no commercial tools to assess the environmental impacts of this type of construction directly Additionally, current green building certification systems do not recognize the sustainable attributes of post-frame construction. Positive attributes of post-frame buildings noted include "reduced site disturbance, less use of wood to create the structural system, engineered systems for the roof structure, and a building cavity with room to accommodate insulation…" Though this research focuses primarily on the operations life-cycle stage, it is clear that buildings comprised of alternate wooden frames to convention light-framing deserve more attention in the green building community. Three post-frame structures of varying assemblies were modeled for a cradle-to-grave analysis using the Athena Impact Estimator as equivalent light-frame structures. The bill of materials for each structure was created by defining light-frame building assemblies with equivalent amounts of wood to the post frame structure. This method was used so that insulation, cladding, windows, and doors could be added to predefined wall and roof systems. Additionally, the 'extra basic materials' option was used to add or subtract materials necessary to equate this light-frame structure to the post-frame structure.

STRUCTURAL LOAD PATH ANALYSIS

In order to observe load paths of transmitted design loads through a structure, structural analysis computer models must be constructed. The modeling methods used to define each structural element and the source of material properties define how the model will predict the performance of the force resisting system. Martin et al. (2011) developed a method for modeling a simple rectangular light-frame (LF) structure in SAP2000. These modeling methods were created with ease of application and accessibility of material properties in mind so that it could be easily adapted by industry. Framing members were modeled as frame elements in SAP2000 with isotropic material properties, and sheathing elements were modeled as shell elements in SAP2000. Joints were modeled as either pinned or rigid connections, thereby eliminating the necessity to quantitatively characterize the stiffness of connections. The effects of nail connections in sheathing were accounted for by adjusting the directional shear modulus for the sheathing, and therefore it was not necessary to model individual connections. Additionally, this model was created to assume linear behavior. The model was created with material properties easily available designers from industry standards and specifications making it a more accessible

method for designers in industry. This model was successfully validated with partial and full-scale models, as well as wind tunnel experiments, from research performed at the University of Florida (Datin 2009).

Pfretzschner et al. (2013) utilized the modeling methods developed by Martin et al. (2011) to create a model in SAP2000 for a more realistic LF residential structure. The residential structure modeled by Pfretzschner et al. (2013) introduced interior walls and a re-entrant corner, and was essentially L-shaped and more typical of a wood-framed home. This model is reflective of a structure built and tested by Paevere et al. (2003) in Australia. Similarly, Pfretzschner's model utilized material properties from industrial specifications rather than experimental results, and incorporated nearly all of the same modeling parameters as Martin et al. (2011). Models in this study were also linear, developed for observations within the elastic range. Where Martin et al. (2011) modeled sheathing members as a thick shell element in SAP2000, Pfretzschner et al. (2013) modeled sheathing as a layered shell element in SAP2000, appropriately accounting for sheathing consisting of both exterior OSB and interior gypsum board. Similarly to Martin et al. (2011), sheathing was modeled as one sheathing element per wall, meshed into smaller elements. The effects of nail connections in the sheathing were accounted for by adjusting the shear modulus. This model was successfully verified by comparison with full-scale testing of two-dimensional trusses, three-dimensional roof assemblies, two-dimensional shear walls, and finally testing performed on a full-scale assembly of the Paevere et al. (2003) house.

There has been considerable research on the modeling of LF wood structures. A detailed literary review of these efforts has been presented by both Martin (2010) and Pfretzschner (2012), and is, therefore, not included here.

Research presented in the iterature pertaining to timber frame (TF) structures has focused primarily on individual joint behavior, or the behavior of small TF assemblies. The majority of research performed has involved full-scale testing of joints and assemblies for stiffness, strength, and failure mode. There have also been several investigations on the strength, bearing capacity, and failure modes of wooden pins (pegs) within these joints. Since the research performed in this study does not relate specifically to experimental testing or behavior of individual joints, only research pertaining to computer modeling of frame systems will be discussed in detail. Note that specific experimental testing research pertaining to timber frame assembly stiffness is, however, briefly discussed.

Early research in timber frame behavior modeling dates back only as far as 1985, when Brungraber (1985) performed full-scale testing on individual joints and frame assemblies, and

created a two-dimensional finite element model to predict joint behavior. This model incorporated three springs, characterizing the stiffness of joints in all three orthogonal directions, with stiffness values based on experimental testing. This research is important because it led to many further investigations pertaining to TF construction.

Sandberg et al. (1996) performed experimental testing on partial frame assemblies, and focused on joint behavior. These assemblies consisted of a post, beam, and for many assemblies tested, a knee brace between the two. Four separate post-beam connections were tested: a mortise-and-tenon joint, a mortise-and-tenon joint with a shoulder, a mortise-and-tenon joint with a knee brace, and a tongue-and-fork joint. Important results related to stiffness from these experiments, published by Bulliet et al. (1999) show that joints exhibit low stiffness at initial loading, and stiffness increases as loads increase. Additionally, joint stiffness was greatly affected by how tightly the joints initially fit together. This was also a result of testing performed on joints by both Schmidt and Daniels (1999) and Schmidt and Scholl (2000) at the University of Wyoming. The research performed by Schmidt and Daniels (1999) was to observe and catalogue failure modes of mortise-and-tenon joints, and the research performed by Schmidt and Scholl (2000) was focused on the difference in performance between seasoned and unseasoned joints. Erikson and Schmidt (2003) point out that this result is likely indicative of full-scale frame behavior. Additionally, modeling efforts by Bulliet et al. (1999) to characterize individual joint behavior included modeling each joint as a combination of a horizontal, a vertical, and a rotational spring. Modeling efforts for frame systems (of three members: a beam, a column, and a brace) included using commercially available modeling systems, SAP IV and SAP90. This complicated modeling method utilizes frame elements only for members, and though joints are modeled as pinned, theoretical frame element members have been introduced to model pin (peg) connections, each assigned an appropriate stiffness. Additionally, eccentricity in loading due to joint configuration is accounted for. For characterization of the stiffness of simulated pegged connections, the shear modulus is defined as the modulus of elasticity (in bending) divided by 16. This modeling technique, performed for all types of joints tested, provided good results for deflection behavior and bending moments.

Lateral stiffness testing and modeling was performed by Erikson et al. (2003). Lateral loads were applied to TF wall systems and stiffness calculations were performed based on deflection. Tests were performed on 1-story, 1-bay frames, and well as 2-story, 2-bay frames. Additionally, stiffness of these wall sections was calculated for the frame alone, as well as for when the frame is sheathed in SIPs. Different connection schedules for wall sheathed with SIPs

were also observed. These included the presence or absence of a sill plate, the use of different fasteners, and installing SIPs such that SIP joints were all located over framing members or using splines where SIP joints were not over framing members. The most important result of this research was that the timber frame alone demonstrated a considerable lack of stiffness. The timber frame with SIPs, however, was shown to significantly increase stiffness. Additionally, recommendations for increasing frame stiffness in TF structures sheathed with SIPs included locating SIP joints over framing members, attaching with screws around the complete SIP perimeter, and avoiding the necessity to use splines. This study also recommends that the framing system of a TF be designed for gravity loads, and SIPs be designed to carry all lateral loads. With respect to modeling, Erikson points out that since the stiffness of a TF is dependent on the stiffness of individual joints, modeling should be performed to include the non-linear stiffness of these connections. Though it is understood that this consideration would add to increased accuracy, the modeling methods designed by Martin et al. (2011) and Pfretzschner et al. (2013) focus on applicability and simplicity, and therefore do not include modeling of specific connections or modeling in the non-linear range. Additionally, since stiffness is completely controlled by sheathing modeling in these methods, individual connection stiffness can be modeled as pinned.

Carradine et al. (2000) performed research to liken the diaphragm action design methodology of post-frame structures (post structures with roof trusses and metal cladding) to TF design. A sample timber frame design for a structure sheathed in SIPs was performed to illustrate the appropriateness of including diaphragm action for its design. To build upon this 2000 paper, Carradine et al. (2004) performed strength and stiffness testing on TF roof assemblies with SIPs for the purpose of establishing procedures for incorporating these values into design procedures. Since it is understood that TF construction, alone, does not provide adequate lateral force resistance, this research was performed to quantify the reduction in lateral burden on the TF by SIPs. Testing was performed on two sizes of roof section, an 8-ft x 24-ft section, and a 20-ft x 24-ft section. Assemblies consisted of vertical rafters and horizontal purlins, and 4-ft x 8-ft SIPs were attached around their complete perimeters to framing members. Loading was applied to a central rafter parallel to the direction of rafters, and strength and stiffness for each assembly were determined. Similar to findings by Pfretzschner et al. (2013), Carradine stated that a reasonable design assumption is that shear stiffness increases linearly with increased length by extrapolating the stiffness of an 8-ft-long section to longer sections. The analysis of a typical residential TF was used to determine the reduction in forces from lateral loading on TF members and joints,

assumed by a SIP diaphragm. Two-dimensional sections of this structure were modeled in PPSA4, and member and joint forces were determined. Note that this analysis showed that the TF, alone, could not sufficiently resist design forces, and certain joints were overstressed by as much as 160%. Data from testing SIPs, incorporated into a stiffness equation, provided a reduction in forces that brought the forces in members and joints down to below allowable loads. Without including diaphragm action, this would not have been possible without increasing member sizes.

Experimental testing performed by He and Lu (2011) comparatively investigated the lateral performance of "post-beam" structures, light wood frame structures, and a hybrid version of these two construction methods. Though the post-beam structure referred to in this study is not assembled with mortise-and-tenon joinery, the interaction of these two framing systems is still indicative of the performance of a hybrid structure between a TF and an LF. Wall sections depicting each structural system described were constructed and tested with lateral loads applied, and deformations were observed. Conclusions show that the LF wall sheathed with OSB could support a significantly higher ultimate lateral load than the post-frame structure (unsheathed). A hybrid of the two structures, however, was able to resist an even higher ultimate lateral load than the light frame alone. Note that the post-frame structures in this study did not employ braces like TF structures do.

Kermani and Hairstans (2006) performed research on the racking performance of SIPs. This paper provides the detailed findings of an experimental study performed at Napier University in Scotland. This testing examined SIPs under racking loads, as well as combined bending and axial compression. Additionally, the effects of openings were examined. Testing was performed under the assumption that a SIP wall system may be a viable replacement for LF, and therefore loads were applied to SIPs alone. Considering the fact that TF modeling is most simply performed by assuming pinned joints and allowing the stiffness to be controlled completely by the SIPs makes these results applicable to modeling efforts. Results show that SIP walls demonstrate superior racking stiffness to a traditional LF wall system. Additionally, this racking stiffness is increased as vertical loads are applied. The racking strength of SIP walls is directly related to the size of openings, and racking strength decreases with increase in opening size. Similar testing was also performed on SIPs by Terntiuk and Memari (2012), in which parameters such as displacement, peak load, and allowable drift were determined. Results from this study showed that connections controlled many of these parameters, and the type of fastener, in particular (screw, nail, or staple), had the greatest effect on performance. Results from tests on

SIP assemblies utilizing splines for connections between ships reinforce the conclusion met by many previous research efforts that SIP joints are most effectively located over framing members (therefore not requiring splines).

APPENDIX B

TIMBER FRAME DESIGN

The timber frame (TF) structure designed for this study was inspired by a traditional TF building designed and constructed by the author in Vermont in 2011. This structure was modified from its original as-built version for simplification and generalization, but has maintained as many of the as-built features as possible, including building envelope and structural materials. Verification of the structural validity of the member sizes chosen was performed with Allowable Stress Design (ASD) methods outlined in the National Design Specification for Wood Construction (NDS) (AF&PA 2005a) using design gravity loads, and the results of this verification are presented below. Note that calculations were performed only on members determined to need structural verification, and only with gravity loads considered. Other members have been determined acceptable based on the results of similar (less conservative) member calculations, presented below.

Design calculations were performed on the ridge beam, rafter plates, 1st floor tie beams, floor joists, 2nd story center posts, and 1st story center posts. Figure B.1 and Figure B.2 are images from a Google Sketch-Up rendering that depicts the location of these members within the structure (Google 2012).

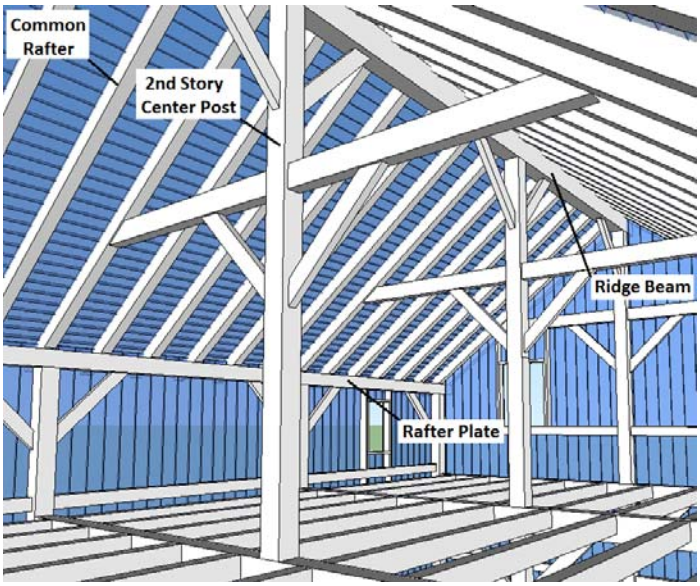

Figure B.1: Timber frame members designed, 2nd story

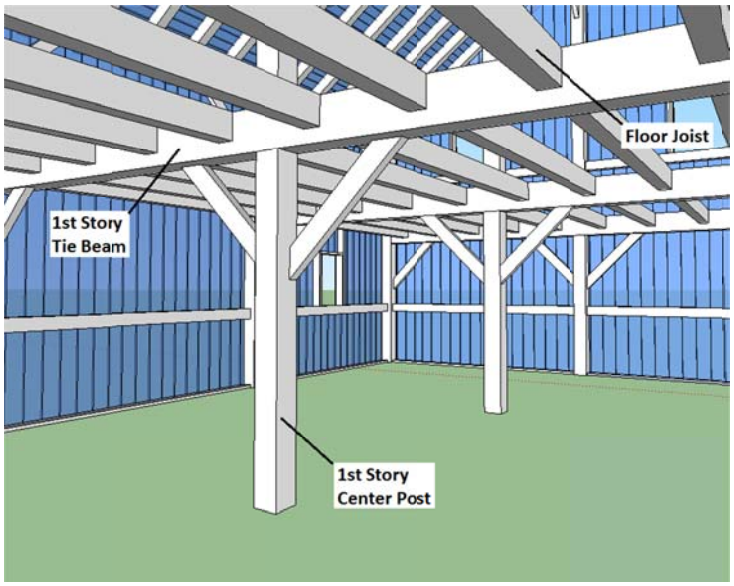

Figure B.2: Timber frame members designed, 1st story

A detailed description of the design of the ridge beam is presented below. The results for other members subject to bending and shear follow. These members were designed by the same general method. The design procedure specific to posts is presented in the following section, "Design of members subject to compression parallel to grain."

DESIGN OF MEMBERS SUBJECT TO BENDING AND SHEAR

Ridge beam

Material properties were determined using the NDS (AF&PA 2005). The species chosen (eastern hemlock) reflects what was used for the construction of the building that inspired this study. The material grade chosen represents the minimum grade allowable, based on this design. The material properties presented in Table B.1 are those necessary for the design of the ridge beam. Note that the material properties necessary for design vary among members based on loading. Beams such as the ridge beam must be checked for bending, shear, and deflection, whereas columns such as the 1st or 2nd story center column must be checked for compression parallel to grain.

Table B.1: Ridge beam material properties

Material Properties		
Species	Eastern Hemlock	
Grade	#1	
Bending (F_b)	1150	lb/in^2
Shear II to Grain (F_v)	155	lb/in^2
Modulus of Elasticity (E)	1,200,000	lb/in^2

Applicable design building loads were determined based on ASCE 7-10, Minimum Design Loads for Buildings and Other Structures (ASCE 2010). These values are listed in Table B.2, and are based on requirements for a typical residential structure. Ground snow load of 60 psf for this location, however, was dictated by local requirements (Jay, Vermont) and is greater than the value reported by ASCE 7-10 of 50 lb/ft^2 (ASCE 2010). The controlling load case is determined by equation B1:

$$\text{Controlling Load Case} = \text{Maximum value of: } \frac{LoadCombination}{C_D} \quad \textbf{(B1)}$$

Where:

C_D = Time duration factor ($C_{D(DEAD)} = 0.9$, $C_{D(LIVE)} = 1.0$, $C_{D(SNOW)} = 1.15$)

This must be calculated for each applicable ASD load combination. The appropriate C_D factor for each calculation is the largest value of possible of the C_D factors associated with the types of loading in each given load combination. The highest resulting value of this calculation coincides with the controlling load case. Note that the value of the above calculation is valid for determination of the controlling load case only.

Table B.2: Ridge beam loading

Loadings Considered		
Dead	15	lb/ft^2
Live	0	lb/ft^2
Snow	60	lb/ft^2
Construction Live	0	lb/ft^2
Wind	0	lb/ft^2
Earthquake	0	lb/ft^2
Total Load	75	lb/ft^2
Controlling Load Case	D+S	

Necessary physical information to determine loading parameters includes member length and tributary area of loading. These values are determined based on the design layout of the structure. With these values, a line loading is calculated (load per linear foot of the member) based on design loads to determine the maximum values of moment and shear which must be supported by the beam. These values are then converted to actual shear and bending stresses. The maximum actual deflection of the beam is also calculated.

The maximum values of moment (M_{actual}) and shear (V_{actual}) for the ridge beam were determined as outlined in equations B2 and B3. Note that equations B2 and B3 are specific to members that are subject to an evenly distributed load such as the ridge beam, and change for alternate load distributions.

$$M_{actual} = \frac{wL^2}{8} \text{ (lbf)} \qquad \textbf{(B2)}$$

$$V_{actual} = \frac{wL}{2} \text{ (lb)} \qquad \textbf{(B3)}$$

Where:

w = line loading (lb/ft)

L = member length (ft)

Calculations for the actual bending stress (f_b), the actual shear stress (f_v), and the actual deflection were performed as outlined in equations A4 through A6.

$$f_b = \frac{M_{actual}}{S} \text{ (lb/in}^2\text{)} \quad \textbf{(B4)}$$

$$f_v = \frac{1.5 * V_{actual}}{A} \text{ (lb/in}^2\text{)} \quad \textbf{(B5)}$$

$$d_{actual} = \frac{5wL^4}{384EI} \text{ (in)} \quad \textbf{(B6)}$$

Where:

S = Section Modulus (in^3)

I = Moment of Inertia (in^4)

E = Modulus of Elasticity (lb/in^2)

A = Cross-Sectional Area (in^2)

The results of the calculations above for the ridge beam are presented in Table B.3.

Table B.3: Ridge beam, beam information and section properties

Beam Information		
Beam Span	12.5	ft
Beam Span	150	in
Tributary Width	13.0	ft
Tributary Area	162.5	ft^2
Line Loading (w)	975	lb/ft
Maximum Moment, M (K-in)	228.5	Kip-in
Maximum Moment, M (lb-in)	228,516	lb-in
Maximum Shear, V	6,094	lb
Actual Bending Stress (f_b)	1,190	lb/in^2
Actual Shear Stress (f_v)	95	lb/in^2
Actual Deflection (d_{actual})	0.39	in
Section Properties		
X-Section Width (b)	8.0	in
X-Section Depth (d)	12.0	in
Cross-Sectional Area (A)	96.0	In^2
Section Modulus (S)	192.0	in^3
Moment of Inertia (I)	1,152.0	in^4

Actual bending stress (fb), shear stress (fv), and deflection (d) are then compared to allowable values for these parameters. The allowable values for bending stress and shear stress are based on material properties (allowable stresses), and are subject to adjustment factors (explained below). The maximum allowable deflection ($d_{allowable}$) is determined based on some fraction of the member's maximum span length, and is outlined in equation B7.

$$d_{allowable} = \frac{L}{240} \qquad \textbf{(B7)}$$

Adjustment factors are employed for the adjustment of material properties which affect the expected performance of the material based on environmental and design parameters. The adjustment factors that are employed in this design include those applicable to sawn lumber.

Time Duration Factor (C_D): The load duration factor accounts for the ability of wood, as a material, to withstand higher loads for shorter periods of time. The load duration factor is

assigned based on the controlling load case for each member, and is determined from Table 2.3.2 of the NDS (AF&PA 2005).

Wet Service Factor (C_M): The wet service factor applies to solid-sawn wood that has a moisture percentage of greater than 19%. This factor applies to this design because it is assumed that the TF is constructed from green timbers. Though these timbers will become dry over time, this assumption must be made based on the structure's initial condition which is most conservative. According to the NDS (AF&PA 2005), the wet service factors for timbers subjected to bending and shear stress are 1.0. When designing axially loaded members, the wet service factor (for members experiencing compression parallel to grain) is 0.91 (AF&PA 2005).

Temperature Factor (C_T): The temperature factor applies to structural members that will experience exposure to sustained temperatures "up to 150-degrees Fahrenheit." This factor does not apply to this design, and therefore equals 1.0 for all members (AF&PA 2005).

Size Factor (C_F): The size factor accounts for the non-linear ability of members of increasing size to withstand increasing loads. Provided the timber is not loaded on its wide face, the size factor is equal to 1.0 for all members that have a depth of less than 12". This applies to all members in this design (AF&PA 2005).

Flat Use Factor (C_{FU}): The flat use factor does not apply to timbers (AF&PA 2005).

Incising Factor (C_i): The Incising factor does not apply to timbers (AF&PA 2005).

Repetitive Member Factor (C_r): The repetitive member factor does not apply to timbers (AF&PA 2005).

Beam Stability Factor (C_L): The beam stability factor accounts for the possibility of lateral torsional buckling. Since the d/b ratio for every applicable member in this structure is less than 2.0, according to section 4.4.1.2 of the NDS, no lateral support is required and therefore $C_L = 1.0$ (AF&PA 2005).

Column Stability Factor (C_p): The column stability factor applies to members subject to axial loading, and affects compression parallel to grain (F_c). This factor accounts for the possibility of flexural buckling.

Adjustment factors are applied to specific material properties as outlined in Table B.4. An "X" indicates that the specified factor is applicable to the given material property.

Table B.4: Applicability of adjustment factors for sawn lumber

	Load Duration Factor	Wet Service Factor	Temperature Factor	Beam Stability Factor	Size Factor	Column Stability Factor
Fb	X	X	X	X	X	-
Fv	X	X	X	-	X	-
Fc	X	X	X	-	X	X
E'	-	X	X	-	-	-

Table B.5 outlines the adjustment factor values applicable to the design of the ridge beam, and the adjusted material properties for this member.

Table B.5: Ridge beam, adjustment factors and adjusted material properties

Adjustment Factors		
(Load Duration) C_D	Controlling Load Case = D+S	1.15
(Wet Service) C_M	Moisture > 19% Limit (Wet)	1.0
(Temperature) C_t	No high temperature exposure	1.0
(Size Factor) C_f	Loaded in strong direction, d not >12"	1.0
(Flat Use) C_{fu}	Not Applicable to Timbers	NA
(Incising) C_i	Not Applicable to Timbers	NA
(Repetitive Member) C_r	Not Applicable to Timbers	NA
(Beam Stability) C_L	d/b < 2	1.0
Adjusted Material Properties		
Bending (Fb')	1323	lb/in^2
Shear II to Grain (Fv')	178	lb/in^2
Modulus of Elasticity (E')	1,200,000	lb/in^2

Structural members subject to bending and shear forces, such as the ridge beam, must be checked for bending, shear, and deflection. The allowable stress or deflection must therefore be greater than the actual stress or deflection expected. Tables B.6 to B.10 compare the adjusted material property or deflection ("allowable") to the stresses and deflection expected ("actual"), as imposed by design forces.

Table B.6: Ridge beam, member selection validation

Bending			
Actual Bending Stress, f_b	1,190	lb/in^2	**Acceptable**
Allowable Bending Stress, F'_b	1,323	lb/in^2	
Shear			
Actual Shear Stress, f_v	95	lb/in^2	**Acceptable**
Allowable Bending Stress, F'_v	178	lb/in^2	
Deflection			
Actual Deflection, d_{actual}	0.39	in	**Acceptable**
Allowable Deflection, $d_{allowable}$	0.63	in	

Table B.7: Rafter plate design validation

Material Properties		
Species	Eastern Hemlock	
Grade	#1	
Bending (F_b)	1150	lb/in^2
Shear II to Grain (F_v)	155	lb/in^2
Modulus of Elasticity (E)	1,200,000	lb/in^2
Loading		
Dead	15	lb/ft^2
Live	0	lb/ft^2
Snow	60	lb/ft^2
Construction Live	0	lb/ft^2
Wind	0	lb/ft^2
Earthquake	0	lb/ft^2
Total Load	75	lb/ft^2
Controlling Load Case	D+S	
Beam Info		
Beam Span	12.5	ft

Beam Span	150		in
Tributary Width	6.5		ft
Tributary Area	81.25		ft^2
Line Loading (w)	487.5		lb/ft
Maximum Moment, M (K-in)	114.3		Kip-in
Maximum Moment, M (lb-in)	114,258		lb-in
Maximum Shear, V	3,046.9		lb
Actual Bending Stress (f_b)	1,339		lb/in^2
Actual Shear Stress (f_v)	71.0		lb/in^2
Actual Deflection	0.65		in
Section Properties			
X-Section Width (b)	8.0		in
X-Section Depth (d)	8.0		in
Cross-Sectional Area (A)	64.0		In^2
Section Modulus (S)	85.3		in^3
Moment of Inertia (I)	341.3		in^4
Adjustment Factors			
(Load Duration) C_D	Controlling Load Case = D+S		1.15
(Wet Service) C_M	Moisture > 19% Limit (Wet)		1.0
(Temperature) C_t	No high temperature exposure		1.0
(Size Factor) C_f	Loaded in strong direction, d not >12"		1.0
(Flat Use) C_{fu}	Not Applicable to Timbers		NA
(Incising) C_i	Not Applicable to Timbers		NA
(Repetitive Member) C_r	Not Applicable to Timbers		NA
(Beam Stability) C_L	d/b < 2		1.0
Adjusted Material Properties			
Bending (F_b')	1323		lb/in^2
Shear II to Grain (F_v')	178		lb/in^2
Modulus of Elasticity (E')	1,200,000		lb/in^2
Member Selection Verification			
Bending			
Actual Bending Stress, f_b	1,339	lb/in^2	**Acceptable***
Allowable Bending Stress, F'$_b$	1,323	lb/in^2	

Shear			
Actual Shear Stress, f_v	71	lb/in^2	**Acceptable**
Allowable Bending Stress, F'_v	178	lb/in^2	
Deflection			
Actual Deflection, d_{actual}	0.65	in	**Acceptable***
Allowable Deflection, $d_{allowable}$	0.63	in	

*Acceptable within small percentage for this hypothetical design.

Table B.8: 1st-floor tie beam design validation

Material Properties		
Species	Eastern Hemlock	
Grade	#1	
Bending (Fb)	1150	lb/in^2
Shear II to Grain (Fv)	155	lb/in^2
Modulus of Elasticity (E)	1,200,000	lb/in^2
Loading		
Dead	10	lb/ft^2
Live	40	lb/ft^2
Snow	0	lb/ft^2
Construction Live	0	lb/ft^2
Wind	0	lb/ft^2
Earthquake	0	lb/ft^2
Total Load	50	lb/ft^2
Controlling Load Case	D+L	
Beam Info		
Beam Span	12.0	ft
Beam Span	144	in
Tributary Width	13.1	ft
Tributary Area	157.2	ft^2
Line Loading (w)	655	lb/ft
Maximum Moment, M (K-in)	141.5	Kip-in
Maximum Moment, M (lb-in)	141,480	lb-in
Maximum Shear, V	3,930	lb
Actual Bending Stress (f_b)	737	lb/in^2
Actual Shear Stress (f_v)	61	lb/in^2
Actual Deflection	0.22	in

Section Properties			
X-Section Width (b)	8.0		in
X-Section Depth (d)	12.0		in
Cross-Sectional Area (A)	96.0		In^2
Section Modulus (S)	192.0		in^3
Moment of Inertia (I)	1152.0		in^4
Adjustment Factors			
(Load Duration) C_D	Controlling Load Case = D+L		1.0
(Wet Service) C_M	Moisture > 19% Limit (Wet)		1.0
(Temperature) C_t	No high temperature exposure		1.0
(Size Factor) C_f	Loaded in strong direction, d not >12"		1.0
(Flat Use) C_{fu}	Not Applicable to Timbers		NA
(Incising) C_i	Not Applicable to Timbers		NA
(Repetitive Member) C_r	Not Applicable to Timbers		NA
(Beam Stability) C_L	d/b < 2		1.0
Adjusted Material Properties			
Bending (F_b')	1150		lb/in^2
Shear II to Grain (F_v')	155		lb/in^2
Modulus of Elasticity (E')	1,200,000		lb/in^2
Member Selection Verification			
BENDING			
Actual Bending Stress, f_b	737	lb/in^2	**Acceptable**
Allowable Bending Stress, F'_b	1,150	lb/in^2	
SHEAR			
Actual Shear Stress, f_v	61	lb/in^2	**Acceptable**
Allowable Bending Stress, F'_v	155	lb/in^2	
DEFLECTION			
Actual Deflection, d_{actual}	0.22	in	**Acceptable**
Allowable Deflection, $d_{allowable}$	0.60	in	

Table B.9: Floor joist design validation

Material Properties		
Species	Eastern Hemlock	
Grade	#2	
Bending (Fb)	750	lb/in^2
Shear II to Grain (Fv)	155	lb/in^2
Modulus of Elasticity (E)	900,000	lb/in^2
Loading		
Dead	10	lb/ft^2
Live	40	lb/ft^2
Snow	0	lb/ft^2
Construction Live	0	lb/ft^2
Wind	0	lb/ft^2
Earthquake	0	lb/ft^2
Total Load	50	lb/ft^2
Controlling Load Case	D+L	
Beam Info		
Beam Span	12.5	ft
Beam Span	150	in
Tributary Width	2.5	ft
Tributary Area	31.25	ft^2
Line Loading (w)	125	lb/ft
Maximum Moment, M (K-in)	29.3	Kip-in
Maximum Moment, M (lb-in)	29,297	lb-in
Maximum Shear, V	781.3	lb
Actual Bending Stress (f_b)	549	lb/in^2
Actual Shear Stress (f_v)	29	lb/in^2
Actual Deflection	0.36	in
Section Properties		
X-Section Width (b)	5.0	in
X-Section Depth (d)	8.0	in
Cross-Sectional Area (A)	40	In^2
Section Modulus (S)	53.3	in^3
Moment of Inertia (I)	213.3	in^4
Adjustment Factors		
(Load Duration) C_D	Controlling Load Case = D+L	1.0

(Wet Service) C_M	Moisture > 19% Limit (Wet)		1.0
(Temperature) C_t	No high temperature exposure		1.0
(Size Factor) C_f	Loaded in strong direction, d not >12"		1.0
(Flat Use) C_{fu}	Not Applicable to Timbers		NA
(Incising) C_i	Not Applicable to Timbers		NA
(Repetitive Member) C_r	Not Applicable to Timbers		NA
(Beam Stability) C_L	d/b < 2		1.0
Adjusted Material Properties			
Bending (F_b')	750		lb/in^2
Shear II to Grain (F_v')	155		lb/in^2
Modulus of Elasticity (E')	900,000		lb/in^2
Member Selection Verification			
Bending			
Actual Bending Stress, f_b	549	lb/in^2	**Acceptable**
Allowable Bending Stress, F'$_b$	750	lb/in^2	
Shear			
Actual Shear Stress, fv	29	lb/in^2	**Acceptable**
Allowable Bending Stress, F'v	155	lb/in^2	
Deflection			
Actual Deflection, d_{actual}	0.36	in	**Acceptable**
Allowable Deflection, $d_{allowable}$	0.42	in	

Table B.10: Common rafter design validation

Material Properties		
Species	Eastern Hemlock	
Grade	#1	
Bending (F_b)	1150	lb/in^2
Shear II to Grain (F_v)	155	lb/in^2
Modulus of Elasticity (E)	1,200,000	lb/in^2
Loading		
Dead	15	lb/ft^2
Live	0	lb/ft^2
Snow	60	lb/ft^2
Construction Live	0	lb/ft^2
Wind	0	lb/ft^2

Earthquake	0	lb/ft^2
Total Load	75	lb/ft^2
Controlling Load Case	D+S	
Beam Info		
Beam Length	15.1	ft
Beam Span	12.1	ft
Beam Span	145.2	in
Tributary Width	2.65	ft
Tributary Area	32.10	ft^2
Line Loading (w)	218	lb/ft
Maximum Moment, M (K-in)	47.8	Kip-in
Maximum Moment, M (lb-in)	47,842	lb-in
Maximum Shear, V	1,317.9	lb
Actual Bending Stress (f_b)	1,172	lb/in^2
Actual Shear Stress (f_v)	56	lb/in^2
Actual Deflection	0.61	in
Section Properties		
X-Section Width (b)	5.0	in
X-Section Depth (d)	7.0	in
Cross-Sectional Area (A)	35	In^2
Section Modulus (S)	40.83	in^3
Moment of Inertia (I)	142.9	in^4
Adjustment Factors		
(Load Duration) C_D	Controlling Load Case = D+S	1.15
(Wet Service) C_M	Moisture > 19% Limit (Wet)	1.0
(Temperature) C_t	No high temperature exposure	1.0
(Size Factor) C_f	Loaded in strong direction, d not >12"	1.0
(Flat Use) C_{fu}	Not Applicable to Timbers	NA
(Incising) C_i	Not Applicable to Timbers	NA
(Repetitive Member) C_r	Not Applicable to Timbers	NA
(Beam Stability) C_L	d/b < 2	1.0
Adjusted Material Properties		
Bending (F_b')	1,323	lb/in^2
Shear II to Grain (F_v')	178	lb/in^2
Modulus of Elasticity (E')	1,200,000	lb/in^2

Member Selection Verification			
Bending			
Actual Bending Stress, f_b	1,172	lb/in^2	**Acceptable**
Allowable Bending Stress, F'_b	1,323	lb/in^2	
Shear			
Actual Shear Stress, f_v	56	lb/in^2	**Acceptable**
Allowable Bending Stress, F'_v	178	lb/in^2	
Deflection			
Actual Deflection	0.61	in	**Acceptable**
Allowable Deflection	0.61	in	

DESIGN OF MEMBERS SUBJECT TO COMPRESION PARALELL TO GRAIN

The design of posts in this structure follows a similar procedure to the design of the bending/shear members described above, with a few important differences. Posts, or columns, are considered subject to purely axial loading. For this reason, the material property "compression parallel to grain" must be validated against the expected (actual) axial load, based on design loads. Validation of bending and shear is not necessary for a member loaded in this manner. In addition, the beam stability factor (C_L) has been replaced with the column stability factor (C_P), described above. The column stability factor must be calculated for both axes of buckling (for a rectangular member) to determine the direction in which the member will buckle first. The lowest value of C_P corresponds to the direction of expected buckling and must therefore be used to calculate adjusted material properties. The procedure for determining C_P for one direction is as follows in equations B7 through B12:

$$C_p = \left(\frac{1+Q}{2c}\right) - \sqrt{\left(\frac{1+Q}{2c}\right)^2 - \frac{Q^2}{c}} \qquad \textbf{(B7)}$$

Where:

c = Interaction Parameter, 0.8 for sawn lumber

Q = Stress Ratio

$$Q = \frac{F_{cE}}{F^*_c} \quad \textbf{(B8)}$$

Where:

F^*_C = Pure crushing stress

$$F^*_c = F_c * (All Adjustment Factors Except C_p) \quad \textbf{(B9)}$$

F_{cE} = Euler Stress

$$F_{cE} = \frac{0.822 * E'_{min}}{R^2} \quad \textbf{(B10)}$$

Where:

R = Slenderness ratio

$$R = \frac{l_e}{d} \quad \textbf{(B11)}$$

Where:

d = Member cross-section depth (parallel to buckling direction)

l_e = Effective length

$$l_e = k_e * l \quad \textbf{(B12)}$$

Where:

l = Member length

k_e = Buckling length coefficient, NDS Table G1 (AF&PA 2005).

For all posts designed for this structure, connections are considered to be pinned at both ends, and therefore k_e = 1.0.

Table B.11: 2nd-story center post design validation

Material Properties		
Species	Eastern Hemlock	
Grade	#2	
Compression II to Grain (F_c)	550	lb/in^2
Loading		
Dead	15	lb/ft^2
Live	0	lb/ft^2
Snow	60	lb/ft^2
Construction Live	0	lb/ft^2
Wind	0	lb/ft^2
Earthquake	0	lb/ft^2
Total Load	75	lb/ft^2
Controlling Load Case	D+S	
Column Info		
Column Length	14.375	ft
Column Length	172.5	in
Tributary Width 1	13.1	ft
Tributary Width 2	13.0	ft
Tributary Area	170.3	ft^2
Actual Axial Load	12,773	lb
Section Properties		
X-Section Width (b)	8.0	in
X-Section Depth (d)	8.0	in
Cross-Sectional Area (A)	64.0	In^2
Section Modulus (S)	85.3	in^3
Moment of Inertia (I)	341.3	in^4
Adjustment Factors		
(Load Duration) C_D	Controlling Load Case = D+S	1.15
(Wet Service) C_M	Moisture > 19% Limit (Wet)	0.91
(Temperature) C_t	No high temperature exposure	1.0
(Size Factor) C_f	Loaded in strong direction, d not >12"	1.0
(Flat Use) C_{fu}	Not Applicable to Timbers	NA
(Incising) C_i	Not Applicable to Timbers	NA
(Repetitive Member) C_r	Not Applicable to Timbers	NA

(Column Stability) C_P	**Intermediate Values (C_P) – Weak Axis**			
	Unbraced Length, l_u (ft)	11.5	ft	
	Unbraced Length, l_u (in)	138	in	
	Buckling Length Coefficient (K_e)	1		
	Effective Length, l_e (ft)	138	in	0.800
	Slenderness Ratio, **R**	17.25		
	Euler Stress, F_{cE}	911.61	lb/in^2	
	Pure Crushing Stress, F^*_c	632.5	lb/in^2	
	Stress Ratio, **Q**	1.44		
	Interaction Parameter, **c**	0.8		
	Intermediate Values (C_p) – Strong Axis			
	Unbraced Length, l_u	6.25	ft	
	Unbraced Length, l_u	75	in	
	Buckling Length Coefficient, K_e	1		
	Effective Length, l_e	75	in	0.954
	Slenderness Ratio, **R**	9.38		
	Euler Stress, F_{cE}	3,086	lb/in^2	
	Pure Crushing Stress, F^*_c	632.5	lb/in^2	
	Stress Ratio, **Q**	4.88		
	Interaction Parameter, **c**	0.8		
Adjusted Material Properties				
Compression II to Grain (Fc')	461			lb/in^2
Member Selection Verification				
Axial Compression				
Allowable Compression Stress Parallel to Grain, F'_c	461	lb/in^2	**Acceptable**	
Allowable Compressive Load Parallel to Grain, P	29,478	lb		
Actual Axial Compressive Load	12,773	lb		

Table B.12: 1st-story center post design validation

Material Properties		
Species	Eastern Hemlock	
Grade	#2	
Compression II to Grain (F_c)	550	lb/in^2
Loading		
Dead	25	lb/ft^2
Live	40	lb/ft^2
Snow	60	lb/ft^2
Construction Live	0	lb/ft^2
Wind	0	lb/ft^2
Earthquake	0	lb/ft^2
Total Load	100	lb/ft^2
Controlling Load Case	D+(0.75*L)+(0.75*S)	
Column Info		
Column Length	7.833	ft
Column Length	94.0	in
Tributary Width 1	13.1	ft
Tributary Width 2	13.0	ft
Tributary Area	170.3	ft^2
Actual Axial Load	17,030	lb
Section Properties		
X-Section Width (b)	8.0	in
X-Section Depth (d)	8.0	in
Cross-Sectional Area (A)	64.0	In^2
Section Modulus (S)	85.3	in^3
Moment of Inertia (I)	341.3	in^4
Adjustment Factors		
(Load Duration) C_D	Controlling Load Case = D+(0.75*L)+(0.75*S)	1.15
(Wet Service) C_M	Moisture > 19% Limit (Wet)	0.91
(Temperature) C_t	No high temperature exposure	1.0
(Size Factor) C_f	Loaded in strong direction, d not >12"	1.0
(Flat Use) C_{fu}	Not Applicable to Timbers	NA
(Incising) C_i	Not Applicable to Timbers	NA
(Repetitive Member) C_r	Not Applicable to Timbers	NA
(Column Stability) C_P	**Intermediate Values (C_P) – Weak Axis**	0.922

	Unbraced Length, $\mathbf{l_u}$	7.83	ft	
	Unbraced Length, $\mathbf{l_u}$	94.0	in	
	Buckling Length Coefficient , $\mathbf{K_e}$	1		
	Effective Length, $\mathbf{l_e}$	94.0	in	
	Slenderness Ratio, **R**	11.75		
	Euler Stress, $\mathbf{F_{cE}}$	1,965	lb/in^2	
	Pure Stress, $\mathbf{F^*_c}$	632.5	lb/in^2	
	Stress Ratio, **Q**	3.11		
	Interaction Parameter, **c**	0.8		
	Intermediate Values (C_p) – Strong Axis			
	Unbraced Length, $\mathbf{l_u}$	5.0	ft	
	Unbraced Length, $\mathbf{l_u}$	60	in	
	Buckling Length Coefficient, $\mathbf{K_e}$	1		
	Effective Length, $\mathbf{l_e}$	60	in	0.972
	Slenderness Ratio, **R**	7.5		
	Euler Stress, $\mathbf{F_{cE}}$	4,822	lb/in^2	
	Pure Stress, $\mathbf{F^*_c}$	632.5	lb/in^2	
	Stress Ratio, **Q**	7.62		
	Interaction Parameter, **c**	0.8		
Adjusted Material Properties				
Compression II to Grain (F_c')	531			lb/in^2
Member Selection Verification				
Axial Compression				
Allowable Compression Stress Parallel to Grain, F'$_c$	531	lb/in^2	**Acceptable**	
Allowable Compressive Load Parallel to Grain, P	33,969	lb		
Actual Axial Compressive Load	17,030	lb		

APPENDIX C

LIGHT-FRAME DESIGN

The light frame (LF) structure was designed based on equivalency with the existing timber frame (TF) structure design. Equivalency for this purpose is defined as maintaining basic building dimensions and functional purpose. The LF was designed according to the 2009 International Residential Code (ICC 2009) for One- and Two-Family Dwellings, published by the International Code Council (ICC), and is considered a residential structure. Where design requirements exceeded the limitations of the IRC, building components were designed according to the 2005 National Design Specification for Wood Construction (NDS) (AF&PA 2005). This applies to the 2nd floor support beams and columns supporting these beams only. The gable-end with garage doors required the design of a portal frame to resist lateral loads, and the design of this component of the structure is outlined in Appendix D.

DESIGN PARAMETERS

This structure is considered to be located in the town of Jay, Vermont, and all environmental design parameters have been assigned based on this location. These parameters are described in Table C.1, and were determined as described.

Table C.1: Light-frame environmental design parameters

Parameter	Value	Units	Source
Ground Snow Load	60	lb/ft^2	*Town of Jay, Vermont*
Design Wind Speed	90	mph	*(ICC 2009) Figure 301.2(4)*
Seismic Design Category	B		*(ICC 2009) Figure 301.2(2)*
Exposure Category	B		*(ASCE 2010) Chapter C26*

Parameters for design wind speed and seismic design category as determined by the IRC for Jay, Vermont were applicable (ICC 2009). Likewise, Exposure Category as indicated in ASCE 7-10 was applicable (ASCE 2010). Ground snow load for this location, however, was dictated by local requirements and is greater than the value reported by ASCE 7-10 of 50 lb/ft^2 (ASCE 2010).

Applicable design loads were determined based on ASCE 7-10, Minimum Design Loads for Buildings and Other Structures (ASCE 2010). These values are listed in Table C.2, and are based on requirements for a typical residential structure.

Table C.2: Building design loads

Parameter	Value	Units	Source
Live Load (2nd Floor)	40	lb/ft^2	ASCE 7-10 Table 4-1
Dead Load (2nd Floor)	10	lb/ft^2	ASCE 7-10 Table C3-1

The live load value is based on the ASCE 7-10 description, "Residential – All other areas except stairs" (ASCE 2010). Note that "other areas" includes a typical residential floor. The dead load value is a conservative summation of the following material descriptions and assigned loads: "Floors, Wood-Joist (No Plaster) – Joist size 2x10 - 16" spacing" = 6 lb/ft^2, "Subflooring, ¾-in" = 3 lb/ft^2. Note that these design building loads for the 2nd floor were required only to design the 2nd floor main support beams and their support columns. All other building components were designed by the prescribed method of the IRC (ICC 2009).

BASIC DESCRIPTION

The following description of this structure is simplified and serves only to give the reader an initial understanding of the structure. A specific design description, based on the requirements of the IRC (ICC 2009), as well as engineering design, follows.

This structure is two stories, and has a rectangular footprint and gable roof. One end of the structure has two garage doors, and additional perforations include a side-entry door and a total of 11 windows. Building footprint dimensions are 26-ft x 40-ft, building height to the ridge is approximately 26-ft, and roof pitch is 9:12. Figure C.1 is a visual representation of the building. This structure is framed with SPF lumber (spruce, pine, fir), assumed to be grade #2 or better. Wall thickness is defined by nominally sized 2x6 framing. Studs, joists, and rafters are spaced at 16-in on center (o.c.). The walls and roof are completely sheathed in 15/32-in-thick oriented strand board (OSB) or plywood. The first floor of the structure is a monolithic concrete slab, and the second floor is framed with lumber and supported by two large wooden beams, each supported by a central wooden column. (See Figure C.2Figure C. for a visual representation of the 2nd floor structural system.) Rather than employing roof trusses, roof framing is performed

with rafters that are fastened with OSB gusset plates at the ridge, and are tied together with rafter ties and collar ties. Figure C.3 is a visual representation of the roof structural system. Figure C.1 through Figure C.3 are images from a 3D model created in Google Sketch-Up (Google 2012).

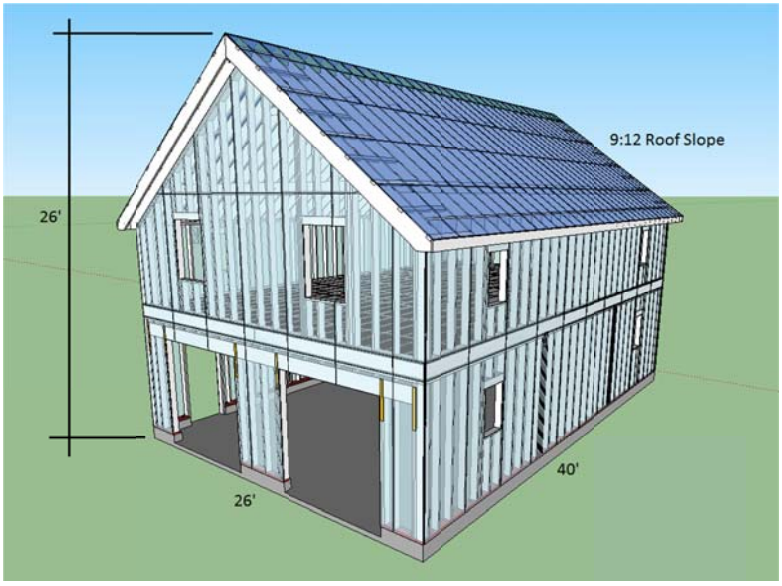

Figure C.1: Light-frame structure

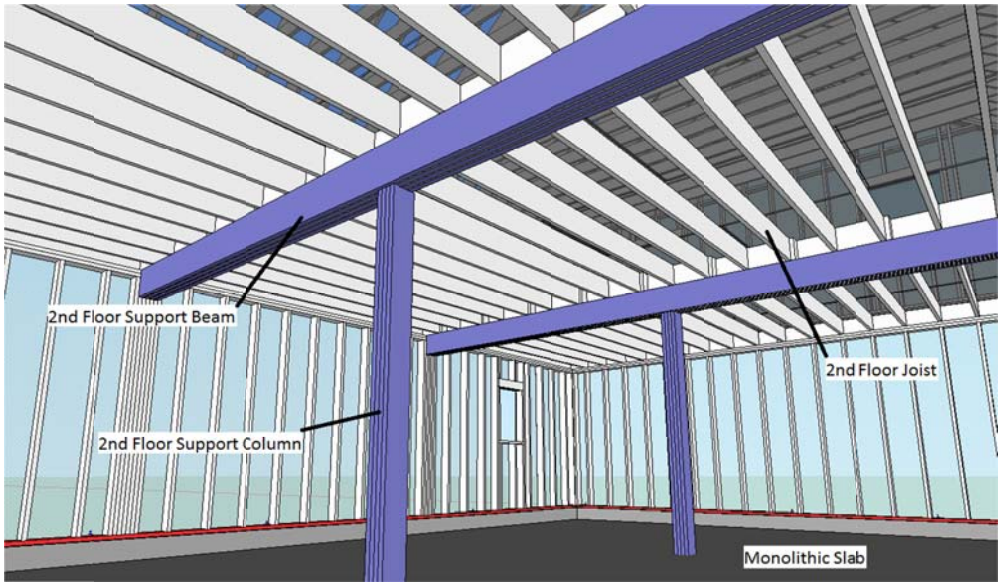

Figure C.2: 2nd floor structural system

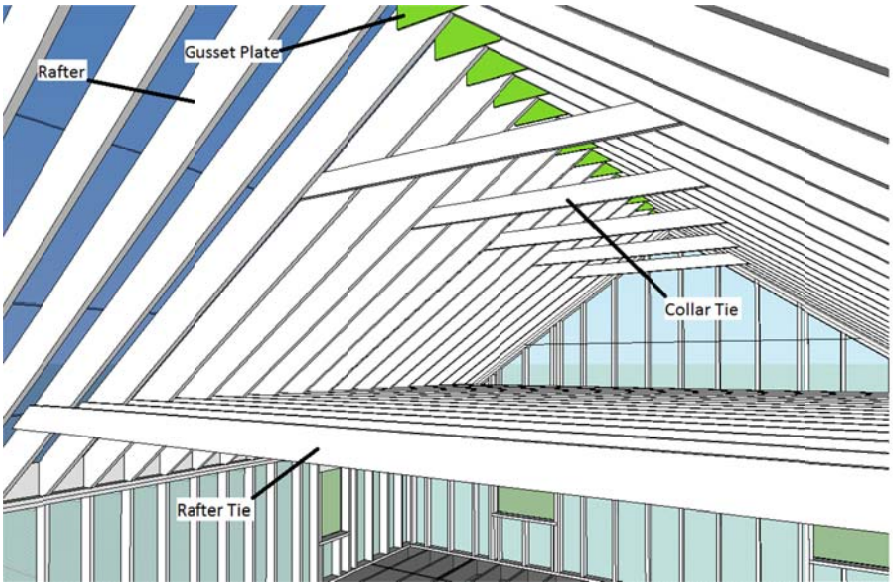

Figure C.3: Roof structural system

INTERNATIONAL RESIDENTIAL CODE DESIGN

The International Residential Code (IRC) (ICC 2009) is a model building code that provides a prescriptive approach to one- and two-family residential buildings, and has been adopted throughout most of the United States. Engineering calculations are not necessary when designing a structure based on the prescriptive method of the IRC. Table C.3 through Table C.9 below outline the IRC requirements applicable to this design, as well as a description of how these requirements have been met. Please refer to the 2009 IRC for a detailed description of these requirements, as well as all tables listed. They have been omitted from this report due to their length.

Table C.3: IRC foundation design (ICC 2009)

Requirement	Design Description	Applicable Tables and Figures
R403.1.6	Sill plates are pressure-treated and anchored to the foundation with 1/2" bolts that extend a minimum of 7 inches into the concrete, and are each fastened with a nut and washer. Anchor bolts are spaced a minimum of every 6 feet. Each sill section is fastened by at least two anchor bolts, and the ends of each sill section are each fastened within 7 to 12 inches.	

Table C.4: IRC floor framing design (ICC 2009)

Requirement	Design Description	Applicable Tables and Figures
R502.3	2nd floor joist size specification: Based on live load (40 lb/ft^2), allowable deflection (L/360), lumber grade (#2): Joist size selection: 2x10 (nominal). Allowable joist span = 15'-5" Actual joist span = 12'-9"	Table 502.3.1(2)
R502.6	All joist ends have greater than 1.5" of bearing support. Joist ends bear the full width of wall framing or support beam.	
R502.6.1	Joist framing from opposite sides over a bearing support lap more than 3 inches, and are assumed to be fastened appropriately.	
R502.7	Joists are supported laterally over support beams by full-depth solid blocking (2x10 material), and at exterior walls by a 2x10 rim board.	
R502.7.1	Additional support for bridging is not required because floor joist size does not exceed 2x12.	
R502.8	No notching or drilling of floor joists is specified.	
R502.9	Nailing and other means of fastening are assumed to meet all requirements and specifications.	Table 502.3(1)

Table C.5: IRC Floor sheathing design (ICC 2009)

Requirement	Design Description	Applicable Tables and Figures
R503.2.1	Floor sheathing specification: based on span (16"), minimum panel thickness (7/16"): Floor sheathing selection: 48/24 OSB or Plywood, 15/32" thick.	Table R503.2.1.1(2)
R5503.2.2	Design loads are less than the maximum allowable loads for the span rating of the floor sheathing selected.	Table R503.2.1.1(1)
R503.2.3	Nailing and other means of fastening are assumed to meet all requirements and specifications.	Table R602.3(1)

Table C.6: IRC wall framing design (ICC 2009)

Requirement	Design Description	Applicable Tables and Figures
R602.2	All lumber is assumed to be Grade #2 or better.	
R602.3	Exterior walls have been designed according to the appropriate figures.	Figure R602.3(1) Figure R602.3(2)
	Structural wall framing is fastened directly to structural framing members.	
	Studs are continuous members, from plate to plate, with the allowable exception of jack studs and trimmer studs.	Table R602.5(1) Table R602.5(2)
R602.3.1	1st floor stud spacing: Based on stud size (2x6 nominal), supporting one floor plus a roof-ceiling assembly, max spacing (24" on center): Allowable laterally unsupported stud height = 10' Actual laterally unsupported stud height = 8'-6" (Note: Actual stud spacing = 16" on center)	Table R602.3(5)

	2nd floor stud spacing: Based on stud size (2x6 nominal), supporting a roof only, max spacing (24" on center): Allowable laterally unsupported stud height = 18' Actual laterally unsupported stud height = 14'-9" (Note: Actual stud spacing = 16" on center)	Table R602.3.1
R602.3.2	Stud walls are capped with a double top plate. Overlapping at corners is assumed. Minimum 24" overlapping at joint ends, occurring over studs, is assumed. Plates are constructed of 2x6 (nominal) lumber.	
R602.3.3	All studs and rafters are spaced at 16" on center, and are in alignment with one another throughout.	
R602.3.4	All wall studs are 2x6 (nominal) width, and bear on a 2x6 (nominal) sill plate.	
R602.6	No notching or drilling of studs is specified.	
R602.7	**Side-entry door header**: Based on supporting roof, ceiling and one center-bearing floor, building width (28'), span (3'-4"): Required: 2, 2x6 (nominal) with 1/2" plywood spacers. Specified: 3, 2x6 (nominal) with 1/2" OSB spacers. **Gable-end window**: Based on supporting roof and ceiling, building width (28'), span (3'-0"): Required: (for span 3'-8") 2, 2x6 (nominal) with 1/2" plywood spacers. Specified: 3, 2x6 (nominal) with 1/2" OSB spacers. **Non-gable-end window**: Based on supporting roof and ceiling, building width (28'), span (2'-0"). Required: (for span 3'-8") 2, 2x6 (nominal) with 1/2" plywood spacers. Specified: 3, 2x6 (nominal) with 1/2" OSB Spacers. **Garage doors**: See Appendix D, Portal Frame Design.	Table R502.5(1)
R602.8	Fire blocking is provided vertically by top and bottom wall plates in between floors, and horizontally by studs.	

Table C.7: IRC wall sheathing design (ICC 2009)

Requirement	Design Description	Applicable Tables and Figures
R602.10.1	Braced wall line lengths: Gable ends = 40’ Side walls = 26'	
R602.10.1.1	Shear wall bracing is achieved using continuous sheathing methods.	
R602.10.1.2 R602.10.1.2(1) R602.10.1.2(3)	**Required bracing for gable end walls, 1st Story**: Based on Exposure Category (B), mean roof height (30'), eave to ridge height (10'), number of braced wall lines (2), basic wind speed (90mph), 1st story of a 2-story structure, continuous sheathing, braced wall line spacing (40'): Required Length = 12' Applicable adjustment Factors: -Eave-to-ridge height = 1.03 (interpolated)*0.95 (note "d")=0.98 Required length of bracing = 11.75' Actual length of bracing (non-garage door end) = 26' Actual length of bracing (garage door end) = 10' (See Appendix D for Portal Frame Design). **Required bracing for side walls, 1st Story:** Based on Exposure Category B, mean roof height (30'), roof eave to ridge height (10'), number of braced wall lines (2), basic wind speed (90 mph), 1st story of a 2-story structure, continuous sheathing, braced wall line spacing (30'): Required length = 9ft Actual length of bracing = significantly greater than minimum. **Required bracing for gable end walls, 2nd story:** Based on Exposure category (B), mean roof height (30'), eave to ridge height (10'), 2 braced wall lines, basic wind speed (90 mph), 2nd story fo a 2-story structure, continuous sheathing, braced wall line spacing (40'):	R602.10.1.2(1)

	Required length = 6' Actual length of bracing significantly greater than minimum. **Required bracing for side walls, 2nd story:** Based on Exposure category (B), mean roof height (30'), eave to ridge height (10'), 2 braced wall lines, basic wind speed (90 mph), 2nd story for a 2-story structure, continuous sheathing, braced wall line spacing (30'): Required length = 5' Actual length of bracing significantly greater than minimum.	
R602.10.1.2.1	Requirements are met for braced wall panel upload path (basic wind speed does not exceed 90 mph, Exposure Category B, roof pitch greater than 5:12, roof span is less than 32').	
R602.10.4	Braced wall lines are continuously sheathed.	
R602.10.4.1	Braced wall panel sheathing method: CS-WSP (continuously sheathed - wood structural panel). Connection criteria: 6" nail spacing along edges, 12" nail spacing throughout interior of panel. (Fastener specification assumed to be met). Panel specification = 24/0 span rating, 1/2" thick. Gable end with garage doors sheathing method: CS-PF (continuously sheathed - portal frame)	Table R602.10.4.1
R602.10.4.1.1	Note: Continuously sheathed portal frame design: See Appendix D.	
R602.10.4.2	CS-WSP: Wall height = 8'-6" CS-PF: Wall height = 8'-4"	Table R602.10.4.2 Figure R602.10.4.2
R602.1.1.2(2)	For length of bracing for continuous sheathing, only full height braced walls meeting requirements are applied.	Table R602.10.4.2
R602.10.4.4	A minimum 24"-long, full-height wood structural panel is provided at both sides of a building corner (corner return).	Figure R602.10.4.4(1)

Table C.8: IRC roof/ceiling design (ICC 2009)

Requirement	Design Description	Applicable Tables and Figures
R802.1.1	Blocking lumber is grade #2 or better.	
R802.2	Roof slope = 9:12, designed according to appropriate figures.	Figure R606.11(1) Figure R606.11(2) Figure R606.11(3)
R802.3	Rafters are framed to each other with an OSB gusset plate. No ridge board exists.	
R802.3.1	Ceiling joists are nonexistent. Rafter ties are installed on every opposing set of rafters. Size specification = 2x8 (nominal). Collar ties are installed on every third set of opposing rafters (4' spacing). Size specification = 2x6 (nominal).	Table R602.3(1)
R802.4	Ceiling Joist tables have been adopted to determine the allowable span for rafter ties. Based on species (SPF), size specification (2x8, nominal): Allowable ceiling joist span (rafter tie span) = 22'-4" Actual rafter tie span = 19'-7".	Table R802.4(1)
R802.5	Rafter spans: Based on ground snow load (70 lb/ft^2), allowable deflection (L/180 for ceiling not attached to rafters), rafter spacing (16"), dead load (20 lb/ft^2), species (SPF #2), rafter size (2x12, nominal): Allowable rafter span = 14'-3" Actual rafter span = 13'	Tables R802.5.(1-8)
R802.6	Every rafter has greater than 1.5" of bearing on plate.	
R802.7	No notching or drilling of rafters is specified.	
R802.8	Blocking is provided in between rafters at their base. Member dimensions do not exceed a 5:1 depth-to-thickness ratio.	

Table C.9: Roof sheathing design (ICC 2009)

Requirement	Design Description	Applicable Tables and Figures
R803.2.1	Roof sheathing is OSB or plywood. Span rating = 32/16. Thickness = 15/32". Load = 40 lb/ft2 total, 30 lb/ft2 live. Edge support not required.	Table R503.2.1(1)
R803.2.3	Roof sheathing is installed staggered.	

ENGINEERED DESIGN OF 2ND FLOOR STRUCTURAL SYSTEM

The design requirements for the second floor structural support system exceeded the limitations of the IRC, and therefore had to be designed using the NDS (AF&PA 2005). These components include the 2nd floor support beams and 2nd floor support columns. The methods for the design of these members, dictated by the NDS, are outlined in Appendix B (Timber Frame Design) (ICC 2009). The methods outlined for beam design and column design apply to the 2nd floor support beam and the 2nd floor support column, respectively. The results of these calculations are outlined in Table C.10 and Table C.11.

Member sizes were assumed, and then checked for validity using this design method. The support beam that spans the width of the building (26') (and is supported at its center by the support column) is constructed out of four (4) 2x12's (nominal), with three (3), ½-in OSB spacers in between each 2x12. Each component of the beam is fastened along its widest face to the others in an alternating pattern to create a large-cross section beam. It is assumed that this member behaves similarly to a solid-sawn member of identical dimensions (6.75" x 11.25"). The support column is constructed from four (4) 2x8's (nominal) that are fastened to each other along their widest faces. This assembly is assumed to behave similarly to a solid-sawn member of identical dimensions (6.75" x 7.25").

Table C.10: 2nd floor support beam design validation

Material Properties		
Species	Spruce - pine - Fir	
Grade	Select Structural	
Bending (Fb)	1100	lb/in^2
Shear II to Grain (Fv)	125	lb/in^2
Modulus of Elasticity	1,300,000	lb/in^2
Loading		
Dead	10	lb/ft^2
Live	40	lb/ft^2
Snow	0	lb/ft^2
Construction Live	0	lb/ft^2
Wind	0	lb/ft^2
Earthquake	0	lb/ft^2
Total Load	50	lb/ft^2
Controlling Load Case	L+D	
Beam Info		
Beam Span	12.3	ft
Beam Span	147.6	in
Tributary Width	13.1	ft
Tributary Area	161.13	ft^2
Line Loading (w)	655	lb/ft
Maximum Moment, M (K-in)	148.6	Kip-in
Maximum Moment, M (lb-in)	14,8642	lb-in
Maximum Shear, V	4,028.3	lb
Maximum Deflection	0.29	in
Section Properties		
X-Section Width (b)	7.5	in
X-Section Depth (d)	11.25	in
Section Modulus (S)	158.20	in^3
Moment of Inertia (I)	889.89	in^4
Adjustment Factors		
(Load Duration) C_D	Controlling Load Case = Live	1.0
(Moisture) C_M	Kiln-dried	1.0
(Temperature) C_t	No high temperature exposure	1.0

(Size Factor) C_f	Loaded in strong direction, d not >12"		1.0
(Flat Use) C_{fu}	Not Applicable to Timbers		NA
(Incising) C_i	Not Applicable to Timbers		NA
(Repetitive Member) C_r	Not Applicable to Timbers		NA
(Beam Stability) C_L	d/b < 2		1.0
Adjusted Material Properties			
Bending (Fb)	1,093		lb/in^2
Shear II to Grain (Fv)	125		lb/in^2
Modulus of Elasticity	1,300,000		lb/in^2
Member Selection Verification			
Bending			
Actual Bending Stress, fb	940	lb/in^2	**Acceptable**
Allowable Bending Stress, F'b	1,093	lb/in^2	
Shear			
Actual Shear Stress, fv	72	lb/in^2	**Acceptable**
Allowable Bending Stress, F'v	125	lb/in^2	
Deflection			
Actual Deflection	0.29	in	**Acceptable**
Allowable Deflection	0.62	in	

Table C.11: 2nd floor support column design validation

Material Properties			
Species	Spruce - pine - Fir		
Grade	#2		
Compression II to Grain (F_c)	425		lb/in^2
Loading			
Dead	10		lb/ft^2
Live	40		lb/ft^2
Snow	0		lb/ft^2
Construction Live	0		lb/ft^2
Wind	0		lb/ft^2
Earthquake	0		lb/ft^2
Total Load	50		lb/ft^2
Controlling Load Case	L+D		
Column Info			
Column Length	8.5		ft
Column Length	102		in
Tributary Width 1	13.3		ft
Tributary Width 2	13.0		ft
Tributary Area	172.9		ft^2
Axial Load	8645		lb
Section Properties			
X-Section Width (b)	6.0		in
X-Section Depth (d)	7.25		in
Section Modulus (S)	52.56		in^3
Moment of Inertia (I)	190.54		in^4
Adjustment Factors			
(Load Duration) C_D	Controlling Load Case = Live		1.0
(Moisture) C_M	Kiln Dried		1.0
(Temperature) C_t	No high temperature exposure		1.0
(Size Factor) C_f	Loaded in strong direction, d not >12"		1.0
(Flat Use) C_{fu}	Not Applicable to Timbers		NA
(Incising) C_i	Not Applicable to Timbers		NA
(Repetitive Member) C_r	Not Applicable to Timbers		NA
(Column Stability) C_P	**Intermediate Values (C_P) – Weak Axis**		0.898
	Unbraced Length, l_u (ft)	8.5	ft

	Unbraced Length, l_u (in)	102	in	0.935
	Buckling Length Coefficient (K_e)	1		
	Unbraced Length : (ft)	17.0		
	Effective Length, $\mathbf{l_e}$ (ft)	102	in	
	Slenderness Ratio, **R**	17.0		
	Euler Stress, $\mathbf{F_{cE}}$	1,052.4	lb/in^2	
	Pure Crushing Stress, $\mathbf{F^*_c}$	425	lb/in^2	
	Stress Ratio, **Q**	2.48		
	Interaction Parameter, **c**	0.8		
	Intermediate Values (C_p) – Strong Axis			
	Unbraced Length, $\mathbf{l_u}$ (ft)	8.5	ft	
	Unbraced Length, l_u (in)	102	in	
	Buckling Length Coefficient (K_e)	1		
	Unbraced Length : (ft)	14.07		
	Effective Length, $\mathbf{l_e}$ (ft)	102	in	
	Slenderness Ratio, **R**	14.07		
	Euler Stress, $\mathbf{F_{cE}}$	1536.6	lb/in^2	
	Pure Crushing Stress, $\mathbf{F^*_c}$	425	lb/in^2	
	Stress Ratio, **Q**	3.62		
	Interaction Parameter, **c**	0.8		
Adjusted Material Properties				
Compression II to Grain (Fc')	382			lb/in^2
Member Selection Verification				
Axial Compression				
Allowable Compression Stress Parallel to Grain, F'c	382	lb/in^2	**Acceptable**	
Allowable Compressive Load Parallel to Grain, P	16,599	lb		
Actual Axial Compressive Load	8,645	lb		

APPENDIX D

PORTAL FRAME DESIGN FOR THE LIGHT FRAME STRUCTURE

Sufficient shear wall length on the gable end of the original-light frame structure was not available, based on the requirements of the 2009 International Residential Code (ICC 2009), to accommodate two 8-ft-wide garage door openings. In order to maintain a building width of 26-ft, accommodate both garage door openings, and maintain all other building dimensions, a portal frame was designed capable of resisting the design horizontal (wind) and vertical (dead, live, snow) loads on the structure. A portal frame is a lateral-force-resisting system that relies on wood structural panels that overlap a continuous header to create a moment-resisting connection for the frame (Martin et al. 2008). In the case of this design, a moment-resisting connection was also created where wood structural panels are fastened to the sill plate. Anchor bolts and tie-downs are also incorporated to increase the lateral-force-resisting capacity, as well as uplift capacity. A portal frame inherently relies on the shear strength of its connections.

The procedure for designing this portal frame consisted of comparing the moment and shear-resisting capacities of the portal frame connections with the design forces generated at these connections, as determined by ASCE 7-10 (ASCE 2010). SAP2000 was used to calculate the actual connection moment and base shear forces on the frame based on design dead, live, and wind loads. The moment and shear strengths of the portal frame connections were determined by following the procedure outlined in the 2008 publication, 'Principles of Mechanics Model for Wood Structural Panel Portal Frames' (Martin et al. 2008).

CALCULATIONS AND ANALYSIS FOR DESIGN LOAD FORCES ON PORTAL FRAME CONNECTIONS

Design wind loads on the structure were calculated using the ASCE 7-10 Envelope Procedure, Simplified Method for enclosed, low-rise buildings (ASCE 2010). See Appendix E for the calculation and explanation of zone forces. Wind loading on the gable-end portal frame was calculated using tributary areas, resulting in a horizontal point load at the top of the portal frame. Figure D.1 depicts the tributary areas that contribute to this lateral point load on the portal frame, and the force in each zone.

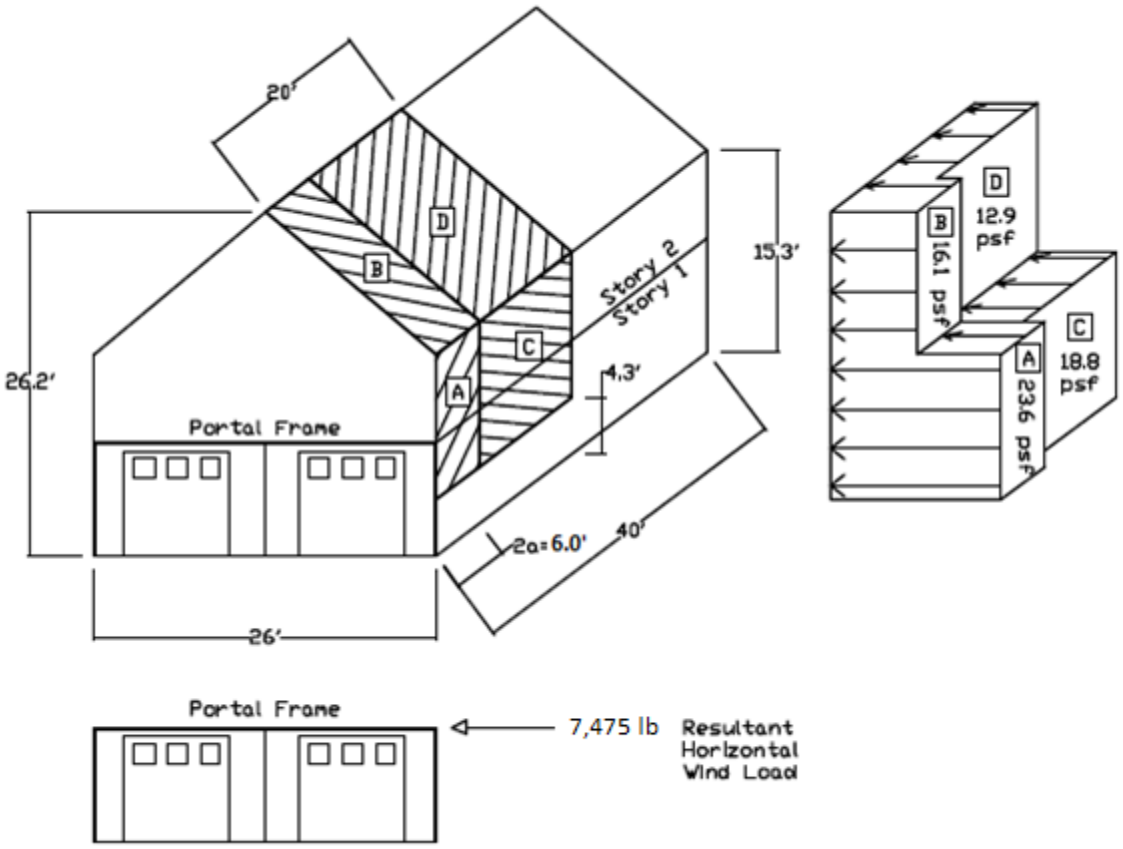

Figure D.1: Wind loading tributary areas acting on the portal frame

Tributary areas contributing to the wind force on the portal frame were determined as follows: it was assumed that the wind force (acting perpendicular to the ridge) on half of the length (20') of the structure would be distributed to each gable-end wall. The portal frame carries the wind loading from the area above its height (story 2 and the roof), as well as half of the area below its height (4.3'). It is assumed that the wind loading on the lower half of the height of the portal frame would go directly to the ground. The width of Zones A and B, which account for wind pressure edge effects is 5.2', and the width of zones C and D is 14.8', calculated as the difference between half the width of the building (20') and the width of zones A and B. Please see Appendix E for the calculation to determine the width of zones A and B. Wind loading zone contributions were summed as shown in Table D.1, and a total horizontal point load of 7,475 lb was determined to act on the portal frame from wind.

Table D.1: Wind loading calculation

Zone	Width	Height	Zone Loading	Total Load Contribution
	ft	ft	lb/ft^2	lb
A	6.0	11.0	23.6	1,558
B	6.0	10.9	16.1	1,053
C	14.0	11.0	18.8	2,895
D	14.0	10.9	12.9	1,969
			Total Wind Point Load	**7,475**

Live and dead loads acting on the portal frame were calculated as shown in Table D.2 and Table D.3.

Table D.2: Live load calculation

	Value	Units	Notes
Tributary Width	6.7	ft	Half the span of supported floor joists
Loading	40	lb/ft^2	Residential Live Load, ASCE 7-10 Table 4-1
Line Loading	**268**	**lb/ft**	Tributary Width * Loading

Table D.3: Dead load calculation

	Value	Units	Notes
OSB Weight	1.6	lb/ft^2	
OSB Surface Area	314	ft^2	
Total OSB Weight	503	lb	OSB Weight * OSB Surface Area
OSB Line Loading	19.3	lb/ft	Total OSB Weight / 26 ft
Lumber Weight	30	lb/ft^3	
Lumber Volume	31	ft^3	Calculated total volume of solid-sawn lumber
Total Lumber Weight	930	lb/ft3	Lumber Weight * Lumber Volume
Lumber Line Loading	35.7	lb/ft	Total Lumber Weight / 26 ft
Dead Line Loading	**55**	**lb/ft**	OSB Line Loading + Lumber Line Loading

Since floor joists on the second floor of the structure rest on the portal frame, live load was calculated using the tributary area of this floor and a residential live load of 40 lb/ft^2 (ASCE 2010). The contributing tributary area for the live load was calculated as the width of the floor (26-ft) multiplied by the half the floor joist length. See Figure D.2, in which this tributary area is visually outlined. Note that 2nd floor gable-end wall framing has been removed from this image for clarity.

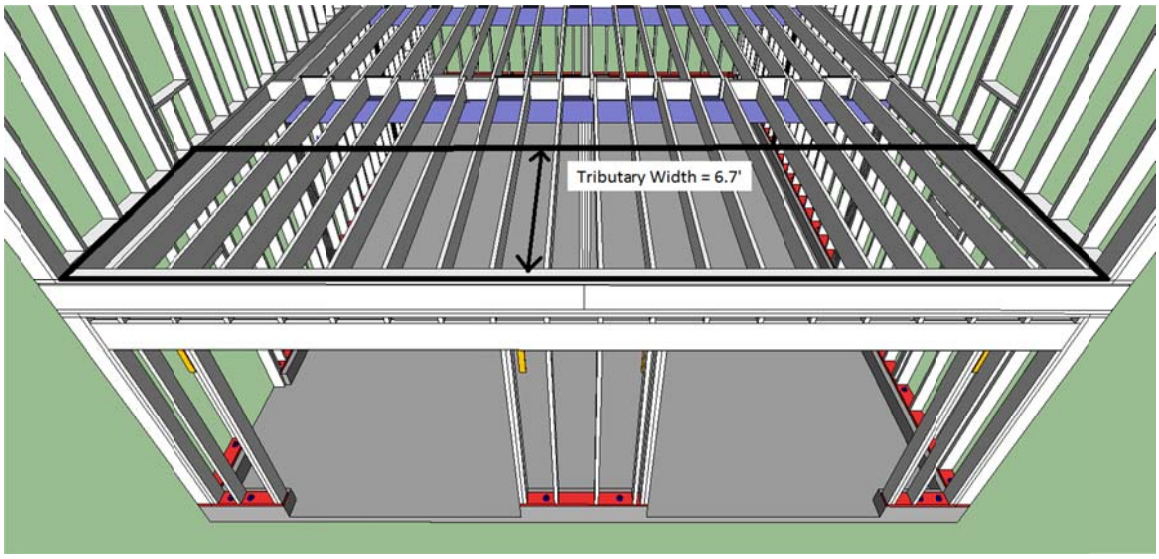

Figure D.2: Live load tributary area acting on the portal frame

No additional roof loading acts on the portal frame because rafters carry these loads (snow, live roof load, etc.) directly to the top plate on the eve side of the structure. Dead loads acting on the portal frame were determined by summing the contributing weight of the wood products in the gable-end wall and contributing tributary area from the second floor. Total distributed loads of 268 lb/ft live load and 55 lb/ft dead load were applied vertically over the length of the portal frame resulting from these calculations. Figure D.3 shows all calculated loads acting on the gable-end portal frame.

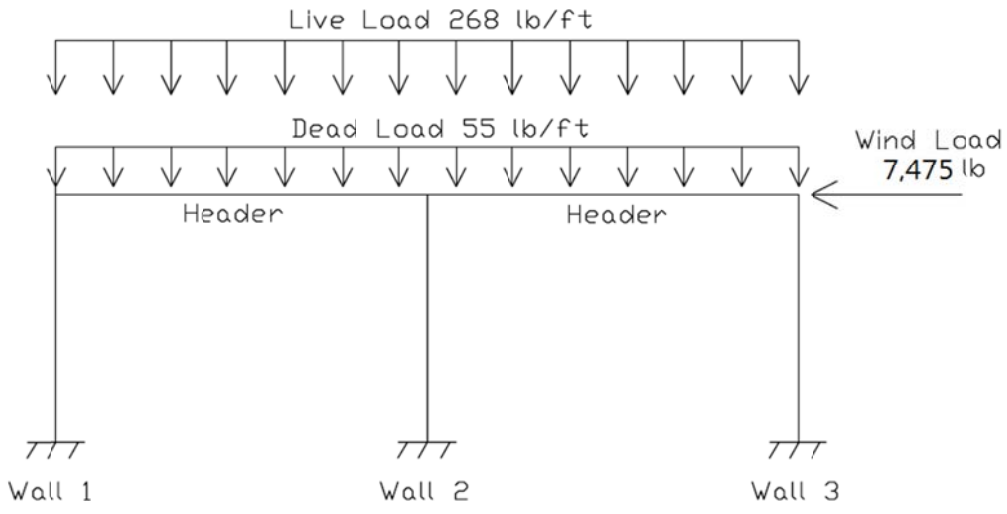

Figure D.3: Portal frame loading

A structural analysis model of the portal frame was created in SAP2000 using these design loads. All joints were modeled as rigid, and appropriate frame section properties for each member were determined. Frame section properties include cross-sectional areas, as well as moments of inertia about the proper bending axis, and were determined either by hand calculation or by using the 'Section Designer' tool in SAP2000. Figure D.4 is a cross-section of Wall 2, drawn using the 'Section Designer' tool.

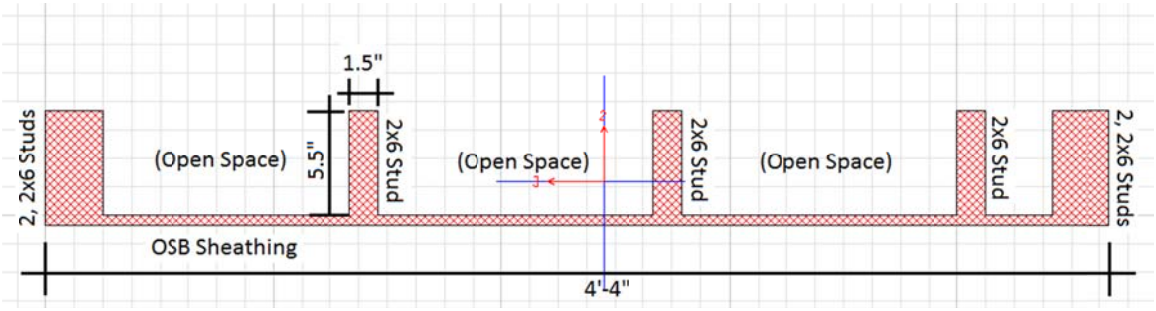

Figure D.4: Wall 2 cross-section draw in 'Section Designer'

This section depicts a wall constructed of 2x6 studs and sheathed with ½" OSB. The Section Designer in SAP 2000 is capable of calculating the cross-sectional area and moments of inertia for complicated sections. Hand calculations of the moment of inertia and cross-sectional area of a similarly complex cross-section were performed with good results to verify that the Section Designer tool calculated these values as intended. A transformed section calculation was also performed to account for the difference in Moduli of Elasticity between the solid-sawn lumber and the OSB sheathing. This calculation, outlined in Table D.4, concluded that the Moduli of Elasticity were similar enough to not require amending a material dimension for the calculation of Moment of Inertia of the assembly.

Table D.4: Transform section, OSB thickness

	Value	Units	Notes
Modulus of Elasticity, E (SPF #1/#2)	510,000	psi	NDS Table 4A
Panel Axial Stiffness , EA (OSB)	3,350,000	lb/ft of panel width	APA Panel Design Specification Table 4A
Panel Area, A (1/2" thickness)	6	in^2/ft of panel width	APA Panel Design Specification Table 6
Modulus of Elasticity, E (OSB)	558,000	psi	Panel Axial Stiffness / Panel Area
OSB Transformed Thickness	**0.54**	**in**	0.5" * (558,000/510,000)

Due to the unit length limitations of drawing cross-sections with the Section Designer tool, it was concluded that the Moduli of Elasticity were similar enough to not require a transformed section. (Note that drawing in ½" increments was as small as comfortably possible in the Section Designer tool.) The section properties for each member of the portal frame modeled are listed in Table D.5. Figure D.5 shows which frame members have been assigned to each section property, as well as wall (column) number assignments.

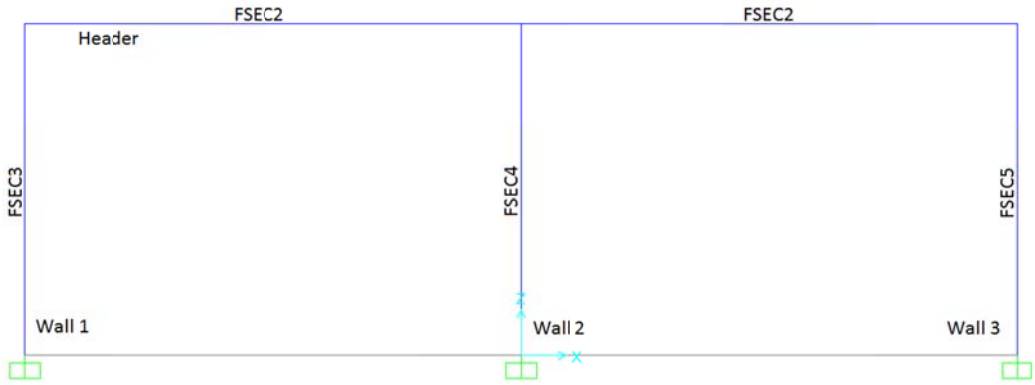

Figure D.5: Portal frame property assignments and member names

Table D.5: Portal frame section properties

Frame Property	Area ,A (in^2)	Moment of Inertia, I (in^4)	Notes
FSEC2	61.9	653	5.5"x11.25" Header
FSEC3	74.5	9885	Wall Section
FSEC4	84.8	33275	Wall Section
FSEC5	74.5	10877	Wall Section

Maximum moments at wall/header connections and wall/sole plate connections, as well as maximum base shear values for each wall were determined based on appropriate load combinations. The ASD loading combinations required for this analysis, which include live, wind, and dead loads are as follows (ASCE 2010):

1. D
2. D + L
4. D + 0.75L
5. D + 0.6W

6a. D + 0.75L + 0.75(0.6W)

7. 0.6D + 0.6W

Results of the SAP2000 analysis for each relevant load case are presented in Table D.6. Note that by inspection load cases 4 and 7 do not control.

Table D.6: SAP2000 analysis results, forces generated by design loads

Load Case 1 (D)

Force	Units	Wall 1	Wall 2	Wall 3
Moment at Wall/Header Connection (M_{TOP})	lb-ft	703	1.95	709
Moment at Wall/Sole Plate Connection (M_{BOTTOM})	lb-ft	577	1.95	587
Base Shear (V)	lb	14.5	0.39	14.1

Force	Units	Wall 1	Wall 2	Wall 3
Moment at Wall/Header Connection (M_{TOP})	lb-ft	4130	8.47	4165
Moment at Wall/Sole Plate Connection (M_{BOTTOM})	lb-ft	3391	11.4	3447
Base Shear (V)	lb	85	2.3	83

Load Case 5 (D + 0.6W)

Force	Units	Wall 1	Wall 2	Wall 3
Moment at Wall/Header Connection (M_{TOP})	lb-ft	1368	690	114
Moment at Wall/Sole Plate Connection (M_{BOTTOM})	lb-ft	10950	12667	12580
Base Shear (V)	lb	1423	1542	1444

Load Case 6a (D + 0.75L + 0.75(0.6W))

Force	Units	Wall 1	Wall 2	Wall 3
Moment at Wall/Header Connection (M_{TOP})	lb-ft	3771	522	2816
Moment at Wall/Sole Plate Connection (M_{BOTTOM})	lb-ft	5957	9493	11276
Base Shear (V)	lb	1123	1156	1028

These results were compared to the allowable capacities of the portal frame connections, as calculated and described in the next section of this appendix.

CALCULATIONS FOR THE ALLOWABLE CAPACITY OF PORTAL FRAME CONNECTIONS

The procedure outlined in the publication, 'Principles of Mechanics Model for Wood Structural Panel Portal Frames' was followed to determine the moment and shear resisting

capacities of the connections in the portal frame (Martin et al. 2008). This procedure takes into account the moment capacity and the shear capacity of each connection. Connection details include the nailing pattern at the wall/header and wall/sole plate connections, anchor bolts, tie-down straps, and header straps.

Figure D.6 shows the dimensions and (some) structural aspects of the portal frame designed for this structure

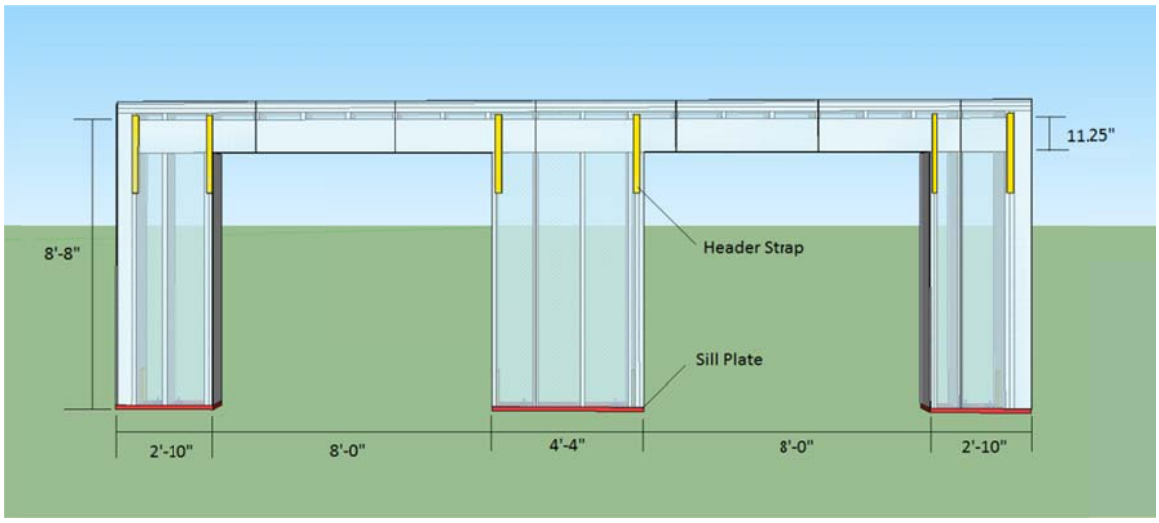

Figure D.6: Portal frame design

The portal frame is a 26-ft-wide gable-end wall section accommodating two 8-ft-wide garage doors. The header is a continuous beam constructed of solid-sawn (nominal) 2-in x 10-in members and ½" OSB spacers, and is modeled as a solid sawn 5.5-in x11.25-in beam. All walls are 8-ft, 8-in tall. Side walls are 2-ft, 10-in wide, and the center wall is 4-ft, 4-in wide. All walls are constructed of (nominal) 2-in x 6-in studs spaced at 16-in on center, and are sheathed with ½" OSB (translucent in Figure D.6). Moment resisting connections are created by overlapping the ½" OSB sheathing over the header, as well as over the sole plate, and connections are made with a (minimum) 3" grid nailing pattern (see example in Figure D.7). Connections are reinforced by anchor bolts and hold down straps anchored into the foundation (installed at the base of each wall, not visible in Figure D.6), and tie-down straps connecting each wall to the header.

The first step to determine the moment and shear resisting capacities of the joints in the portal frame is to determine the fastener resisting capacity of the grid nailing pattern at each connection. Figure D.7 shows the grid nailing pattern designed for each end-wall moment

connections to the header. This example nailing pattern indicates the joint numbering pattern, as well as the origin and center of rotation, used for calculations.

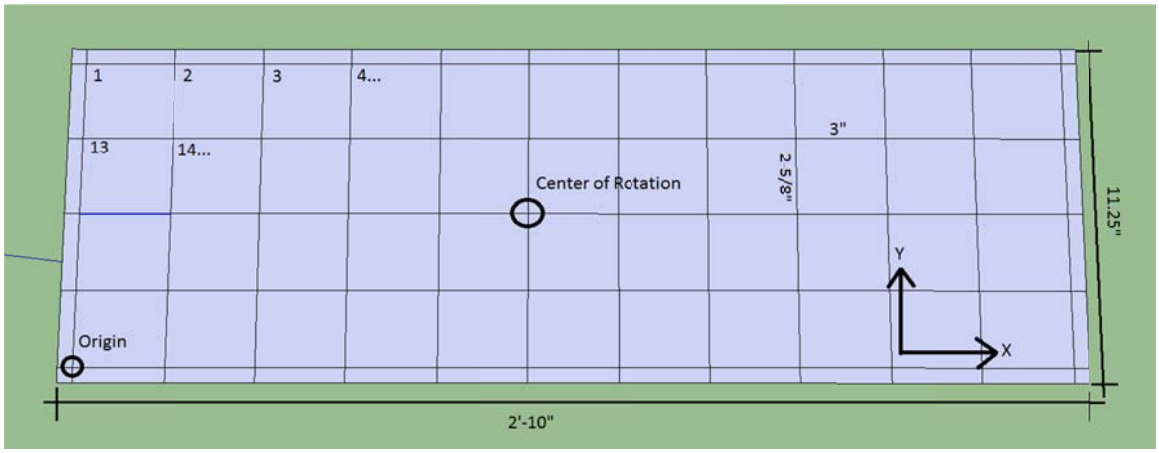

Figure D.7: Nailing pattern for end wall/header connection

The moment capacity of each grid nailing pattern connection is determined by first calculating the polar moment of inertia of the fastener group, and the single fastener lateral load capacity. The moment capacity of the connection was calculated using the critical fastener. This means that the moment was calculated such that the fastener furthest from the center of rotation would not exceed its allowable shear strength. The polar moment of inertia, J, was calculated by equation D1.

$$J = \text{Sum of } (dx^2 + dy^2) \quad \textbf{(D1)}$$

Where:

dx = x distance from the fastener to the center of rotation.

dy = y distance from the fastener to the center of rotation.

The sum of the results of this equation for every nail represents the polar moment of inertia for the nail pattern connection. The results of this calculation for each nail in the wall 1/header connection, as well as the polar moment of inertia for the connection are presented in Table D.7. The Critical Fastener Moment capacity of the grid nailing pattern moment connection was calculated by equation D2, and is outlined in Table D.7 for the example end-wall/header connection shown in Figure D.6.

$$M = Z'(J)/ r_{MAX} \quad \textbf{(D2)}$$

Where:

Z' = single fastener allowable shear capacity for 8d common nails and ½" OSB (adjusted for load duration with C_D=1.6).

J = polar moment of inertia.

r_{MAX} = longest moment arm.

Table D.7: Critical fastener moment capacity of end-wall/header connection

Z	67	lbf/nail per 2005 NDS
C_D	1.6	(Wind)
Z'	107.2	lbf/nail

Fastener	**X** (in)	**Y** (in)	**dx** (in)	**dy** (in)	**dx^2** (in^2)	**dy^2** (in^2)	**dx^2+dy^2** (in^2)	**r** (in)
1	0	10.25	-16.5	-5.125	272.25	26.27	298.52	17.28
2	3	10.25	-13.5	-5.125	182.25	26.27	208.52	14.44
3	6	10.25	-10.5	-5.125	110.25	26.27	136.52	11.68
4	9	10.25	-7.5	-5.125	56.25	26.27	82.52	9.08
5	12	10.25	-4.5	-5.125	20.25	26.27	46.52	6.82
6	15	10.25	-1.5	-5.125	2.25	26.27	28.52	5.34
7	18	10.25	1.5	-5.125	2.25	26.27	28.52	5.34
8	21	10.25	4.5	-5.125	20.25	26.27	46.52	6.82
9	24	10.25	7.5	-5.125	56.25	26.27	82.52	9.08
10	27	10.25	10.5	-5.125	110.25	26.27	136.52	11.68
11	30	10.25	13.5	-5.125	182.25	26.27	208.52	14.44
12	33	10.25	-16.5	-5.125	272.25	26.27	298.52	17.28
13	0	7.6875	-16.5	-2.5625	272.25	6.57	278.82	16.70
14	3	7.6875	-13.5	-2.5625	182.25	6.57	188.82	13.74
15	6	7.6875	-10.5	-2.5625	110.25	6.57	116.82	10.81
16	9	7.6875	-7.5	-2.5625	56.25	6.57	62.82	7.93
17	12	7.6875	-4.5	-2.5625	20.25	6.57	26.82	5.18
18	15	7.6875	-1.5	-2.5625	2.25	6.57	8.82	2.97

19	18	7.6875	1.5	-2.5625	2.25	6.57	8.82	2.97
20	21	7.6875	4.5	-2.5625	20.25	6.57	26.82	5.18
21	24	7.6875	7.5	-2.5625	56.25	6.57	62.82	7.93
22	27	7.6875	10.5	-2.5625	110.25	6.57	116.82	10.81
23	30	7.6875	13.5	-2.5625	182.25	6.57	188.82	13.74
24	33	7.6875	-16.5	-2.5625	272.25	6.57	278.82	16.70
25	0	5.125	-16.5	0	272.25	0.00	272.25	16.50
26	3	5.125	-13.5	0	182.25	0.00	182.25	13.50
27	6	5.125	-10.5	0	110.25	0.00	110.25	10.50
28	9	5.125	-7.5	0	56.25	0.00	56.25	7.50
29	12	5.125	-4.5	0	20.25	0.00	20.25	4.50
30	15	5.125	-1.5	0	2.25	0.00	2.25	1.50
31	18	5.125	1.5	0	2.25	0.00	2.25	1.50
32	21	5.125	4.5	0	20.25	0.00	20.25	4.50
33	24	5.125	7.5	0	56.25	0.00	56.25	7.50
34	27	5.125	10.5	0	110.25	0.00	110.25	10.50
35	30	5.125	13.5	0	182.25	0.00	182.25	13.50
36	33	5.125	-16.5	0	272.25	0.00	272.25	16.50
37	0	2.5625	-16.5	2.5625	272.25	6.57	278.82	16.70
38	3	2.5625	-13.5	2.5625	182.25	6.57	188.82	13.74
39	6	2.5625	-10.5	2.5625	110.25	6.57	116.82	10.81
40	9	2.5625	-7.5	2.5625	56.25	6.57	62.82	7.93
41	12	2.5625	-4.5	2.5625	20.25	6.57	26.82	5.18
42	15	2.5625	-1.5	2.5625	2.25	6.57	8.82	2.97
43	18	2.5625	1.5	2.5625	2.25	6.57	8.82	2.97
44	21	2.5625	4.5	2.5625	20.25	6.57	26.82	5.18
45	24	2.5625	7.5	2.5625	56.25	6.57	62.82	7.93
46	27	2.5625	10.5	2.5625	110.25	6.57	116.82	10.81
47	30	2.5625	13.5	2.5625	182.25	6.57	188.82	13.74
48	33	2.5625	-16.5	2.5625	272.25	6.57	278.82	16.70
49	0	0	-16.5	5.125	272.25	26.27	298.52	17.28
50	3	0	-13.5	5.125	182.25	26.27	208.52	14.44
51	6	0	-10.5	5.125	110.25	26.27	136.52	11.68
52	9	0	-7.5	5.125	56.25	26.27	82.52	9.08
53	12	0	-4.5	5.125	20.25	26.27	46.52	6.82
54	15	0	-1.5	5.125	2.25	26.27	28.52	5.34
55	18	0	1.5	5.125	2.25	26.27	28.52	5.34
56	21	0	4.5	5.125	20.25	26.27	46.52	6.82

57	24	0	7.5	5.125	56.25	26.27	82.52	9.08
58	27	0	10.5	5.125	110.25	26.27	136.52	11.68
59	30	0	13.5	5.125	182.25	26.27	208.52	14.44
60	33	0	-16.5	5.125	272.25	26.27	298.52	17.28
						J =	7222.97	in^2
						r_{MAX} =	17.28	in
						Critical Fastener Moment =	**44815**	**lb-in**

Where:

x = x distance from the origin to the fastener.

y = y distance from the origin to the fastener.

r = distance from fastener to the center of rotation.

Table D.8 indicates the Critical Fastener Allowable Moment capacity for the grid nailing pattern moment connections for the wall/header and wall/sole plate connection for each wall. Note that the nailing patterns, and therefore the Critical Fastener Allowable Moment capacity of each end wall are identical.

Table D.8: Critical fastener allowable moment capacities

		Value	Units
End Walls	Header Connection ($M_{HEADER.FASTENER}$)	44815	lb-in
	Sole Plate Connection (M_{WSP} to Sill)	9719	lb-in
Center Wall	Header Connection ($M_{HEADER.FASTENER}$)	99602	lb-in
	Sole Plate Connection (M_{WSP} to Sill)	18331	lb-in

With the critical fastener allowable moment capacities for the grid nailing pattern at each connection determined, the total moment capacity of the header fastener moment, the sole plate fastener moment, and the base shear of each wall can now be calculated with the following procedure. Additional required design values for this procedure are presented in Table D.9.

Table D.9: Design values for Wall 1 moment and shear capacities

	Value	Units
Width	34	in
Height	100	in
Tiedown Strap	5000	lbf
Fb_{WSP}	600	psi
t	0.5	in
$Strap_{HEADER}$	1000	lbf
Fvtv	155	lb/in
Z	67	lb
n	16	
$V_{BASE\ CONNECTION}$	1600	lb

Where:

Width and Height = Wall 1 dimensions, including sole plate and header overlap.

Tie-down Strap = Allowable design strength of the base tie-down strap.

Fb_{WSP} = Allowable bending strength of OSB for 24/0 sheathing (APA 2012).

t = Thickness of OSB sheathing panel.

$Strap_{HEADER}$ = Allowable design strength of the wall/header strap.

Fvtv = Panel shear through the thickness (APA Panel Design Specification).

n = Number of nails along wall/sole plate connection (assuming 1 row).

$V_{BASE\ CONNECTION}$ = Cumulative shear strength of two 5/8" anchor bolts bearing on one SPF sole plate (AF&PA 2005).

The first portion of this procedure is to calculate the moment capacity of the connections at the top and bottom of each wall, as well as the shear strength of the moment connections (shear capacity based on moment couples).

Equation D3 was used to calculate the total moment capacity for the connection at the bottom of each wall (M_{BOTTOM}). This value depends on the location of the tie-down strap (installed on the inside of each of the outer two studs), as well as the moment resisting capacity of the nailing of the sheathing to the sole plate (M_{WSP} to Sill).

$$M_{BOTTOM} = \text{Tie-down Strap} * (\text{Width} - 3") + M_{WSP} \text{ to Sill} \quad \textbf{(D3)}$$

Note that 3" is subtracted from the moment arm to sum the moment about the tie-down strap center line.

Calculation of the moment capacity of the top connection of the portal frame is determined based on the moment-resisting capacities of the wood structural panel (M_{WSP}), the header strap ($M_{HEADER.STRAP}$), and the nailing pattern that connects the OSB to the header ($M_{HEADER.FASTENER}$). Equation D4 calculates the moment capacity contribution of the wood structural panel.

$$M_{WSP} = Fb_{WSP} * (t*\text{Width}^2)/6) * 1.6 \quad \textbf{(D4)}$$

The contribution to the moment-resisting capacity of the top connection by the header strap ($M_{HEADER.STRAP}$) is calculated by equation D5, and is limited by the lesser of the values of the moment-resisting capacity of the strap itself, and the wood structural panel to which it is fastened.

$$M_{HEADER.STRAP} = \text{Min of } [Strap_{HEADER} * (\text{Width}-1.5)), M_{WSP}] \quad \textbf{(D5)}$$

The total moment-resisting capacity at the top of the wall is the sum of the moment-resisting capacity contribution of the strap and the lesser of the moment-resisting capacities of the wood structural panel and the nailing pattern, as indicated by equation D6.

$$M_{TOP} = \text{Min of } (M_{WSP}, M_{HEADER.FASTENER}) + M_{HEADER.STRAP} \quad \textbf{(D6)}$$

The lateral load capacity based on moment couples ($V_{MOMENT\ COUPLES}$) is calculated by equation D7. Note that the lesser of the values for the lateral load capacity, based on moment couples or the shear strength of connections (see below), will control the total allowable base shear.

$$V_{MOMENT\ COUPLES} = (M_{BOTTOM} + M_{TOP}) / \text{Height} \quad \textbf{(D7)}$$

Table D.10 indicates the results of the procedure outlined above.

Table D.10: Wall/header and wall/sole plate moment capacities, and shear capacity based on moment couples for Wall 1

Lateral Load Capacity, V, Based on Moment Couples

Moment Capacity at Bottom of Portal Frame Wall Segment, M_{BOTTOM}				
	Wall 1	**Wall 2**	**Wall 3**	
M_{BOTTOM}	164719	263331	164719	lb-in
Moment Capacity at Top of Portal Frame Wall Segment, M_{TOP}				
	Wall 1	**Wall 2**	**Wall 3**	
M_{WSP}	92480	216320	92480	lb-in
$M_{HEADER.STRAP}$	32500	50500	39000	lb-in
M_{TOP}	77315	150102	83815	lb-in
Portal Frame Lateral Load Capacity Based on Moment Couples, $V_{MOMENT\ COUPLES}$				
	Wall 1	**Wall 2**	**Wall 3**	
$V_{MOMENT\ COUPLES}$	2420	4134	2485	lb-in

The second step of this procedure is to calculate the base shear capacity of each wall based on the shear strength of the nails, the OSB panel, and the base connection (anchor bolts).

The shear strength of the OSB (V_{PANEL}) is determined by equation D8, and the shear strength of the wall/sole plate nailing pattern connection (V_{NAIL}) is calculated with equation D9. Note that the calculation for the nailing shear capacity assumes one row of nails.

$$V_{PANEL} = F_v t_v * 1.6 * \text{Width} \quad \textbf{(D8)}$$

$$V_{NAIL} = Z * 1.6 * \#\text{of nails on bottom} \quad \textbf{(D9)}$$

The lateral load capacity of the portal frame based on shear strength is controlled by the minimum value of the panel shear capacity, the nail shear capacity, and the anchor bolt shear capacity, as indicated in equation D10.

$$V_{SHEAR\ STRENGTH} = \text{Min of } (V_{PANEL}, V_{NAILS}, (V_{BASE\ CONNECTION} * 1.6)) \quad \textbf{(D10)}$$

Note that the value for the anchor bolt shear capacity ($V_{BASE\ CONNECTION}$) was previously determined and is listed in Table D.9. Table D.11 indicates the results of this portion of this procedure, as outlined above, for each wall.

Table D.11: Lateral load capacity based on shear strength

Panel Shear Capacity, V_{PANEL}				
	Wall 1	**Wall 2**	**Wall 3**	
V_{PANEL}	8432	12896	8432	lb
Nail Shear Capacity, V_{NAILS}				
	Wall 1	**Wall 2**	**Wall 3**	
V_{NAIL}	1715	1930	1715	lb
Portal Frame Lateral Load Capacity Based on Shear Strength, $V_{SHEAR\ STRENGTH}$				
	Wall 1	**Wall 2**	**Wall 3**	
$V_{BASE\ CONNECTION}$	2560	2560	2560	lb
Portal Frame Lateral Load Capacity Based on Shear Strength, $V_{SHEAR\ STRENGTH}$				
	Wall 1	**Wall 2**	**Wall 3**	
$V_{SHEAR\ STRENGTH}$	1715	1930	1715	lb

For this design, the shear strength capacity of the nailing controls for each wall. Ultimately, the lesser of the values of lateral load capacity based on moment couples and lateral load capacity based on shear strength controls the base shear strength capacity of each wall. For this portal frame design, the lateral load capacity based on shear strength controlled for every wall. Table D.12 presents the results of this procedure for all three walls, including the calculations of moment capacity at the top and bottom of the wall, as well as base shear capacity.

Table D.12: Moment capacities and base shear of portal frame connections

Wall 1		
CD = 1.6		
V	1715	lb
M_{BOTTOM}	13727	lb-ft
M_{TOP}	6443	lb-ft
CD = 1.0		
V	1072	lb
M_{BOTTOM}	8579	lb-ft
M_{TOP}	4027	lb-ft
CD = 0.9		
V	965	lb
M_{BOTTOM}	7721	lb-ft
M_{TOP}	3624	lb-ft

Wall 2		
CD = 1.6		
V	1930	lb
M_{BOTTOM}	21944	lb-ft
M_{TOP}	12508	lb-ft
CD = 1.0		
V	1206	lb
M_{BOTTOM}	13715	lb-ft
M_{TOP}	7818	lb-ft
CD = 0.9		
V	1085	lb
M_{BOTTOM}	12344	lb-ft
M_{TOP}	7036	lb-ft

Wall 3		
CD = 1.6		
V	1715	lb
M_{BOTTOM}	13727	lb-ft
M_{TOP}	6985	lb-ft
CD = 1.0		
V	1072	lb
M_{BOTTOM}	8579	lb-ft
M_{TOP}	4365	lb-ft
CD = 0.9		
V	965	lb
M_{BOTTOM}	7721	lb-ft
M_{TOP}	3929	lb-ft

It is important to note that the procedure described above assumes design for wind loading, and therefore a load duration factor (C_D) of 1.6 is incorporated throughout. For loading combinations controlled by live load (C_D = 1.0) or dead load (C_D = 0.9), these values have been adjusted appropriately and included in Table D.13. The procedure for this adjustment requires multiplying each moment or shear capacity by the appropriate load duration factor, and dividing by 1.6 (the load duration factor for wind, already incorporated).

DESIGN VALIDATION

This portal frame design was verified by comparing the actual connection forces calculated by SAP2000 based on design loadings with the moment capacities of each connection, as well as the base shear capacity of each wall calculated by the procedure outlined above. Table D.13 through Table D.16 outline the comparison of these values for all applicable loading combinations (1, 2, 5, and 6a), and shows that in all cases the allowable design values are greater than actual values for all connection forces.

Table D.13: Design validation, load case 1

Load Case 1, C_D = 0.9

Wall 1					
Allowable Load (Calculated)				**Actual Load (SAP)**	
V	965	lb	>	14.5	lb
M_{BOTTOM}	7721	lb-ft	>	577	lb-ft
M_{TOP}	3624	lb-ft	>	703	lb-ft
Wall 2					
Allowable Load (Calculated)				**Actual Load (SAP)**	
V	1085	lb	>	0.39	lb
M_{BOTTOM}	12344	lb-ft	>	1.95	lb-ft
M_{TOP}	7036	lb-ft	>	1.95	lb-ft
Wall 3					
Allowable Load (Calculated				**Actual Load (SAP)**	
V	965	lb	>	14.1	lb
M_{BOTTOM}	7721	lb-ft	>	587	lb-ft
M_{TOP}	3929	lb-ft	>	709	lb-ft

Table D.14: Design validation, load case 2

Load Case 2, C_D = 1.0

Wall 1					
Allowable Load (Calculated)				**Actual Load (SAP)**	
V	1072	lb	>	85	lb
M_{BOTTOM}	8579	lb-ft	>	3391	lb-ft
M_{TOP}	4027	lb-ft	>	4130	lb-ft
Wall 2					
Allowable Load (Calculated)				**Actual Load (SAP)**	
V	1206	lb	>	2.3	lb
M_{BOTTOM}	13715	lb-ft	>	11.4	lb-ft
M_{TOP}	7818	lb-ft	>	8.47	lb-ft
Wall 3					
Allowable Load (Calculated)				**Actual Load (SAP)**	
V	1072	lb	>	83	lb
M_{BOTTOM}	8579	lb-ft	>	3447	lb-ft
M_{TOP}	4365	lb-ft	>	4165	lb-ft

Table D.15: Design validation, load case 5

Load Case 5, C_D = 1.6

Wall 1					
Allowable Load (Calculated)				**Actual Load (SAP)**	
V	1715	lb	>	1423	lb
M_{BOTTOM}	13727	lb-ft	>	10950	lb-ft
M_{TOP}	6443	lb-ft	>	1368	lb-ft
Wall 2					
Allowable Load (Calculated)				**Actual Load (SAP)**	
V	1930	lb	>	1542	lb
M_{BOTTOM}	21944	lb-ft	>	12667	lb-ft
M_{TOP}	12508	lb-ft	>	690	lb-ft
Wall 3					
Allowable Load (Calculated)				**Actual Load (SAP)**	
V	1715	lb	>	1444	lb
M_{BOTTOM}	13727	lb-ft	>	12580	lb-ft
M_{TOP}	6985	lb-ft	>	114	lb-ft

Table D.16: Design validation, load case 6a

Load Case 6a, C_D = 1.6

Wall 1					
Allowable Load (Calculated)				**Actual Load (SAP)**	
V	1715	lb	>	1123	lb
M_{BOTTOM}	13727	lb-ft	>	5957	lb-ft
M_{TOP}	6443	lb-ft	>	3771	lb-ft
Wall 2					
Allowable Load (Calculated)				**Actual Load (SAP)**	
V	1930	lb	>	1156	lb
M_{BOTTOM}	21944	lb-ft	>	9493	lb-ft
M_{TOP}	12508	lb-ft	>	522	lb-ft
Wall 3					
Allowable Load (Calculated)				**Actual Load (SAP)**	
V	1715	lb	>	1028	lb
M_{BOTTOM}	13727	lb-ft	>	11276	lb-ft
M_{TOP}	6985	lb-ft	>	2816	lb-ft

REDESIGN FOR PLYWOOD

This portal frame design was performed specifying ½" OSB sheathing because this was the panel product used in the method outlined in the APA publication that was followed (APA 2008). Since the light frame structure that this portal frame was designed for is sheathed in plywood, however, material properties for 4-ply plywood were substituted for necessary OSB material properties. These property substitutions are outlined in Table D.17.

Table D.17: Plywood material property substitutions

Property	OSB	4-Ply Plywood	Units
Fb_{WSP}	600	550	psi
Fvtv	155	69	lb/in

Since the moment capacity of the header strap (M_{HEADER_STRAP}) remained less than the moment capacity of the wood structural panel (M_{WSP}), substituting the allowable bending strength of plywood for the allowable bending strength of OSB (Fb_{WSP}) did not affect controlling

conditions. Similarly, since the shear capacity of nailing (V_{NAIL}) remained less than the shear capacity of the panel (V_{PANEL}), substituting the panel shear strength through its thickness (F_{VTV}) also did not affect controlling conditions. For this reason, the capacity of the portal frame designed did not change when OSB was substituted for 4-ply plywood of an equivalent thickness.

APPENDIX E

DESIGN WIND PRESSURE CALCULATION

Design wind pressures were calculated with the ASCE 7-10, "Minimum Design Loads for Buildings and Other Structure," Envelope Procedure, Simplified Method for enclosed, low-rise buildings (ASCE 2010). This method is outlined in section 28.5, Part 2 of ASCE 7-10. The following conditions outlined in Table E.1 were met to utilize this method:

Table E.1: Design wind pressure calculation conditions

Condition	Met By	Source
1. The building is a simple diaphragm building.	"Building, Simple Diaphragm: A building in which both windward and leeward wind loads are transmitted by roof and vertically spanning wall assemblies, through continuous floor and roof diaphragms, to the MWFRS."	ASCE 7-10, Section 26.2
2. The building is a low-rise building.	"Building, Low-Rise: Enclosed or partially enclosed buildings that comply with the following conditions: 1. Mean roof height, h less than or equal to 60 ft. 2. Mean roof height, does not exceed least horizontal dimension [26']." Note: Mean roof height, h = 20.75	ASCE 7-10, Section 26.2
3. The building is enclosed as defined in Section 26.2 and conforms to the wind-borne debris provisions of Section 26.10.3.	1. "Building, Enclosed: A building that does not comply with the requirements for open or partially enclosed buildings." Note: This building does not comply with the definitions for open or partially enclosed. 2. "Protection of Glazed Openings: Glazed openings in Risk Category II, III, or IV buildings located in hurricane-prone regions	1. ASCE 7-10, Section 26.2 2. ASCE 7-10, Section 26.10.3

	shall be protected as specified in this section." Note: This building is not in a hurricane-prone region.	
4. The building is a regular-shaped building or structure.	"Building or Structure, Regular Shaped: A building or other structure having no unusual geometrical irregularity in special form.	ASCE 7-10, Section 26.2
5. The building is not classified as a flexible building.	"Building and Other Structure, Flexible: Slender buildings and other structures that have a fundamental natural frequency less than 1 Hz." Note: the fundamental natural frequency of this building is 5.14 Hz (ASCE 7-10, Section 12.8.2.1). See below in this appendix.	ASCE 7-10, Section 26.2
6. The building does not have response characteristics making it subject to across wind loading, vortex shedding, instability due to galloping or flutter; and it does not have a site location for which channeling effects or buffeting in the wake of upwind obstructions warrant special consideration.	Note: These effects are not of consideration	
7. The building has an approximately symmetrical cross-section in each	Note: The building shape is perfectly symmetrical, and it has a 37-degree roof slope.	

direction with either a flat roof or a gable or hip roof with no greater than a 45-degree roof slope.		
8. The building is exempted from torsional load cases.	"Exception: …buildings two stories or less framed with light-frame construction"	ASCE 7-10, Figure 28.4-1, Note 5

The parameters listed in Table E.2 were determined for this design. Note that both the light-frame and the timber frame structure designed have the same design wind loading. All design parameters are based on a theoretical site location, located in northern Vermont. Both structures are considered to be located on the same footprint.

Table E.2: Design wind load design parameters

Parameter			Source
Risk Category	II		ASCE 7-10, Table 1.5-1
Basic Wind Speed	115	mph	ASCE 7-10, Figure 26.5-A
Wind Load Parameters:			
Exposure Category	B		ASCE 7-10, Chapter C26
Topography Factor, K_{zt}	1.0		ASCE 7-10, 26.8.1
Adjustment Factor for building height and exposure category, λ	1		ASCE 7-10, Figure 28.6-1

With these design wind load parameters and a known roof angle of 37-degrees (9:12 slope) for Case A and 0-degrees for Case B, the unadjusted horizontal and vertical wind pressures on the structures were determined using Figure 28.6-1(ASCE 7-10). The values obtained from this figure assume an exposure category B and an average building height of 30 ft. An

adjustment to these values to account for a variation in exposure, roof angle, and topographic features is calculated by equation E1:

$$p_S = \lambda * K_{zt} * p_{30} \quad \textbf{(E1)}$$

Where:

p_s = Simplified design wind pressure

p_{30} = simplified design wind pressure for exposure B at h = 30ft (values obtained from Figure 28.6-1)

Since the adjustment factor for this building design (Exposure category B, mean roof height 20.75 ft) and the topography factor, K_{zt} (no significant topographic effects assumed), both equal 1.0, the values for horizontal and vertical wind pressures determined using Figure 28.6-1 are valid and do not require adjustment. Figure E.1 and Figure E.2 show the results of this procedure and depict their acting locations on the structure for Cases A and B.

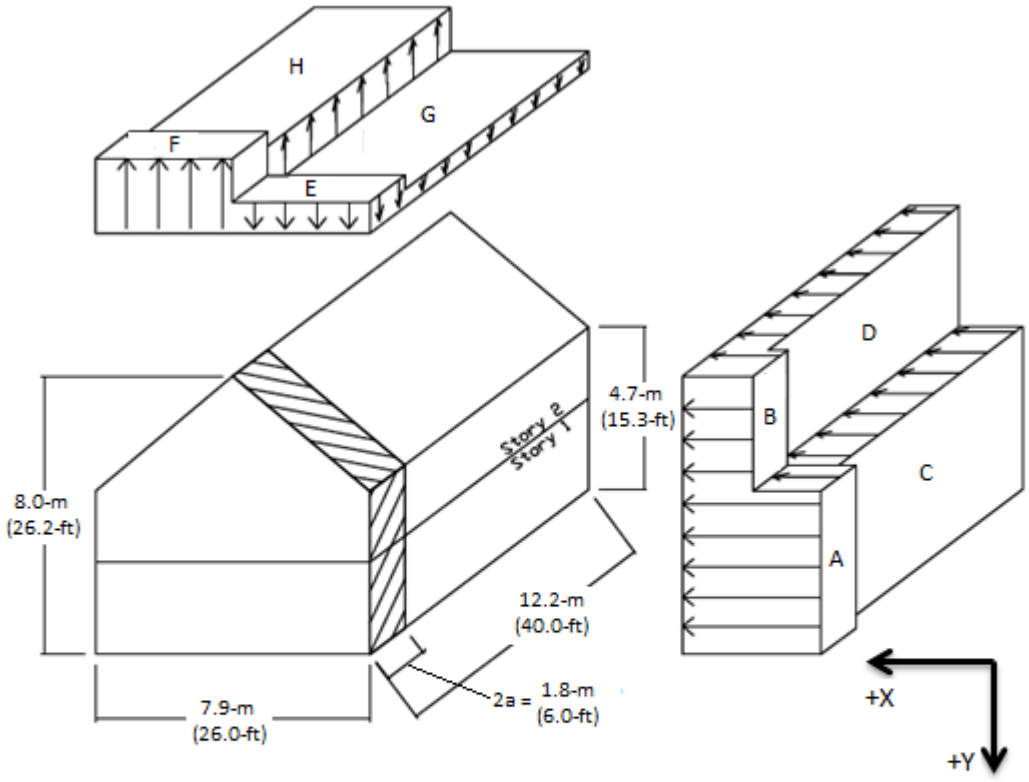

Zone	A	B	C	D	E	F	G	H	E_{OH*}	G_{OH*}
Wind Pressure kN/m^2 (lb/ft^2)	1.13 (23.6)	0.77 (16.1)	0.90 (18.8)	0.62 (12.9)	0.09 (1.8)	-0.68 (-14.3)	0.03 (0.6)	-0.59 (-12.3)	-0.46 (-9.5)	-0.40 (-8.3)

*Overhang wind pressures not shown in figure

Figure E.1: Simplified design wind pressure acting, Case A

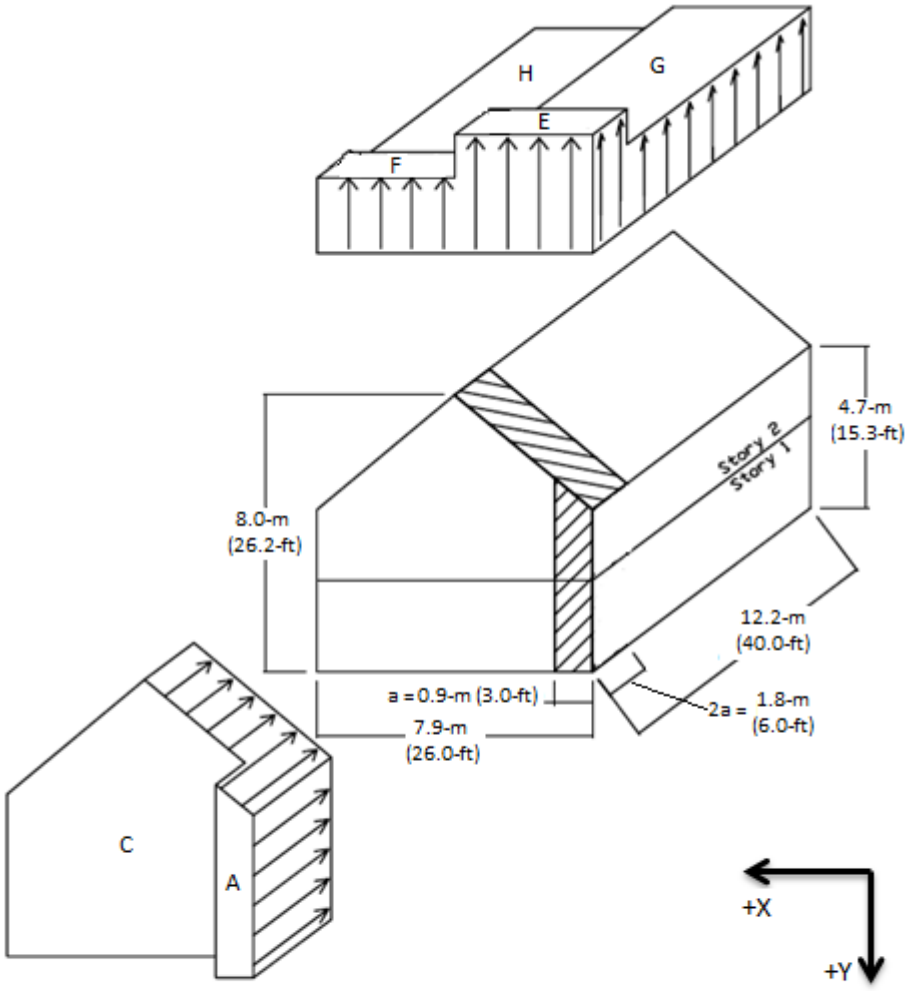

Zone	A	C	E	F	G	H	E_{OH*}	G_{OH*}
Wind Pressure kN/m^2 (lb/ft^2)	1.13 (23.6)	0.90 (18.8)	0.09 (1.8)	-0.68 (-14.3)	0.03 (0.6)	-0.59 (-12.3)	-1.30 (-27.2)	-1.69 (-35.3)

*Overhang wind pressures not shown in figure

Figure E.2: Simplified design wind pressure acting, Case B

Zones A, B, E and F account for a change in wind pressure due to edge effects. The width of these zones equals "2a", where "a" is calculated as the lesser of the following three quantities: 10% of the least horizontal dimension, 40% of the design building height, or a minimum of 3-ft. See footnote 9 of Figure 28.6-1 of ASCE 7-10 for this requirement (ASCE 2010). This calculation is outlined in Table E.3.

Table E.3: End effect zone width

10% least horizontal dimension	0.1 * 26-ft	2.6	ft
40% of design building height	0.4 * 20.75-ft	8.3	ft
Min: 4% of least horizontal dimension	0.04 * 26-ft	1.04	ft
Min: 3ft	3ft	3.0	ft
"*a*"	Lesser of top two values, not less than greater of min. values	3.0	ft
End effect zone width, 2*a*	2 * 3.0-ft	**6.0**	**ft**

Edge effects on the windward side of the building, therefore, act over the first 6.0 feet of length of the structure, on both the wall and the roof.

BUILDING FUNDAMENTAL NATURAL FREQUENCY

Condition 5 of the conditions required to use the method for calculating design wind pressure (outlined in Table E.1) states that in order to calculate the design wind pressure using this method, the building must not be classified as flexible. Flexible buildings are defined as having a fundamental natural frequency of less than 1.0 Hz (ASCE 7-10). Equation E2 was used to verify that the fundamental natural frequency of the building is greater than 1.0.

$$T_a = C_t h_n^{\,x} \qquad \textbf{(E2)}$$

Where:

T_a = fundamental natural period of the building (seconds)

h_n = the structural height (ASCE 7-10, Section 11.2) (ft)

C_t = Approximate period parameter coefficient

x = Approximate period parameter coefficient

Values for C_t and x are located in ASCE 7-10 Table 12.8-2, and are based on the type of structure. For this design, the type of structure is under the category “all other structural

systems." Note that the fundamental natural frequency is the inverse of the fundamental natural period, as indicated in equation E3.

$$f = 1/T_a \quad \textbf{(E3)}$$

Where:

f = fundamental natural frequency of the building (Hz)

Table E.4 outlines the values and results for the determination of the fundamental natural frequency of this building.

Table E.4: Fundamental natural frequency

h_n	20.75	ft
C_t	0.02	
x	0.75	
T_a	0.194	s
f	**5.14**	**Hz**

APPENDIX F

STRUCTURAL SYSTEM DESCRIPTIONS

TRADITIONAL TIMBER FRAME

This structure is the most traditional timber frame (TF), constructed of large-dimension green eastern hemlock. Members are fastened with mortise-and-tenon joinery, and fastened primarily with wooden pegs. Fastening of rafter ends to rafter plates, however, is performed with 10-in screws to provide for increased uplift resistance. Roof sheathing is (nominal) 2-in x 6-in kiln-dried dimensional SPF (spruce-pine-fir) lumber nailed directly to rafters with 16d nails, for continuous covering. Walls are sheathed with vertical (nominal) 1-in x 10-in kiln-dried shiplap pine boards, nailed to wall framing members with 8d nails. Flooring is comprised of 2-in x 8-in unseasoned (green) hemlock boards attached to floor joists with 16d nails. Attachment of the frame to the foundation is made by a connection similar to two, ½-in-diameter anchor bolts at each post bottom. A sill plate located between each post bottom is fastened to the foundation with 10-in-long, ½-in-diameter anchor bolts. Sill plates provide a nailing surface for siding. Structural design of the traditional TF structure was verified with the National Design Specification (NDS) (AF&PA 2005), and member size was dictated largely by the size necessary to facilitate mortise-and-tenon-style joinery. Verification calculations show that some members, such as posts, are over-conservative, where others, such as rafters, are adequate. See Appendix B for a thorough description of the design of this structure and for engineering calculations validating member selection. Further design alterations (below) maintaining "timber frame" in their title reflect this design unless specified. This structure was based on the Jay, Vermont structure built by the author in 2011, and serves as the basis for which all other structures in this study have been designed.

KILN-DRIED TIMBER FRAME

The option to use kiln-dried materials for TF construction is common for high-end homes where tolerance for the shrinkage of structural members is extremely low. Kiln-drying timbers helps to increase frame quality by cutting joinery after member dimensions have stabilized. For this environmental impact assessment (EIA) model, all framing members and floor boards are assumed to be kiln dried rather than green. Sheathing for the roof and walls remain unchanged from the "traditional TF" design.

TIMBER FRAME WITH LIGHT-FRAMING INFILL

Where the traditional TF design for this study is sheathed with vertical pine shiplap boards, this option replaces these boards with a light-frame (LF) wall system. The purpose for this design option is to allow exterior wall sheathing to be performed with standard-sized panel products. LF studs are installed in between timber framing members, on which $^{15}/_{32}$-in-thick OSB sheathing is fastened. Light framing is (nominal) 2-in x 6-in, kiln-dried dimensional SPF lumber, spaced 16" on center, and installed to accommodate both the timber structural system and the sheathing. Roof and floor sheathing are also performed with $^{15}/_{32}$-in-thick OSB for this design, fastened directly to rafters and floor joists, respectively. Light framing members are fastened with 16d nails, and OSB is fastened with 8d nails. The TF, itself, remains unchanged from that of the "traditional TF" design.

TIMBER FRAME WITH SIPS

This design option also serves to replace the traditional TF wall and roof sheathing materials, and does so with structural insulated panels (SIPs). SIPs are a manufactured product commonly used in the timber framing industry. They consist of a thick layer of insulating foam, most commonly expanded polystyrene, fastened on each side to a sheet of $^{3}/_{8}$-in-thick OSB. This option is employed in practice primarily for its high isolative value, and ease of installation. Though other options for foam material and sheet product are widely available, this assembly is common. For this design, SIPs have been utilized for walls and roof sheathing, and floor sheathing is $^{15}/_{32}$-in-thick OSB. SIP thickness for walls is 6-1/2", and SIP thickness for the roof is 10-1/8", providing approximate R-Values of R-24 and R-38, respectively. SIP thicknesses chosen reflect those most commonly used in Vermont, and are most comparable to the thickness of 2x6 LF walls (Delabruere 2012). The TF, itself, remains unchanged from that of the "traditional TF" design.

TIMBER FRAME WITH SIPS (NO FOAM)

This subheading ("No Foam") indicates that the EIA has been performed neglecting the environmental effects of the expanded polystyrene (SIP insulation foam). Note that SIPs are not available without a foam core, and this option has been proposed for comparison purposes only.

STANDARD LIGHT-FRAME

An equivalent LF was designed based on the "traditional TF" structure. Equivalence for this design was defined as maintaining an identical building envelope and shape, and meeting the same operational needs as the TF structure. Structures designed for this study reflect a typical design for each framing technique. The design of the standard LF was performed in accordance with the guidelines outlined in the International Residential Code (ICC 2009). Where design requirements could not be met by these guidelines, necessary components of the structural system were engineered according to the NDS (AF&PA 2005). Where design direction was determined by the author, decisions were made based on what would have been constructed if the original as-built structure had employed an LF instead of a TF. Walls are framed with (nominal) 2-in x 6-in kiln-dried dimensional SPF lumber, studs spaced 16-in on center. Roof and wall sheathing were performed with 3/8" OSB, and floors were sheathed with ¾" OSB. See Appendix C for all additional design specifications and for verification of the structural integrity of engineered components.

Further design alterations (below) maintaining "light-frame" in their title reflect this design unless otherwise specified.

LIGNT-FRAME WITH 2X4 WALLS

Wall thickness, dictated by stud size for LF residential buildings, is typically either (nominal) 2-in x 6-in and (nominal) 2-in x 4-in (Allen & Thallon 2011) members (Allen & Thallon 2011). For this design option, all wall framing has been downsized to (nominal) 2-in x 4-in sizes. Other aspects of the standard LF, including sheathing options and joist and rafter sizes, remain unchanged.

LIGNT-FRAME WITH PLYWOOD

Though OSB is a very common sheathing product for residential construction, plywood is another option (Allen & Thallon 2011). For this design option, all OSB sheathing for roofing, flooring, and siding has been substituted with equivalent-thickness plywood. Other aspects of the standard LF, including all framing sizes, remain unchanged.

LIGHT-FRAME INSULATED

This design is identical to the standard LF design, with the addition of fiberglass batt insulation for the walls and roof. Batt thickness is dictated by wall and roof thickness as 5.5-in

and 9.25-in, respectively. Though this study focuses on the environmental impacts of the wood structural system, itself, it was necessary to provide this option for comparison with the timber frame with SIPs. The LF with fiberglass batt insulation EIA also serves to compare the effects of adding this common insulation option to the standard LF.

APPENDIX G

CALCULATION OF CARBON STORED IN WOOD PRODUCTS

Results for global warming potential (GWP) generated by the Athena Impact Estimator for Buildings software (AIE) reflect direct emissions to the atmosphere only. These results accurately account for the emission of all releases that contribute to global climate change from the manufacturing and construction life-cycle phases for each structural assembly considered. Since this software does not give credit for carbon stored in wood products, however, these values present an incomplete picture of the cumulative effect wood structures have on global climate change.

As a tree grows, CO_2 is sequestered from the atmosphere and carbon is stored in the wood fiber to make up approximately 50% of its composition by weight (Florides et al. 2008). It is therefore a more accurate portrayal of a wooden structure's global warming potential to present its GWP emission value alongside a summation of the carbon that it stores in its cellular structure. Note that since GWP is reported in units of kilograms of CO_2-equivalence, carbon stored in wood products must also be reported in these units for comparison, effectively representing the CO_2 that has been kept out of the atmosphere.

The amount of carbon stored in any wood product can be calculated based on the weight of wood fiber material in that product, and so the total weight of wood in each structure was calculated. Since exact moisture content and dimension of each member is not specifically known, weight calculations were based on the assumption that member dimensions reflect oven-dry volume. Weight was based on the oven-dry specific gravity of solid-sawn members (based on species) and panel products, as reported by the National Design Specification (NDS) (AF&PA 2005) and the Panel Design for panel products (APA 2012), respectively. Table G.1 shows the oven-dry specific gravity and unit weight of every wood product included in the structures studied. All calculations for the carbon content of structures were performed with metric units to match the output of AIE.

Table G.1: Wood product specific gravity and unit weight

Wood Product	Specific Gravity (Oven-Dry)	Unit Weight kg/m^3	Source
Solid-Sawn SPF	0.42	420	*NDS (AF&PA 2005)*
Solid-Sawn Eastern Hemlock	0.41	410	*NDS (AF&PA 2005)*
Solid-Sawn Eastern White Pine	0.36	360	*NDS (AF&PA 2005)*
OSB	0.50	500	*Panel Design Spec. (APA 2012)*
Plywood	0.42	420	*Panel Design Spec. (APA 2012)*

The bill of materials for each structure was used to calculate total mass of wood products per structure, based on known volumes of each. Note that only wood product weights were calculated since other materials, including metal fasteners and insulation, do not store carbon. Since each bill of materials reflects the total materials required for purchase for the assembly of each structure, a 10% reduction in total wood fiber material weight was taken before calculating carbon storage. This conservative reduction accounts for waste material from the construction life cycle stage. This reduction is also assumed to account roughly for the mass of adhesives in OSB and plywood, which though inherently included in the specific gravity of these products, do not store carbon.

Carbon makes up approximately 50% of the weight of wood fiber in solid-sawn wood (Lamlom and Savidge 2003). Based on this generally-accepted assumption across most wood species, the total weight of carbon in a given structure is half of the weight of this structure. Conversion from total weight of carbon stored to weight of CO_2-equivalent emissions, for comparison with global warming potential (GWP) values generated by the Impact Estimator, the atomic weight of oxygen must be included. The atomic weight of carbon is approximately 12 atomic mass units (u), the atomic weight of oxygen is approximately 16 u, and the atomic weight of CO_2 is approximately 44 u. The conversion from carbon stored to CO_2-equivalent storage is presented in Equation G1.

$$\text{kg Carbon Stored} * \frac{44}{12} = \text{kg } CO_2\text{-Equivalent} \qquad \textbf{(G1)}$$

Values for volume and weight of each wood product in each structural system, as well as a calculation of total carbon stored and total CO_2-equivalent carbon stored in each structural system are presented in Table G.2.

Table G.2: $C0_2$-equivalence of carbon stored in structures

Wood Product	Units	Light Frame				Timber Frame				
		Standard	2x4 Walls	Plywood	Standard Insulated	Standard	Kiln Dried	Light Frame Infill	SIPs	SIPs No Foam
VOLUME										
Solid-Sawn SPF	m^3	14.64	15.31	12.84	14.64	0	0	0	0	0
Solid-Sawn Eastern Hemlock	m^3	0	0	0	0	32.03	32.03	22.91	18.59	18.59
Solid-Sawn Eastern White Pine	m^3	0	0	0	0	4.37	4.37	0	0	0
OSB	m^3	7.52	7.52	0	7.52	0	0	7.48	8.74	8.74
Plywood	m^3	0	0	7.52	0	0	0	0	0	0
WEIGHT										
Solid-Sawn SPF	kg	6149	6432	5392	6149	0	0	0	0	0
Solid-Sawn Eastern Hemlock	kg	0	0	0	0	13130	13130	9392	7620	7620
Solid-Sawn Eastern White Pine	kg	0	0	0	0	1575	1575	0	0	0
OSB	kg	3761	3761	0	3761	0	0	3742	4372	4372
Plywood	kg	0	0	3160	0	0	0	0	0	0
Total Weight of Wood Products	kg	9911	10193	8552	9911	14705	14705	13135	11992	11992
10% Reduction for Material Waste	kg	991	1019	855	991	1470	1470	1313	1199	1199
Total Weight of Carbon Stored	kg	4460	4587	3848	4460	6617	6617	5911	5396	5396
CO_2-Equivalence of Carbon Stored	kg-CO_2	**16341**	**16807**	**14100**	**16341**	**24245**	**24245**	**21656**	**19773**	**19773**

APPENDIX H

COMPLETE ENVIRONMENTAL IMPACT ASSESSMENT LCIA RESULTS

The following life cycle impact analysis (LCIA) reports were generated by the Athena Impact Estimator (AIE) (ASMI 2012), and indicate values determined by AIE based on building and material data input. Note that only the manufacturing and construction phase results are included. Summary measures included in these results are: Fossil Fuel Consumption, Global Warming Potential, Acidification Potential, Human Health Criteria, Eutrophication Potential, Ozone Depletion Potential, and Smog Potential. Additionally, results pertaining to Energy Consumption, Resource Use, and Land Emissions are included. Results for Air Emissions and Water Emissions have been omitted due to their length, and because none of their results were analyzed in this study.

The tables below outline the environmental impact assessment (EIA) results of each wooden structural system considered. Analyzed are two major structural systems, a light frame and a traditional timber frame. Within each major structural system are several structural options exhibiting material substitutions. Please see Appendix F for a detailed description of each structural system.

SUMMARY MEASURES REPORTS

Table H.1: Summary measures, standard light-frame

	Manufacturing			Construction		
Summary Measures	Material	Transportation	**Total**	Material	Transportation	**Total**
Fossil Fuel Consumption (MJ)	26,260	2,795	**29,055**	964	7,588	**8,552**
Global Warming Potential (kg CO2 eq)	1,220	215	**1,435**	65	340	**405**
Acidification Potential (moles of H+ eq)	661	66	**727**	3	166	**170**
HH Criteria (kg PM10 eq)	16	0	**16**	0	0	**0**
Eutrophication Potential (kg N eq)	2	0	**2**	0	0	**0**
Ozone Depletion Potential (kg CFC-11 eq)	0	0	**0**	0	0	**0**
Smog Potential (kg O3 eq)	192	35	**227**	0	94	**94**

Table H.2: Summary measures, light-frame with 2x4 walls

	Manufacturing			Construction		
Summary Measures	Material	Transportation	**Total**	Material	Transportation	**Total**
Fossil Fuel Consumption (MJ)	25,340	2,611	**27,951**	899	7,259	**8,158**
Global Warming Potential (kg CO2 eq)	1,159	201	**1,360**	60	315	**375**
Acidification Potential (moles of H+ eq)	628	62	**689**	3	159	**162**
HH Criteria (kg PM10 eq)	15	0	**15**	0	0	**0**
Eutrophication Potential (kg N eq)	2	0	**2**	0	0	**0**
Ozone Depletion Potential (kg CFC-11 eq)	0	0	**0**	0	0	**0**
Smog Potential (kg O3 eq)	179	33	**211**	0	90	**90**

Table H.3: Summary Measures: Light Frame – Plywood

	Manufacturing			Construction		
Summary Measures	Material	Transportation	**Total**	Material	Transportation	**Total**
Fossil Fuel Consumption (MJ)	18,023	2,392	**20,415**	876	9,607	**10,483**
Global Warming Potential (kg CO2 eq)	1,043	184	**1,227**	59	289	**348**
Acidification Potential (moles of H+ eq)	535	56	**592**	3	203	**206**
HH Criteria (kg PM10 eq)	9	0	**9**	0	0	**0**
Eutrophication Potential (kg N eq)	1	0	**1**	0	0	**0**
Ozone Depletion Potential (kg CFC-11 eq)	0	0	**0**	0	0	**0**
Smog Potential (kg O3 eq)	172	30	**202**	0	118	**118**

Table H.4: Summary Measures: Light Frame – Standard Insulated

	Manufacturing			Construction		
Summary Measures	Material	Transportation	**Total**	Material	Transportation	**Total**
Fossil Fuel Consumption (MJ)	51,394	3,057	**54,451**	1,072	7,730	**8,802**
Global Warming Potential (kg CO2 eq)	2,996	234	**3,230**	72	351	**423**
Acidification Potential (moles of H+ eq)	1,320	72	**1,392**	4	170	**174**
HH Criteria (kg PM10 eq)	58	0	**58**	0	0	**0**
Eutrophication Potential (kg N eq)	2	0	**2**	0	0	**0**
Ozone Depletion Potential (kg CFC-11 eq)	0	0	**0**	0	0	**0**
Smog Potential (kg O3 eq)	239	38	**278**	0	95	**96**

Table H.5: Summary Measures: Timber Frame – Standard

	Manufacturing			Construction		
Summary Measures	Material	Transportation	**Total**	Material	Transportation	**Total**
Fossil Fuel Consumption (MJ)	12,077	2,705	**14,782**	1,078	10,970	**12,047**
Global Warming Potential (kg CO2 eq)	797	208	**1,005**	72	362	**434**
Acidification Potential (moles of H+ eq)	273	64	**337**	4	234	**237**
HH Criteria (kg PM10 eq)	6	0	**7**	0	0	**0**
Eutrophication Potential (kg N eq)	1	0	**1**	0	0	**0**
Ozone Depletion Potential (kg CFC-11 eq)	0	0	**0**	0	0	**0**
Smog Potential (kg O3 eq)	74	34	**108**	0	135	**135**

Table H.6: Summary Measures: Timber Frame – Kiln Dried

	Manufacturing			Construction		
Summary Measures	Material	Transportation	**Total**	Material	Transportation	**Total**
Fossil Fuel Consumption (MJ)	15,191	2,926	**18,117**	1,078	10,970	**12,047**
Global Warming Potential (kg CO2 eq)	991	225	**1,215**	72	362	**434**
Acidification Potential (moles of H+ eq)	502	69	**571**	4	234	**237**
HH Criteria (kg PM10 eq)	10	0	**10**	0	0	**0**
Eutrophication Potential (kg N eq)	1	0	**1**	0	0	**0**
Ozone Depletion Potential (kg CFC-11 eq)	0	0	**0**	0	0	**0**
Smog Potential (kg O3 eq)	183	37	**220**	0	135	**135**

Table H.7: Summary Measures: Timber Frame – Light Frame Infill

	Manufacturing			Construction		
Summary Measures	Material	Transportation	**Total**	Material	Transportation	**Total**
Fossil Fuel Consumption (MJ)	24,676	2,758	**27,434**	1,010	9,413	**10,423**
Global Warming Potential (kg CO2 eq)	1,124	212	**1,336**	68	347	**415**
Acidification Potential (moles of H+ eq)	509	65	**574**	4	202	**206**
HH Criteria (kg PM10 eq)	13	0	**14**	0	0	**0**
Eutrophication Potential (kg N eq)	1	0	**1**	0	0	**0**
Ozone Depletion Potential (kg CFC-11 eq)	0	0	**0**	0	0	**0**
Smog Potential (kg O3 eq)	117	35	**152**	0	116	**116**

Table H.8: Summary Measures: Timber Frame – SIPs

	Manufacturing			Construction		
Summary Measures	Material	Transportation	**Total**	Material	Transportation	**Total**
Fossil Fuel Consumption (MJ)	128,164	2,967	**131,131**	1,232	10,401	**11,633**
Global Warming Potential (kg CO2 eq)	6,356	228	**6,584**	83	423	**506**
Acidification Potential (moles of H+ eq)	2,137	70	**2,207**	4	226	**230**
HH Criteria (kg PM10 eq)	20	0	**20**	0	0	**0**
Eutrophication Potential (kg N eq)	2	0	**2**	0	0	**0**
Ozone Depletion Potential (kg CFC-11 eq)	0	0	**0**	0	0	**0**
Smog Potential (kg O3 eq)	552	37	**589**	0	128	**129**

Table H.9: Summary Measures: Timber Frame – SIPs No Foam

	Manufacturing			Construction		
Summary Measures	Material	Transportation	**Total**	Material	Transportation	**Total**
Fossil Fuel Consumption (MJ)	31,579	2,966	**34,545**	1,054	9,630	**10,685**
Global Warming Potential (kg CO2 eq)	1,336	228	**1,563**	71	364	**435**
Acidification Potential (moles of H+ eq)	620	70	**690**	4	207	**211**
HH Criteria (kg PM10 eq)	17	0	**17**	0	0	**0**
Eutrophication Potential (kg N eq)	1	0	**1**	0	0	**0**
Ozone Depletion Potential (kg CFC-11 eq)	0	0	**0**	0	0	**0**
Smog Potential (kg O3 eq)	126	37	**164**	0	118	**119**

ENERGY CONSUMPTION

Table H.10: Energy Consumption: Light Frame – Standard

	Manufacturing			Construction		
Energy Source	Material	Transportation	**Total**	Material	Transportation	**Total**
Hydro (MJ)	6,118	1	**6,120**	0	2	**2**
Coal (MJ)	106	18	**124**	6	29	**35**
Diesel (MJ)	7,544	2,601	**10,145**	901	7,286	**8,187**
Feedstock (MJ)	9,340	0	**9,340**	0	0	**0**
Gasoline (MJ)	275	0	**275**	0	0	**0**
Heavy Fuel Oil (MJ)	302	63	**365**	20	94	**114**
LPG (MJ)	11	3	**13**	1	4	**5**
Natural Gas (MJ)	8,682	110	**8,792**	36	175	**211**
Nuclear (MJ)	217	5	**221**	2	8	**9**
Wood (MJ)	27,250	0	**27,250**	0	0	**0**
Total Primary Energy Consumption (MJ)	59,845	2,801	**62,645**	966	7,598	**8,563**

Table H.11: Energy Consumption: Light Frame – 2x4 Walls

	Manufacturing			Construction		
Energy Source	Material	Transportation	**Total**	Material	Transportation	**Total**
Hydro (MJ)	5,844	1	**5,845**	0	2	**2**
Coal (MJ)	102	17	**119**	6	26	**32**
Diesel (MJ)	7,103	2,430	**9,533**	840	6,980	**7,819**
Feedstock (MJ)	9,300	0	**9,300**	0	0	**0**
Gasoline (MJ)	275	0	**275**	0	0	**0**
Heavy Fuel Oil (MJ)	290	59	**349**	18	87	**106**
LPG (MJ)	10	3	**13**	1	4	**5**
Natural Gas (MJ)	8,259	103	**8,362**	34	162	**195**
Nuclear (MJ)	205	4	**209**	1	7	**8**
Wood (MJ)	26,031	0	**26,031**	0	0	**0**
Total Primary Energy Consumption (MJ)	57,420	2,617	**60,037**	900	7,268	**8,168**

Table H.12: Energy Consumption: Light Frame – Plywood

	Manufacturing			Construction		
Energy Source	Material	Transportation	**Total**	Material	Transportation	**Total**
Hydro (MJ)	4,511	1	**4,512**	0	2	**2**
Coal (MJ)	162	15	**177**	5	24	**30**
Diesel (MJ)	6,387	2,225	**8,611**	819	9,351	**10,169**
Feedstock (MJ)	2,827	0	**2,827**	0	0	**0**
Gasoline (MJ)	107	0	**107**	0	0	**0**
Heavy Fuel Oil (MJ)	168	55	**223**	18	80	**98**
LPG (MJ)	45	2	**47**	1	4	**4**
Natural Gas (MJ)	8,328	94	**8,422**	33	148	**181**
Nuclear (MJ)	84	4	**88**	1	7	**8**
Wood (MJ)	18,566	0	**18,566**	0	0	**0**
Total Primary Energy Consumption (MJ)	41,184	2,397	**43,581**	878	9,616	**10,493**

Table H.13: Energy Consumption: Light Frame – Standard Insulated

	Manufacturing			Construction		
Energy Source	Material	Transportation	**Total**	Material	Transportation	**Total**
Hydro (MJ)	8,157	1	**8,158**	0	2	**2**
Coal (MJ)	407	20	**427**	7	30	**36**
Diesel (MJ)	8,849	2,839	**11,688**	1,002	7,419	**8,420**
Feedstock (MJ)	9,340	0	**9,340**	0	0	**0**
Gasoline (MJ)	275	0	**275**	0	0	**0**
Heavy Fuel Oil (MJ)	597	75	**671**	22	98	**119**
LPG (MJ)	21	3	**24**	1	4	**5**
Natural Gas (MJ)	31,905	120	**32,025**	40	180	**221**
Nuclear (MJ)	310	5	**315**	2	8	**10**
Wood (MJ)	27,250	0	**27,250**	0	0	**0**
Total Primary Energy Consumption (MJ)	87,110	3,064	**90,174**	1,074	7,740	**8,814**

Table H.14: Energy Consumption: Timber Frame – Standard

	Manufacturing			Construction		
Energy Source	Material	Transportation	**Total**	Material	Transportation	**Total**
Hydro (MJ)	5,469	1	**5,470**	0	2	**3**
Coal (MJ)	150	17	**167**	7	30	**37**
Diesel (MJ)	5,756	2,515	**8,270**	1,007	10,648	**11,655**
Feedstock (MJ)	849	0	**849**	0	0	**0**
Gasoline (MJ)	35	0	**35**	0	0	**0**
Heavy Fuel Oil (MJ)	162	64	**226**	22	101	**123**
LPG (MJ)	99	3	**102**	1	5	**6**
Natural Gas (MJ)	5,027	107	**5,134**	41	186	**226**
Nuclear (MJ)	222	5	**226**	2	8	**10**
Wood (MJ)	6,640	0	**6,640**	0	0	**0**
Total Primary Energy Consumption (MJ)	24,408	2,711	**27,119**	1,080	10,980	**12,060**

Table H.15: Energy Consumption: Timber Frame – Kiln Dried

	Manufacturing			Construction		
Energy Source	Material	Transportation	**Total**	Material	Transportation	**Total**
Hydro (MJ)	5,828	1	**5,829**	0	2	**3**
Coal (MJ)	169	19	**188**	7	30	**37**
Diesel (MJ)	6,191	2,720	**8,912**	1,007	10,648	**11,655**
Feedstock (MJ)	849	0	**849**	0	0	**0**
Gasoline (MJ)	22	0	**22**	0	0	**0**
Heavy Fuel Oil (MJ)	173	69	**241**	22	101	**123**
LPG (MJ)	63	3	**66**	1	5	**6**
Natural Gas (MJ)	7,724	115	**7,839**	41	186	**226**
Nuclear (MJ)	226	5	**231**	2	8	**10**
Wood (MJ)	17,857	0	**17,857**	0	0	**0**
Total Primary Energy Consumption (MJ)	39,101	2,932	**42,034**	1,080	10,980	**12,060**

Table H.16: Energy Consumption: Timber Frame – Light Frame Infill

	Manufacturing			Construction		
Energy Source	Material	Transportation	**Total**	Material	Transportation	**Total**
Hydro (MJ)	6,045	1	**6,046**	0	2	**2**
Coal (MJ)	125	18	**143**	6	29	**35**
Diesel (MJ)	7,524	2,565	**10,089**	944	9,105	**10,049**
Feedstock (MJ)	9,398	0	**9,398**	0	0	**0**
Gasoline (MJ)	283	0	**283**	0	0	**0**
Heavy Fuel Oil (MJ)	304	63	**367**	21	97	**117**
LPG (MJ)	39	3	**42**	1	4	**5**
Natural Gas (MJ)	7,002	109	**7,111**	38	178	**216**
Nuclear (MJ)	218	5	**222**	2	8	**9**
Wood (MJ)	19,320	0	**19,320**	0	0	**0**
Total Primary Energy Consumption (MJ)	50,259	2,764	**53,022**	1,012	9,423	**10,435**

Table H.17: Energy Consumption: Timber Frame – SIPs

	Manufacturing			Construction		
Energy Source	Material	Transportation	**Total**	Material	Transportation	**Total**
Hydro (MJ)	8,879	1	**8,881**	1	2	**3**
Coal (MJ)	332	19	**351**	8	36	**43**
Diesel (MJ)	8,451	2,757	**11,208**	1,152	10,025	**11,177**
Feedstock (MJ)	85,815	0	**85,815**	0	0	**0**
Gasoline (MJ)	410	0	**410**	0	0	**0**
Heavy Fuel Oil (MJ)	23,496	71	**23,567**	25	118	**143**
LPG (MJ)	64	3	**66**	1	5	**6**
Natural Gas (MJ)	9,596	117	**9,713**	46	217	**264**
Nuclear (MJ)	452	5	**457**	2	10	**11**
Wood (MJ)	24,659	0	**24,659**	0	0	**0**
Total Primary Energy Consumption (MJ)	162,155	2,973	**165,128**	1,235	10,413	**11,648**

Table H.18: Energy Consumption Timber Frame – SIPs No Foam

	Manufacturing			Construction		
Energy Source	Material	Transportation	**Total**	Material	Transportation	**Total**
Hydro (MJ)	7,256	1	**7,257**	0	2	**3**
Coal (MJ)	180	19	**199**	7	31	**37**
Diesel (MJ)	8,394	2,757	**11,151**	986	9,307	**10,292**
Feedstock (MJ)	13,618	0	**13,618**	0	0	**0**
Gasoline (MJ)	410	0	**410**	0	0	**0**
Heavy Fuel Oil (MJ)	383	71	**453**	22	101	**123**
LPG (MJ)	41	3	**44**	1	5	**6**
Natural Gas (MJ)	8,553	117	**8,670**	40	187	**227**
Nuclear (MJ)	351	5	**356**	2	8	**10**
Wood (MJ)	24,659	0	**24,659**	0	0	**0**
Total Primary Energy Consumption (MJ)	63,845	2,973	**66,818**	1,056	9,641	**10,697**

RESOURCE USE

Table H.19: Resource Use: Light Frame – Standard

	Manufacturing			Construction		
Resource	Material	Transportation	**Total**	Material	Transportation	**Total**
Limestone (kg)	7	0	**7**	0	0	**0**
Iron Ore (kg)	19	0	**19**	0	0	**0**
Water (L)	2,337	0	**2,337**	0	0	**0**
Obsolete Scrap Steel (kg)	45	0	**45**	0	0	**0**
Coal (kg)	8	1	**9**	0	1	**2**
Wood Fiber (kg)	13,469	0	**13,469**	0	0	**0**
Uranium (kg)	0	0	**0**	0	0	**0**
Natural Gas (m^3)	243	3	**246**	1	5	**6**
Natural Gas as feedstock (m^3)	72	0	**72**	0	0	**0**
Crude Oil (L)	226	70	**295**	24	193	**217**
Crude Oil as feedstock (L)	143	0	**143**	0	0	**0**
Prompt Scrap Steel as feedstock (kg)	29	0	**29**	0	0	**0**

Table H.20: Resource Use: Light Frame – 2x4 Walls

	Manufacturing			Construction		
Resource	Material	Transportation	**Total**	Material	Transportation	**Total**
Limestone (kg)	7	0	**7**	0	0	**0**
Iron Ore (kg)	17	0	**17**	0	0	**0**
Water (L)	2,181	0	**2,181**	0	0	**0**
Obsolete Scrap Steel (kg)	42	0	**42**	0	0	**0**
Coal (kg)	7	1	**8**	0	1	**2**
Wood Fiber (kg)	12,586	0	**12,586**	0	0	**0**
Uranium (kg)	0	0	**0**	0	0	**0**
Natural Gas (m^3)	231	3	**233**	1	4	**5**
Natural Gas as feedstock (m^3)	72	0	**72**	0	0	**0**
Crude Oil (L)	213	65	**278**	22	185	**207**
Crude Oil as feedstock (L)	143	0	**143**	0	0	**0**
Prompt Scrap Steel as feedstock (kg)	27	0	**27**	0	0	**0**

Table H.21: Resource Use: Light Frame – Plywood

	Manufacturing			Construction		
Resources	Material	Transportation	**Total**	Material	Transportation	**Total**
Limestone (kg)	7	0	**7**	0	0	**0**
Iron Ore (kg)	19	0	**19**	0	0	**0**
Water (L)	2,339	0	**2,339**	0	0	**0**
Obsolete Scrap Steel (kg)	45	0	**45**	0	0	**0**
Coal (kg)	10	1	**11**	0	1	**1**
Wood Fiber (kg)	11,508	0	**11,508**	0	0	**0**
Natural Gas (m3)	231	2	**234**	1	4	**5**
Natural Gas as feedstock (m3)	26	0	**26**	0	0	**0**
Crude Oil (L)	185	60	**245**	22	247	**269**
Crude Oil as feedstock (L)	29	0	**29**	0	0	**0**
Prompt Scrap Steel as feedstock (kg)	29	0	**29**	0	0	**0**

Table H.22: Resource Use: Light Frame – Standard Insulated

	Manufacturing			Construction		
Resource	Material	Transportation	**Total**	Material	Transportation	**Total**
Limestone (kg)	484	0	**484**	0	0	**0**
Iron Ore (kg)	19	0	**19**	0	0	**0**
Sand (kg)	768	0	**768**	0	0	**0**
Other (kg)	367	0	**367**	0	0	**0**
Water (L)	3,124	0	**3,124**	0	0	**0**
Obsolete Scrap Steel (kg)	45	0	**45**	0	0	**0**
Coal (kg)	35	1	**36**	0	1	**2**
Wood Fiber (kg)	13,469	0	**13,469**	0	0	**0**
Uranium (kg)	0	0	**0**	0	0	**0**
Natural Gas (m3)	857	3	**861**	1	5	**6**
Natural Gas as feedstock (m3)	72	0	**72**	0	0	**0**
Crude Oil (L)	268	76	**344**	27	197	**224**
Crude Oil as feedstock (L)	143	0	**143**	0	0	**0**
Prompt Scrap Steel as feedstock (kg)	29	0	**29**	0	0	**0**

Table H.23: Resource Use: Timber Frame – Standard

	Manufacturing			Construction		
Resource	Material	Transportation	**Total**	Material	Transportation	**Total**
Limestone (kg)	10	0	**10**	0	0	**0**
Iron Ore kg	33	0	**33**	0	0	**0**
Water (L)	2,690	0	**2,690**	0	0	**0**
Obsolete Scrap Steel (kg)	54	0	**54**	0	0	**0**
Coal (kg)	9	1	**10**	0	1	**2**
Wood Fiber (kg)	13,004	0	**13,004**	0	0	**0**
Uranium (kg)	0	0	**0**	0	0	**0**
Natural Gas (m3)	147	3	**150**	1	5	**6**
Crude Oil (L)	166	68	**234**	27	281	**308**
Metallurgical Coal as feedstock (kg)	4	0	**4**	0	0	**0**
Prompt Scrap Steel as feedstock (kg)	34	0	**34**	0	0	**0**

Table H.24: Resource Use: Timber Frame – Kiln Dried

	Manufacturing			Construction		
Resource	Material	Transportation	**Total**	Material	Transportation	**Total**
Limestone (kg)	10	0	**10**	0	0	**0**
Iron Ore (kg)	33	0	**33**	0	0	**0**
Water (L)	2,690	0	**2,690**	0	0	**0**
Obsolete Scrap Steel (kg)	54	0	**54**	0	0	**0**
Coal (kg)	10	1	**11**	0	1	**2**
Wood Fiber (kg)	14,076	0	**14,076**	0	0	**0**
Uranium (kg)	0	0	**0**	0	0	**0**
Natural Gas (m3)	219	3	**222**	1	5	**6**
Crude Oil (L)	179	73	**252**	27	281	**308**
Metallurgical Coal as feedstock (kg)	4	0	**4**	0	0	**0**
Prompt Scrap Steel as feedstock (kg)	34	0	**34**	0	0	**0**

Table H.25: Resource Use: Timber Frame – Light Frame Infill

	Manufacturing			Construction		
Resource	Material	Transportation	**Total**	Material	Transportation	**Total**
Limestone (kg)	8	0	**8**	0	0	**0**
Iron Ore (kg)	24	0	**24**	0	0	**0**
Water (L)	2,206	0	**2,206**	0	0	**0**
Obsolete Scrap Steel (kg)	52	0	**52**	0	0	**0**
Coal (kg)	9	1	**10**	0	1	**2**
Wood Fiber (kg)	13,272	0	**13,272**	0	0	**0**
Natural Gas (m3)	199	3	**202**	1	5	**6**
Natural Gas as feedstock m3	71	0	**71**	0	0	**0**
Crude Oil (L)	225	69	**294**	25	241	**266**
Crude Oil as feedstock (L)	143	0	**143**	0	0	**0**
Prompt Scrap Steel as feedstock (kg)	33	0	**33**	0	0	**0**

Table H.26: Resource Use: Timber Frame – SIPs

	Manufacturing			Construction		
Resource	Material	Transportation	**Total**	Material	Transportation	**Total**
Limestone (kg)	11	0	**11**	0	0	**0**
Iron Ore (kg)	42	0	**42**	0	0	**0**
Water (L)	9,979	0	**9,979**	0	0	**0**
Obsolete Scrap Steel (kg)	59	0	**59**	0	0	**0**
Coal (kg)	19	1	**20**	0	2	**2**
Wood Fiber (kg)	14,256	0	**14,256**	0	0	**0**
Uranium (kg)	0	0	**0**	0	0	**0**
Natural Gas (m3)	268	3	**271**	1	6	**7**
Natural Gas as feedstock (m3)	721	0	**721**	0	0	**0**
Crude Oil (L)	866	74	**940**	31	265	**296**
Crude Oil as feedstock (L)	1,373	0	**1,373**	0	0	**0**
Metallurgical Coal as feedstock (kg)	4	0	**4**	0	0	**0**
Prompt Scrap Steel as feedstock (kg)	38	0	**38**	0	0	**0**

Table H.27: Resource Use: Timber Frame – SIPs No Foam

	Manufacturing			Construction		
Resource	Material	Transportation	**Total**	Material	Transportation	**Total**
Limestone (kg)	11	0	**11**	0	0	**0**
Iron Ore (kg)	42	0	**42**	0	0	**0**
Water (L)	1,427	0	**1,427**	0	0	**0**
Obsolete Scrap Steel (kg)	59	0	**59**	0	0	**0**
Coal (kg)	12	1	**13**	0	2	**2**
Wood Fiber (kg)	14,256	0	**14,256**	0	0	**0**
Uranium (kg)	0	0	**0**	0	0	**0**
Natural Gas (m3)	240	3	**243**	1	5	**6**
Natural Gas as feedstock (m3)	104	0	**104**	0	0	**0**
Crude Oil (L)	254	74	**328**	26	246	**273**
Crude Oil as feedstock (L)	208	0	**208**	0	0	**0**
Metallurgical Coal as feedstock (kg)	4	0	**4**	0	0	**0**
Prompt Scrap Steel as feedstock (kg)	38	0	**38**	0	0	**0**

LAND EMISSIONS

Table H.28: Land Emissions: Light Frame – Standard

	Manufacturing			Construction		
Land Emissions	Material	Transportation	**Total**	Material	Transportation	**Total**
Bark/Wood Waste (kg)	104	0	**104**	0	0	**0**
Blast Furnace Slag (kg)	7	0	**7**	0	0	**0**
Blast Furnace Dust (kg)	2	0	**2**	0	0	**0**
Other Solid Waste (kg)	207	2	**209**	1	3	**4**

Table H.29: Land Emissions: Light Frame – 2x4 Walls

	Manufacturing			Construction		
Land Emissions	Material	Transportation	**Total**	Material	Transportation	**Total**
Bark/Wood Waste (kg)	93	0	**93**	0	0	**0**
Blast Furnace Slag (kg)	6	0	**6**	0	0	**0**
Blast Furnace Dust (kg)	2	0	**2**	0	0	**0**
Other Solid Waste (kg)	196	2	**198**	1	3	**4**

Table H.30: Land Emissions: Light Frame – Plywood

	Manufacturing			Construction		
Land Emissions	Material	Transportation	**Total**	Material	Transportation	**Total**
Bark/Wood Waste (kg)	91	0	**91**	0	0	**0**
Blast Furnace Slag (kg)	7	0	**7**	0	0	**0**
Blast Furnace Dust (kg)	2	0	**2**	0	0	**0**
Other Solid Waste (kg)	138	2	**140**	1	3	**3**

Table H.31: Land Emissions: Light Frame – Standard Insulated

	Manufacturing			Construction		
Land Emissions	Material	Transportation	**Total**	Material	Transportation	**Total**
Bark/Wood Waste (kg)	104	0	**104**	0	0	**0**
Blast Furnace Slag (kg)	7	0	**7**	0	0	**0**
Blast Furnace Dust (kg)	2	0	**2**	0	0	**0**
Other Solid Waste (kg)	272	2	**274**	1	3	**4**

Table H.32: Land Emissions: Timber Frame – Standard

	Manufacturing			Construction		
Land Emissions	Material	Transportation	**Total**	Material	Transportation	**Total**
Bark/Wood Waste (kg)	138	0	**138**	0	0	**0**
Blast Furnace Slag (kg)	10	0	**10**	0	0	**0**
Blast Furnace Dust (kg)	2	0	**2**	0	0	**0**
Other Solid Waste (kg)	67	2	**69**	1	3	**4**

Table H.33: Land Emissions: Timber Frame – Kiln Dried

	Manufacturing			Construction		
Land Emissions	Material	Transportation	**Total**	Material	Transportation	**Total**
Bark/Wood Waste (kg)	138	0	**138**	0	0	**0**
Blast Furnace Slag (kg)	10	0	**10**	0	0	**0**
Blast Furnace Dust (kg)	2	0	**2**	0	0	**0**
Other Solid Waste (kg)	156	2	**158**	1	3	**4**

Table H.34: Land Emissions: Timber Frame – Light Frame Infill

	Manufacturing			Construction		
Land Emissions	Material	Transportation	**Total**	Material	Transportation	**Total**
Bark/Wood Waste (kg)	111	0	**111**	0	0	**0**
Blast Furnace Slag (kg)	8	0	**8**	0	0	**0**
Blast Furnace Dust (kg)	2	0	**2**	0	0	**0**
Other Solid Waste (kg)	145	2	**147**	1	3	**4**

Table H.35: Land Emissions: Timber Frame – SIPs

	Manufacturing			Construction		
Land Emissions	Material	Transportation	**Total**	Material	Transportation	**Total**
Bark/Wood Waste (kg)	99	0	**99**	0	0	**0**
Blast Furnace Slag (kg)	11	0	**11**	0	0	**0**
Blast Furnace Dust (kg)	2	0	**2**	0	0	**0**
Other Solid Waste (kg)	220	2	**223**	1	4	**5**

Table H.36: Land Emissions: Timber Frame – SIPs No Foam

	Manufacturing			Construction		
Land Emissions	Material	Transportation	**Total**	Material	Transportation	**Total**
Bark/Wood Waste (kg)	99	0	**99**	0	0	**0**
Blast Furnace Slag (kg)	11	0	**11**	0	0	**0**
Blast Furnace Dust (kg)	2	0	**2**	0	0	**0**
Other Solid Waste (kg)	176	2	**178**	1	3	**4**

APPENDIX I

SAP2000 MODEL MATERIAL AND SECTION PROPERTIES

Table I.1 through Table I.5 include all material input defined within all SAP2000 light-frame (LF) and timber frame (TF) models. Where wall material and section labels indicate direction (North-N, South-S, East-E, and West-W), story number, or refer to the portal frame when describing wall materials, please refer to Figure I.1 to verify location. Though directional orientation is described with respect to the LF in Figure I.1, please note that all labels (except 'portal frame') apply to the TF structure as well.

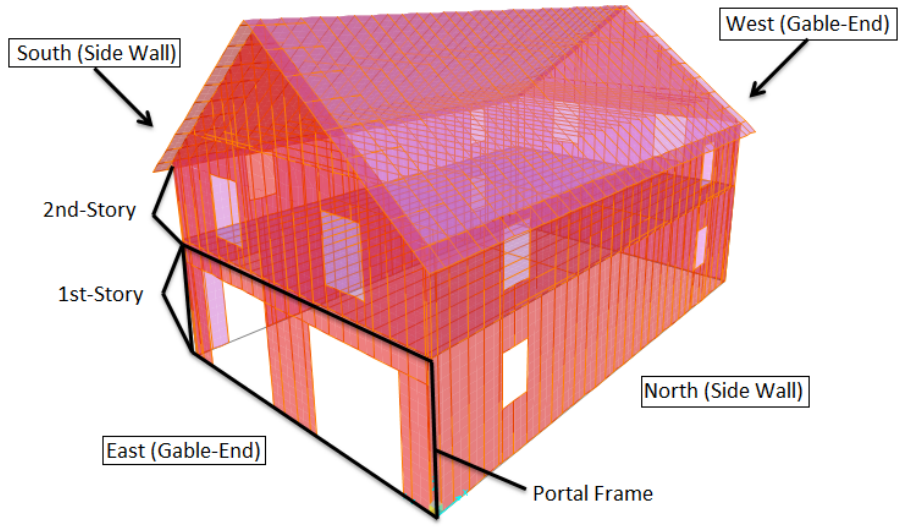

Figure I.1: Directional orientation of structures

Though section properties and framing element material properties are constant among LF or TF models loaded with different load combinations, sheathing material properties used in the models vary based on wind loading direction. For this reason, each wall or diaphragm sheathing material has been defined with either flexural properties or in-plane properties, based on the loading scenario. For gravity loading only (load combination 4), diaphragms are considered to act in flexure, and walls are considered to act in-plane.

Plywood material properties have been determined using OSULaminates (Nairn 2007). Please refer to Table I.1 for an outline of the input parameters this program requires to produce the material properties necessary for modeling.

Table I.1: OSULaminates input values for plywood material properties

Material	Plywood Species 1
Number of Plies	4
Ply Thickness	0.30 cm (0.117 in)
Ply Orientation	0° - 90° - 90° - 0°

LIGHT-FRAME SECTION PROPERTIES

Section properties defined for framing and sheathing elements define the actual cross-section or thickness of the material, respectively. Additionally, material properties are assigned to each section, depending on species and/or wood product type. The position of sheathing elements with respect to the distance from the center line to wall studs, rafters, or joists for wall sheathing, roof sheathing, and floor sheathing, respectively, are also defined. All LF solid-sawn framing element cross-sections are defined using the section designer tool in SAP2000 (Computers and Structures, 2012). Where members are longitudinally adjacent, such as double top plates or built-up posts, one single framing element is defined with a cross-section equivalent to the sum of the cross-sections of the individual members. For specific framing member or sheathing sizes, please refer to Appendix C of Malone (2013), LF Design.

TIMBER FRAME SECTION PROPERTIES

Section properties defined for the TF follow the same procedure as those defined for the LF. Note that structural insulated panels (SIPs) are defined as two layers of 9.5 mm (3/8-in) OSB, each offset the appropriate respective distance from the wall or roof center line. For specific framing member sizes, please refer to Appendix B.

LIGHT-FRAME MATERIAL PROPERTIES

Table I.2: Light-frame isotropic (framing) material properties

Isotropic Material (Framing Materials)	Applied to	Weight per Unit Volume kN/m3 (lb/ft3)	Modulus of Elasticity MPa (ksi)	Poisson's Ratio	Source
Dimensional SPF Lumber	Framing elements	4.12 (26.2)	9,653 (1,400)	0.3	NDS (AF&PA 2005)

Table I.3: Light-frame orthotropic (sheathing) material properties

Orthotroic Materials (Sheathing Materials)	Applied to	Weight per Unit Volume kg/m^3 (lb/ft^3)	Modulus of Elasticity, E MPa (ksi)		Poisson's Ratio, U		Shear Modulus, G_{12}	Source
			E1	E2	U1	U2	Mpa (ksi)	
Floor Sheathing (Plywood)	2^{nd} Floor (in-plane)	420 (26.2)	5,336 (774)	5,336 (774)	0.021	0.021	194 (28.2)	**All material properties except G_{12}:** *OSULaminates* (Nairn 2007) **G_{12} values from calibration with:** *NDS Equation 4.3.2-2* (AF&PA 2005), (Al Mamun et al. 2011)
	2^{nd} Floor (flexural)		9,101 (1,320)	1,558 (226)	0.07	0.012	NA	
Roof Sheathing (Plywood)	Roof (in-plane)	420 (26.2)	5,336 (774)	5,336 (774)	0.021	0.021	195 (28.3)	
	Roof (flexural)		9,101 (1,320)	1,558 (226)	0.07	0.012	NA	
1^{st}-Story Walls (Plywood)	N, S Walls - 1^{st}-Story (in-plane)	420 (26.2)	5,336 (774)	5,336 (774)	0.021	0.021	195 (23.8)	
	N, S Walls - 1^{st}-Story (flexure)		9,101 (1,320)	1,558 (226)	0.07	0.012	NA	
2nd-Story walls (Plywood)	N, S Walls - 2nd Story (in-plane)	420 (26.2)	5,336 (774)	5,336 (774)	0.021	0.021	150 (21.7)	
	N, S Walls - 2nd-Story (flexure)		9,101 (1,320)	1,558 (226)	0.07	0.012	NA	
1^{st}-Story Gable-Ends (Plywood)	E, W Gables- 1^{st}-Story (in-plane)	420 (26.2)	5,336 (774)	5,336 (774)	0.021	0.021	170 (24.7)	
	E, W Gables - 1^{st}-Story (flexure)		9,101 (1,320)	1,558 (226)	0.07	0.012	NA	
2nd-Story Gable-Ends (Plywood)	E, W Gables - 2nd Story (in-plane)	420 (26.2)	5,336 (774)	5,336 (774)	0.021	0.021	167 (24.2)	
	E, W Gables - 2nd-Story (flexure)		9,101 (1,320)	1,558 (226)	0.07	0.012	NA	
Portal Frame Sheathing (Plywood)	Portal Frame (in-plane)	420 (26.2)	5,336 (774)	5,336 (774)	0.021	0.021	158 (22.9)	

TIMBER FRAME MATERIAL PROPERTIES

Table I.4: Timber frame isotropic (framing) material properties

Isotropic Material (Framing Materials)	Applied to	Weight per Unit Volume kN/m3 (lb/ft3)	Modulus of Elasticity MPa (ksi)	Poisson's Ratio	Source
Eastern Hemlock Timbers	Framing elements	4.12 (26.2)	8,274 (1,200)	0.3	NDS (AF&PA 2005)

Table I.5: Timber frame orthotropic (sheathing) material properties

Orthotroic Materials (Sheathing Materials)	Applied to	Weight per Unit Volume kg/m^3 (lb/ft^3)	Modulus of Elasticity, E MPa (ksi)		Poisson's Ratio, U		Shear Modulus, G_{12}	Source
			E1	E2	U1	U2	Mpa (ksi)	
Floor Sheathing (OSB)	2^{nd} Floor (in-plane)	500 (31.2)	5,336 (774)	3,833(556)	0.23	0.16	194 (28.2)	**Material properties except U1,2:** *Panel Design Spec. (APA 2012)* **Poisson's Ratio:** (*Thomas 2003)* **G_{12} values from calibration with:** *(Erikson 2003, Carradine 2004)*
	2^{nd} Floor (flexural)		7,860 (1,140)	1,441 (209)	0.23	0.16	NA	
Roof Sheathing (OSB SIPs)	Roof (in-plane)	500 (31.2)	5,336 (774)	3,833(556)	0.23	0.16	553 (80.2)	
	Roof (flexural)		7,860 (1,140)	1,441 (209)	0.23	0.16	NA	
Walls (OSB SIPs)	Walls (in-plane)	500 (31.2)	5,336 (774)	3,833(556)	0.23	0.16	159 (23.1)	
	Walls (flexure)		7,860 (1,140)	1,441 (209)	0.23	0.16	NA	

APPENDIX J

SHEATHING G_{12} STIFFNESS CALIBRATION

The stiffness of sheathing elements, expressed as the shear modulus (G_{12}), was determined by calibration with expected deflections. The adjustment of this material property in SAP2000 controls the stiffness of shear walls and diaphragms. G_{12} calibration for light-frame (LF) sheathing was determined in accordance with the methods used by Pfretzschner et al. (2013). G_{12} calibration for the LF portal frame, as well as timber frame (TF) sheathing, were determined by calibration with expected deflections from existing experimental data.

Expected deflections for sheathing fastened to light-framing were calculated using Equation C4.3.2-2 from the National Design Specification (NDS) (AF&PA 2005b). A simple calibration model was created in SAP2000 depicting the parameters set by this equation, and the G_{12} value was altered until the calculated expected deflection (and therefore the expected stiffness) was met. The deflection calculated by this equation is based on "framing bending deflection, panel shear deflection, deflection from nail sip, and deflection due to tie-down slip" (AF&PA 2005b). For more information on this adjustment procedure, see Pfretzschner (2012).

Since NDS equation C4.3.2-2 applies only to walls constructed by typical light framing methods, it was not possible to use this method to determine the stiffness (G_{12}) of the LF portal frame or the walls or roof of the TF. These calibration models, and the experimental testing they are based on, are explained below.

LIGHT-FRAME

Portal Frame

Experimental testing was performed on a single-bay portal frame by Al Mamun et al. (2011) for the purpose of investigating the behavior of LF wood portal frames. The portal frame assembly tested that was most similar to the portal frame designed for the LF in this study was selected for calibration. The test assembly considered was constructed with 38-mm x 89-mm (nominal 2-in x 4-in) spruce-pine-fir (SPF) studs and sheathed on one side with 12.5-mm-thick (0.5-in) OSB. The header was constructed from built-up 38-mm x 286-mm (nominal 2-in x 12-in) SPF. Hold-downs (Simpson Strong-Tie, model HTT 16) were installed at both ends of the portal frame, as well as on both sides of the opening. A lateral load was applied in the in-plane direction at the top of the frame, and deflection was allowed in only in this direction. Deflection

of the top of the portal frame was measured with a displacement transducer, and a stiffness value of 0.62 kN/mm (3,597 lb/in) was calculated based on measured deflection and applied load.

A simple calibration model depicting this test setup was created in SAP2000. Modeling techniques used mimic those developed by Martin et al. (2011) and Pfretzschner et al. (2013), and are identical to those used throughout this study. Framing members (studs, sills, and header) were modeled as frame elements with their actual cross-section, and assigned isotropic material properties for SPF. Orthotropic material properties assigned to sheathing were determined with the APA Panel Design Specification (APA 2012), and are identical to those assigned to OSB in the structural models created for this study. For more information on material properties of SPF and OSB, refer to Appendix I. Figure J.1 is an image of the calibration model for this portal frame created in SAP2000, shown before and during deflection (Computers and Structures, Inc. 2012).

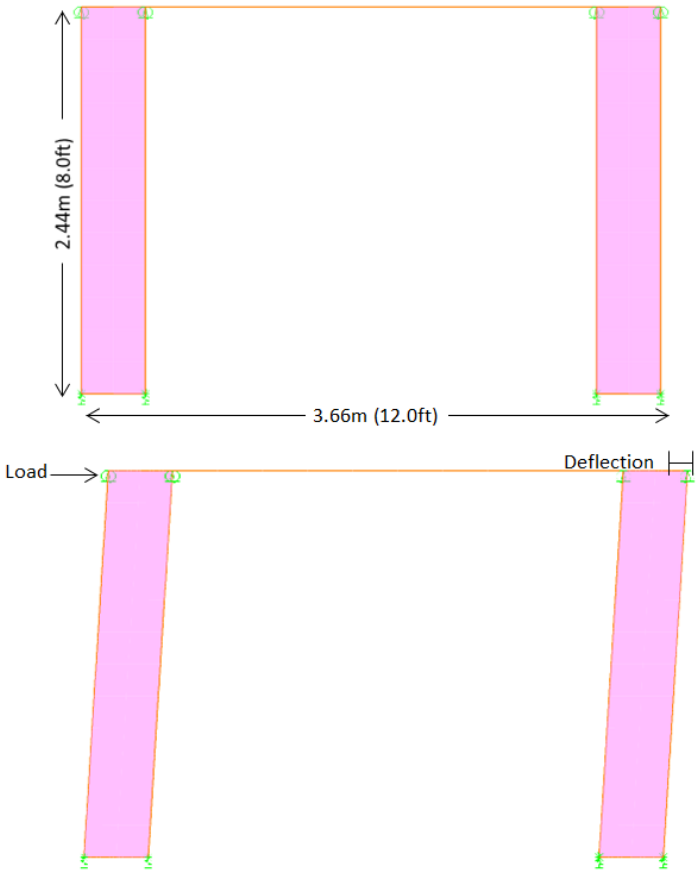

Figure J.1: Portal frame calibration model (Computers and Structures, Inc. 2012)

A load was applied at the top of the portal frame in the calibration model, and deflection at the top of the portal frame was observed. (Note that for this calibration model and all others necessary in this study, the force applied is negligible. Since the stiffness of an assembly is calculated by dividing the force by the deflection, and calibration models created in SAP2000 are linear, the stiffness result will be equal for any load/deflection combination considered.) The G_{12} sheathing element material property was then altered until a calculation of stiffness based on applied load and observed deflection matched the stiffness value reported by Al Mamun et al. (2011) of 0.62 kN/mm (89 ksi). The shear modulus (G_{12}) of the sheathing elements of portal frame was 553 MPa (80.2 ksi). This value was applied to the material property for all meshed sheathing elements in the LF portal frame.

TIMBER FRAME

Walls

The stiffness of TF walls was calibrated by the same methods against experimental testing performed by Erikson et al. (2003). In-plane stiffness tests performed on a 2-story, 2-bay TF wall sheathed with SIPs generated stiffness results that were matched by a simple calibration model created in SAP2000. Erikson's 2-story, 2-bay eastern white pine (EWP) TF wall assembly was sheathed entirely with four, 102-mm (4-in)-thick SIP panels composed of OSB and extruded polystyrene. The framing assembly tested included three vertical posts, equally spaced at 3.66-m (12-ft) apart, spanning the entire height of the wall. Posts were 197-mm x 197-mm (7.75-in x 7.75-in) in cross-section. Beams positioned in between each bay, at mid-height, the top of the wall, and at the base of the wall (sill plate) were spaced 2.44-m (8-ft) apart, and were 146-mm x 248-mm (5.75-in x 9.75-in) in cross-section. Typical TF braces were also included, and were 70-mm x 146-mm (2.75-in x 5.75-in) in cross-section. The edges of all four panels, and therefore the joints in between each, coincided over framing members and SIPs were attached to the frame around the entire perimeter of each panel by 102-mm (4-in) screws, every 306-mm (12-in). OSB splines were therefore not necessary. Cyclic loads were applied to the TF wall system by a spreader bar, distributing half of the total applied a force at each horizontal beam level. Deflections were measured at the top of the wall. Using the applied load and the initial displacement observed (indicating the maximum stiffness of the wall) Erikson calculated a shear stiffness of 0.259 kN/mm (37.56 ksi) for this assembly.

A simple calibration model was created in SAP2000 to mimic this exact testing setup to determine a G_{12} (stiffness) value. Modeling techniques were identical to all others used in this study. Framing members were modeled with their identical cross-sections, and assigned isotropic material properties for eastern white pine, as defined in the NDS (AF&PA 2005a). These material properties included a modulus of elasticity of 7,585 MPa (1,100 ksi) and a Poisson's ratio of 0.3. Each layer of sheathing material was modeled with the orthotropic material properties used throughout this study for OSB. Figure J.2 shows the calibration model created in SAP2000 to determine the stiffness of TF walls, before and during deflection.

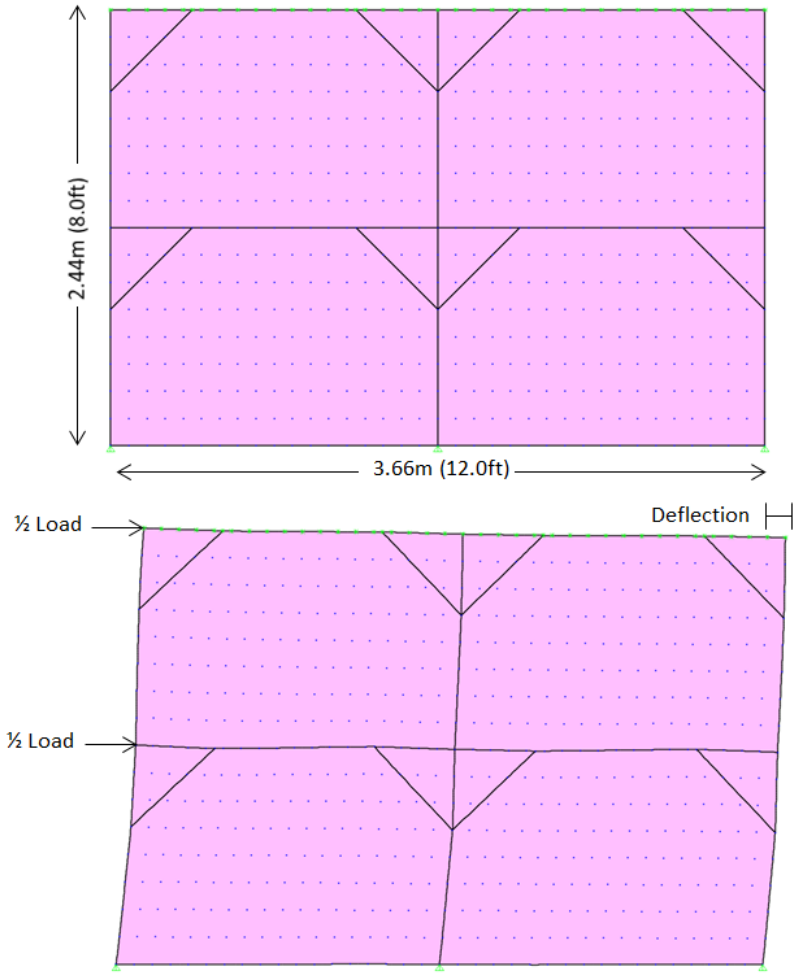

Figure J.2: Timber frame wall calibration model (Computers and Structures, Inc. 2012)

Identical to the loading for testing, the total force for the calibration model was applied in two equal parts at the center and top beams, acting in-plane. Also similar to testing, deflection was only allowed in the in-plane direction. A force was applied, and the G_{12} (stiffness) value of

the sheathing elements was adjusted until the observed deflection resulted in a calculated stiffness of 259 MPa (37.56 ksi). Based on this calibration model, a G_{12} (stiffness) value of 23.1 was applied to all TF wall sheathing elements.

Roof

The stiffness of the roof assembly of the TF was calibrated with the results of testing performed by Carradine et al. (2004). Testing for both strength and stiffness was performed on a series of roof section diaphragm assemblies to examine the capability of TF roof systems to resist lateral loads. The roof assembly selected for calibration consists of three, 127-mm x 178-mm (5-in x 7-in) southern pine rafters separated by three sets of 127-mm x 178-mm (5-in x 7-in) southern pine purlins (horizontal roof beams), sheathed with 165-mm (6.5-in)-thick SIPs. Rafters were spaced 3.66-m (12-ft) apart, and sets of purlins were spaced at 1.22-m (4-ft) apart, connecting to rafters with mortise-and-tenon-style joinery at the center and both ends of rafters. SIP dimensions were 1.22-m x 3.66-m (4-ft x 12-ft), and long edges coincided with framing members (purlins). One short edge of each SIP coincided with the center rafter, and the other short edge overhung 305-mm (12-in) past its respective side rafter. SIP connections to framing members were made with 229-mm (9-in) screws every 305-mm (12-in) along all framing members (rafters and purlins). Load was applied to a center rafter, in a simple beam test scenario, in the direction parallel to the rafters. Deflection was measured at the opposite side of end center rafter. Results from testing of this roof section show a shear stiffness of 7.58 kN/mm (43.2 k/in).

A simple calibration model depicting this testing setup was created, similar to methods described for TF walls, in SAP2000 (Computers and Structures, Inc. 2012). Modeling techniques were identical to all others used in this study. Framing members were modeled with their identical cross-sections, and assigned isotropic material properties for southern pine, as defined in the NDS (AF&PA 2005a). These material properties included a MOE of 8,275 MPa (1,200 ksi) and a Poisson's ratio of 0.3. Each layer of sheathing material was modeled with the orthotropic material properties used throughout this study for OSB. Figure J.3 shows the calibration model created in SAP2000 to determine the stiffness of TF roof sheathing, undeformed and deformed.

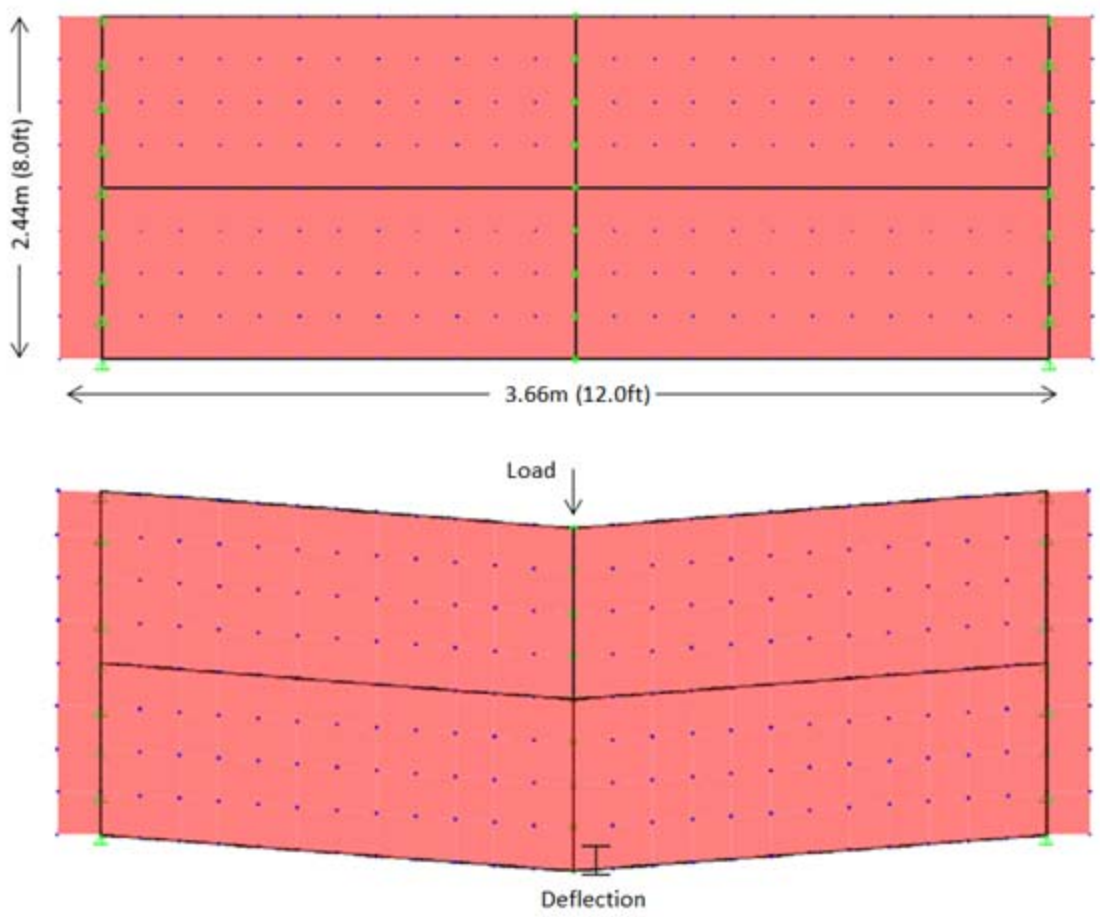

Figure J.3: Timber frame roof calibration model (Computers and Structures, Inc. 2012)

Testing was performed with a similar configuration roof, so the stiffness observed should be the same in the model and experiment. Unfortunately, a load twice the magnitude of that used in the test was applied at the center rafter in the model. Deflection was only allowed in the in-plane direction. Based on this calibration model, a G_{12} value of 80.2 ksi was applied to all TF roof sheathing elements, and was twice as large as it should be. To examine the effects of this error, several of the models were examined with the correct value of 40.1 ksi for G_{12}. These models included those depicting a fully-enclosed TF structure, loaded with gravity loads only (load combination 4), as well as with dead load and wind load from both general directions (load combination 5). Results showed that reactions at the foundation were minimally affected, with a maximum variation in foundation connection magnitude of 5% for load combination 4 (gravity loads only), and a maximum variation in foundation connection magnitude of 3% for load combination 5 (dead and wind load).

APPENDIX K

LOAD PATH ANALYSIS RESULTS:

The following graphs represent the location and magnitude of foundation connection reactions (anchor bolts, hold downs, post bottoms) resulting from design loading for timber frame and light frame structures modeled with and without openings (doors, windows). Magnitude is represented by the size of each "bubble," and its position is in the actual location of the reaction along the base of the structure. Dark bubbles and light bubbles represent reactions in the positive and negative directions, respectively. For reactions in the Z direction (vertical direction), positive reactions represent those resisting downward gravity forces. For reactions in the X and Y directions, the positive direction is shown on each plot. Note that all plots representing reactions in the Z direction are scaled relative to one another only. Plots representing reactions in the X and Y directions are scaled relative to one another (but do not match the scale of plots representing reactions in the Z direction). Reactions observed are based on design loading from Allowable Stress Design (ASD) load combinations 4, 5, and 6a (ASCE 2010). For load combinations including wind loading, wind loads were considered from each respective direction. "North-South" wind loading represents wind loading ranging from perpendicular to the side of each structure to 45-degrees off of perpendicular in the direction of the windward corner, as indicated in each plot considering this wind loading direction. Similarly, "East-West" wind loading represents wind loading ranging from perpendicular to the gable end of each structure to 45-degrees off of perpendicular in the direction of the windward corner, as indicated on each plot considering this wind loading direction. For scale, the maximum absolute reaction observed for every plot is highlighted and assigned its value. Reaction magnitudes were observed in metric units of force (kN). The following plots are graphic results from structural models created in SAP2000 Version 15 (Computers and Structures, 2012).

LIGHT FRAME – FULLY ENCLOSED

Load Combination 4

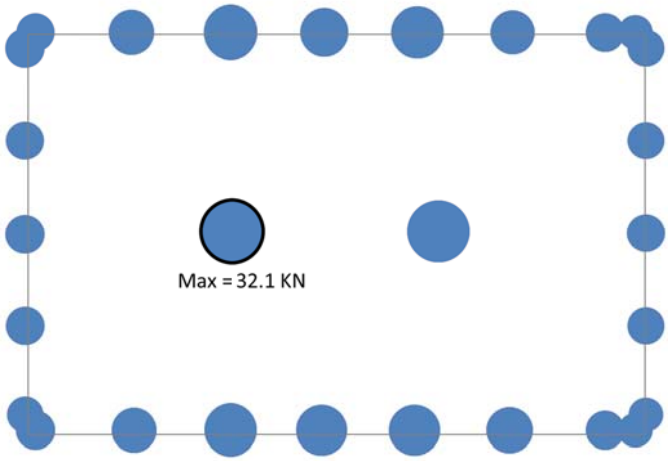

Figure K.1: Light frame, enclosed, load combination 4, Z-reaction

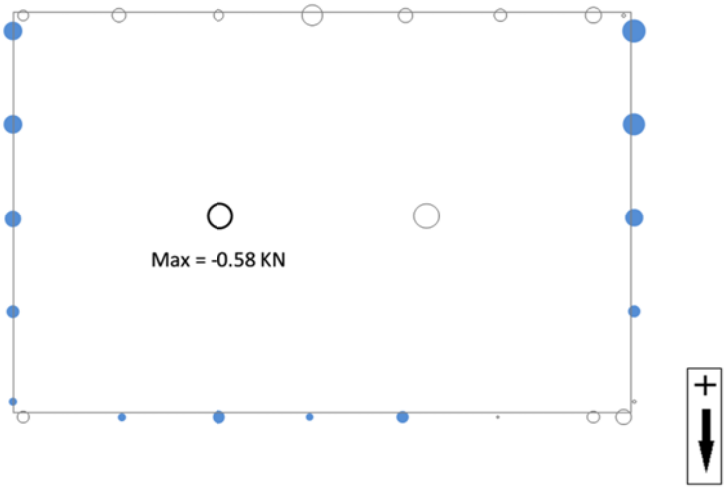

Figure K.2: Light frame, enclosed, load combination 4, Y-reaction

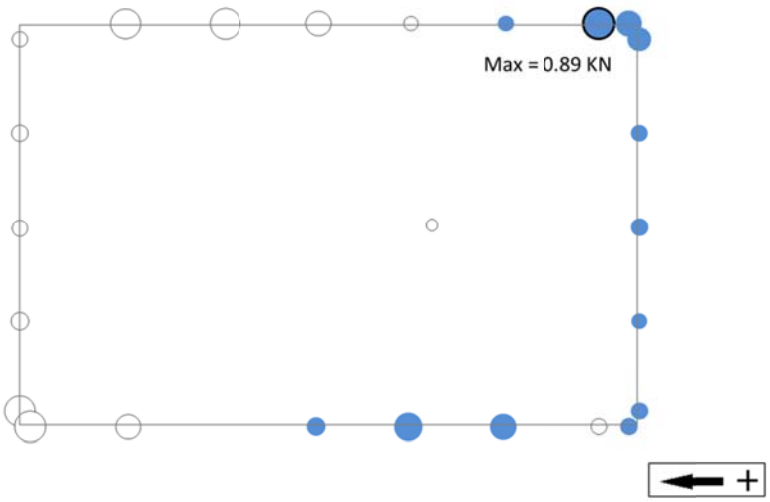

Figure K.3: light frame, enclosed, load combination 4, X-reaction

Load Combination 5

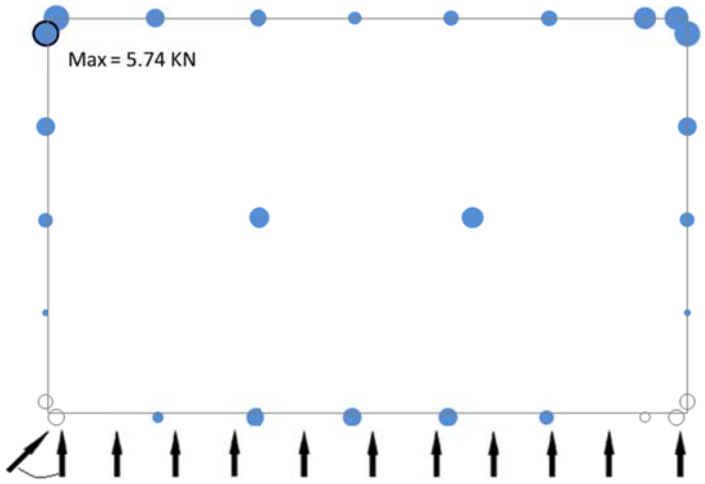

Figure K.4: Light frame, enclosed, load combination 5, north-south wind, Z-reaction

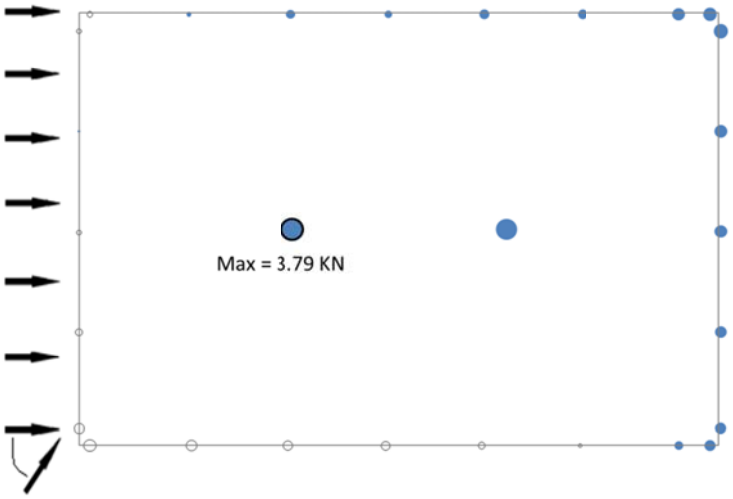

Figure K.5: Light frame, enclosed, load combination 5, east-west wind, Z-reaction

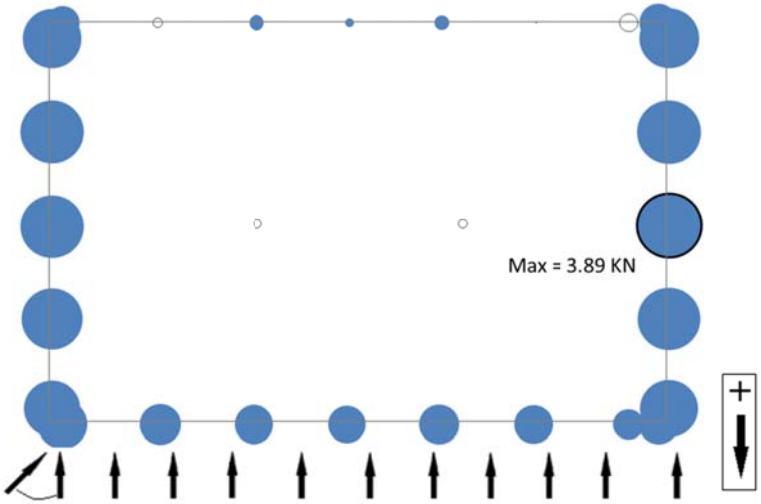

Figure K.6: Light frame, enclosed, load combination 5, north-south wind, Y-reaction

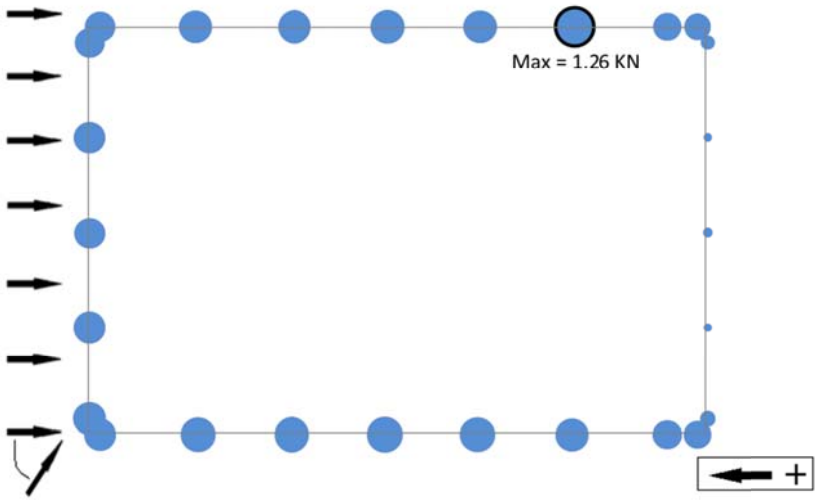

Figure K.7: Light frame, enclosed, load combination 5, east-west wind, X-reaction

Load Combination 6a

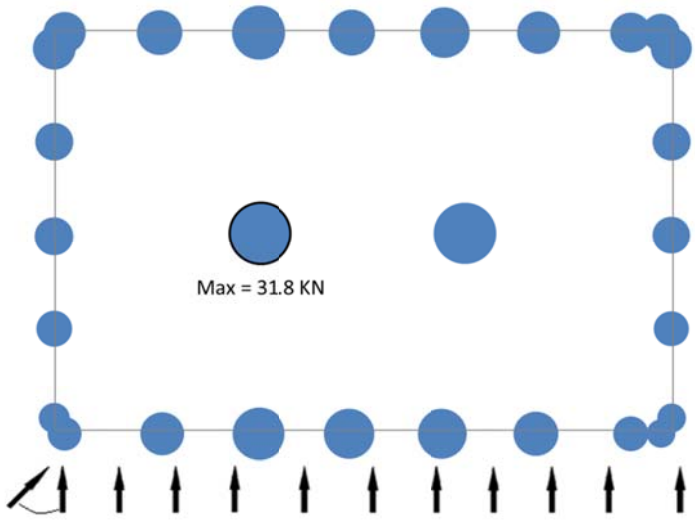

Figure K.8: Light frame, enclosed, load combination 6a, north-south wind, Z-reaction

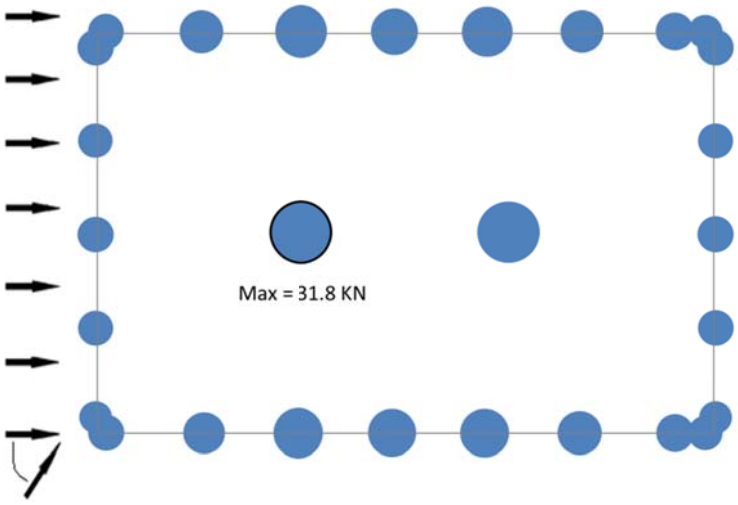

Figure K.9: Light frame, enclosed, load combination 6a, east-west wind, Z-reaction

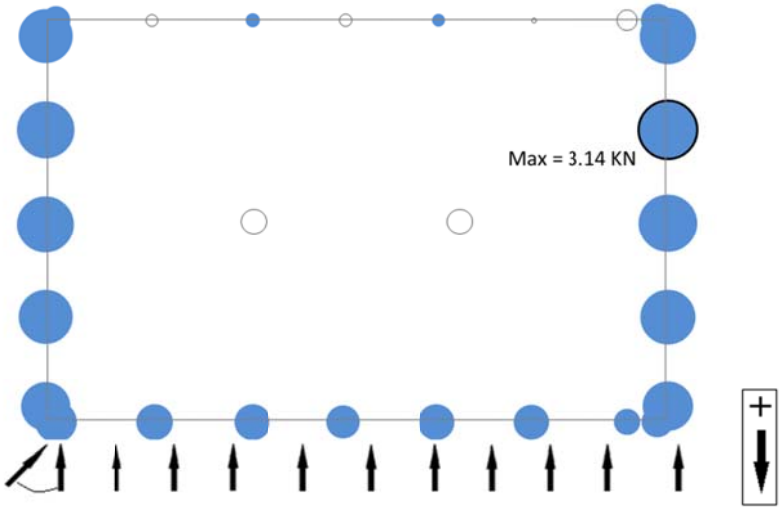

Figure K.10: Light frame, enclosed, load combination 6a, north-south wind, Y-reaction

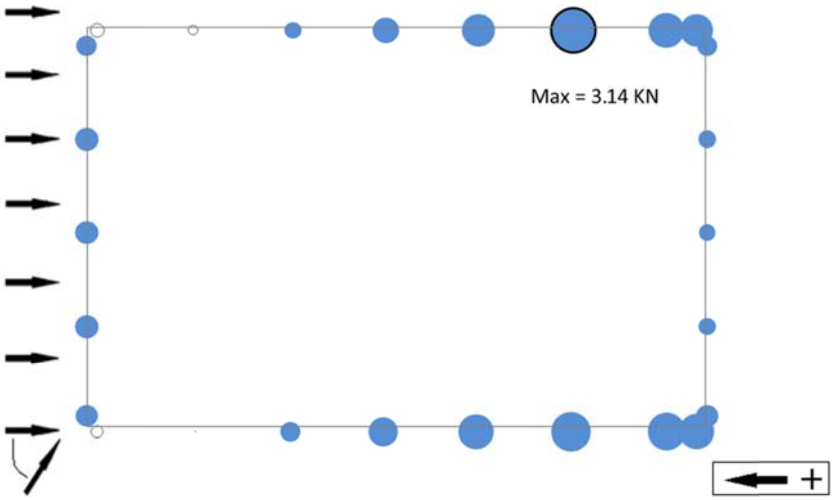

Figure K.11: Light frame, enclosed, load combination 6a, east-west wind, X-reaction

LIGHT FRAME – WITH OPENINGS

Load Combination 4

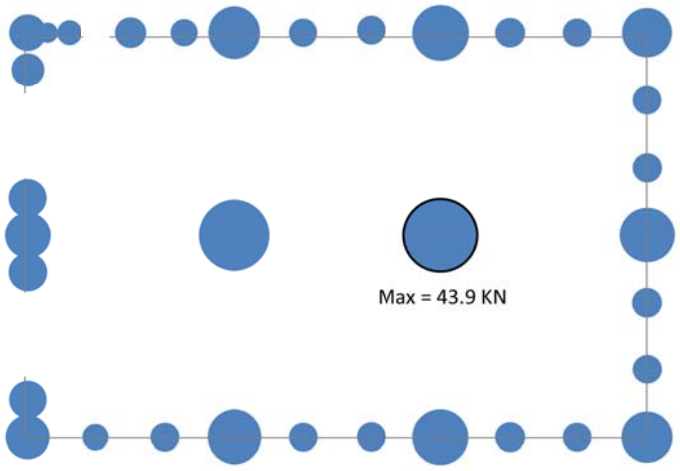

Figure K.12: Light frame, with openings, load combination 4, Z-reaction

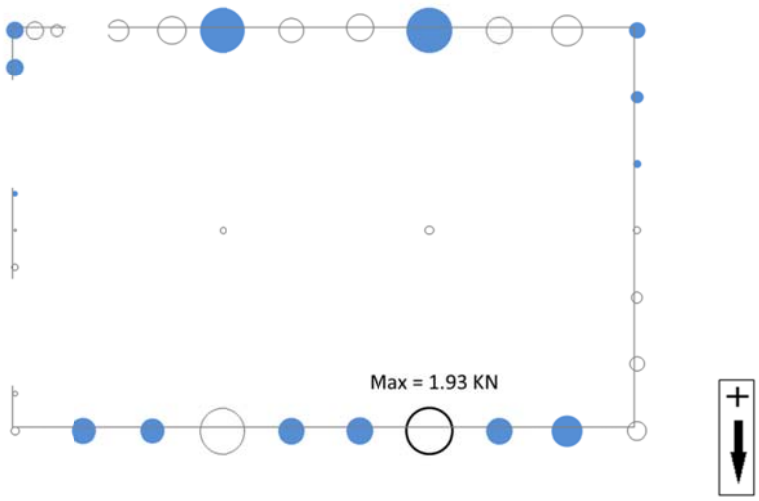

Figure K.13: Light frame, with openings, load combination 4, Y-reaction

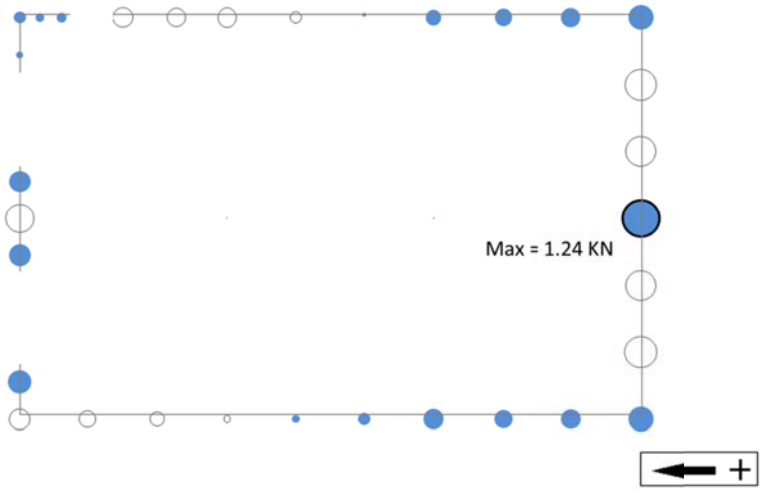

Figure K.14: Light frame, with openings, load combination 4, X-reaction

Load Combination 5

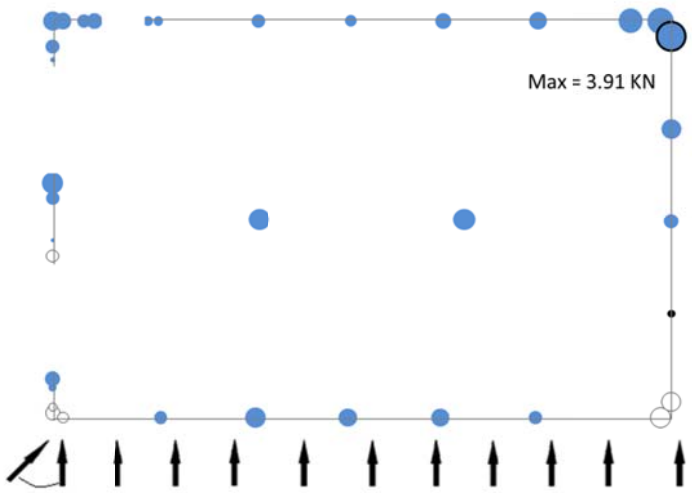

Figure K.15: Light frame, with openings, load combination 5, north-south wind, Z-reaction

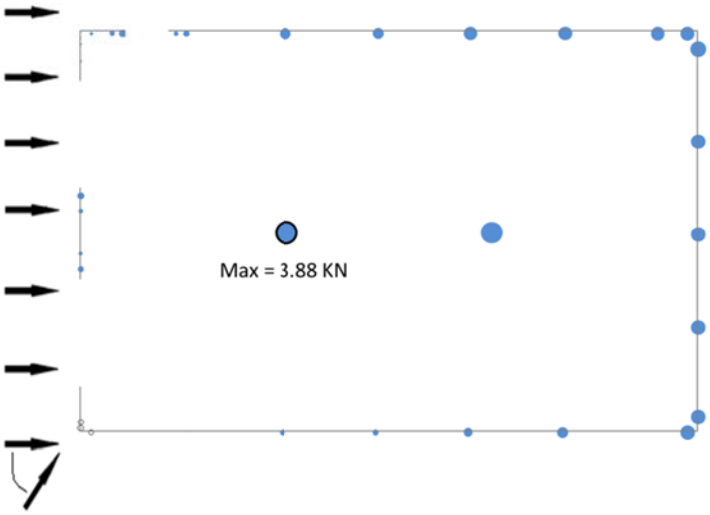

Figure K.16: Light frame, with openings, load combination 5, east-west wind, Z-reaction

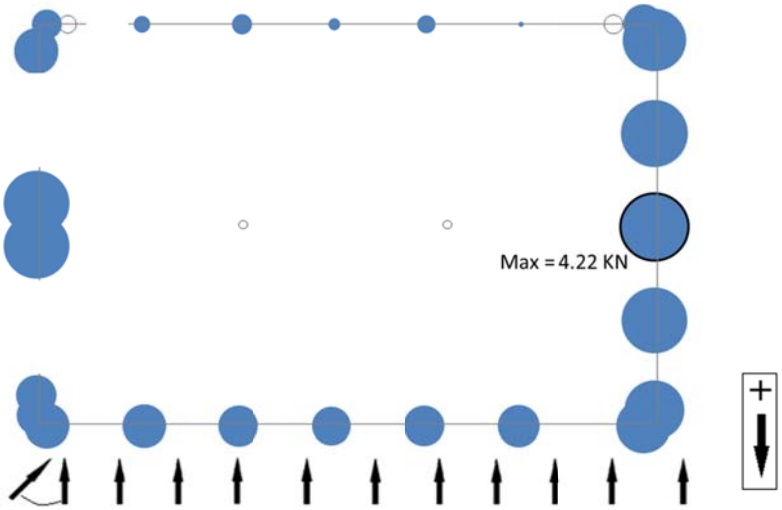

Figure K.17: Light frame, with openings, load combination 5, north-south wind, Y-reaction

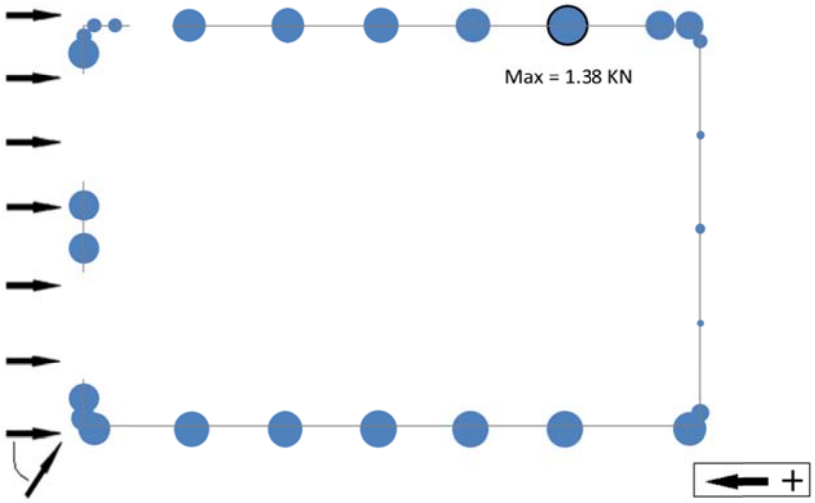

Figure K.18: Light frame, with openings, load combination 5, east-west wind, X-reaction

Load Combination 6a

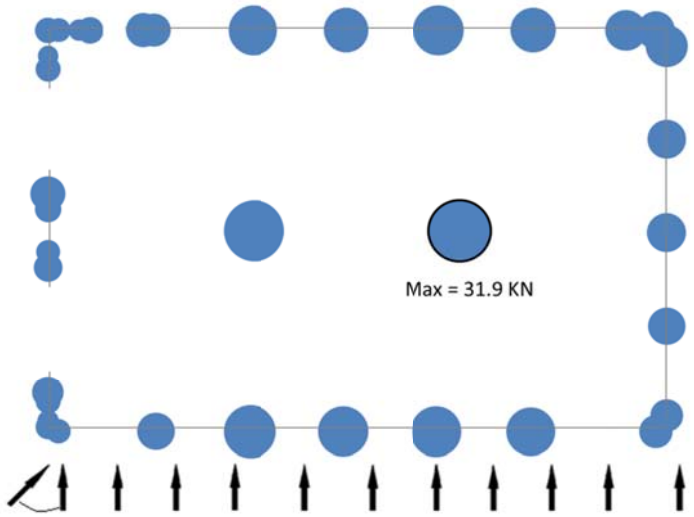

Figure K.19: Light frame, with openings, load combination 6a, north-south wind, Z-reaction

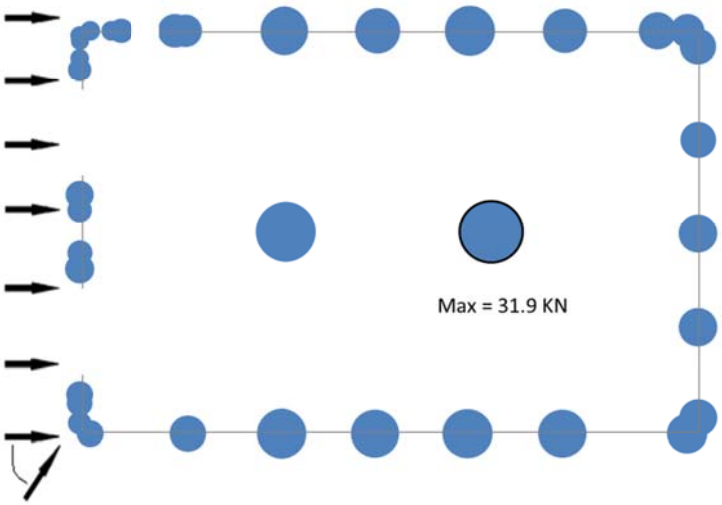

Figure K.20: Light frame, with openings, load combination 6a, east-west wind, Z-reaction

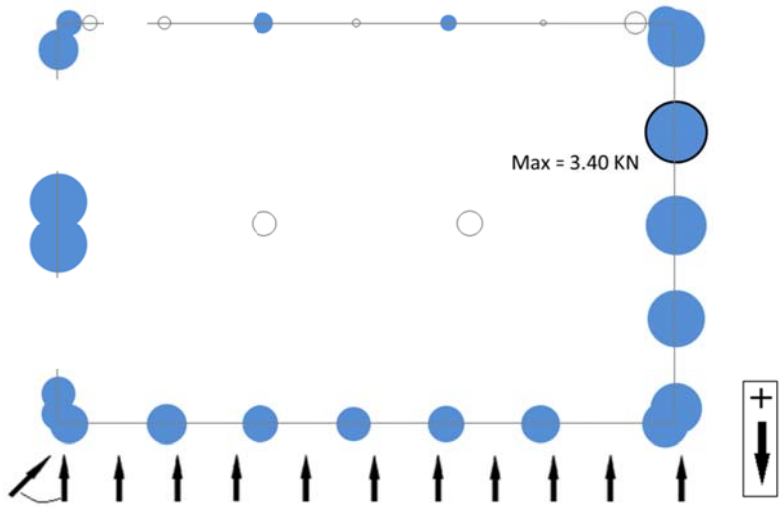

Figure K.21: Light frame, with openings, load combination 6a, north-south wind, Y-reaction

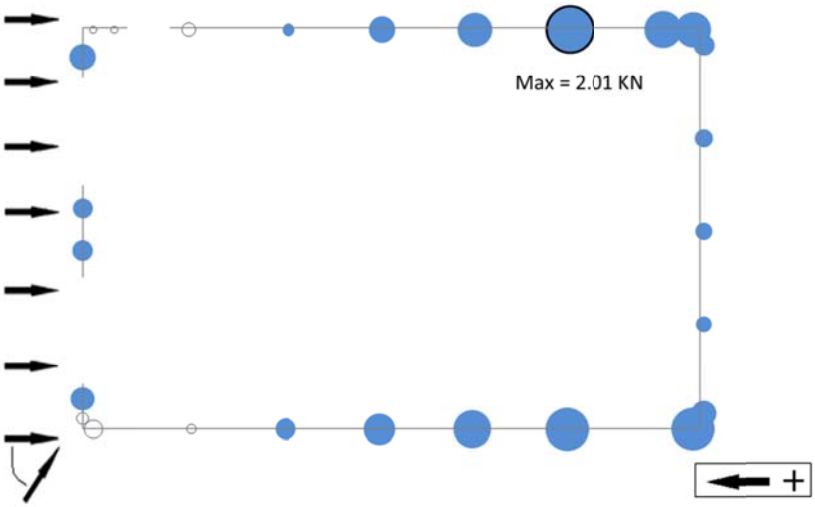

Figure K.22: Light frame, with openings, load combination 6a, east-west wind, X-reaction

TIMBER FRAME – FULLY ENCLOSED

Load Combination 4

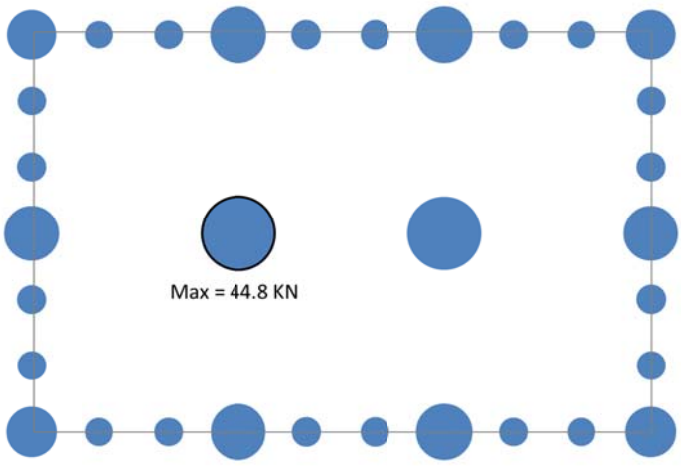

Figure K.23: Timber frame, enclosed, load combination 4, Z-reaction

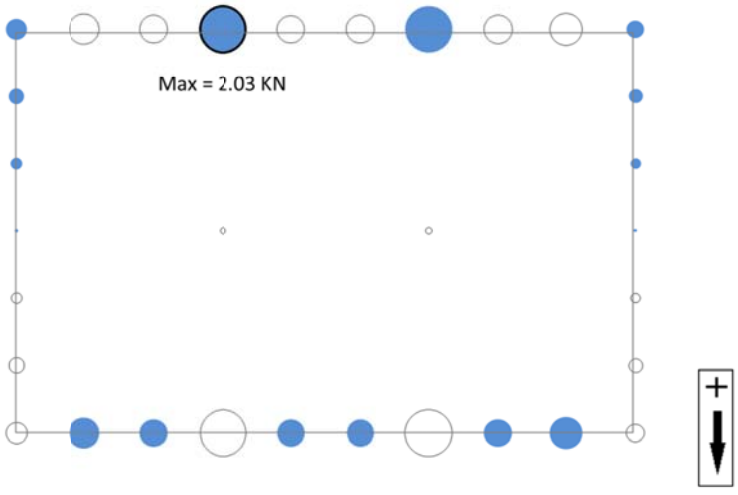

Figure K.24: Timber frame, enclosed, load combination 4, Y-reaction

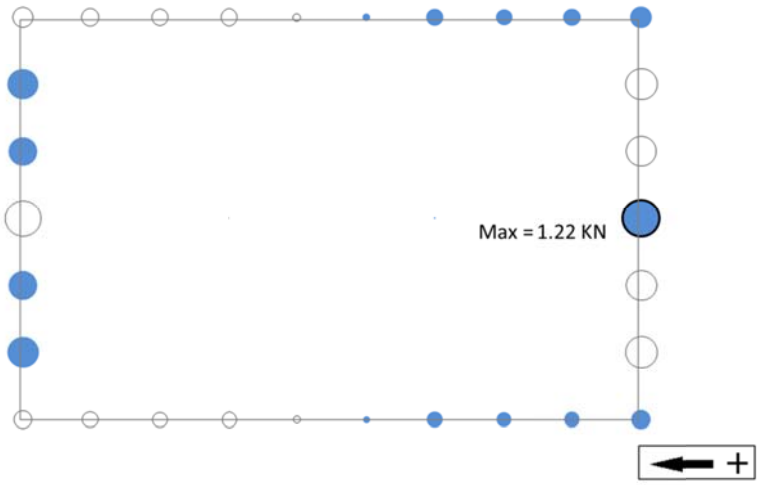

Figure K.25: Timber frame, enclosed, load combination 4, X-reaction

Load Combination 5

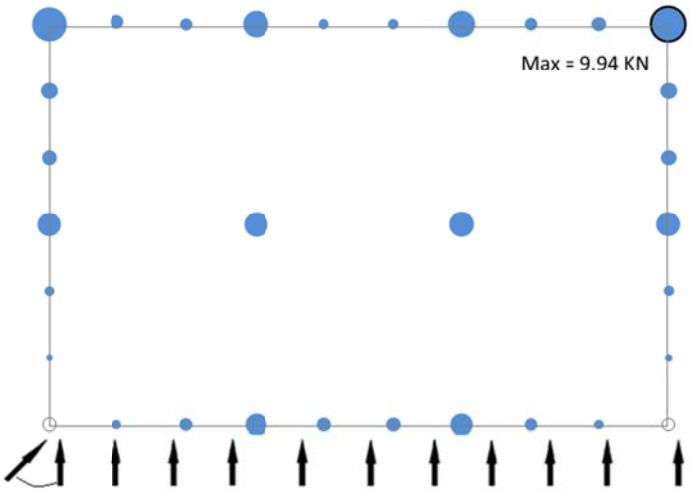

Figure K.26: Timber frame, enclosed, load combination 5, north-south wind, Z-reaction

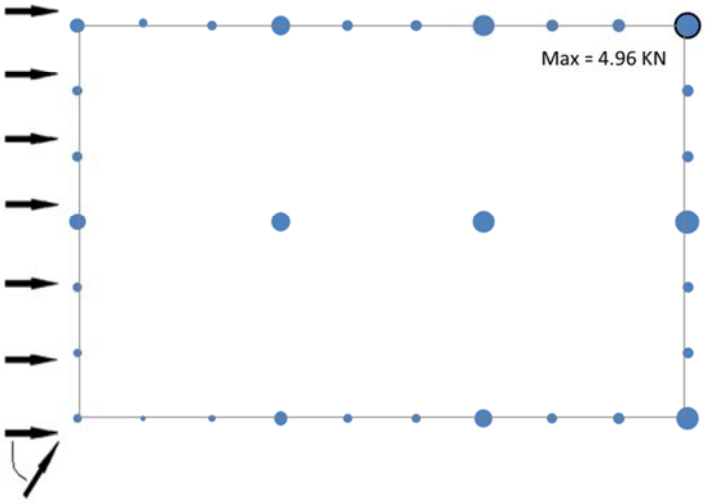

Figure K.27: Timber frame, enclosed, load combination 5, east-west wind, Z-reaction

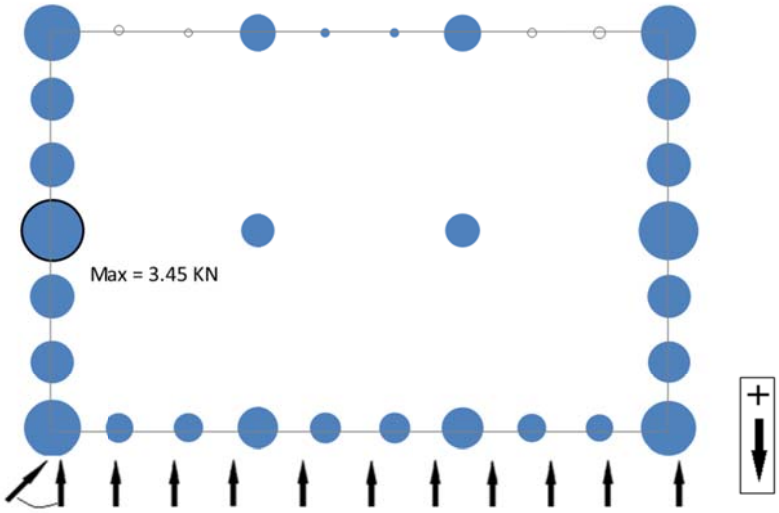

Figure K.28: Timber frame, enclosed, load combination 5, north-south wind, Y-reaction

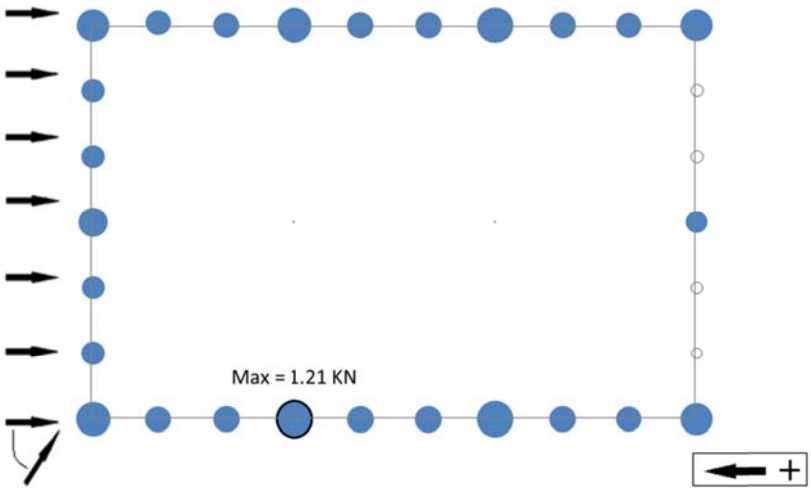

Figure K.29: Timber frame, enclosed, load combination 5, east-west wind, X-reaction

Load Combination 6a

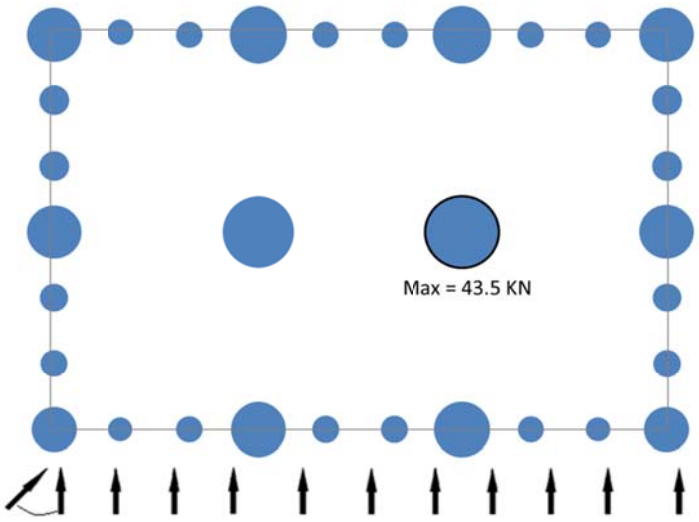

Figure K.30: Timber frame, enclosed, load combination 6a, north-south wind, Z-reaction

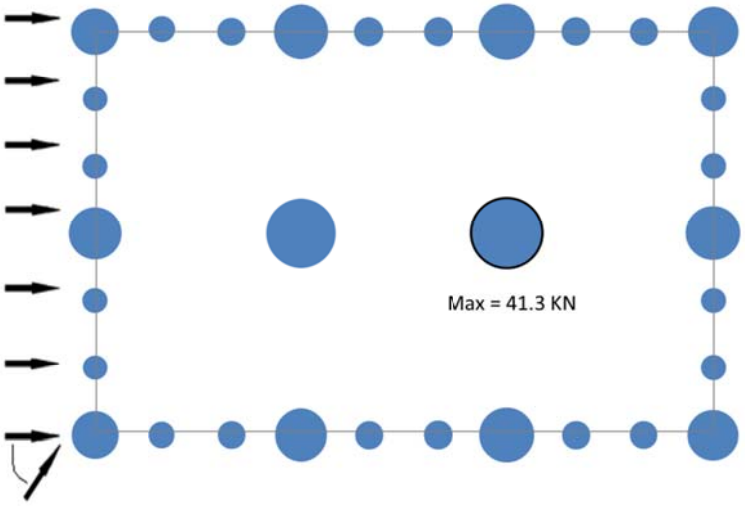

Figure K.31: Timber frame, enclosed, load combination 6a, east-west wind, Z-reaction

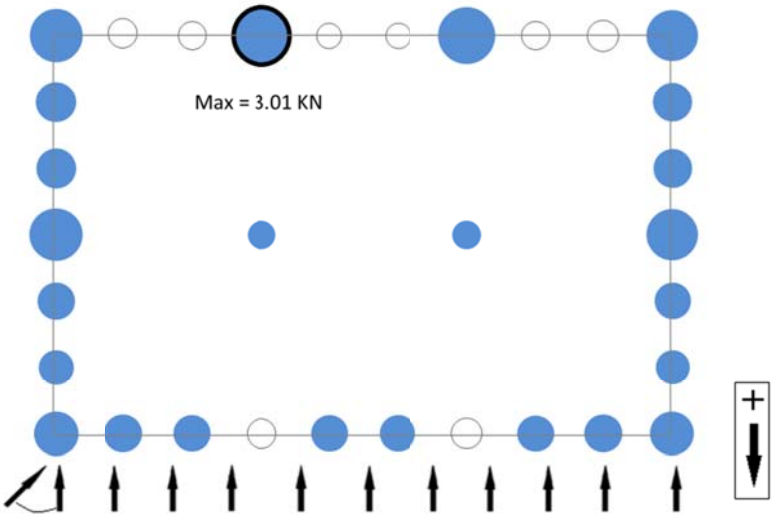

Figure K.32: Timber frame, enclosed, load combination 6a, north-south wind, Y-reaction

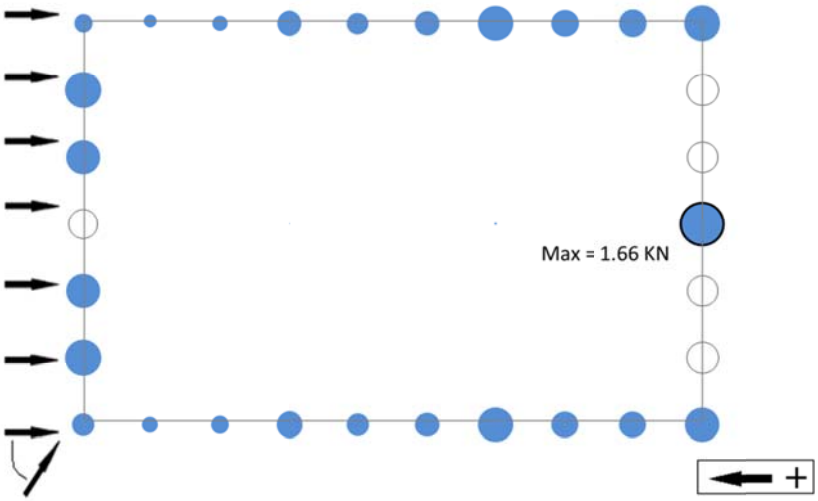

Figure K.33: Timber frame, enclosed, load combination 6a, east-west wind, X-reaction

TIMBER FRAME – WITH OPENINGS

Load Combination 4

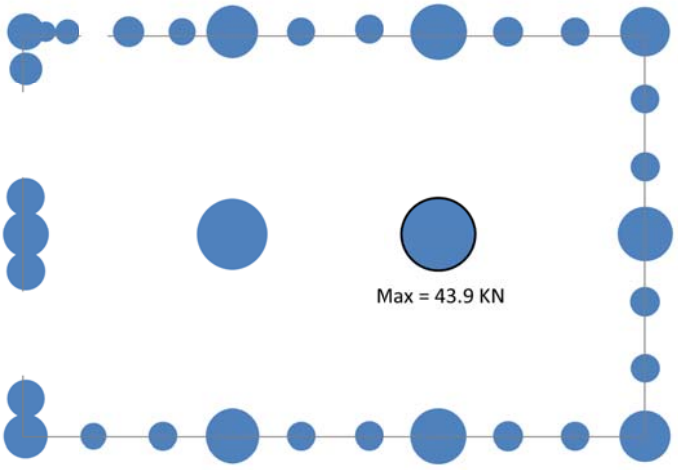

Figure K.34: Timber frame, with openings, load combination 4, Z-reaction

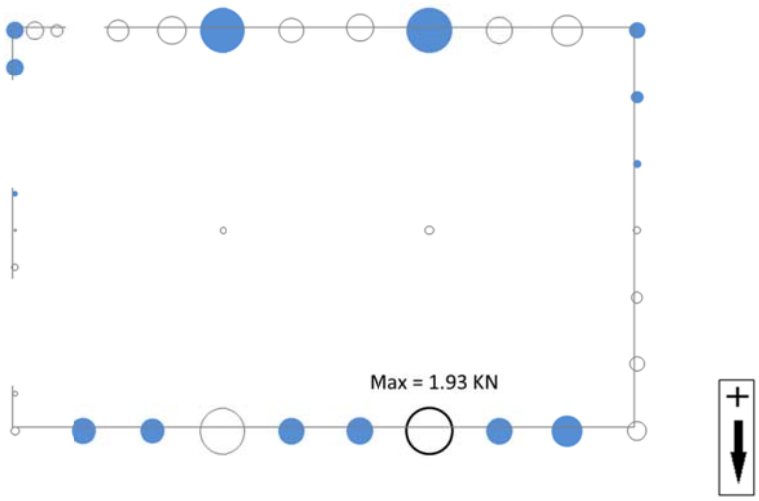

Figure K.35: Timber frame, with openings, load combination 4, Y-reaction

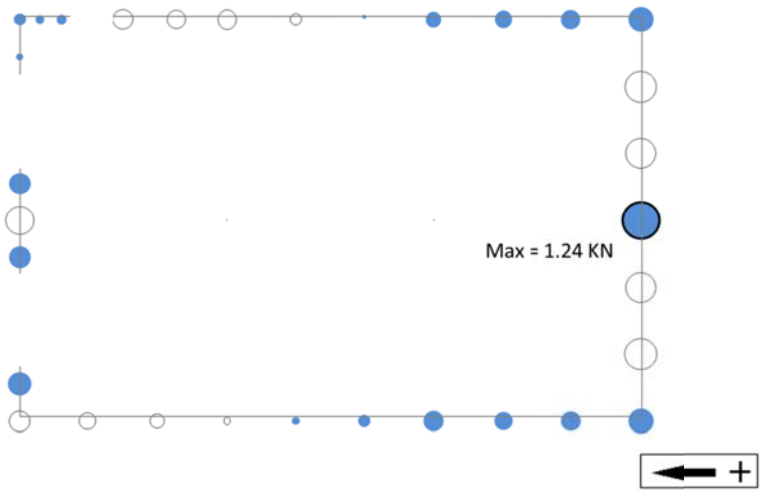

Figure K.36: Timber frame, with openings, load combination 4, X-reaction

Load Combination 5

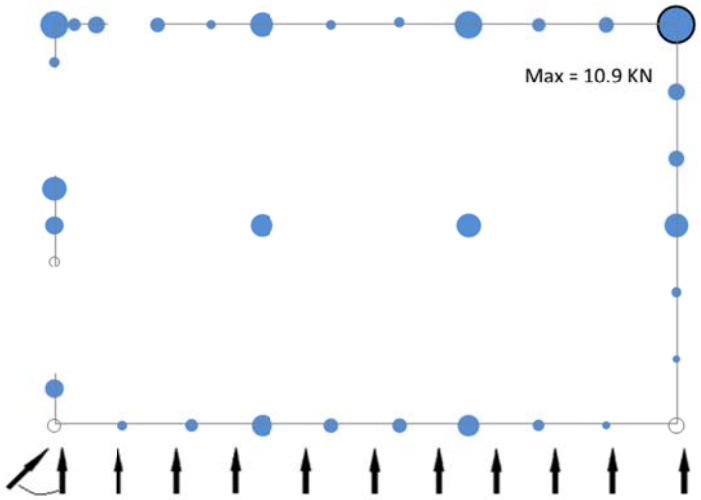

Figure K.37: Timber frame, with openings, load combination 5, north-south wind, Z-reaction

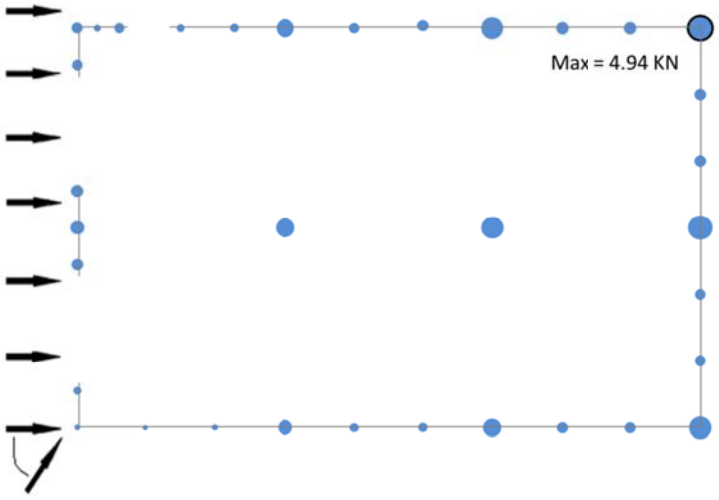

Figure K.38: Timber frame, with openings, load combination 5, east-west wind, Z-reaction

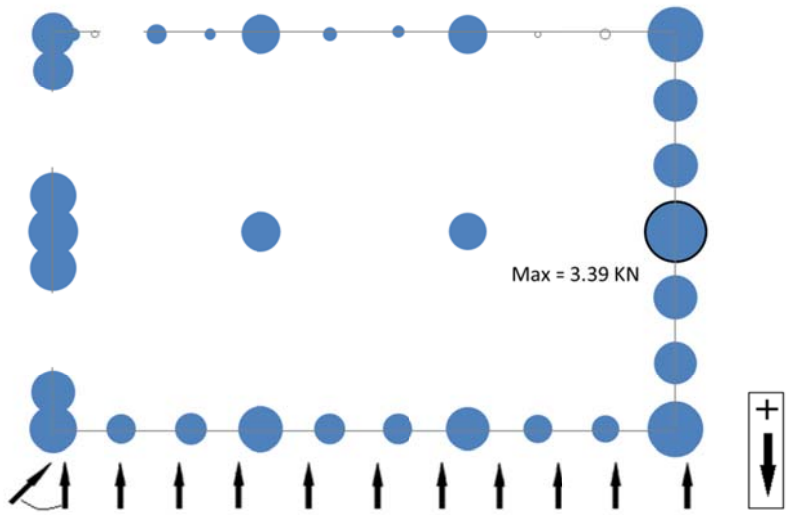

Figure K.39: Timber frame, with openings, load combination 5, north-south wind, Y-reaction

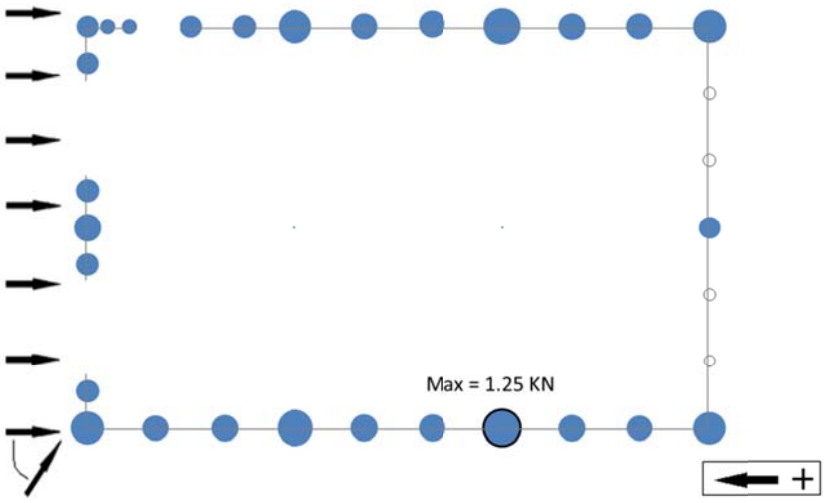

Figure K.40: Timber frame, with openings, load combination 5, east-west wind, X-reaction

Load Combination 6a

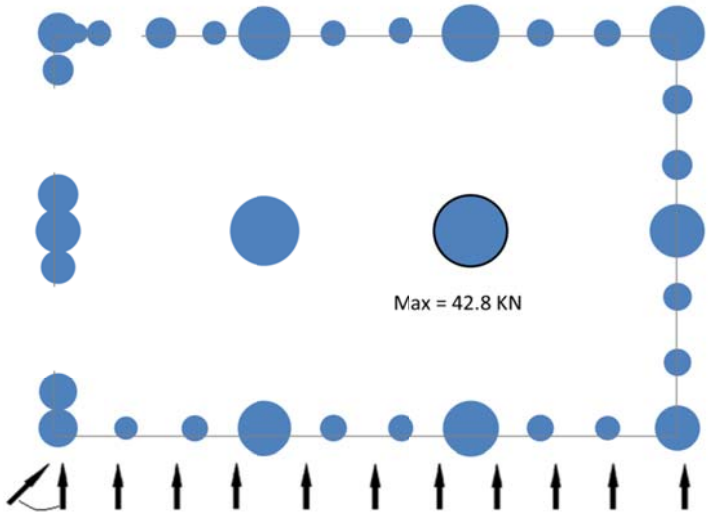

Figure K.41: Timber frame, with openings, load combination 6a, north-south wind, Z-reaction

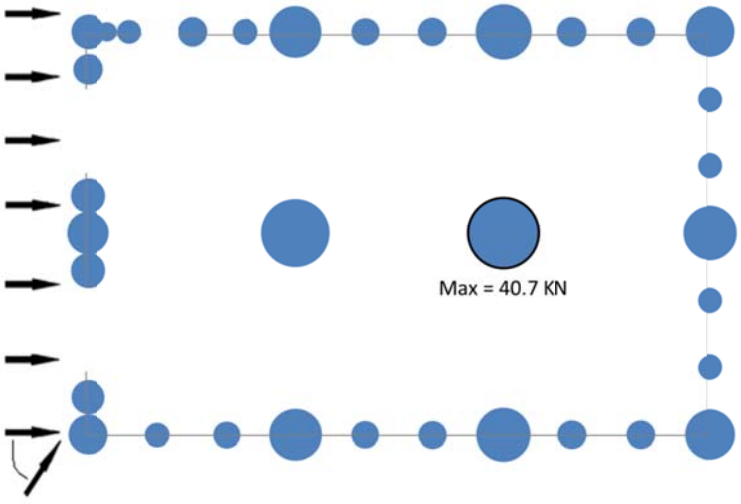

Figure K.42: Timber frame, with openings, load combination 6a, east-west wind, Z-reaction

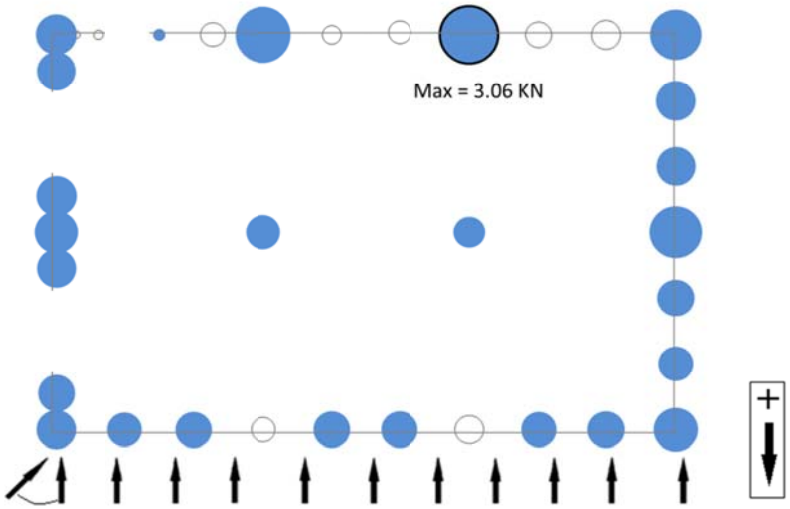

Figure K.43: Timber frame, with openings, load combination 6a, north-south wind, Y-reaction

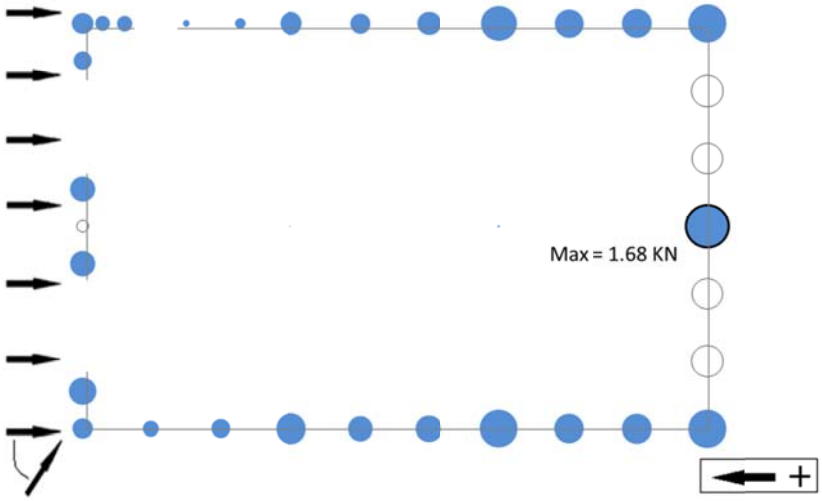

Figure K.44: Timber frame, with openings, load combination 6a, east-west wind, X-reaction